THE ROLE OF ENDOPLASMIC RETICULUM STRESS IN VASCULAR CALCIFICATION

Furmanik, Malgorzata

Awarding institution:
King's College London

THE ROLE OF ENDOPLASMIC RETICULUM STRESS IN VASCULAR CALCIFICATION

SUBMITTED FOR THE DEGREE OF DOCTOR OF PHILOSOPHY

BY

MALGORZATA FURMANIK

SUPERVISORS

PROFESSOR CATHERINE M. SHANAHAN

DR ALEXANDER KAPUSTIN

KING'S COLLEGE LONDON

LONDON 2015

Acknowledgements

I would like to thank my supervisor, Professor Cathy Shanahan, for her guidance, endless support and encouragement, patience, putting up with my negativity and being an amazing role model.

I would also like to thank my second supervisor, Dr Alexander Kapustin, for teaching me about various aspects of being a good scientist and doing that with extraordinary sense of humour.

Special thanks to Leilani for being an amazing friend, for endless supplies of marshmallows and letting me hide in her office when I needed to cry. I would like to thank Jo for keeping me entertained with her lost phone stories and cheese jokes, but mainly for being a good friend and labmate. I would like to thank the rest of the Shanahan lab, current and former lab members: Qiuping, Derek, Robert, Rosie, Flavia, Ally, CanCan, Anne, Chin Yee, Andrew, Jayanta, CiCi, Nina, Sundeep, Roshni, Dipen, Chen, Serena, Lauren, Daniel J. Brayson and Yiwen. I learned loads from all of you and you made my time in the lab special. I will miss lunch club, disputes over which radio station to listen to and Christmas parties. I will probably not miss having to listen to your lab meeting presentations every Monday though.

A big thank you goes to (in no particular order) Natalia, Paweł, Katrin, Zuzia, Wojtek and Irenka for always being there for me. Life would have been much tougher without people to discuss the miseries of PhD life with, and without people who use the word 'aliquot' when referring to food. I do not want to go all soppy in here so I will limit my thanks to you all to just that. I would also like to thank Brecht, who had to endure vast amounts of complaining over many hours of Skype conversations when I was writing.

Last but not least, I would like to thank my parents, Jola and Jacek, whose complete support of all my decisions led me to pursue a PhD.

Abbreviations

AB	Apoptotic body
acLDL	Acetylated LDL
AGEs	Advanced Glycation End-products
ALP	Alkaline Phosphatase (ALPL)
ASK1	Apoptosis Signal Regulating Kinase 1 (MAP3K5)
ATF4	Activating Transcription Factor 4
ATF5	Activating Transcription Factor 5
ATF6	Activating Transcription Factor 6
Bak	BCL2-Antagonist/Killer (BAK1)
Bax	BCL2-Associated X Protein
BBF2H7	BBF2 Human Homolog On Chromosome 7 (CREB3L2)
Bcl-2	B-Cell CLL/Lymphoma 2
Bim	Bcl-2 Interacting Mediator Of Cell Death (BCL2L11)
BMP-2	Bone Morphogenetic Protein 2
BMP-7	Bone Morphogenetic Protein 7
BSP	Bone Sialoprotein (IBSP)
Ca	Calcium (Ca^{2+})
CAII	Carbonic Anhydrase II (CA2)
CD63	CD63 Molecule
CHOP	C/EBP-Homologous Protein (DDIT3)
CKD	Chronic Kidney Disease
CNN1	Calponin 1
COL1A1	Collagen Type I α1
COL14A1	Collagen Type XIV α1
COMP	Cartilage Oligomeric Matrix Protein
COPII	Coat Protein Complex II (vesicle)
CREB	cAMP Responsive Element Binding Protein
DAD1	Defender Against Cell Death 1
Dlx5	Distal-Less Homeobox 5
DR5	Death Receptor 5 (TNFRSF10B)
ECM	Extracellular Matrix
EEA1	Early Endosome Antigen 1
eIF2α	Eukaryotic Translation Initiation Factor 2, Subunit 1 Alpha (EIF2S1)
ENPP1	Ectonucleotide Pyrophosphatase/Phosphodiesterase 1
ER	Endoplasmic Reticulum
ERAD	Endoplasmic Reticulum-Associated Protein Degradation
ERSE	ER Stress Response Element
FGF	Fibroblast Growth Factor

Fzd	Frizzled Class Receptor
GADD34	Growth Arrest And DNA Damage-Inducible 34 (PPP1R15A)
Grp78	Glucose Regulated Protein, 78kDa (HSPA5)
Grp94	Glucose Regulated Protein, 94kDa (HSP90B1)
HAp	Hydroxyapatite
HEK239T	Human Embryonic Kidney cell line
Hsp70	Heat Shock Protein, 70kDa (HSPA1A)
IGF	Insulin-like Growth Factor
IRE1	Inositol-Requiring Enzyme 1 (ERN1)
JNK	JUN N-Terminal Kinase (MAPK8)
LAMP-1	Lysosomal-Associated Membrane Protein 1
LDL	Low Density Lipoprotein
Lrp	Low Density Lipoprotein Receptor
MAPK	Mitogen Activated Protein Kinase
MCL1	Myeloid Cell Leukemia 1
MGP	Matrix Gla Protein
miRNA	Micro RNA
MMP	Matrix Metalloproteinase
MOVAS-1	Mouse Vascular Smooth Muscle Cell Line
MSCs	Mesenchymal Stem Cells
Msx2	Msh Homeobox 2
MV	Matrix Vesicle
OASIS	Old Astrocyte Specifically-Induced Substance (CREB3L1)
OCN	Osteocalcin (BGLAP)
OPG	Osteoprotegerin (TNFRSF11B)
OPN	Osteopontin (SPP1)
Osterix	(SP7)
oxLDL	Oxidised LDL
P	Phosphate (PO_4^{3-})
p-MLC	Phosphorylated Myosin Light Chain (MYL2)
PBA	4-phenylbutyric acid
PDGF	Platelet-Derived Growth Factor
PDGFRB	Platelet-Derived Growth Factor Receptor, Beta Polypeptide
PDI	Protein Disulphide Isomerase
PERK	PRKR-Like Endoplasmic Reticulum Kinase (EIF2AK3)
PHEX	Phosphate Regulating Endopeptidase Homolog, X-Linked
Pit-1	Phosphate Transporter 1 (SLC20A1)
PTH1R	Parathyroid Hormone 1 Receptor
PTHrP	Parathyroid Hormone Related Peptide
ROS	Reactive Oxygen Species

Runx2	Runt-Related Transcription Factor 2
SAOS-2	Human Bone Osteosarcoma Cell Line
SEC23A	Sec23 Homolog A (S. Cerevisiae)
shRNA	Short Hairpin RNA
siRNA	Short Interfering RNA
SM22α	Smooth Muscle Protein 22 Alpha (TAGLN)
SMAD	Mothers Against Decapentaplegic Homolog Family Member
Sox9	SRY (Sex Determining Region Y)-Box 9
SSP	Staurosporine
TG	Thapsigargin
TGFβ	Transforming Growth Factor β
TGFBR1/2	Transforming Growth Factor β Receptor 1/2
TM	Tunicamycin
TNFα	Tumour Necrosis Factor α
TRAF2	TNF Receptor-Associated Factor 2
Twist1/2	Twist Family BHLH Transcription Factor 1/2
U2OS	Human Osteosarcoma Cell Line
UPR	Unfolded Protein Response
UPRE	Unfolded Protein Response Element
VDR	Vitamin D Receptor
VSMC	Vascular Smooth Muscle Cell
Wnt	Wingless-Type MMTV Integration Site Family Member

Abstract

Vascular calcification (VC) is a health problem common in ageing populations, diabetes and chronic kidney disease. It leads to vascular stiffening and heart failure. VC is a regulated process mediated by vascular smooth muscle cells (VSMCs), with similarities to developmental osteogenesis. The exact molecular events responsible for triggering it are unknown. The endoplasmic reticulum (ER) is involved in folding of proteins. ER stress occurs as a result of unfolded protein accumulation and has been implicated in osteoblast differentiation and bone mineralization. Therefore, I hypothesized that ER stress signalling regulates osteogenic differentiation and calcification of VSMCs.

I showed that calcification of human aortas was associated with changes in ER stress marker expression. Warfarin and TNFα, which are both established inducers of vascular calcification, increased expression of ER stress markers in VSMCs. ER stress modelled in human primary VSMCs *in vitro* increased their calcification and was shown to modulate expression of a number of bone related genes, such as BMP-2, Runx2, Osterix, ALP, BSP and OPG in VSMCs *in vitro*. I also demonstrated that ER stress activated features characteristic of a secretory phenotype in VSMCs, such as downregulation of SMC markers and components of TGFβ signalling related to contractile differentiation, as well as BMP-2. Taken together these results suggested that ER stress can induce changes that lead to osteogenic differentiation.

To further explore the relationship between ER stress and osteogenic differentiation of VSMCs Osterix and ALP were studied in more detail. ALP activity was upregulated by ER stress, but did not change when VSMCs calcified. Promoter analysis showed that ALP might be regulated by ER stress via indirect mechanisms and potential regulators of ALP transcription were identified using proteomic analysis.

Table of Contents

List of Figures

List of Tables

Chapter 1: Introduction

1.1. Vascular calcification

1.1.1. What is vascular calcification?

Vascular calcification is the process of deposition of hydroxyapatite in the extracellular matrix (ECM) of the blood vessel wall. Hydroxyapatite (HAp) is the main mineral component of bones and consists of calcium (Ca^{2+}) and phosphate (HPO_4^{2-}) ions that crystallise in matrix vesicles on a scaffold of ECM proteins secreted by calcifying cells (Demer *et al.* 2008; Kapustin *et al.* 2012).

The presence of vascular calcification poses an increased risk of cardiovascular and all-cause mortality. Nearly all patients with cardiovascular disease have some degree of calcification, and, in asymptomatic adults, prevalence of coronary calcification corresponds with age; among 60-year-olds, approximately 60% have vascular calcification (Rennenberg *et al.* 2009; Sage *et al.* 2010).

Vascular calcification can be categorised into two main types: medial and intimal, depending on its localisation in the vessel wall (Karwowski *et al.* 2012; Proudfoot *et al.* 2001). Each type of calcification is caused by different conditions and is associated with different risk factors for the cardiovascular system, summarised in Table 1.1 (Sage *et al.* 2010).

Medial calcification, also called Mönckenberg's sclerosis, most often presents itself as continuous areas of calcified structures along the elastic lamellae of vessels. The direct result of medial vascular calcification is blood vessel wall stiffening, that leads to many cardiovascular complications such as hypertension and aortic stenosis, which in turn give rise to cardiac hypertrophy, myocardial and lower-limb ischemia, congestive heart failure and can eventually result in death (London *et al.* 2011). Vascular calcification is a risk factor predictive of cardiac events (Sage *et al.* 2010; Karwowski *et al.* 2012). Medial calcification is associated primarily with ageing, diabetes and chronic kidney disease (CKD). Patients on dialysis are exposed to a host of risk factors that promote vascular calcification; the most potent of these

are associated with elevated levels of calcium and phosphate and are caused by the dysregulated mineral metabolism induced by renal failure (Shanahan 2013). Much research on vascular calcification is focused on CKD as prevalence of vascular calcification in patients suffering from this disease is very high and nearly half the deaths in dialysis patients are due to cardiovascular disease (Speer *et al.* 2004).

Intimal calcifications are dispersed in the vessel wall, discontinuous and co-localise with atherosclerotic plaques (Sage *et al.* 2010). Intimal calcification is caused by the same factors as atherosclerosis, such as lipids, oxidative stress and inflammation. The result of intimal calcification is an increased risk of plaque rupture (Hoshino et al. 2009), which is believed to cause most myocardial infarction and stroke events.

Vascular smooth muscle cells (VSMCs) play a crucial role in regulating both these types of calcification (Shanahan 2005; Shanahan *et al.* 2011; Shroff *et al.* 2007) and therefore they are the focus of this PhD thesis. However, other cell types are also known to contribute to the process of vascular calcification. Macrophages and endothelial cells, which are known to play a role in atherosclerosis (Weber and Noels, 2011), have also been shown to mediate some of the mechanisms leading to calcification (New *et al.* 2013; Yao *et al.* 2013). It has also been argued that vascular stem cells present in the vessel wall can contribute to vascular disease (Tang *et al.* 2012).

Table 1.1. Types of vascular calcification. References are in the text.

Calcification	Medial	Intimal
Causes	CKD, diabetes, ageing	atherosclerosis, ageing
Results	Vascular stiffening, leads to hypertension and heart failure.	Plaque rupture, leads to strokes and myocardial infarcts.
Cells involved	VSMCs, vascular stem cells?	VSMCs, endothelial cells, macrophages

1.1.2. Mechanisms of vascular calcification

Vascular calcification has long been considered as a passive, degenerative process related to tissue ageing. However, it is now recognised that both intimal and

medial calcification are regulated and mediated by VSMCs (Shanahan *et al.* 1999a; Sage *et al.* 2013). In response to cellular stress VSMCs undergo vascular calcification via several mechanisms: apoptosis, release of matrix vesicles, loss of calcification inhibitors, ageing-related DNA damage and osteogenic differentiation (Figure 1.1). All these processes are discussed in detail in the following sections.

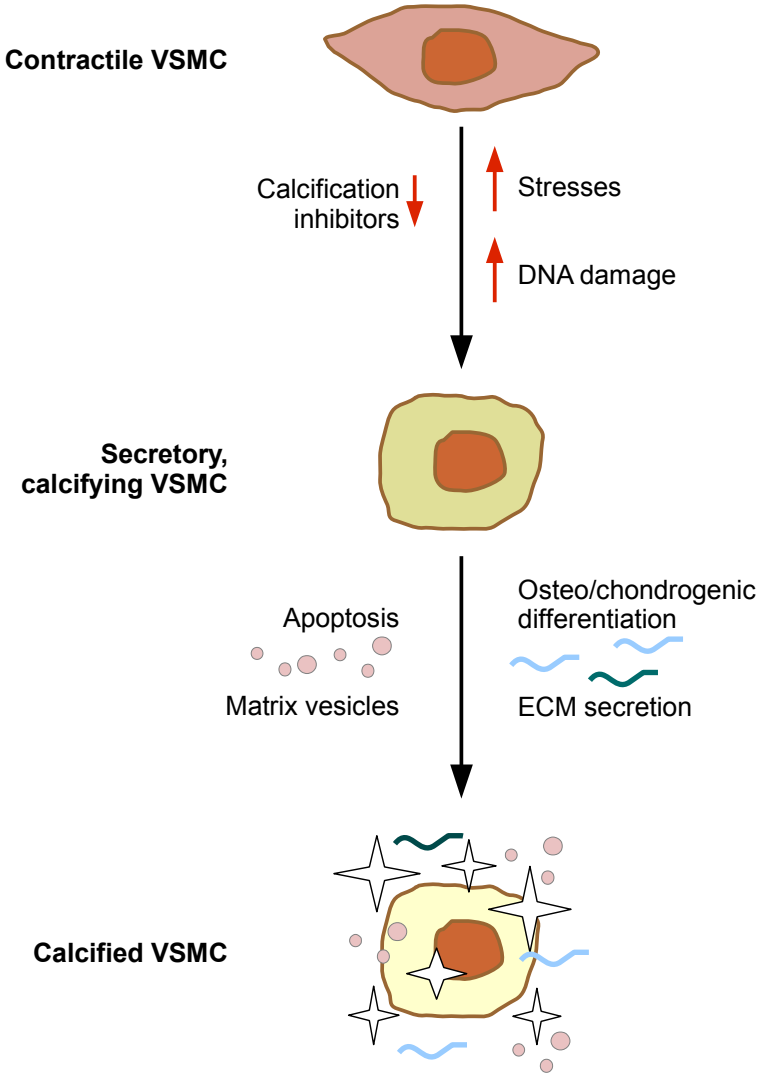

Figure 1.1. Mechanisms of vascular calcification. Stresses such as inflammation or serum mineral imbalance cause a reduction in natural calcification inhibitors and trigger VSMC calcification. Calcifying VSMCs exhibit a secretory phenotype during which they secrete matrix vesicles and express osteo- and chondrogenic markers (transcription factors and extracellular matrix proteins).

1.1.2.1. Loss of calcification inhibitors

In healthy organisms concentrations of calcium (Ca) and inorganic phosphate (P) in serum and interstitial fluid normally reach saturation point (concentrations at

which they spontaneously precipitate). Their spontaneous precipitation in soft tissues is prevented by proteins that act as natural calcification inhibitors, which are produced by various tissues and circulating in blood. Some of these endogenous calcification inhibitors (fetuin-A, MGP, OPG, Klotho) have well established roles in regulating vascular calcification, others (SMAD6, fibrillin-1 and CAII) are hypothesized to play a role based on the phenotypes of mouse knock-out models (Shroff *et al.* 2007) (Table 1.2).

Table 1.2. Summary of natural calcification inhibitors and the effects of their disruption in mice and humans.

Protein	Mouse knock-out phenotype	Human mutation/ polymorphism phenotype	References
BMP-7	Death 1 month after birth, skeletal malformations, retarded ossification of bones, a reduced number of nephrons, polycystic kidney, lack of retinal pigmentation, and retarded lens development.	Polymorphisms associated with inverse relationships between bone mineralization and vascular calcification in the coronary, carotid, and abdominal aorta in a diabetes.	(Freedman *et al.* 2009) (Jena *et al.* 2007)
Carbonic anhydrase II (CAII)	Age dependent medial calcification of small arteries in a number of organs.	Mutations cause CAII deficiency syndrome osteopetrosis, renal tubular acidosis, and cerebral calcification.	(Spicer *et al.* 1989) (Shah *et al.* 2004)
ENPP1	Calcification of joints and the spine and arterial calcification.	Loss of ENPP1 causes 'idiopathic' infantile arterial calcification: calcification of the internal elastic lamina of muscular arteries and stenosis due to intimal thickening.	(Okawa *et al.* 1998) (Rutsch *et al.* 2003)
Fetuin-A	Organ calcification on mineral and vitamin D–rich diet or normal diet depending on the genetic background. Serum has decreased ability to inhibit HAp crystal nucleation.	Polymorphisms associated with high serum phosphate levels, prevalence of calcified atherosclerotic plaques and cardiovascular mortality.	(Schafer *et al.* 2003) (Stenvinkel *et al.* 2005) (Lehtinen *et al.* 2007)
Fibrillin-1	Death 2 weeks after birth, dissecting aneurysm and rupture of the ascending aorta, vascular calcifications	Mutations cause Marfan syndrome: skeletal abnormalities, mental retardation, cardiovascular defects including vascular calcification.	(Ramirez *et al.* 1999) (Fietta et al. 2002)
Klotho	Short lifespan, infertility, vascular calcification, soft tissue calcifications, skin atrophy, osteoporosis and emphysema.	Mutations cause tumoral calcinosis with dural and carotid artery calcifications and ectopic calcification of organs.	(Ichikawa *et al.* 2007) (Kuro-o *et al.* 1997)

Protein	Mouse knock-out phenotype	Human mutation/ polymorphism phenotype	References
MGP	Death within 2 months of birth due to arterial calcification that leads to blood vessel rupture; calcification of cartilages that lead to osteopenia and fractures.	Mutations cause Keutel syndrome: calcification of cartilage in the ears, nose, larynx, trachea, and ribs and extensive medial vascular calcification at an early age. Polymorphisms linked to risk of plaque calcification and cardiovascular events.	(Munroe *et al.* 1999) (Luo *et al.* 1997) (Herrmann *et al.* 2000)
OPG	Osteoporosis and medial calcification of the aorta and renal arteries.	Polymorphism in OPG promoter associated with intimal thickening of the common carotid artery, indicative of early atherosclerosis.	(Bucay *et al.* 1998) (Brändström *et al.* 2004)
SMAD6	Heart defects and aortic calcification.	Not known.	(Galvin *et al.* 2000)

The first inhibitor, fetuin-A (also known as α2-Heremans-Schmid glycoprotein), is constitutively produced in the liver and can be found in serum and extracellular fluids of tissues (Jahnen-Dechent *et al.* 1997). Mice lacking fetuin-A develop ectopic calcifications of soft tissues (Schäfer *et al.* 2003). Certain polymorphisms of this gene have been associated with high serum phosphate levels (Osawa *et al.* 2005), high prevalence of calcified atherosclerotic plaques (Lehtinen *et al.* 2007) and cardiovascular mortality (Stenvinkel *et al.* 2005) in humans. Low levels of circulating fetuin-A in CKD have been correlated to a higher risk of vascular calcification (Ketteler *et al.* 2003). Fetuin-A inhibits calcification by forming complexes with mineral and another calcification inhibitor, matrix γ-carboxyglutamic acid protein (MGP), and thus preventing mineral precipitation (Ketteler *et al.* 2002; Schäfer *et al.* 2003). Fetuin-A has been shown to colocalise with calcified VSMCs *in vivo*, shown by immunohistochemistry of aortic sections. *In vitro* fetuin-A has been shown to be taken up by VSMCs from serum, packaged into vesicles and subsequently secreted to the extracellular space (Reynolds *et al.* 2005). Fetuin-A was also shown to inhibit VSMC apoptosis and increase phagocytosis of apoptotic bodies (Reynolds *et al.* 2005). This shows that fetuin-A not only inhibits mineral precipitation but also provides additional mechanisms of inhibiting VSMC calcification.

Another potent calcification inhibitor is MGP, which is synthesized by

chondrocytes and VSMCs and directly inhibits calcium phosphate crystal nucleation by binding mineral ions to its γ-carboxylated glutamic acid residues (Luo *et al.* 1997). MGP knock-out mice die within 2 months of birth due to arterial calcification that leads to blood vessel rupture, and show calcification of cartilage which leads to osteopenia and fractures (Luo *et al.* 1997). Mutations of MGP in humans, which cause MGP to be inactive or absent, result in Keutel syndrome. Keutel syndrome manifests as calcification of cartilage in the ears, nose, larynx, trachea, and ribs and extensive medial vascular calcification at an early age (Munroe *et al.* 1999). MGP polymorphisms have been linked to increased risk of atherosclerotic plaque calcification and myocardial infarction (Herrmann *et al.* 2000). MGP has been shown to be highly expressed in human atherosclerotic plaques (Shanahan *et al.* 1994). Calcifying human VSMCs *in vitro* also showed elevated expression of MGP (Proudfoot *et al.* 1998). These findings demonstrate that in stress conditions VSMCs synthesise high levels of MGP in order to protect themselves from calcification. In addition, MGP has been shown to negatively regulate BMP-2, a potent bone-inducing cytokine, by binding BMP-2 and preventing it from reaching its receptor on the cell surface (Zebboudj *et al.* 2002).

Osteoprotegerin (OPG) and Klotho are two proteins whose knock-outs in mice have seemingly contradictory effects because they cause both osteoporosis and soft tissue calcification. OPG deficient mice exhibit a decrease in bone density and mass and at the same time medial calcification of the aorta and renal arteries (Bucay *et al.* 1998). OPG is a secreted factor that decreases osteoclast activity by inhibiting receptor activator of nuclear factor kappa B ligand (RANKL) activation of its receptor RANK. This signalling is essential for the maturation of osteoclast progenitors (Katagiri *et al.* 2002), thus the increased bone resorption and osteoporosis in its absence. OPG is endogenously expressed in the media of the aorta (Bucay *et al.* 1998), but the mechanisms by which it inhibits vascular calcification are yet unknown. However, increased levels of serum OPG were observed in patients with vascular calcification and cardiovascular disease (Collin-Osdoby 2004) and polymorphisms in the OPG promoter have been associated with intimal thickening of the common carotid artery, indicative of early atherosclerosis

(Brandstrom *et al.* 2004).

Klotho deficient mice develop normally until 2 weeks of age and then exhibit symptoms resembling accelerated ageing, including a short lifespan, infertility, skin atrophy, osteoporosis and calcification of the aorta and other arteries, accompanied by intimal thickening. In addition, ectopic calcification of various organs is observed (Kuro-o *et al.* 1997). In humans, a homozygous Klotho mutation causes tumoral calcinosis, which manifests itself with carotid and dural artery calcifications and ectopic calcifications of soft tissues (Ichikawa *et al.* 2007). Klotho is a cofactor of FGF23, a hormone that promotes renal phosphate excretion by decreasing phosphate reabsorption and reducing circulating vitamin D. Therefore its deficiency results in symptoms produced by a disrupted mineral metabolism (Ichikawa *et al.* 2007). Decreased Klotho levels have been observed in calcified arteries showing its important role in inhibiting vascular calcification (Lim *et al.* 2012).

ENPP1 (ectonucleotide pyrophosphatase/phosphodiesterase 1) is an enzyme expressed in bone and cartilage on the surface of cells, that produces inorganic pyrophosphate (PPi), a major inhibitor of calcification. ENPP1 deficient mice develop calcification of joints and spine and arterial calcification (Okawa *et al.* 1998). In humans the loss of ENPP1 causes 'idiopathic' infantile arterial calcification, a syndrome characterised by calcification of the internal elastic lamina of arteries and stenosis due to intimal thickening (Rutsch *et al.* 2003). PPi directly inhibits HAp deposition and its levels are controlled by alkaline phosphatase (ALP), an enzyme that catalyses its hydrolysis. It has been shown that in a rat renal failure model of vascular calcification the activity of ALP is increased in the aorta (Lomashvili *et al.* 2008), suggesting that increased PPi hydrolysis is a hallmark of calcification.

Smad6 belongs to the Smad family of proteins, which mediate intracellular TGFβ superfamily signalling. It has been shown to be expressed predominantly in the heart and blood vessels. Smad6 deficient mice develop heart defects and aortic calcification (Galvin *et al.* 2000). Smad6 inhibits bone morphogenetic protein (BMP) signalling, which is why the loss of inhibition results in soft tissue calcification in Smad6 null mice. Because of its effect on mouse development Smad6 is a potential calcification inhibitor, however its role in vascular calcification in humans is not

known.

Fibrillin-1 is another interesting inhibitor of calcification. It is an ECM glycoprotein that forms elastic microfibrills in blood vessel walls. Mice lacking functional fibrillin-1 die within the first 2 weeks after birth because of dissecting aneurysms and rupture of the ascending aorta. They also develop vascular calcifications (Pereira *et al.* 1997; Ramirez *et al.* 1999a). In humans various mutations of the fibrillin-1 gene result in Marfan syndrome with a spectrum of skeletal abnormalities and cardiovascular defects including vascular calcification (Ramirez *et al.* 1999b). However, the role of fibrillin-1 in vascular calcification induced by other factors is unknown.

Carbonic anhydrase II (CAII) is the most widespread of 13 isoforms of this enzyme, which forms protons (H^+) and bicarbonate ions (HCO_3^-) from CO_2 and H_2O and thus contributes to the regulation of pH in body fluids. Mice with CAII deficiency show calcification in small and medium arteries and arterioles (Spicer *et al.* 1989). In humans, mutations of the CAII gene are manifested as cerebral calcification and osteopetrosis (bones become denser, opposite to osteoporosis; Shah *et al.* 2004). These findings highlight the importance of pH in formation of calcified plaques, but the exact role of CAII in vascular calcification in other contexts is unknown.

Bone morphogenetic protein 7 (BMP-7), a member or the TGFβ superfamily, is an example of an inhibitor of vascular calcification, whose knock-out in mice, however, does not have a vascular or soft tissue calcification phenotype. Mice lacking BMP-7 show skeletal abnormalities, delayed ossification of bones as well as kidney and eye defects (Jena *et al.* 1997). Polymorphisms in the BMP-7 gene have been linked to inverse relationships between bone mineralization and vascular calcification in the coronary, carotid, and abdominal aorta in diabetes patients (Freedman *et al.* 2009). BMP-7 has also been shown to play a role in VSMC differentiation and maintaining of their differentiated phenotype *in vitro* (Dorai *et al.* 2000). Moreover, treatment with BMP-7 prevented vascular calcification in a mouse model of this disease (Davies *et al.* 2005). This shows that not all BMPs favour calcification and that a balance in the signalling of these molecules results in correct development.

1.1.2.2. VSMC calcification is vesicle-mediated

VSMCs are the source of two distinct types of vesicles released to the ECM, apoptotic bodies (ABs) and matrix vesicles (MVs), and both of these play important roles in initiating vascular calcification (Kapustin and Shanahan 2012).

ABs are membrane-bound fragments of cells, that result from apoptotic cell death. Through apoptosis the body disposes of damaged cells in a way that does not elicit an inflammatory response, as ABs are immediately phagocytosed by macrophages (Maiuri *et al.* 2007). Apoptosis has been shown to be important for both physiological and pathological calcification. ABs have been shown to have HAp crystal nucleating properties in cartilage (Hashimoto *et al.* 1998). It was shown later that in VSMCs cultured *in vitro* apoptosis occurs prior to the onset of their calcification and that ABs accumulate calcium and may be sites of crystal nucleation (Proudfoot *et al.* 2000). These findings are confirmed by i*n vivo* studies showing that dialysis triggers VSMC apoptosis and thus accelerates vascular calcification (Shroff *et al.* 2008). Apoptosis was also shown to accelerate plaque formation and induce its calcification in a mouse model of atherosclerosis (Clarke *et al.* 2008). In addition to that, acetylated low density lipoproteins (acLDL), which are potent inducers of atherosclerosis, have been shown to induce VSMC calcification by inhibiting AB phagocytosis (Proudfoot *et al.* 2002).

MVs are small (100nm in diameter) extracellular membranous particles, which contrary to ABs, are released by living cells. They play a crucial role in regulating the mineralisation of ECM during bone growth at the growth plate, where they are secreted by chondrocytes and initiate the first crystals of HAp (Anderson 2003). It is now well recognised that MVs are very different from ABs, but they also play an important regulatory role in vascular calcification. MVs have been shown to mediate calcification of VSMCs treated with elevated concentrations of Ca and P *in vitro* and to be loaded with natural calcification inhibitors fetuin-A and MGP (Reynolds *et al.* 2004). This suggests that VSMCs secrete MVs to protect themselves by discarding an excess Ca and P bound to calcification inhibitors, however if the inhibitors are depleted, they nucleate calcification. *In vivo* studies confirm the presence of MVs in the ECM of healthy arteries and calcified MVs in the ECM of

arteries from patients with atherosclerosis, diabetes and CKD (Kapustin *et al.* 2011). In addition to VSMCs, macrophages have been proposed to be an alternative source of MVs in the calcifying vessel wall (New *et al.* 2013).

Proteomic analysis of MVs secreted by VSMCs carried out by our laboratory has shown that they contain various endoplasmic reticulum (ER)-resident proteins (Kapustin *et al.* 2011) such as chaperones (Hsp70, Grp94, Grp78), various protein disulphide isomerases (PDIA1, PDIA3, PDIA6), calumenin and protein glycosyltransferase (DAD1) and that their levels in MVs change as VSMCs are calcifying. This has provided the first hint that the ER might play a role in VSMC calcification.

1.1.2.3. Osteogenic transdifferentiation of calcifying VSMCs

VSMC phenotypic plasticity

In contrast to other muscle cells VSMCs do not differentiate terminally and show phenotypic plasticity. In physiological conditions in the vessel wall they exist as contractile cells and regulate vascular tone. In response to stress and injury VSMCs lose expression of contractility-related genes such as SM22α, calponin (CNN1), and myosin light chain (MLC) (Frid et al. 1992; Huang *et al.* 1999; Feil *et al.* 2004). They also proliferate, migrate and secrete ECM related proteins, and thus are able to repair the injured vessel (Shanahan *et al.* 1998; Shanahan *et al.* 1993). This is the mechanism that leads to formation of a fibrous cap over an atherosclerotic plaque (Dzau *et al.* 2002). When vascular injury is persistent the phenotypic transition is dysregulated and VSMCs can undergo an unfavourable transdifferentiation into cells with characteristics of osteoblasts or chondrocytes (Iyemere *et al.* 2006; Shanahan *et al.* 1999b; Speer *et al.* 2009). This observation led researchers to the idea that vascular calcification is caused by pathological induction of a process similar to bone formation, which normally only occurs during bone development in the embryo.

VSMC osteogenic transdifferentiation and endochondral bone formation

During embryonic development bone formation occurs via two mechanisms: endochondral and membranous. During membranous ossification, which gives rise to flat bones of the skull, osteocytes differentiate directly from mesenchymal stem cells (MSCs). During endochondral ossification, by which most bones in the body are made, there is an intermediate step in which MSCs differentiate into chondrocytes that proliferate and secrete extracellular matrix to form a scaffold for osteoblasts (Karsenty *et al.* 2009). Chondrocytes also secrete MVs that later initiate calcification of the ECM (Anderson 2003). Then they become hypertrophic and direct perichondral cells to differentiate into osteoblasts (Karsenty *et al.* 2009; Michigami 2013), and finally undergo apoptosis. All stages of endochondral bone formation can be found in calcified lesions, including fully formed trabecular bone, and markers characteristic for both osteoblasts and chondrocytes have been found to be expressed by calcifying VSMCs (Qiao et al 2003; Neven *et al.* 2007; Speer *et al.* 2009, Sage *et al.* 2010).

Chondrocyte and osteoblast proliferation and maturation during endochondral bone formation is regulated by a tightly orchestrated transcription programme activated in MSCs, mediated by secreted factors such TGFβ, Ihh (Indian hedgehog), PTHrP (parathyroid hormone-related protein), FGFs (fibroblast growth factors), BMPs (bone morphogenetic proteins), Wnts and IGFs (insulin-like growth factors). Several key transcription factors act downstream of these pathways and regulate expression of ECM genes in chondrocytes and osteoblasts. Among these are Sox9, Runx2 (Cbfa1), Osterix, Dlx5, Msx2, β-catenin Twist-1 and Twist-2, which regulate transcription of various bone ECM such as collagens, cartilage oligomeric matrix protein (COMP), bone sialoprotein (BSP), osteocalcin (OCN) and other regulatory bone proteins such as ALP and osteoprotegerin (OPG), thus leading to maturation of osteoblasts, mineralisation and bone formation (Karsenty *et al.* 2009). Here I will discuss in more detail some of these factors, that were found to be relevant to vascular calcification and are relevant to this project (Figure 1.2).

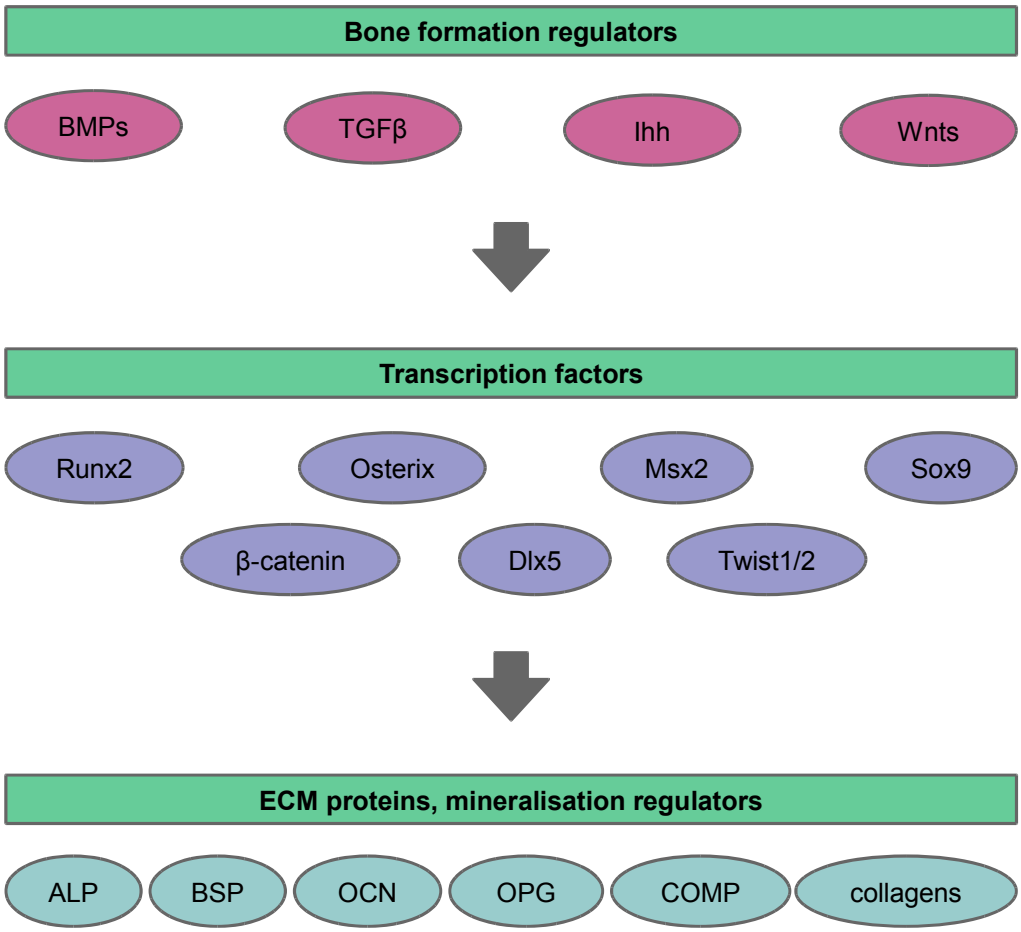

Figure 1.2. Factors involved in bone formation during embryonic development, which are relevant for vascular calcification.

BMP-2, a cytokine that belongs to the TGFβ superfamily, regulates organ formation during embryonic development. The knock-out of BMP-2 is embryonic lethal, with the mice not surviving 10 days of gestation due to heart defects (Zhang and Bradley 1996). In later stages of embryonic development BMP-2 is also an important regulator of osteoblast maturation; MSCs treated with BMP-2 differentiate into osteoblasts (Nishimura *et al.* 1998; Chen *et al.* 2012). BMP-2, as well as other members of the TGFβ superfamily, binds to its respective cell surface receptors, which transduce the signal to the cytoplasm by phosphorylating signalling molecules called SMADs (Liu *et al.* 1996). These act by activating target transcription factors. BMP-2 is an established inducer of VSMC osteogenic transdifferentiation and calcification *in vitro* (Li *et al.* 2008; Nakagawa *et al.* 2010). *In vivo* it has been

shown to be expressed in human calcified aortas and not in healthy vessels (Bostrom *et al.* 1993; Kaden *et al.* 2004) and to accelerate plaque calcification in a mouse model of atherosclerosis (Nakagawa *et al.* 2010). However, BMP-2 has also been shown to be expressed in the aorta during embryonic development and promote neural crest stem cells to differentiate into smooth muscle cells (Shah *et al.* 1996), therefore its role in vascular calcification might not be as definite as studies suggest.

TGFβ1 is a cytokine with an established role in regulating chondrocyte growth by inhibiting their hypertrophy and maintaining expression of ECM proteins (Ballock *et al.* 1993). This effect appears to be partly mediated by induction of PTHrP expression (see below). TGFβ1 has also been shown to induce physiological death of chondrocytes crucial for bone mineralisation (Mackie *et al.* 2008). In VSMCs cultured *in vitro* TGFβ1 promotes contractile differentiation (Shah et al 1996; Hirschi *et al.* 1998). However, it has also been shown to induce osteogenic gene expression (Simionescu *et al.* 2005, Liu *et al.* 2014) and to be present at high levels in calcified human aortas (Jian *et al.* 2003). This suggests that similar to BMP-2, the role of this cytokine in vascular calcification and modulation of VSMC phenotype is not clear.

Ihh and PTHrP play complementary roles during endochondral bone formation. Ihh promotes chondrocyte hypertrophy and maturation of osteoblasts, while PTHrP promotes chondrocyte proliferation and delays hypertrophy (Kronenberg 2003; Nakashima *et al.* 2003). The role of Ihh in VSMC osteogenic transdifferentiation is still unknown. PTHrP has been shown to inhibit bovine VSMC calcification (Jono *et al.* 1997). However, another study has shown that it can increase expression of osteogenic genes BMP-2 and Runx2 in human VSMCs (Liu *et al.* 2012)

Wnts are secreted, lipid-modified glycoproteins that activate cell surface receptor-mediated signal transduction pathways to regulate a variety of cellular activities, including cell fate determination, proliferation, migration, polarity, and gene expression. The canonical Wnt signaling pathway, where Wnts interact with Lrp/Fzd receptor complexes to inhibit β-catenin degradation, promotes the proliferation, expansion and survival of osteoblasts. β-catenin is essential for skeletal

development, null murine embryos died after 7 days of gestation. Specific depletion of β-catenin in osteoblasts caused a low bone mass phenotype in mice (Westendorf *et al.* 2004). There is some evidence that Wnt3a and Wnt7a signalling via the canonical pathways is involved in regulation of mouse VSMC calcification by osteogenic transcription factor Msx2 (Shao *et al.* 2005). Wnt5a has also been implicated in promoting VSMC calcification, and is inhibited by PPARγ (Woldt et al. 2005). In addition, another study has shown that TGFβ1 upregulates β-catenin expression and thus promotes calcification of rat VSMCs (Liu *et al.* 2014). These studies show that the Wnt signalling pathway is a regulator of vascular calcification.

An important aspect of bone formation is its regulation by osteoblst- and chondrocyte-specific transcription factors which are expressed at various stages of maturation of these cells. Some of these transcription factors have also been shown to be expressed in calcified aortas and have been hypothesized to regulate VSMC calcification.

Sox9 is the main transcription factor associated with regulating chondrogenesis, essential for its early stages. Sox9 drives transcription of cartilage matrix proteins such as type 10 and type 2 collagen, aggrecan and COMP (Bi *et al.* 1999; Liu et al. 2007; Nishimura *et al.* 2012). Sox9 mutations cause skeletal dysplasia and XY sex reversal, which reflects the fact that apart from skeletogenesis it is required for the formation of other organs, such as testis (Akiyama 2008). Sox9 has been shown to regulate VSMC chondrogenic transdifferentiation by suppressing expression of smooth muscle cell markers and activating expression of chondrogenic markers (Xu *et al.* 2012; Neven *et al.* 2007; Neven *et al.* 2010). Sox9 has been shown to be expressed in calcified human aortas (Tyson *et al.* 2003).

Runx2 knock-out mice die just after birth and their skeletons show complete lack of mineralisation (Komori *et al.* 1997). Runx2, whose transcriptional targets include OCN, BSP, osteopontin (OPN) and Ihh, is essential for osteoblast maturation as well as chondrocyte hypertrophy (Nishimura *et al.* 2012). Runx2 has been shown to be important for VSMC osteogenic transdifferentiation, as it drives expression of osteogenic genes (Speer *et al.* 2010) and it has been shown to be expressed in calcified blood vessels (Tyson *et al.* 2003). More recently its crucial role in regulating

vascular calcification has been demonstrated in a VSMC-specific knock-out mouse model. The mice exhibited decreased calcification compared to wild type counterparts, when fed a high fat diet. Decreased RANKL expression and macrophage infiltration into the calcified lesions was observed in aortas of the knock-out mice, as well as decreased expression of ALP (Sun *et al.* 2012).

Dlx5 is a transcription factor that belongs to the distal-less, homeodomain-containing family of transcription factors. Dlx5-knockout mice have craniofacial abnormalities with a delayed cranial ossification and abnormal osteogenesis (Acampora *et al.* 1999). It has been shown to regulate expression of Osterix in osteoblasts (Lee *et al.* 2003; Ulsamer *et al.* 2008). The involvement of Dlx5 in VSMC calcification is not yet known.

Msx2, a homeobox gene, is a mammalian homologue of the Drosophila muscle segment homeobox. Msx2-deficient mice show reduced bone formation, abnormal calvarial development, and defects in the ectodermal organs including the teeth, hair, and mammary glands (Ichida *et al.* 2004). The bone phenotype is caused by impaired chondrocyte hypertrophy as well as osteoblast maturation. Msx2 has been shown to promote VSMCs calcification by activating the Wnt pathway (Shao *et al.* 2005). It has been shown to mediate TNFα-induced ALP expression in human VSMCs (Lee *et al.* 2010) and oxidised LDL-induced Osterix and ALP expression and calcification of bovine VSMCs (Taylor *et al.* 2011).

Osterix (Osx, SP7), a zinc-finger containing transcription factor from the SP1 family, is expressed in MSCs and osteoblasts and is essential for extracellular matrix deposition, osteoblast maturation and bone formation; in Osterix null mice no bone formation occurs (Nakashima *et al.* 2002). Osterix was shown to act both downstream of Runx2 and independently of Runx2 (Lee *et al.* 2003; Matsubara *et al.* 2008). It has also been demonstrated to act downstream of both Dlx5 and Msx2 in osteoblasts (Matsubara *et al.* 2008; Ulsamer *et al.* 2008). Interestingly, Osterix inhibits the Wnt/β-catenin pathway in osteoblasts, forming a negative feedback loop mechanism regulating mineralisation (Zhang et al 2008). Osterix was shown to be expressed in calcified human coronary arteries alongside other bone markers (Alexopoulos *et al.* 2011). Recently three studies have been published shedding light

on the function of Osterix in VSMCs. The first one shows that upon oxidised LDL treatment bovine VSMCs undergo an osteogenic transdifferentiation, during which Osterix is upregulated in an Msx2-dependent manner (Taylor *et al.* 2011). Another study shows that Osterix is upregulated in rat VSMCs upon treatment with vitamin D, a known inducer of calcification (Zebger-Gong *et al.* 2011). In addition, a miRNA, miR-125b, which targets Osterix in human VSMCs undergoing osteogenic transdifferentiation has been identified (Goettsch *et al.* 2011). Inhibition of miR-125b was shown to increase calcification of human coronary artery VSMCs, which was accompanied by increased ALP activity and expression of Runx2. These findings show that Osterix plays a role in VSMC osteogenic transdifferentiation and calcification, but there is poor understanding of what its transcriptional targets and exact functions in those cells are.

An important group of bone formation regulators are the Twist proteins, Twist-1 and Twist-2. Twist-1 has long been known to be implicated in skeletogenesis because haploinsufficiency at its locus causes Saethre-Chatzen syndrome, which manifests with an increase in bone formation in the skull (Howard *et al.* 1997). Twist-1 in the skull and Twist-2 in the appendicular skeleton inhibit osteoblast differentiation early during skeletogenesis, by interacting with Runx2 and preventing it from binding to the OCN promoter (Yousfi *et al.* 2002; Bialek *et al.* 2004). Expression of the Twist genes decreases later during embryogenesis and osteoblast differentiation can proceed. Twist-1 also inhibits Runx2 function in the perichondrium and thus controls chondrocyte maturation (Bialek *et al.* 2004). Twist-1 has also been shown to negatively regulate Runx2 activity in valvular interstitial cells from calcified human aortic valves and decreased their osteogenic differentiation (Zhang *et al.* 2014).

It has recently emerged that for both osteoblasts and chondrocytes to secrete ECM, mature and form bones efficiently ER stress and the unfolded protein response signalling are essential. This together with the proteomic analysis of MV data in our laboratory provided evidence for a potential role of ER stress in vascular calcification.

1.1.3. Stresses that induce vascular calcification

Further evidence supporting the idea that ER stress could play a role in vascular calcification comes from the fact that various factors that cause VSMC calcification *in vitro* and vascular calcification *in vivo* have already been shown to induce or reduce ER stress in other cell types and tissues. A list of calcification inducers and what is known about their ability to induce ER stress is presented in Table 1.3 below. Many of these factors are associated with diseases known to aggravate vascular calcification such as atherosclerosis (LDLs, inflammation, oxidative stress, cholesterol), CKD (high calcium and phosphate, oxidative stress, vitamin D, warfarin) or diabetes (AGEs, oxidative stress, inflammation).

Table 1.3. Inducers of vascular calcification and what is known about their ability to modulate ER stress. Key: "+" induces, "-" decreases, "?" not known.

What?	**Induces calcification of VSMCs**		**Induces ER stress**		**References**
	In vitro	***In vivo***	***In vitro***	***In vivo***	
Advanced glycation endproducts (AGEs)	+	+	+ rat cortical neurons, human neuroblastoma cells, HUVECs, stromal cells, human and mouse chondrocytes	?	(Ren *et al.* 2009) (Wang *et al*. 2012a) (Yin *et al.* 2012) (Rasheed *et al.* 2012) (Tanaka *et al.* 2013) (Yamabe et al. 2013) (Wu *et al.* 2014)
BMP-2	+	+	+ osteoblasts VSMCs	?	(Kaden *et al.* 2004) (Li *et al.* 2008) (Murakami *et al.* 2009) (Nakagawa *et al.* 2010) (Liberman et al. 2011)
Calcium and phosphate	+	+	+ rat VSMCs	?	(Block *et al.* 1998) (Shanahan *et al.* 2011) (Duan *et al.* 2013)
Calcium phosphate crystals	+	?	?	?	(Ewence *et al.* 2008) (Sage *et al.* 2011)
Cholesterol	+	+	+ VSMCs, macrophages, valvular interstitial cells	Mouse aortic valves	(Watson *et al.* 1994) (DeVries-Seimon *et al.* 2005) (Musunuru *et al.* 2008) (Kedi *et al.* 2009) (Cai *et al.* 2013)

What?	Induces calcification of VSMCs		Induces ER stress		References
	In vitro	*In vivo*	*In vitro*	*In vivo*	
Dexamethasone	+	?	- HEK293 cells	- mouse intestine	(Mori *et al.* 1999) (Fujii *et al.* 2006) (Das *et al.* 2013)
Estrogen	+/-	?	- endothelial cells, pancreatic β-cells, mouse osteoblasts	- mouse liver	(Balica *et al.* 1997) (Osako *et al.* 2010) (Fukui *et al.* 2011) (Haas *et al.* 2012) (Guo *et al.* 2014c) (Kooptiwut *et al.* 2014)
Inflammation	+	+	+ many cell types	+ many tissues	(Parhami *et al.* 2002) (Moe *et al.* 2005) (Garg *et al.* 2012)
Low density lipoprotein (LDL)	+	+	+ endothelial cells, macrophages, valvular interstitial cells	+ macrophages in atherosclerotic plaque	(Proudfoot *et al.* 2002) (Sanson *et al.* 2009) (Orsó *et al.* 2011) (Taylor *et al.* 2011) (Cai *et al.* 2013) (Yao *et al*. 2013)
Leptin	+	+	? ER stress induces leptin resistance, leptin decreases ER stress in HEPG2 and A549 cells	? ER stress induces leptin resistance	(Parhami *et al.* 2001) (Iribarren *et al.* 2007) (Hosoi *et al.* 2008) (Wang *et al.* 2013) (Xiong *et al.* 2014)
Oxidative stress	+	+	+ many cell types	+ many tissues	(Miller *et al.* 2008) (Byon *et al.* 2008) (Kaneto *et al.* 2005) (Cao *et al.* 2014)
Shear stress (hypertension)	?	+	?	+ mouse aortas	(Kalra *et al.* 2012) (Kassan *et al.* 2012)
Stearate	+	?	+ mouse VSMCs	?	(Ting *et al.* 2011) (Masuda *et al.* 2012)
TGFβ	+	+	+ lung fibroblasts	?	(Watson *et al.* 1994) (Jian *et al.* 2003) (Simionescu *et al.* 2005) (Baek *et al.* 2012)
TNFα	+	+	+ murine fibrosarcoma L929, mouse VSMCs	?	(Barath *et al.* 1990) (Tintut *et al.* 2000) (Xue *et al.* 2005) (Masuda *et al.* 2013)
Vitamin D3	+	+	- macrophages	?	(Wolisi *et al.* 2005) (Duan *et al.* 2009) (Riek *et al.* 2012)

What?	Induces calcification of VSMCs		Induces ER stress		References
	In vitro	*In vivo*	*In vitro*	*In vivo*	
Vitamin D3 + Nicotine (VDN model)	+	+	+ rat VSMCs	+ rat aortas	(Niederhoffer et al. 1997) (Duan *et al.* 2009) (Duan *et al.* 2013)
Warfarin	+	+	?	?	(Danziger 2008) (Lomashvili *et al.* 2011)
β-glycerophosphate	+	?	+ human dental pulp cells	?	(Shioi *et al.* 1995) (Kim et al. 2014)

1.2. Endoplasmic reticulum stress and the unfolded protein response

The ER is the first organelle of the secretory pathway, where most secreted and transmembrane proteins are folded and mature. ER stress occurs when the influx of unfolded proteins to the ER exceeds its capacity to fold them. It results in activation of a signalling pathway called the unfolded protein response (UPR) (Ron and Walter, 2007; Walter and Ron, 2011). ER stress and the UPR can also be activated by disturbances in calcium homeostasis as storing Ca^{2+} is an important function of the ER. Ca^{2+} is required for the maintenance of protein synthesis as the majority of the ER resident chaperones (for example calreticulin) are Ca^{2+} -binding proteins. Therefore, fluctuations of the levels of Ca^{2+} in the ER can severely impact folding capacity (Gorlach *et al.* 2006).

There are three proteins responsible for sensing an increased load of unfolded proteins in the ER, which define three branches of the UPR: inositol-requiring protein-1 (IRE1), activating transcription factor-6 (ATF6) and protein kinase RNA (PKR)-like ER kinase (PERK). These transmembrane proteins, which have ER luminal and cytosolic domains, are called ER stress transducers as upon sensing ER stress they transmit the signal from the ER to downstream effectors (Figure 1.3) (Ron and Walter, 2007; Walter and Ron, 2011).

The first ER stress transducer ever to be described is IRE1. Upon unfolded protein accumulation it oligomerizes and undergoes autophosphorylation (Shamu

et al. 1996). This activates its effector function, which is cleavage of only one known substrate, XBP1 mRNA. This splicing of XBP1 causes a frameshift and results in a completely different protein being translated (Yoshida *et al.* 2001). The spliced XBP1 is more stable and acts as a transcription activator for UPR regulated genes (Calfon *et al.* 2002; Yoshida *et al.* 2001). The protein resulting from unspliced XBP1 mRNA is unstable and represses UPR target genes (Calfon *et al.* 2002). The XBP1 branch of the UPR has a role in regulating lipid biosynthetic enzymes and ER-associated degradation components, as well as ER biogenesis (Walter and Ron, 2011). It has also been shown that, apart from splicing XBP1, IRE1 can mediate RIDD (regulated IRE1-dependent decay), whereby ER-localised mRNAs are degraded to limit the number of newly synthesized proteins and decrease the protein load in the ER (Hollien and Weissman, 2006).

The second branch of the UPR is represented by ATF6. When unfolded proteins accumulate in the ER, its Golgi localisation sequences are revealed and it is translocated to this organelle. In the Golgi ATF6 is processed by site 1 and site 2 proteases, which cleave off the ER luminal and transmembrane domains (Haze *et al.* 1999). The resulting cytosolic fragment, which has DNA binding activity, moves to the nucleus and is a transcription factor that activates transcription of UPR-regulated genes, for example XBP1, Grp78 and Grp94 chaperones (78kDa and 94kDa glucose regulated proteins) and PDI (protein disulphide isomerase; Haze *et al.* 1999; Yoshida *et al.* 2001).

The third branch of the UPR is mediated by PERK (also known as eukaryotic initiation factor 2-alpha kinase, 3EIF2AK3). Similar to IRE1 it undergoes oligomerisation and autophosphorylation upon accumulation of unfolded proteins in the ER (Harding *et al.* 1999). However, unlike IRE1, PERK also phosphorylates eukaryotic translation initiation factor 2α (eIF2α). This results in lower translation initiation levels and decreased flux of new proteins into the ER (Harding *et al.* 2000). Some transcripts involved in the UPR are able to avoid this translational block and are preferentially translated when eIF2α is limiting, due to short upstream open reading frames in their 5' untranslated regions. An example of such a gene is ATF4, a transcription factor that is translationally induced by phosphorylation of eIF2α

(Vattem *et al.* 2004). Another two are CHOP (transcription factor C/EBP homologous protein) and GADD34 (growth arrest and DNA damage–inducible 34; Walter and Ron, 2011).

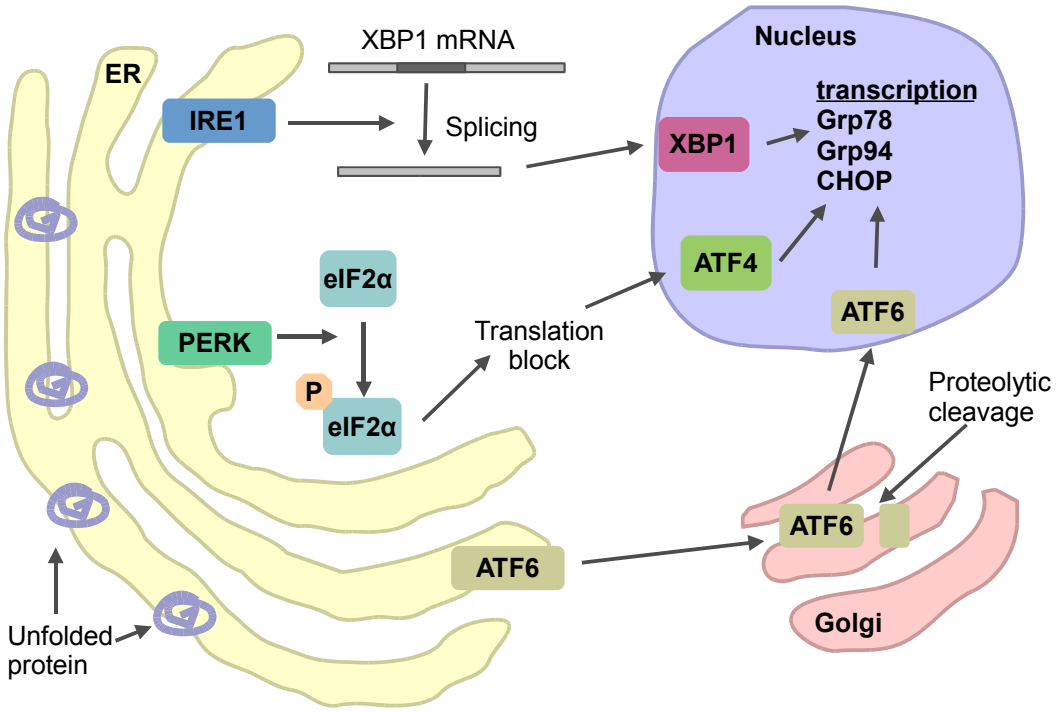

Figure 1.3. ER stress caused by accumulation of unfolded proteins triggers the UPR, which consists of three branches mediated by IRE1, PERK and ATF6, which transduce the ER stress signal to the nucleus. This results in transcription of genes whose products help resolve ER stress.

Activation of all three branches of the UPR results in a decrease in protein influx to the ER and expression of various genes that help cope with an increased load of unfolded proteins, such as mentioned before chaperones (for example Grp78 and Grp94; Kozutsumi *et al.* 1988; Luo *et al.* 2003), PDIs and genes involved in phospholipid synthesis and ER biogenesis (Sriburi *et al.* 2004), which leads to expansion of the ER and its protein folding capacity. Another mechanism activated in order to cope with an overabundance of unfolded proteins is ERAD (ER-associated degradation). In this process misfolded proteins are retrotranslocated to the cytoplasm and degraded by the the proteasome (Travers *et al.* 2000). Large aggregates of severely unfolded proteins that are difficult to degrade via ERAD can also be disposed of via autophagy, which has been shown to be activated during ER stress (Deegan *et al.* 2013). However, if ER stress is too overwhelming and cannot be

resolved it may lead to cell death (Sano and Reed, 2013).

Apoptosis is activated by ER stress via several mechanisms (Szegzedi *et al.* 2006; Sano and Reed, 2013). First of all, IRE1α activates TRAF2 (tumour necrosis factor receptor associated factor 2) which activates apoptotic-signaling kinase-1 (ASK1), causing activation downstream of stress kinases Jun-N-terminal kinase (JNK) and p38 MAPK (mitogen-activated protein kinase), that promote apoptosis (Urano *et al.* 2000). Among the apoptosis-inducing substrates of JNK are anti-apoptotic Bcl-2 and pro-apoptotic Bim, which are inhibited and activated, respectively, by JNK phosphorylation. In addition to IRE1, the ER stress-specific transcription factor CHOP has been implicated in ER-stress induced apoptosis (Zinszner *et al.* 1998). CHOP expression can be activated by all three UPR branches. It increases expression of pro-apoptotic Bim and DR5, while decreasing expression of anti-apoptotic Bcl-2 (Yamaguchi and Wang, 2004; Sano and Reed, 2013). Finally, ER stress can mediate cell death by disturbance in its calcium metabolism; Bax and Bak have been shown to regulate Ca^{2+} release from the ER upon ER stress (Scorrano *et al.* 2013). All upstream signals, such as the activation of transcription factors, kinase pathways and the regulation of Bcl-2 family members, ultimately lead to caspase activation, resulting in the ordered and sequential dismantling of the cell. Caspase 12 has been proposed as a key mediator of ER stress-induced apoptosis (Nakagawa *et al.* 2000), however this caspase is expressed only in rodents; its human homologue has been silenced by several mutations during evolution. Caspase 4 has been proposed to fulfil the function of caspase 12 in humans (Hitomi *et al.* 2004), but this is under debate, since it has been shown that apoptosis can be induced by ER stress without its activation (Obeng and Boise, 2005).

ER stress has been shown to be essential for many physiological processes, especially those involving professional secretory cells (Moore and Hollien, 2012). For example differentiation of B cells into plasma cells (Reimold *et al.* 2001) or insulin secretion by pancreatic β-cells (Harding *et al.* 2001) are associated with increases of protein folding demand that activate the UPR. However, ER stress has been also implicated in many pathological processes such as viral infections (Dimcheff *et al.* 2003) and atherosclerosis (Minamino *et al.* 2012).

1.3. Unfolded protein response regulates bone formation

When bone formation occurs during embryonic development, osteoblasts and chondrocytes need to secrete large amounts of ECM and regulatory proteins. It has been well documented, that in order to cope with the high demand of protein synthesis and secretion osteoblasts and chondrocytes employ UPR signalling (Tohmonda *et al.* 2011; Tsang *et al.* 2010) and the UPR has been shown to activate transcription of some bone specific genes.

The first hint that ER stress is involved in bone formation comes from a study which showed that XBP1 was highly expressed in developing skeletons of mouse embryos using *in situ* hybridisation. XBP1 was found to be expressed in osteoblasts forming bones via intramembranous bone formation and chondroblasts, which take part in the process of endochondral bone formation (Clauss *et al.* 1993). It was later shown that XBP1 mRNA expression can be induced by BMP-2 via IRE1 and that IRE1 and XBP1 are required for maturation of preosteoblasts to osteoblasts. XBP1 directly activated the promoter of Osterix, a key osteogenic transcription factor (Tohmonda *et al.* 2011). Moreover, XBP1 has been implicated in hypertrophic chondrocyte differentiation. It was shown to be a transcription target of ATF6 in BMP-2 stimulated chondrocytes and to form a complex with Runx2. Cells in which expression of XBP1 was abolished did not express Ihh and expressed low levels of chondrocytic collagen types 2 and 10, which showed that their differentiation was impaired (Liu *et al.* 2012). Another study has shown that transcription of parathyroid hormone (PTH)/PTH-related peptide receptor (PTH1R) was regulated by the IRE1-XBP1 pathway in osteoblasts (Tohmonda et al. 2013). In addition, overexpression of IRE1 was shown to inhibit differentiation of chondrocytes and enhance expression of PTHrP, which promoted their undifferentiated, proliferating phenotype (Guo *et al.* 2014a).

It has also been demonstrated that BMP-2 can upregulate IRE1, XBP1, CHOP, PERK, ATF4 and ATF6 expression (Tohmonda *et al.* 2011; Han *et al.* 2013). The findings about ATF6 were confirmed in a different study, which showed that BMP-2 activated Runx2 expression in mouse preosteoblasts, which in turn activated transcription of ATF6. It was also shown that ATF6 directly induced transcription of

OCN (Jang *et al.* 2011) and XBP1 (Guo *et al.* 2014b).

The most evidence about the involvement of ER stress in bone formation comes from studies of the PERK-ATF4 branch of the UPR. PERK knock-out mice exhibited skeletal dysplasias at birth and postnatal growth retardation. Skeletal defects included deficient mineralization, osteoporosis, and abnormal bone development (Zhang *et al.* 2002). Their osteoblast proliferation and differentiation was delayed, which was associated with decreased expression of Runx2 and Osterix. Also, mineralisation was reduced and defects of the ER were present due to accumulation of procollagen. Interestingly, ATF4 levels in these osteoblasts were normal, suggesting the presence of other factors downstream of PERK that regulate osteoblast maturation (Wei *et al.* 2008). However, Saito *et al.* placed ATF4 downstream of PERK in osteoblasts showing that knock-outs of these two genes have the same effects on bone formation. They have also shown that this branch of UPR can be induced by BMP-2 in osteoblasts and confirmed that this drives osteoblast differentiation (Saito *et al.* 2011). Upregulation of PERK has been observed in spinal ligament fibroblasts of patients with ossification of the posterior longitudinal ligament (Chen *et al.* 2014). In addition, the PERK-ATF4 pathway was demonstrated to be crucial for transdifferentiation of myoblasts into osteoblasts (Tanaka *et al.* 2014). This suggests that aberrant activation of these signalling pathways could lead to VSMCs assuming an osteo/chondrogenic phenotype.

The role of ATF4 in bone formation was confirmed in another study which demonstrated that ATF4-deficient mice exhibited a reduction in bone volume and they failed to ever achieve normal bone mass. This was because ATF4 directly activates transcription of OCN. What is more, ATF4 is involved in amino acid metabolism, so its absence resulted in insufficient amino acid availability for protein synthesis further disrupting normal bone formation (Yang *et al.* 2004b). The bones of mice lacking ATF4 have also been shown to be less tough and more brittle compared to those of their wild type conterparts (Makowski *et al*. 2014). ATF4 has also been shown to activate the transcription of Ihh, a cytokine that regulates chondrocyte proliferation in the growth plate (Wang *et al.* 2009). Ihh secreted by chondrocytes due to ATF4 activation has been shown to also have a paracrine effect

on osteoblasts and contribute to their differentiation (Wang *et al.* 2012). ATF4 has also been shown to regulate the expression of β-catenin and form complexes with this transcription factor in pre-osteoblasts (Yu *et al.* 2013). In addition, ATF4 transcriptional activity has been demonstrated to be regulated in osteoblasts by Twist-1, an important regulator of Runx2 activity (Dnaciu *et al.* 2102). Importantly, ATF4 is not detectable in any other adult tissues except bone, eye and cartilage, but it can induce the expression of OCN in non-osteoblast cell types (Yang *et al.* 2004a), suggesting that pathological activation of ATF4 in tissues other than those mentioned could cause calcification.

CHOP, the main mediator or ER-stress induced apoptosis has also been implicated in bone formation and metabolism in recent studies. CHOP knock-out in a pseudoachondroplasia mouse model decreased chondrocyte apoptosis and aggravated the bone malformation phenotype, suggesting that CHOP-mediated apoptosis is important for normal bone formation (Pirog *et al.* 2014). In addition, the UPR, and specifically CHOP, have been shown to play a role in response to injury and inflammation in osteoarthritic cartilage, where they mediate pro-inflammatory signals in chondrocytes (Husa *et al.* 2013).

In addition to the canonical ER stress transducers, two tissue-specific ER stress transducers, OASIS and BBF2H7, have been shown to be involved in osteoblast and chondrocyte maturation respectively (Murakami *et al.* 2009; Saito *et al.* 2009). Both of these transcription factors belong to the CREB/ATF family, have a bZIP (basic leucine zipper) and a transmembrane domain and are ATF6 homologues (Murakami *et al.* 2009).

OASIS was first discovered in astrocytes, and not until an *in situ* hybridisation experiment in mouse embryos was performed was its role in bone formation revealed. In mouse embryos OASIS expression was shown to overlap with expression of osteogenic markers such as osteonectin, type 1 collagen and OPN, suggesting that it played a role in bone development (Nikaido *et al.* 2001). A later study confirmed that the function of OASIS is osteoblast specific, as OASIS deficient mice exhibited severe osteopenia, involving a decrease in type 1 collagen in the bone matrix and a decline in the activity of osteoblasts. That is explained by the fact

that OASIS activates the transcription of COL1A1 through an unfolded protein response element (UPRE)-like sequence in its promoter region. Moreover, expression of OASIS and mild ER stress was induced in osteoblasts by BMP-2 (Murakami *et al.* 2009, Murakami *et al.* 2010). Mutations in OASIS in humans have been linked to severe recessive osteogenesis imprefecta, a genetic condition where bones are brittle and fail to mineralise properly (Symoens *et al*. 2013).

BBF2H7 is, like OASIS, another member of the CREB/ATF family of transcription factors (Kondo *et al.* 2007). BBF2H7 knock-out mice displayed severe chondrodysplasia and suffocated shortly after birth. The cartilage of these mice had disrupted structure and the chondrocytes had abnormally enlarged ER with accumulated ECM proteins inside, therefore it was concluded that this ER stress transducer is chondrocyte-specific. It was shown that upon ER stress induction BBF2H7 was activated by cleavage similarly to ATF6 and OASIS and activated transcription of Sec23a, a component of the protein coat of secretory COPII vesicles. In the absence of BBF2H7 chondrocytes could not secrete ECM, which impaired cartilage formation. It was also shown that Sox9, the main chondrogenic transcription factor, can induce mild ER stress in chondrocytes and activate BBF2H7 (Saito *et al.* 2009). A later study by the same group has demonstrated that Sox9 directly regulated transcription of BBF2H7 by binding to its promoter (Hino *et al.* 2014). In addition to that BBF2H7 was found to control chondrocyte maturation via another mechanism, by inhibiting ER-stress induced apoptosis via ATF5 and MCL1 (Izumi *et al.* 2012).

Finally, the chaperone protein Grp78 (BiP, hspa5, DnaK) has been shown to be involved in ECM mineralisation. GRP78 is a member of the heat shock protein 70 family. Its primary function is to act as a molecular chaperone in the ER and facilitate proper protein folding. However, It has been shown to be expressed and secreted by osteoblasts; Grp78 also localised on the surface of these cells. It has been shown to bind collagen type 1 and nucleate calcium and phosphate crystals *in vitro*, suggesting that it plays a role in bone ECM mineralisation (Ravindran *et al.* 2011). In a follow-up study the same group has shown that Grp78 expression is increased during embryonic development in condensing cartilage and MSCs of the alveolar

bone, endochondral bone and dental pulp, further supporting its important role in bone formation (Ravindran *et al.* 2012).

It is evident that ER stress signalling via the canonical ER stress pathways as well as tissue-specific ER stress transducers plays a major role in bone formation. The signalling pathways that link the UPR with bone formation have been summarized in the diagram in Figure 1.4.

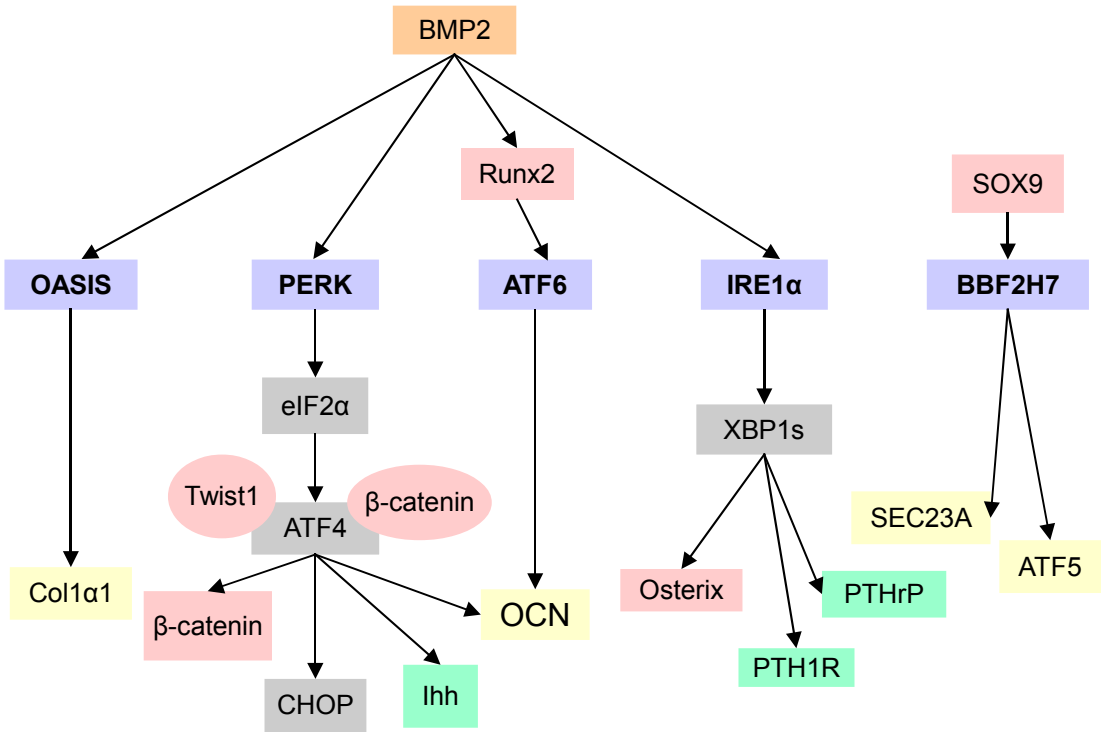

Figure 1.4. UPR regulation of bone formation signalling. BMP-2 signalling has been shown to activate all three branches of the canonical unfolded protein response in osteoblasts as well as OASIS. The pathway that begins with Sox9 represents chondrocyte-specific signalling. Blue – ER stress transducers; grey – other components of the UPR; red – osteogenic transcription factors; yellow – mineralisation regulating proteins; green – components of the Ihh/PTHrP pathways regulating chondrocyte maturation.

1.4. Endoplasmic reticulum stress in VSMCs and vascular calcification

Because ER stress and the unfolded protein response play an important role during bone formation and calcification of VSMCs resembles osteoblast maturation I hypothesised that ER stress plays a role in vascular calcification. This idea is supported by recently published studies.

It has been shown that vascular calcification induced in rats with nicotine and vitamin D is accompanied by upregulation of Grp78 and Grp94 chaperone expression in the aorta, which is indicative of ER stress (Duan *et al.* 2009). Moreover, markers of ER stress-induced apoptosis, CHOP and caspase 12 were also upregulated in those aortas. A more recent study from the same lab has shown that ATF4 was a mediator of ER stress-induced calcification, both in the rat model *in vivo* and in rat VSMCs *in vitro* (Duan *et al.* 2013). They also demonstrated that changes in calcification and ER stress markers correlated with osteogenic gene expression (OPN, ALP, Runx2).

The next line of evidence comes from a study which shows that in human coronary artery vascular smooth muscle cells (HCASMCs) BMP-2-mediated oxidative stress increased ER stress, demonstrated by increased expression of GRP78, phospho-IRE1 and XBP1 (Liberman *et al.* 2011). An increase in NADPH oxidase activity and oxidative stress occurred via activation of the BMP-2 receptor 2 and Smad1 signalling. This study also showed that XBP1 binds to the Runx2 promoter in BMP-2-treated HCASMCs. Inhibition of oxidative stress or ER stress decreased Runx2 expression, intracellular calcium deposition, and mineralization of BMP-2-treated HCSMCs.

It has also been shown that in a mouse VSMC line MOVAS-1, stearate (a saturated fatty acid) induced calcification and ER stress (Masuda *et al.* 2012). Stearate induced ATF4 mRNA and protein expression through activation of the PERK-eIF2α pathway. It also increased CHOP expression and XBP1 splicing. ATF4 knock-down blocked osteogenic differentiation (assessed by measurements of OCN and phosphate transporter Pit-1 mRNA) and mineralization induced by stearate. The same lab has shown that TNFα induced calcification of MOVAS-1 cells by activating the PERK-ATF4-CHOP branch of the UPR. They also presented evidence that this pathway was activated in aortas of mice with CKD induced by 5/6 nephrectomy (Masuda *et al.* 2013).

In addition to these studies, several others point to the role of UPR components in vascular disease and calcification. CHOP has been found to be upregulated by cyclic stretch in rat VSMCs, suggesting that hypertension might

induce ER stress (Cheng *et al.* 2008). An *in vivo* study in mice reported that inducing ER stress resulted in hypertension (Liang *et al.* 2013) suggesting that there might be a positive feedback loop mechanism regarding VSMC contractility and phenotype under mechanical stress.

Furthermore, a study in mouse VSMCs lacking the ENPP1 enzyme, which synthesizes pyrophosphate, a natural calcification inhibitor, showed that the absence of CHOP in these conditions increased calcification (Serrano *et al.* 2014). These results suggest that in these conditions CHOP protects cells from calcification.

The studies described above show that ER stress accompanies vascular calcification induced by various means *in vivo* and that it can increase VSMC mineralisation *in vitro* (Figure 1.5). However, these findings are very limited and therefore there remains a lack of definitive evidence that would explain what causes ER stress *in vivo* and whether it is activated in human calcified aortas. It is unclear via what mechanisms the factors mentioned in these studies induce ER stress. In addition, they did not explain how activation of UPR signalling lead to calcification of VSMCs, apart from increased apoptosis and potential activation of Runx2 expression by XBP1. A very limited number of osteogenic genes was examined in each of these reports, hardly allowing any conclusions as to osteogenic transdifferentiation and phenotype of VSMCs to be made. Each of these studies focused on one branch of the UPR, not reporting whether others are activated and lead to the same results.

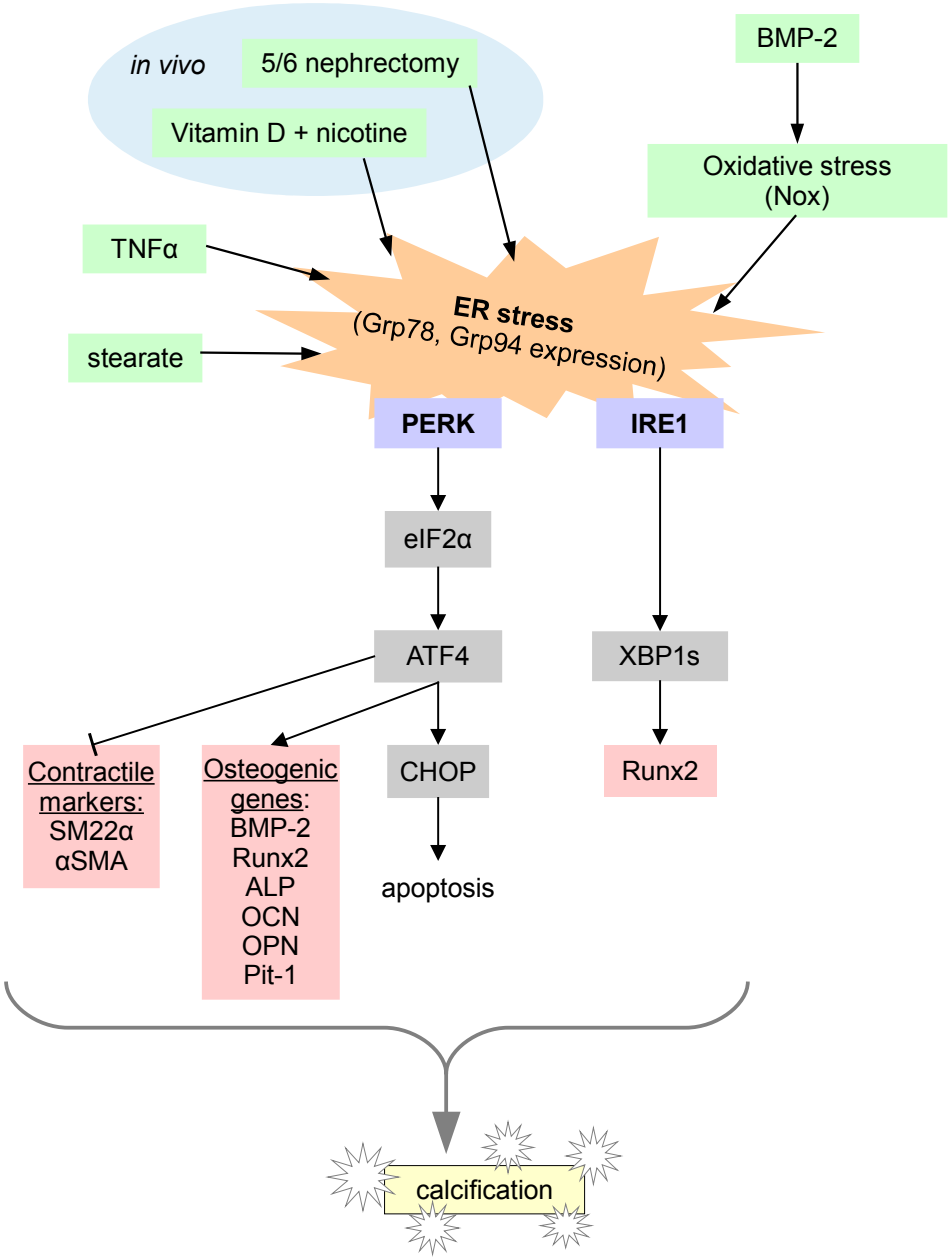

Figure 1.5. ER stress and the UPR in VSMC calcification (references in the text). Several factors that activate ER stress *in vitro* or in rodent models of calcification have been identified. It is still unclear how UPR activation leads to vascular calcification.

1.5. Aims

Vascular calcification is a regulated, VSMC-mediated process, however the exact molecular events that lead to vascular calcification are unknown. The resemblance of vascular calcification to bone formation lead to the hypothesis that ER stress could play an important role in vascular calcification, as it is a crucial process in osteogenesis. Therefore the main aim of my project was to examine the role of ER stress in vascular calcification.

I set out to examine potential changes in ER stress associated with vascular calcification in human aortas *in vivo,* as well as changes in calcification of VSMCs *in vitro* associated with ER stress. Another way of exploring the relationship between ER stress and vascular calcification was determining whether ER stress can be induced *in vitro* by known calcification-promoting factors.

Another part of the project was focused around vascular calcification mechanisms that ER stress could potentially modulate, and therefore I looked at apoptosis and osteogenic transdifferentiation of VSMCs.

The final aim was to look at regulation of osteogenic genes in response to ER stress in VSMCs in detail, and analyse whether osteogenic gene expression can be directly regulated by ER stress transcription factors.

Chapter 2: Materials and methods

2.1. Cell culture

2.1.1. Passaging

Human primary vascular smooth muscle cells (VSMCs) were used for most experiments. The cells were of aortic origin, collected from organ transplant donors, characterised and archived in the laboratory. All human materials were handled in compliance with the Human Tissue Act (2004, UK).

VSMCs were grown in M199 supplemented with 20% foetal bovine serum (FBS) and 100 U/ml penicillin, 100 U/ml streptomycin and 0.29 mg/ml glutamine (PSG), in a 4% CO_2 at 37°C incubator (Thermo Heraeus HERAcell 150). Cells were split 1:2 upon reaching 80% of confluency. For splitting VSMCs were washed with Earl's balanced salt solution (EBSS) twice and then incubated with 0.25% Trypsin/EDTA for 5 minutes at 37°C. Trypsin was neutralized by addition of complete culture medium, cells were centrifuged 5 minutes at 700x*g* at 4°C and cell pellet resuspended in complete culture medium. Cells were used for experiments between passages 8-12.

SAOS-2 and U2OS osteosarcoma cell lines were used as positive controls in some experiments. They were grown in Dulbecco's Modified Eagle's Medium (DMEM) supplemented with 10% FBS and PSG. They were passaged 1:5 when confluent, as described above.

2.1.2. Freezing

For freezing cells were trypsinized and cell pellet was resuspended in freezing medium (M199 supplemented with 30% FBS and 10% dimethyl sulfoxide - DMSO). Freezing vials containing cells were gradually frozen to -80°C in a Mr. Frosty Freezing Container (Thermo Scientific) for 24 hours and then transferred to liquid nitrogen.

2.1.3. Cell counting

Cells were trypsinised as described above and resuspended in complete

culture medium (1 ml of medium per 75cm^2 flask surface). 10 µl of the suspension was pipetted into an improved Neubauer hemocytometer (Marienfeld). Cells in three squares were counted and their number averaged, the value multiplied by 10000 to give the number of cells per 1ml.

2.1.4. Cell treatment with cytokines, growth factors, inhibitors and mineral ions

Cells were passaged as described above and incubated in complete cell medium for 24-48 hours. Then they were washed with EBSS twice and incubated in the presence or absence of additional components (Table 2.1) For the short treatment (24 hours or less) cells were incubated in M199 supplemented with 0.5% FBS and PSG. For treatments longer than 24 hours cells were treated in M199 supplemented with 5% FBS and PSG.

Table 2.1. Reagents for cell treatments.

Treatment	Catalog no	Solvent	Stock concentration	Final concentration
4-phenylbutyric acid (PBA)	Sigma, P2,100-5	M199	20mM	0.5mM
BMP-2	Cell Signalling, 4697S	10mM HCl	0.1mg/ml	100ng/ml
$CaCl_2$ (Ca)	Sigma, C7902	H_2O	100mM	2.7mM
H_2O_2	Sigma, H1009	PBS	30%	1-20µM
Hydroxyapatite (HAp)	Sigma, 289396	HBSS	15mg/ml	50-150µg/ml
NaK_2PO_4 (P)	Sigma, S-5011	H_2O	100mM	2.5mM
PDGF	Gibco, PHG0045	0.1M acetic acid/ 0.1% BSA	100µg/ml	10 pg/µl
Staurosporine (SSP)	Sigma, S5921	DMSO	1 mg/ml	0.5µg/ml
TGFβ1	PeproTech, 100-21	PBS/0.1% BSA	20 ng/µl	2 pg/µl
Thapsigargin (TG)	Sigma, T9033	DMSO	1mg/ml	0.01-0.2µg/ml
TNFα	R&D Systems, 210-TA	PBS/0.1% BSA	100 ug/mL	10 pg/µl
Tunicamycin (TM)	Sigma, T7765	DMSO	1mg/ml	0.04-0.4µg/ml

Vitamin D3	Sigma, D1530	20% ethanol	10^{-5}M	10^{-9} - 5x10^{-7}M
Warfarin	Sigma, P5104	DMSO	100mM	10-200µM

2.1.5. Transient gene knock-down with siRNA and miRNA

SiRNA transfection was performed in order to knock down ATF4, ATF6 and Osterix in VSMCs. Cells were incubated in the complete medium for 24 hours and then transfection medium was applied for 48 hours. For one well of a 48 well plate the transfection medium contained 250µl M199 with 20% FBS and PSG, 25µl OptiMEM, 3µl HiPerfect and 3pmol siRNA oligouncleotide smartpool (GE Dharmacon). MiRNA transfections were performed using the same protocol, MISSION miRNA mimcs were purchased from Sigma.

2.1.6. Retroviral transduction

PG13 cells constitutively producing retroviruses with an Osterix shRNA, human Osterix cDNA or empty vectors were kindly provided by professor Kurt Hankenson (University of Pennsylvania, Philadelphia, United States) (Zhu *et al.* 2012). PG13 cells were maintained in DMEM supplemented with 10% FBS and PSG and passaged 1:5 every 2 days.

Virus-containing media was collected from cells and filtered through 0.45µM filters and added to VSMCs (70% of confluency, 24 hours post-plating) in complete VSMC growth medium (M199 with 20% FBS and PSG) supplemented with 8µg/ml polybrene. For the treatment virus-containing medium was diluted with M199 with 20% FBS and PSG in the following proportions: 1:2, 1:4 or 1:10. VSMCs were incubated with viral media for 48 hours, and harvested for gene expression analysis.

Alternatively, 24 hours after plating VSMCs (70% of confluency) were centrifuged 90 minutes at 1200x*g* in the culture plates with undiluted viral supernatants and then virus-containing medium was changed to complete growth medium. The procedure was repeated the following day. Gene expression was analysed in 24 hours after the last spin.

2.1.7. Lentiviral transduction

VSMCs (80% of confluency) were transduced with four different clones of TRC1 pLKO.1 Osterix shRNA MISSION Lentiviral Transduction Particles (Sigma), according to the manufacturer's protocol. Empty vector (TRC1 pLKO.1) was used as a negative control. Viral particles were added to growth media at MOI (multiplicity of infection) 2 and 10 in the complete growth medium supplemented with 8µg/ml hexadimethrine bromide and cell were incubated for 24 hours. The growth media were changed next day and cells were incubated another 24 hours and protein expression was evaluated by Western blotting.

To measure the transduction efficiency, SAOS-2 cells were transduced with pLKO.1-CMV-tGFP MISSION Lentiviral Transduction Particles (Sigma) as described above and GFP fluorescence was observed with Olympus IX81 microscope and pictures were taken with Hamamatsu 1394 ORCA-ERA camera using Volocity software (PerkinElmer).

2.2. Cell viability assays

2.2.1. MTT assay

In an MTT assay cell viability is assessed by measuring the activity of mitochondrial NAD-dependent dehydrogenases. In viable cells the soluble yellow MTT salt (3-(4,5-Dimethylthiazol-2-yl)-2,5-diphenyltetrazolium bromide) is converted by enzymes to purple insoluble formazan crystals. Formazan crystals are solubilised with acidified isopropanol (isopropanol mixed with hydrochloric acid), and light absorbance of the solution is measured.

VSMCs were seeded in a 96-well plate in triplicate (5000 cells/well) and treated with tunicamycin and thapsigargin. The assay was performed using *In Vitro* Toxicology Assay Kit, MTT Based (Sigma) according to the manufacturer's protocol. MTT solution (10µl per well) was added and cells were incubated in the cell culture incubator for 2 hours at 37°C. Next, 100µl of the solubilisation solution was added to each well to dissolve the formazan crystals. Absorbance was measured at 560nm with TECAN Genios Pro Multifunction Microplate Reader. Absorbance at 710nm was also measured and subtracted from the 560nm measurements as background.

2.2.2. Apoptosis and necrosis analysis

Analysis of cell death was carried out using the Green FLICA Caspases 3&7 Assay Kit (Immunohistochemistry) according to the manufacturers' protocols. In this assay Hoechst 33342 is added to cells to stain the nuclei and enable counting the total number of cells. Carboxyfluorescein FLICA reagent is based on the caspase inhibitor zVAD-FMK, and therefore is bound by apoptotic cells with activated caspases 3 and 7. Propidium iodide (PI) is used to stain necrotic cells, as it binds to DNA in cells with disintegrated plasma membranes.

For each assay cells from a 24 well plate were trypsinized and resuspended in 80µl of fresh medium. 61µl of the cell suspension were then taken and 3.3µl of FLICA reagent and 1.3µl Hoechst 33342 were added for 1 hour at 37°C. Then cells were pelleted at 400x*g* for 5 min at 4°C and washed with apoptosis wash buffer twice (included in the FLICA assay kit). Cell pellet was resuspended in 60µl of apoptosis wash buffer containing 10 µg/ml of PI and 30µl was transferred into a measurement chamber of the NC-Slide A2 (Chemometec) and immediately scanned in the NucleoCounter NC-3000 (Chemometec) using a predefined caspase assay protocol.

The percentage of healthy, apoptotic and necrotic cells in each sample was determined based on the scatter plots generated by the NucleoCounter software. Cells with low green fluorescence signal (FLICA) and low PI signal were deemed healthy, cells with high FLICA signal were deemed apoptotic and cells with a high PI signal were considered necrotic.

2.3. Animal tissue preparations

All animal procedures were performed under Home Office license authority in accordance with the Guidance on the Operation of the Animals (Scientific Procedures) Act, 1986 (UK Home Office).

2.3.1. Mouse aortic rings

Aortas were harvested from wild type C57BL/6 and DBA/2 mice (male and female), purchased from Harlan Laboratories (UK) and maintained in a pathogen-

free environment with food and water provided *ad libitum*.

Mouse aortas (staring from the arch and including the abdominal aorta) were harvested into serum free M199 and washed extensively in sterile HBSS. The adventitia was gently stripped away and each vessel was cut into 6-9 pieces (rings), which were randomly assigned to experimental conditions. The vessel rings were treated with tunicamycin and thapsigargin for 24 hours, 36 hours, 7 days or 14 days.

Incubated rings were harvested, each was weighted and homogenised either for Western blotting or ALP activity assay. For homogenisation aortic ring was placed in a tube with ceramic beads (MP Bio) with a small volume of lysis buffer, shaken in a Bertin Technologies Precellys 24 tissue homogeniser twice for 20 seconds, and centrifuged in benchtop centrifuge (Eppendorf) at 13 000 rpm for 5 minutes at 4°C to pellet the tissue debris. Supernatants were transferred to a fresh tubes.

Alternatively, intact treated vessel rings were fixed for histological analysis as described in the following sections.

2.3.2. Rat aortic samples

Samples of thoracic aorta from 21-28 day old wild type male Sprague-Dawley rats were kindly provided by Mr Jayanta Bordoloi, Cardiovascular Division, King's College London, UK. The rats were purchased from Charles River Laboratories (UK) and fed 3 mg warfarin and 1.5 mg vitamin K1 per 1g of food for 11 days. The control group consisted of rats fed a standard diet.

For Western blotting the tissue samples were homogenised as described above. Fragments of the same vessels were analysed with immunohistochemistry as described below.

2.4. Western blotting

2.4.1. Cell lysis

Cells were washed twice with PBS and scraped in lysis buffer. Samples were sonicated for 10 seconds (Branson Sonifier 150) and centrifuged for 15 minutes at 15000 rpm at 4°C. Supernatants were transferred to new tubes and protein concentration was determined using BioRad DC Protein Assay kit and TECAN Genios

Pro Multifunction Microplate Reader. Samples were mixed 1:3 with 4x SDS-PAGE loading buffer and incubated 5 minutes at 95°C.

2.4.2. Nuclear fractionation

Cells were washed with PBS, scraped with a small volume of PBS and centrifuged for 5 minutes at 5000 rpm at 4°C. Supernatants were discarded and cell pellets were resuspended in buffer A. Samples were incubated 20 minutes on ice and then centrifuged for 5 minutes at 5000 rpm at 4°C and the supernatants were collected (cytoplasmic fraction). The pellets were washed once with buffer A (resuspended, centrifuged for 5 minutes at 5000 rpm at 4°C and supernatant discarded) and resuspended in IP buffer. Then samples were centrifuged for 5 minutes at 5000 rpm at 4°C the supernatants were collected into new tubes (nuclear fraction). Protein assay was performed and samples for SDS-PAGE were prepared as described above.

2.4.3. Sodium dodecyl sulphate – polyacrylamide gel electrophoresis (SDS-PAGE)

Samples were analysed by using 10% acrylamide resolving gel and 5% stacking gel. Equal amounts of protein (determined by protein assay) were loaded on gels. Gels were immersed in SDS-PAGE running buffer and ran at 80-120V until bromphenol blue indicator reached the end of the gel.

2.4.4. Western blotting

After SDS-PAGE proteins were transferred to PVDF membranes (Immobilon-P, Milipore) using a Trans-Blot SD Semi-Dry Transfer Cell (Bio-Rad) in Western blotting transfer buffer at 25V for 1 hour. Membranes were blocked in PBST with 5% milk for 1 hour at room temperature and then incubated with primary antibody (see Table 2.2) diluted in blocking buffer, overnight at 4°C. Membranes were washed in blocking buffer (10 minutes) and HRP-conjugated secondary antibody (diluted 1:5000 in the blocking buffer) was applied for 1 hour at room temperature. Next, membranes were washed for 1.5 hours with 4 changes of PBST. Amersham ECL Prime Western Blotting Detection Reagent (GE Healthcare) was applied for 5

minutes. Protein bands were visualised on X-ray film (Xograph) developed in an automatic X-ray film processor (Xograph).

Alternatively, proteins were transferred to Immobilon-FL PVDF membranes, and infrared dye-conjugated secondary antibodies diluted 1:10000 in blocking buffer were used. Then protein bands were visualised by using the Li-Cor Odyssey CLx infrared scanner.

2.4.5. Membrane stripping

Membranes were incubated with 0.2 M NaOH for 10 minutes, thoroughly washed in double-distilled H_2O and PBS and then blocked and re-probed.

Table 2.2. Antibodies used for Western blotting.

	Antibody	Species	Dilution	Company
Primary	ALP	rabbit	1:10000	Abcam, ab108337
	ATF4	rabbit	1:1000	Santa Cruz, sc-200
	BBF2H7	rabbit	1:1000	Abcam, ab102989
	CNN1	rabbit	1:5000	Abcam, ab46794
	GAPDH	rabbit	1:5000	Santa Cruz, sc-25778
	Grp78 and Grp94 (KDEL)	mouse	1:2500	Assay Designs, SPA-827
	OASIS	rabbit	1:500	Abcam, ab33051
	Osterix	rabbit	1:1000	Abcam, ab22552
	p-MLC	mouse	1:500	Cell Signalling, 36755
	Runx2	rabbit	1:500	Abcam, ab48812
	SM22a	rabbit	1:1000	Abcam, ab14106
	SMAD1	rabbit	1:1000	Cell Signalling, 9743S
	SMAD2	rabbit	1:1000	Cell Signalling, 3122S
	SMAD3	rabbit	1:1000	Abcam, ab40854
	SMAD4	rabbit	1:1000	Cell Signalling, 9515S
	Sox9	rabbit	1:300	Abcam ab3697
	VDR	mouse	1:500	Santa Cruz, sc-13133
	β-actin	mouse	1:10000	Sigma, A2228

	Antibody	Species	Dilution	Company
Secondary	anti-mouse	sheep	1:5000	GE Healthcare, NA931V
	anti-rabbit	donkey	1:5000	GE Healthcare, NA934V
	Anti-Mouse IRDye 800 CW	goat	1:10000	Li-Cor, 926-32210
	Anti-Rabbit IRDye 680 RD	goat	1:10000	Li-Cor, 926-68071

2.4.6. Quantification of western blots

X-ray films were scanned in an EPSON Perfection 2400 Photo scanner and densitometry was carried out in Image J. Blots scanned with Odyssey were analysed using Li-Cor Image Studio Lite 4.0.

Quantification was carried out in Apache Open Office Calc 4.1.1, graphics and statistical analysis were carried out in GraphPad Prism 5. Signal intensity was normalised to the intensity of expression of house-keeping proteins (GAPDH or β-actin). Where appropriate one way ANOVA with Tukey or Dunnet *post hoc* test or t-tests were carried out to determine statistical significance.

2.5. Immunocytochemistry

VSMCs were grown on glass coverslips in 24 well plates (15000 cells/well). After treatments cells were washed twice with PBS and fixed with 4% PFA for 10 minutes at 37°C. Then cells were washed with PBS and were permeabilized with 0.5% NP-40 for 5 minutes at room temperature, washed with PBS twice and blocked in 2% BSA for 1 hour at room temperature. After blocking cells were incubated with primary antibody (see Table 2.3) diluted in blocking buffer, overnight at 4°C. The following day cells were washed three times with PBS and fluorescent dye-labelled secondary antibodies were applied for 1 hour at room temperature, the coverslips were protected from light from this stage on. After that DAPI (0.1µg/ml) was applied for 1 minute at room temperature to visualise nuclei, the coverslips were washed three times with PBS and mounted in Mowiol mounting medium. The following day the cells were observed with Olympus IX81 microscope and pictures were taken with Hamamatsu 1394 ORCA-ERA camera using Volocity software.

Table 2.3. Antibodies used for immunocytochemistry.

	Antibody	Species	Dilution	Company
Primary	CD63	mouse	1:500	BD Pharmingen, 556019
	CD107a (LAMP1)	mouse	1:250	BD Pharmingen, 555798
	EEA1	mouse	1:500	BD Transduction Laboratories, 610456
	Osterix	rabbit	1:500	Abcam, ab22552
	p-PERK	rabbit	1:250	Santa Cruz, sc-32577
	IRE1	rabbit	1:250	Santa Cruz, sc-20790
Secondary	Alexa fluor 488 anti-rabbit	goat	1:500	Invitrogen, A-11008
	Alexa fluor 568 anti-mouse	goat	1:500	Invitrogen, A-11004

2.6. Histological analysis of mouse and rat aortas

2.6.1. Hematoxylin and eosin staining of mouse aortic rings

Mouse rings treated as described above were fixed in 4% PFA for 4 hours and then incubated in 70% ethanol for another 24 hours. After that the tissue samples were dehydrated and infiltrated in paraffin in a Shandon Hypercenter XP and embedded in paraffin wax blocks using a Sakura Tissue-TEK TEC tissue embedding console. A rotary microtome (Leica RM2125RTF) was used to cut 5 µm sections of the aortas.

The sections were dewaxed in xylene for 10 minutes and rehydrated twice in 100% ethanol for 3 minutes and in 70% ethanol for 3 minutes and then in water for 5 minutes. The sections were stained with hematoxylin to visualise nuclei for 5 minutes, fixed with acid alcohol (1% HCl in 70% ethanol) and washed in water for 5 minutes. They were incubated in eosin, which stains the cytoplasm, for 3 minutes and rinsed 5 times with water. Next, samples were dehydrated in 70% ethanol for 1 minute, twice in 100% ethanol for 3 minutes, twice in xylene for 5 minutes and mounted with DPX mounting medium.

The following day the sections were observed with Olympus IX81 microscope and pictures were taken with a Q Imaging Micropublisher 3.3 RTV camera using

Volocity software (PerkinElmer).

2.6.2. Immunohistochemical staining of rat aortas

Rat aortas were fixed, sectioned and dehydrated as described above. Next, antigens disrupted by PFA fixing were retrieved by steaming the sections in citrate buffer (Vector Labs) in a steamer (Russel Hobbs) for 15 minutes. Slides were washed in PBST and incubated 10 minutes in PBS containing 3% H_2O_2 and 10% methanol to quench endogenous horseradish peroxidase (HRP) activity. Then slides were washed three times with PBST and then were blocked in normal horse or goat serum from the relevant VECTASTAIN ABC kit (Vector Labs) for 1 hour at room temperature in a humidifying chamber. After that primary antibodies were applied (Table 2.4) overnight at 4°C. The next day sections were washed three times in PBST and incubated with HRP-linked secondary antibodies from the VECTASTAIN ABC kit 1 hour at room temperature. They were then washed 3 times in PBST and incubated 30 minutes with the ABC reagent, which amplifies the HRP signal. After another 3 washes sections were incubated with the DAB reagent (Vector Labs) until brown colour developed, the reaction was stopped in water. The sections were stained with hematoxylin, dehydrated and mounted as described above.

Table 2.4. Antibodies used for immunohistochemistry.

	Antibody	Species	Dilution	Company
Primary	Grp78 and Grp94 (KDEL)	mouse	1:500	Assay Designs, SPA-827
	ATF4	rabbit	1:250	Santa Cruz, sc-200
	ALP	rabbit	1:250	Abcam, ab108337
	Osterix	rabbit	1:250	Abcam, ab22552
Secondary	VECTASTAIN ABC Kit mouse	horse	-	Vector Labs, PK6102
	VECTASTAIN ABC Kit rabbit	goat	-	Vector Labs, PK6101

2.7. Quantitative real-time PCR

2.7.1. RNA isolation

RNA was extracted from cells using RNA-STAT 60 according to manufacturer's protocol. Briefly, cells were scraped with RNA STAT 60, transferred to 1.5ml tubes and incubated for 5 minutes at room temperature to let nucleic acids dissociate from protein complexes. Chloroform was added (in a 1:5 proportion to the cell lysate) to extract proteins and samples were vortexed. Samples were centrifuged 15 minutes at 12,000x*g* at 4°C and isopropanol was added to supernatant to precipitate RNA for 30 minutes on ice, and then centrifuged for 10 minutes at 12,000x*g* at 4°C. The pellet was washed with 75% ethanol, air-dried and then resuspended in DEPC-treated water.

Concentration of isolated RNA was determined using a Nanodrop ND-1000 spectrophotometer. A sample was considered pure enough for experiments if the absorbances at 260/280 and 260/230 ratio were at least 1.8 and 1, respectively.

2.7.2. Reverse transcription

Reverse transcription (RT) was carried out in 20µl reactions using 0.1µg/µl RNA, with 7.5ng/µl of Random and Oligo dT primers, dNTP mix (0.25 mM each nucleotide), 0.5 U/µl RNAsin RNase inhibitor, 5x MU-MLV buffer and 1 U/µl Mu-MLV reverse transcriptase.

Primers, RNA and dNTPs were added to 0.2ml PCR tubes and incubated for 5 minutes at 65°C prior to the reaction in order to allow the primers to denature. Then buffer, RNAsin and DEPC-treated water were added and incubated for 3 minutes 37°C incubation to activate the RNAsin. The reverse transcriptase was added and the RT was carried out for 10 minutes at 25°C and then 50 minutes at 37°C with a final incubation at 95°C for 5 minutes, in an Applied Biosystems 2720 Thermal Cycler. The cDNA was diluted with double-distilled water to the final volume 100µl for each 2µg RNA used.

2.7.3. Quantitative real-time PCR

Expression of all genes was quantified using the $2^{-\Delta\Delta Ct}$ method (Livak and

Schmittgen 2001). All primers (see Table 2.5.) were validated for this method (see appendix). qPCR was carried out in 20µl reactions with 2x MESA GREEN qPCR MasterMix and a final concentration of 0.125µM of each primer in a Corbette RotorGene 3000. 40 cycles of 95°C for 15 seconds and 60°C for 60 seconds were carried out, with a melt curve analysis step at the end.

Table 2.5. Primers used for qPCR.

Gene	Primer sequence (5'-3')	Annealing temperature	Amplicon size
ALP	F: ACGAGCTGAACAGGAACAACGT R: CACCAGCAAGAAGAAGCCTTTG	55°C	104bp
ATF4	F: CAACAACAGCAAGGAGGATGCCTT R: TGTCATCCAACGTGGTCAGAAGGT	55°C	143bp
ATF6	F: CAGCAGCACCCAAGACTCAAACAA R: ACCACAGTAGGCTGAGACAGCAAA	55°C	163bp
BBF2H7	F:CTCATGGTTGTGGTGCTGTGCTTT R:AGCCATCTTGGTGGCAGAAGGATA	55°C	87bp
BMP-2	From QIAGEN, QT00012544	60°C	148bp
BSP	F: AGTTTCGCAGACCTGACATCCAGT R: TTCATAACTGTCCTTCCCACGGCT	55°C	161bp
CHOP	F: AGTCATTGCCTTTCTCCTTCGGGA R: AAGCAGGGTCAAGAGTGGTGAAGA	55°C	165bp
Col1α1	F: TGTGGCCCAGAAGAACTGGTACAT R: ACTGGAATCCATCGGTCATGCTCT	55°C	89bp
COMP	F: GCAGATGGAGCAAACGTATTGGCA R: AGGACTTCTTGTCCTTCCAACCCA	55°C	200bp
DLX5	F: GACTCAGTACCTCGCCTTGC R: GAGACTGCGGCGAGTTACAC	56°C	188bp
GAPDH	F: CGACCACTTTGTCAAGCTC R: CAAGGGGTCTACATGGCAAC	55°C	229bp
IRE1	F: CCTCCGAGCCATGAGAAATAAG R: GGGAAGCGAGATGTGAAGTAG	62°C	114bp
MSX2	F: AAATTCAGAAGATGGAGCGGCGTG R: CGGCTTCCGATTGGTCTTGTGTTT	59°C	115bp
OASIS	F:TCAACAATGCGCACTTTCCTGAGC R:TCTCATCCAGCACAGGGTCATCAA	55°C	108bp

Gene	Primer sequence (5'-3')	Annealing temperature	Amplicon size
OCN	F: GGCAGCGAGGTAGTGAAGAG R: CGATAGGCCTCCTGAAAGC	60°C	138bp
OPG	From QIAGEN, QT00014294	60°C	107bp
OSX	F: TGCTTGAGGAGGAAGTTCAC R: AGGTCACTGCCCACAGAGTA	54°C	148bp
PERK	F: AGGCTTTGGAATCTGTCACTAA R: CAGGAGTTCTGGAAGGAGAATG	57°C	93bp
RUNX2	From QIAGEN, QT00020517	60°C	101bp
SEC23A	F:TCCTGGAGATGAAATGCTGTCCCA R:TTCTAGCGTACCACCAAAGCCCAT	55°C	152bp
SOX9	F: AGCTCTGGAGACTTCTGAACGAGA R: ACTTGTAATCCGGGTGGTCCTTCT	55°C	99bp

Initial analysis of qPCR results was carried out in the Rotor Gene software provided with the thermocycler. Melt curves were inspected for the presence of only one sharp peak per primer pair. The cycle thresholds (Ct values) were set in the middle of amplification curves. Fold change ($2^{-\Delta\Delta Ct}$) calculations were carried out in Apache Open Office Calc. Graphs and statistical analyses were carried out in GraphPad Prism. Where appropriate, one way ANOVA with Tukey or Dunnet *post hoc* test or t-tests were carried out to determine statistical significance. Graphs show n=3 unless stated otherwise.

2.7.4. Human Osteogenesis Primer Library

Human Osteogenesis Primer Library (HOST-1, RealTimePrimers.com) was used to analyse osteogenic marker expression in VSMCs treated with tunicamycin. The library consisted of 96 primer pairs, including 8 housekeeping genes.

RNA was isolated from tunicamycin-treated and control VSMC samples and RT was carried out as described above. 5µg of RNA was used as a template and cDNA final volume was 1120µl.

β-2-microglobulin was the housekeeping gene used to normalise the gene expression, as no changes in β-2-microglobulin expression were detected in the

tunicamycin-treated sample. The results were analysed using the $2^{-\Delta\Delta Ct}$ method as described above.

The mRNA expression data was then overlayed over a protein-protein interaction network retrieved by Cytoscape 3.2.0 software. The network was created by feeding names of genes included in the library into Cytoscape and retrieving information from all available online interaction databases.

2.7.5. Analysis of gene expression in human aortic samples

Expression of 4 ER stress markers and 7 osteogenic markers was measured in RNA from human aortic samples previously characterised and archived in our laboratory. Human materials were handled in accordance with the ethical guidelines of University of Cambridge, where they originated from.

Ten samples of each of the following groups were chosen for analysis: healthy, fatty streak and calcified. RT and real-time PCRs were carried out as described above. Analysis of each primers pair had to be split into two qPCRs because of the large number of samples. Therefore the $2^{-\Delta\Delta Ct}$ analysis could not be used, as fold changes cannot be compared between separate real-time PCR runs. Instead, all analyses show –ΔCt values, which reflect the changes in gene expression in the same way.

2.8. XBP1 splicing assay

2.8.1. Reverse transcription and polymerase chain reaction (RT-PCR)

In order to detect splicing of XBP1 mRNA as indicator of ER stress, RNA extraction and reverse transcription were carried out as described above, followed by PCR for XBP1. PCR reactions were carried out with 2x Go Taq Green PCR mastermix in 50µl reactions with 0.25µM of each primer (Table 2.6) with 35 cycles of 94°C for 10s, 64°C for 30s, 72°C for 30s in an Applied Biosystems 2720 Thermal Cycler.

Table 2.6. Primers used for XBP1 assay.

Gene	Primer sequence (5'-3')	Annealing temperature	Amplicon size
XBP1	F: AAACAGAGTAGCAGCTCAGACTGC R: TCCTTCTGGGTAGACCTCTGGGAG	64°C	473 bp

2.8.2. Restriction enzyme digestion

In order to differentiate between the spliced and unspliced XBP1 mRNA, the PCR product was purified with a QIAquick PCR Purification Kit (Qiagen) according to the manufacturers protocol and digested with PstI restriction enzyme (Promega). Only unspliced PCR product of XBPI gene is susceptible to PstI digestion. The digestion was carried out in 20µl reactions with buffer H (Promega) for 4 hours at 37°C.

2.8.3. Agarose gel electrophoresis

Following the digest products were resolved on a 2% agarose gel in TAE buffer. Samples were resolved at 70V for 30 minutes. Gels images were acquired using UVP BioSpectrum Imaging System.

2.9. Calcification assays

Cells were plated in 48-well plates (10000 cell/well, for cresolphthalein assay) or 24-well plates (20000 cells/well, for Alizarin Red S staining) and incubated for 24 hours. Then the cells were washed twice with EBSS and treated with calcification media (M199 supplemented with 5% FBS and PSG, with the addition of Ca^{2+} and PO_4^{3-}) in the presence or absence of TM, TG and PBA. The cells were incubated for 8 days with the media changed every 3 days.

2.9.1. Cresolphthalein assay

This assay was carried out in order to quantify the calcium deposition mediated by VSMCs. It is based on the ability of o-cresolphthalein to form a purple

complex with calcium at basic pH.

Cells were plated with duplicates for each condition, so that they could be analyased both for calcium deposits and protein content for assay normalisation. Cells were washed with HBSS and then incubated overnight at 4°C with 100µl 0.1M HCl in order to lyse the cells and dissolve the mineral deposited in the well, or with 20µl 1%SDS/0.1MNaOH in order to lyse the cells for protein measurements. The following day, 55µl of each HCl-lysed sample was transferred to a 96-well plate and 25µl of ddH2O, 10µl of o-cresolphthalein solution and 200µl of ammonia buffer were added. Serial dilutions of $CaCl_2$ were made to form a standard calibration curve. Absorbance was measured at 540nm by using TECAN Genios Pro Multifunction Microplate Reader.

Calcium concentrations were calculated in Apache Open Office Calc 4.1.1 and normalised to protein concentrations which were determined using the Biorad DC Protein Assay. Fold changes of normalised calcium content were plotted in GraphPad Prism 5 and where appropriate one way ANOVA and Dunnet or Tukey *post hoc* statistical significance tests were performed.

2.9.2. Alizarin Red S staining

This assay was used to visualise calcification in wells, as Alizarin Red S stains calcium deposits red.

Cells were washed twice in PBS and fixed with 4% PFA for 10 minutes at 37°C, washed twice with water and stained with 2% Alizarin Red S for 5 minutes and then washed with water twice. The plate was scanned using an EPSON Perfection 2400 Photo scanner.

2.10. Alkaline phosphatase activity assay

2.10.1. Human primary vascular smooth muscle cells

Alkaline phosphatase (ALP) assay is a colorimetric test based on the hydrolysis of phosphate group from a colourless substrate p-nitrophenyl phosphate (pNPP) by ALK yielding coloured p-nitrophenyl (pNP) product.

Cells were washed with PBS, scraped with 1% Triton X-100 in PBS and lysed

by freeze-thawing twice. The lysates were centrifuged at 13,000x*g* for 5 minutes at 4°C and supernatants transferred to fresh tubes. Equal volumes of each sample were loaded in triplicate on a 96-well plate. 5mg pNPP was dissolved in 5ml ALP assay buffer and 100µl of the solution was added to each well with sample and negative control and mixed. The plate was covered and incubated at 37°C for 30 minutes. After that serial dilutions of 10mM pNP were prepared in the same plate (to form a standard calibration curve) and absorbance was measured at 405nm by using a TECAN Genios Pro Multifunction Microplate Reader. Protein concentration in each sample was measured using the DC Protein Assay according to the manufacturer's protocol.

Alkaline phosphatase activity was normalised to protein concentration in each sample and was expressed as µM of pNP generated per minute.

2.10.2. Mouse aortic rings

Aortic ring homogenates were prepared as described in section 3.1. ALP assay was carried out using the same protocol as for cells, with the exception of the freeze-thaw step, which was omitted.

2.11. Alkaline phosphatase promoter analysis

Ten deletion constructs containing fragments of the human tissue-nonspecific alkaline phosphatase (ALP) promoter cloned into the pGL3-BV vector with the firefly luciferase gene were kindly provided by Dr Hideo Orimo from Nippon Medical School in Tokyo, Japan (Orimo and Shimada 2005). The pRL-TK renilla luciferase control vector was kindly provided by Dr Alison Brewer from the Cardiovascular Division, King's College London, UK.

2.11.1. Bioinformatic analysis of ALP promoter DNA sequence

The sequence corresponding to the -122 to -4556 (counting from the first nucleotide of the initiation codon) of the ALP promoter was analysed with Matinspector (Genomatix) for the presence of transcription factor binding sites.

2.11.2. Generation of competent *E. coli* DH5α cells and transformation with luciferase constructs

E. coli DH5α cells were cultured in 5ml of antibiotic-free LB broth at 37°C in a shaking (220rpm) incubator for 18 hours. The following day 2ml of culture was diluted in fresh LB broth and cultured until the OD_{600} was 0.3. Bacteria cells were then pelleted by centrifugation at 1200x*g* for 10 minutes and resuspended in 20ml of sterile, ice cold 100mM $CaCl_2$. This step was repeated and then after a final centrifugation the bacteria were resuspended in 10ml 15% glycerol/100mM $CaCl_2$ and stored in -80°C in 100µl aliquots.

Competency of bacteria was determined by transforming 0.5, 1, 5 and 10ng pEQPAM plasmid into 50µl competent cells and plating out onto ampicillin-LB agar (100µg/ml ampicillin) palates. Briefly, plasmid DNA was added to cells in pre-chilled Falcon 2059 tubes, the reactions were swirled gently and incubated 30 minutes on ice. They were then heat shocked for 45 seconds at 42°C and cooled on ice for 2 minutes. After that 0.3ml of S.O.C. medium (pre-heated to 37°C) was added and bacteria were incubated 1 hour at 37°C with shaking at 220rpm. Each reaction was then spread on two ampicillin-LB agar palates and incubated overnight at 37°C. The number of colonies formed on each plate was divided by the amount of plasmid (in µg), anything above 10^4 CFU/µg was deemed competent.

In order to prepare sufficient quantities of the pGL3-BV and the pRL-TK constructs, the plasmids were transformed into *E. coli* DH5α as described above. A single colony was picked from each plate and grown in 100ml of LB broth supplemented with 100µg/ml ampicillin overnight at 37°C with shaking. Plasmids were isolated using the NucleoBond Xtra Midi plasmid purification kit (Machery-Nagel) according to the manufacturer's protocol. Concentration and quality of isolated plasmids were determined using a Nanodrop ND-1000 spectrophotometer. A sample was considered pure enough for experiments if the absorbance 260/280 ratio was at least 1.8.

2.11.3. Luciferase reporter assay

Luciferase reporter assays measure the ability of a DNA sequence

(hypothetical promoter) to initiate transcription of a luciferase gene that is cloned downstream of the tested promoter, in this case firefly luciferase behind the ALP promoter. The two luciferase enzymes used (firefly and renilla) have different substrate requirements and emit different wavelengths of light. In each experiment light emitted by the firefly luciferase is normalised to that of renilla luciferase, which serves as a 'loading control'.

VSMCs were plated in 48-well plates (10000 cells/well) in triplicates for each condition. After 24 hours they were transfected with the pGL3-BV ALP promoter constructs and pRL-TK using Lipofectamine LTX (Table 2.7). 24 hours after transfection cells were washed and treated with TM and TG, as described previously for 24 hours. Luciferase assays were carried out using the Dual-Luciferase Reporter Assay kit (Promega) according to the manufacturer's protocol. Cells were washed with PBS and lysed in the supplied passive lysis buffer on a rotary shaker for 15 minutes. 20µl of each lysate was transferred to a white 96-well plate with 100ul of LARII reagent. Firefly luciferase luminescence was measured in a Berthold Mithras LB 940 luminometer. After that 100ul of Stop&Glo reagent was added and renilla luciferase luminescence was measured.

Table 2.7. Transfection of VSMCs with luciferase reporter constructs.

Reagent	Amount per well
M199+20%FBS+PSG	250µl
OptiMEM	25µl
Lipofectamine LTX	1.25µl
Plus reagent	0.75µl
pGL-BV3	0.5µg
pRL-TK	20ng

2.11.4. Analysis of transcription factors binding to the alkaline phosphatase promoter

In order to examine whether ATF4 binds to the ER stress-responsive fragment of the ALP promoter DNA binding assays were performed. In this assay streptavidin coated beads were conjugated with a biotinylated fragment of the ALP

promoter and then incubated with nuclear extracts from VSMCs. Proteins eluted from the biotinylated DNA were then analysed by Western blotting or mass spectrometry.

2.11.4.1. Generation of biotinylated oligonucleotides

First, a biotinylated oligonucleotide with the promoter sequence was produced carrying out a PCR reaction using a biotinylated forward and normal reverse primers (Table 2.8). The oligonucleotide was then precipitated by adding 1/5 volumes of 3M sodium acetate (pH 5.5), 2.5 volumes of 95% ethanol and incubating for 30 minutes at -20°C. The DNA was pelleted at 14,000 rpm at 4°C for 15 minutes, washed with 70% ethanol and centrifuged again. The pellet was resuspended in double-distilled water and the concentration and purity was determined using the ND-1000 Nanodrop spectrophotometer.

Table 2.8. Primers used to amplify the ALP promoter for DNA binding assays.

Primer sequence (5'-3')	Annealing temperature	Amplicon size
F: GGAGTGTAGTGGCGTGATCT R: GCAATAGAGTGGGACCCTGT	54°C	1582bp

2.11.4.2. Nuclear extraction

Cells were plated in a T25 flask (100 000 cells per flask) and treated as described. Then cells were washed with cold PBS/phosphatase inhibitor buffer (PIB, 1:20), scraped with PBS/PIB and centrifuged at 350x*g* for 5 minutes at 4°C. The pellet was resuspended in 1ml of hypotonic buffer and incubated 15 minutes on ice to allow cells to swell. Next, 50µl of 10% NP-40 was added to disrupt the cell membranes without damaging nuclear membranes and samples were thoroughly mixed and centrifuged 1 minute at 14,000x*g* at 4°C to pellet the nuclei. Then pellets werein 40µl nuclear lysis buffer and incubated 30 minutes on ice with gentle rocking. During the incubation the pellets were resuspended every 10 minutes. The samples were then centrifuged 10 minutes at 14000x*g* at 4°C, after which supernatants containing nuclear proteins extracts were saved. Concentrations of the

extracts were measured with DC Protein Assay and they were stored in -80°C.

2.11.4.3. DNA binding assay

For each tested condition 6µg of the oligonucleotide was conjugated with 20µl of magnetic streptavidin-coated beads (Dynabeads M-270 Streptavidin, Invitrogen). The optimal amount of DNA for this amount of beads was determined experimentally (appendix).

Magnetic beads were washed 3 times with 10 volumes of B&W buffer. Biotinylated DNA was added to the beads resuspended in B&W buffer and incubated with rotation 30 minutes at room temperature. After that the beads were washed 3 times with B&W buffer, twice with transcription factor binding buffer and aliquoted into fresh tubes. Competitor DNA poly(dI:dC) was added to each aliquot (5µg for each 20µl of beads) and samples were incubated for 15 minutes at room temperature with rotating, to decrease unspecific interactions of DNA with proteins. Next, nuclear extracts (20µg) were added to each sample and incubated 30 minutes rotating. After that the beads were washed 3 times with transcription factor binding buffer and bound transcription factors were eluted by resuspending the beads in SDS-PAGE sample buffer and boiling 5 minutes at 95°C. Samples were analysed by Western blotting for ATF4 or mass spectrometry.

2.11.4.4. Mass spectrometry

Mass spectrometry analysis was carried out in order to identify other proteins that bind with the tested fragment of the ALP promoter.

A DNA binding assay was carried out as described above, with a sample of thapsigargin treated VMSCs, and samples were ran on an SDS-PAGE acrylamide gel. The gel was washed in water, then stained with BioSafe Coomassie for 30 minutes and then washed 3 times with water, 15 minutes each to wash away unspecific staining.

The gel was taken to the Proteomics Facility at the Institute of Psychiatry (King's College London) for proteomics analysis. Briefly, fragments of the gel were cut out and in-gel reduction, alkylation and digestion with trypsin were performed

prior to subsequent analysis by liquid chromatography - tandem mass spectrometry (LC-MS/MS). Raw mass spectrometry data were analysed in Proteome Discoverer (ThermoScientific; v1.3.0.339) utilising the Mascot database. Samples were searched against Uniprot database to identify proteins bound to the biotinylated ALP promoter and compared with proteins that nonspecifically bound to unconjugated beads.

2.12. Data analysis

All results represent n=3, unless stated otherwise. Data was analysed using Apache OpenOffice 4.1.1 and GraphPad Prism software. Graphs show mean with SEM. Where appropriate t-tests or one way ANOVA with Tukey's or Dunnett's *post hoc* tests were performed. Results were considered statistically significant when $p<0.05$. Statistical significance is indicated with asterisks: * denotes p between 0.05 and 0.01, ** denotes p between 0.01 and 0.001, *** denotes $p<0.001$.

2.13. Appendix

2.13.1. Real-time PCR primer validations

Before real-time PCR was carried out, primers were tested on a U2OS cDNA sample to confirm the amplification of one product by each pair of primers. Single products of the expected sizes (see Table 2.5) were obtained, seen as single bands in each lane of an agarose gel (Figure 2.1).

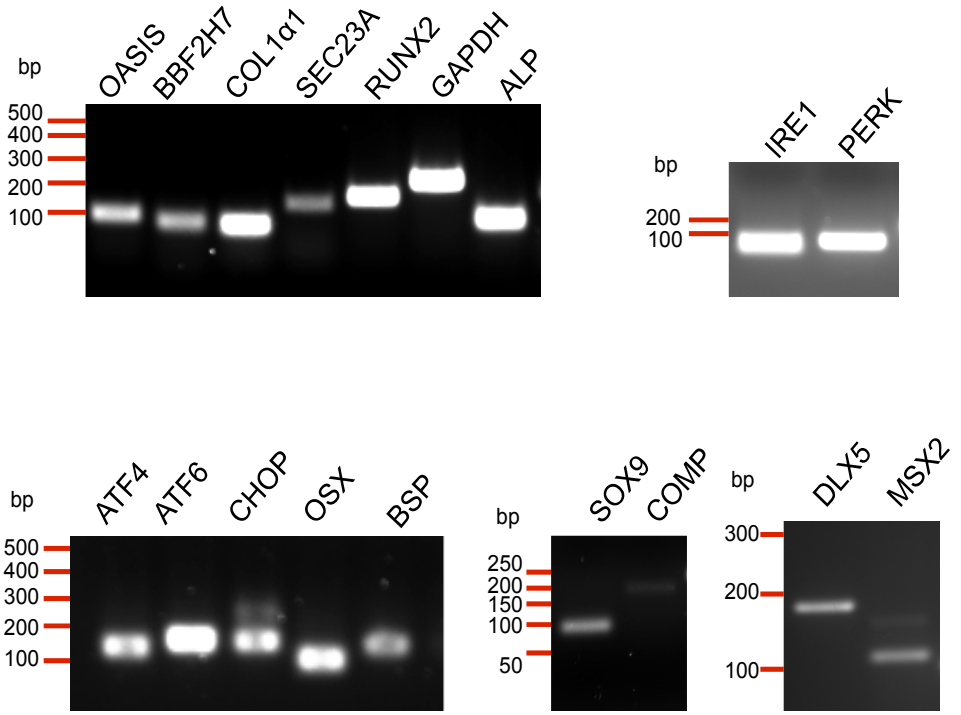

Figure 2.1. Validation of qPCR primers - agarose gels confirming the amplicon size for each primer pair. RNA was isolated from U2OS cells, reverse transcription and conventional PCR were carried out, the products were resolved on 2% agarose gels.

Next, validation reactions were carried out to assess whether amplification efficiencies are the same for each tested pair of primers and GAPDH primers, which were used as an internal control. ΔC_T values were plotted against dilution factor of the cDNA samples on a logarithmic scale and trend lines were fitted (Figure 2.2 and Figure 2.3). If the absolute value of the trend line slope is very small (smaller than 0.5) that means that the target and reference gene amplification efficiencies are similar and the $2^{-\Delta\Delta CT}$ method may be used for these two sets of primers.

A

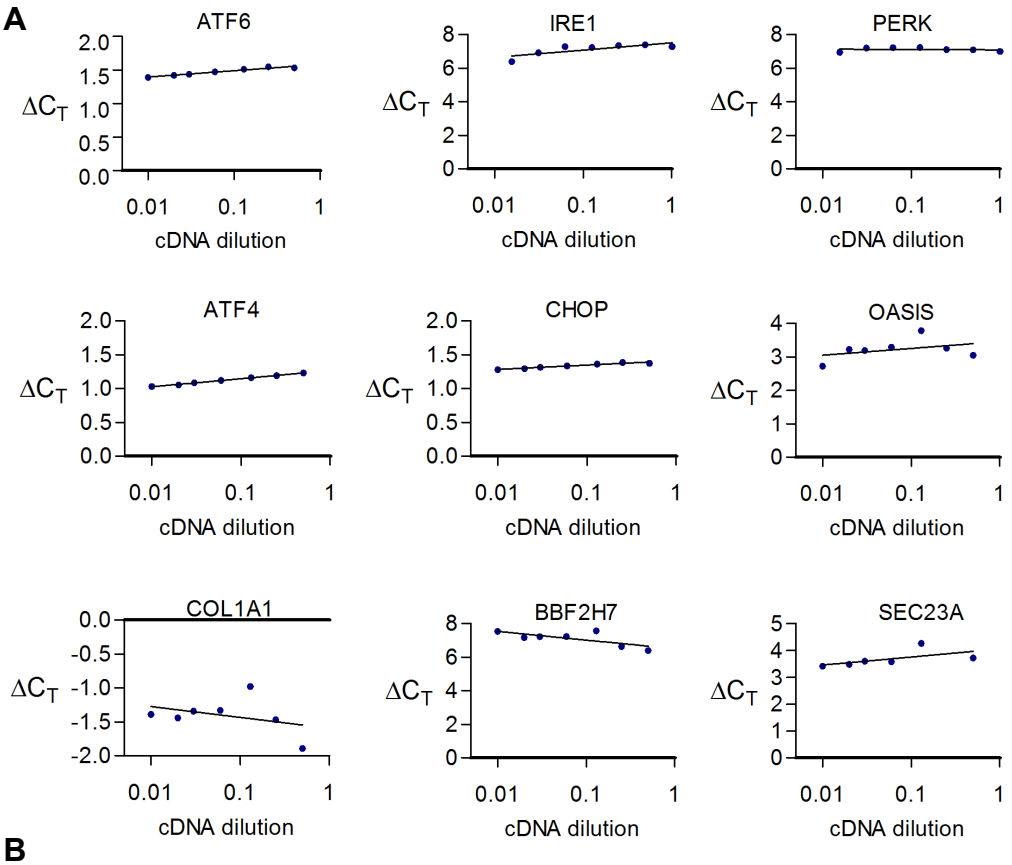

B

Gene	ATF6	IRE1	PERK	ATF4	CHOP	OASIS	BBF2H7	COL1A1	SEC23A
Slope	0.094	0.438	-0.02136	0.1207	0.00789	0.2022	-0.5216	-0.1590	0.2994

Figure 2.2. Validation of qPCR primers – ER stress markers, osteoblast- and chondrocyte-specific ER stress transducers and their target genes. Seven 1:2 serial dilutions were made of VSMC cDNA and qPCR reactions were carried out with these samples. **A** ΔC_T values plotted against dilution factors (log scale). **B.** Slopes of the resulting curves.

A

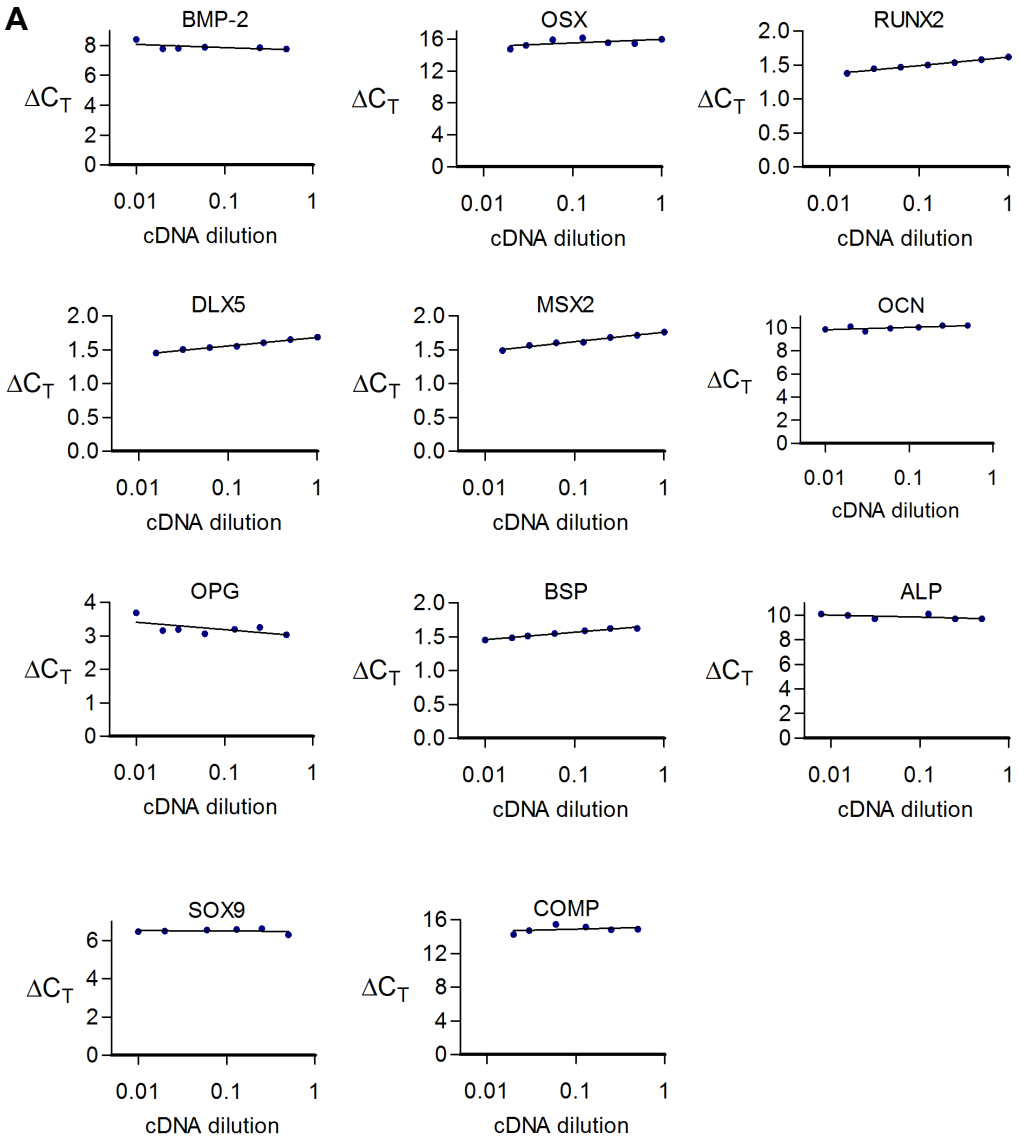

B

Gene	BMP-2	OSX	RUNX2	DLX5	MSX2	OCN	OPG	BSP	ALP	SOX9	COMP
Slope	-0.213	0.451	0.125	0.126	0.142	0.207	-0.219	0.008	-0.165	-0.026	0.261

Figure 2.3. Validation of qPCR primers – osteo/chondrogenic markers. Seven 1:2 serial dilutions were made of VSMC cDNA and qPCR reactions were carried out with these samples. **A** ΔC_T values plotted against dilution factors (log scale). **B.** Slopes of the resulting curves.

2.13.2. Optimisation of biotinylated oligonucleotide amount

A test experiment was carried out in order to establish what amount of the biotinylated ALP promoter fragment will saturate the amount of beads used and therefore allow for maximal protein binding. Magnetic beads (20µl per sample) were washed three times with 10 volumes of B&W buffer. 10, 8, 6, 4, 2 or 0µg of the biotinylated DNA was added to the beads resuspended in B&W buffer and incubated with rotation 30 minutes at room temperature. DNA was eluted with DNA release buffer for 5 minutes at 70°C and resolved on a 1% agarose gel (Figure 2.4). The results show that 6µg was the amount that saturated the beads, as increased amounts of DNA did not result in an increase in eluted DNA.

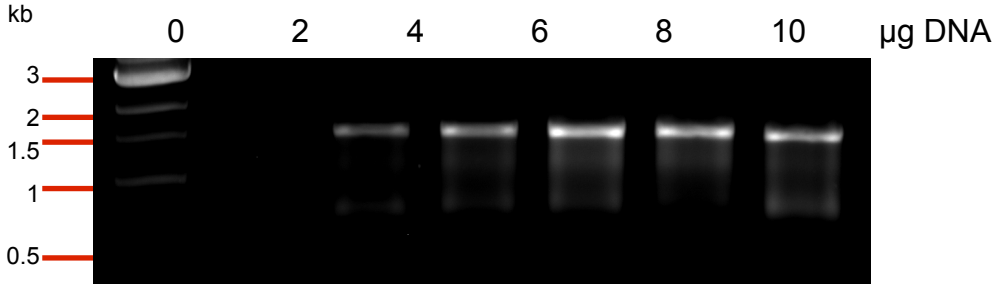

Figure 2.4. Optimisation of the amount of biotinylated oligonucleotide for DNA binding assay. The indicated amounts of the oligonucleotide were incubated with 20µl of streptavidin-coated magnetic beads. Beads were washed, DNA eluted off and resolved on a 1% agarose gel.

2.13.3. List of reagents (in alphabetical order)

Reagent	Company
Acetic acid	Sigma
Acrylamide/Bis 37.5:1, 30%	National Diagnostics/Geneflow
Agarose	Starlab
Alizarin Red S	Sigma
Ampicillin, sodium salt	Sigma
APS	BioRad
b-mercaptoethanol	Sigma
BioSafe Coomassie	BioRad
Bromophenol blue	BDH
BSA	Sigma

Reagent	Company
Chlorophorm	Sigma
DAPI	Sigma
DEPC treated H_2O	Invitrogen
DMEM	Sigma
DMSO	Sigma
DNA loading dye	Promega
dNTP mastermix	Eurogentec
DPBS	Sigma
DPX	VWR
DTT	Sigma
EBSS	Sigma
EDTA	Sigma
Eosin	Sigma
EtBr	Sigma
Ethanol	Fisher Scientific
FBS	PAA
Formamide	Sigma
Glycerol	Sigma
Glycine	Sigma
Go Taq Green PCR mastermix	Promega
HBSS	Sigma
HCl	Sigma
Hematoxylin	Sigma
HEPES	Sigma
Hexadimethrine bromide	Sigma
HiPerFect	Qiagen
Isopropanol	Sigma
Kanamycin	Sigma
KCl	Sigma
KOH	Sigma
LB agar	Sigma
LB broth	Sigma
Lipofectamine LTX	Invitrogen

Reagent	Company
M199	Sigma
MESA GREEN qPCR MasterMix	Eurogentec
Methanol	Fisher Scientific
$MgCl_2$	Sigma
Milk	Marvel
Mowiol	Calbiochem
Mu-MLV reverse transcriptase	Promega
NaCl	Fisher Scientific
NaF	Sigma
NaOH	Sigma
$NaVO_3$	Sigma
NP-40 alternative	Calbiochem
o-cresolphthalein	Sigma
Oligo dT primer	Promega
OptiMEM	Gibco
PBS	Fisher
PFA	Sigma
pNP	Sigma
pNPP	Sigma
Polybrene	Sigma
poly(dI:dC)	Sigma
Primers	IDT
Protease inhibitor cocktail	Sigma
PSG	Sigma
Random primer	Promega
RNA-STAT 60	Amsbio
RNAsin	Promega
S.O.C. medium	Invitrogen
SDS, 20%	Sigma
SiRNA Smartpools	Dharmacon/Sigma
Spermidine	Sigma
TEMED	BioRad
Triton X-100	Sigma

Reagent	Company
Trizma base (Tris)	Sigma
Trypsin/EDTA	Sigma
Tween 20	Sigma
Xylene	Sigma
$ZnCl_2$	Sigma

2.13.4. Buffers and stock solutions (in alphabetical order)

Alizarin Red S

- 2% Alizarin Red S
- pH to 4.2 (adjusted with 10% NH_4OH)

ALP assay buffer

- 0.1M glycine
- 1mM $MgCl_2$
- 1mM $ZnCl_2$
- pH 10.4

Ammonia/chloride buffer

- 0.24% NH_4Cl
- 5% NH_4OH
- pH 10.5

APS

- 10% ammonium persulfate
- H_2O

Binding and washing (B&W) Buffer (2X):

- 10 mM Tris-HCl (pH 7.5)
- 1 mM EDTA
- *2 M NaCl*

$CaCl_2$

- 1mg/ml $CaCl_2$

DNA Release Buffer:

- 50% Formamide in water

Hypotonic buffer

- 20mM HEPES
- 5mM NaF
- 0.1mM EDTA
- pH 7.5

Mowiol mounting medium for immunocytochemistry

- 10% Mowiol
- 25% glycerol
- 0.1M Tris
- pH 8.5

Nuclear fractionation buffer A

- 10mM HEPES pH 7.9
- 10mM KCl
- 1.5 mM $MgCl_2$
- 0.5mM DTT
- 0.05% NP-40
- 2µl/ml protease inhibitor cocktail

Nuclear fractionation IP buffer

- 10mM Tris pH 7.5
- 100mM NaCl
- 1mM EDTA
- 1% Triton
- 2µl/ml protease inhibitor cocktail

Nuclear lysis buffer

- 50 mM Tris HCl (pH 8)
- 150 mM NaCl
- 1% NP-40
- 0.5% sodium deoxycholate
- 1% glycerol
- 1mM $NaVO_3$
- 2µl/ml protease inhibitor cocktail

o -cresolphthalein solution

- 1mg/ml o-cresolphthalein
- 0.0672% NH_4Cl
- 1.4% NH_4OH
- *pH 10.5*

PBST

- 10x PBS tablets
- 0.1% Tween 20
- 1l H_2O

PFA (Paraformaldehyde)

- 4% PFA
- PBS
- pH 7.5

Phosphatase inhibitor buffer

- 125mM NaF
- 250mM β-glycerophosphate
- 25mM $NaVO_3$

Resolving gel buffer

- 1.5 M Tris
- pH 8.8

SDS-PAGE running buffer

- 25 mM Tris
- 250 mM glycine
- 0.1% SDS
- *pH 8.3*

SDS-PAGE sample (loading) buffer, 4x

- 40% glycerol
- 240 mM Tris/HCl pH 6.8
- 8% SDS
- 0.04% bromophenol blue
- 5% β-mercaptoethanol

Stacking gel buffer

- 0.5 M Tris
- *pH 6.8*

TAE (Tris-acetic acid-EDTA)

- 40mM Tris
- 20mM acetic acid
- and 1mM EDTA

Transcription Factor Binding Buffer (2X):

- 40 mM HEPES–KOH pH 7.9
- 50 mM KCl
- 0.2 mM EDTA
- 4 mM $MgCl_2$
- 1 mM dithiothreitol (DTT)
- 0.05% NP-40
- *4 mM spermidine*

Western blotting lysis buffer

- 0.1M Tris-HCL
- 0.15M NaCl
- 1% Triton X-100
- 2µl/ml protease inhibitor cocktail
- pH 8.1

Western blotting transfer buffer

- 20% (v/v) methanol
- 25mM Tris
- 0.2M glycine
- 1% SDS
- pH 8.3

Chapter 3: Endoplasmic reticulum stress is involved in vascular calcification

3.1. Introduction

3.1.1. ER stress and vascular calcification

The unfolded protein response (UPR) is a signalling pathway activated in response to ER stress, which occurs as a result of unfolded protein accumulation or perturbations of intracellular Ca^{2+} homoeostasis. It consists of three branches, each mediated by a separate ER stress transducer: PERK, ATF6 or IRE1. Each of these activates expression of genes that help resolve ER stress such as Grp78 and Grp94 chaperones, via distinct downstream targets (Ron and Walter, 2007). In cases when ER stress cannot be resolved, it can lead to cell death (Rao *et al.* 2004)

ER stress signalling has been shown to be crucial for bone development. XBP1 was shown to be highly expressed in developing skeletons of mouse embryos (Clauss *et al.* 1993). In addition BMP-2, the main bone morphogenetic protein, can upregulate IRE1, XBP1, CHOP, PERK, ATF4 and ATF6 expression in osteoblasts (Tohmonda *et al.* 2011; Han *et al.* 2013). PERK knock-out mice exhibit skeletal dysplasias at birth and postnatal growth retardation highlighting its important role in bone formation (Zhang *et al*. 2002). Mice deficient in ATF4, which acts downstream of PERK, exhibit a reduction in bone volume and fail to achieve normal bone mass (Yang *et al.* 2004b). Finally, the chaperone Grp78 was shown to localise on the surface of osteoblasts, bind collagen type 1 and nucleate calcium and phosphate crystals *in vitro*, suggesting that it plays a role in bone ECM mineralisation (Ravindran *et al.* 2011). Grp78 expression is increased during embryonic development in condensing cartilage and mesenchymal cells (Ravindran *et al.* 2012).

Vascular calcification shares similarities with bone formation. Calcifying VSMCs have been shown to undergo an osteogenic transdifferentiation, which resembles osteoblast maturation, during which they lose expression of VSMC

markers and start expressing osteo/chondrogenic markers (Shanahan *et al.* 1999a; Speer *et al.* 2009). In addition, it was shown that in VSMCs cultured *in vitro* apoptosis occurs prior to the onset of calcification and that apoptotic bodies accumulate calcium and are sites of crystal nucleation (Proudfoot *et al.* 2000). These findings were confirmed by *in vivo* studies showing that dialysis triggers VSMC apoptosis and thus accelerates vascular calcification (Shroff *et al.* 2008). Apoptosis was also shown to accelerate plaque formation and induce its calcification in a mouse model of atherosclerosis (Clarke *et al.* 2008). This is important because apoptosis of chondrocytes is an important step that induces bone mineralisation (Karsenty *et al.* 2009). Because vascular calcification has similarities with bone formation, I hypothesized that ER stress and UPR signalling are involved in this pathological process.

VSMC calcification has been linked to ER stress and the UPR in five studies to date. It has been shown that calcification induced in rat aortas and VSMCs cultured *in vitro* is associated with increased apoptosis as well as expression of ER stress markers ATF4, Grp78, Grp94 and CHOP, and osteogenic markers OPN and ALP (Duan *et al.* 2009, 2013). Liberman *et al.* (2011) have shown that BMP-2, the main inducer of osteoblast differentiation, activates oxidative stress, which results in ER stress and increased calcification of human coronary artery VSMCs. Finally, Masuda *et al.* (2012, 2013) have shown that in mouse VSMCs stearate and TNFα induce calcification via the PERK-ATF4-CHOP branch of the UPR. However, these studies offer limited explanation of what mechanisms link ER stress to vascular calcification, which UPR pathways are involved or whether ER stress can be activated *in vivo* in human aortas.

3.1.2. Modelling ER stress

ER stress can be modelled *in vitro* using tunicamycin and thapsigargin treatments. Tunicamycin is an inhibitor of N-glycosylation, and causes accumulation of unglycosylated proteins in the ER (Olden *et al.* 1979) and therefore it imitates ER stress induced by an increased load of proteins. This type of ER stress occurs in osteoblasts, which are professional secretory cells and therefore under greater

demand to fold and process large quantities of proteins when secreting ECM (Wu and Kaufman, 2006). Thapsigargin is an inhibitor of SERCA (sarco/endoplasmic reticulum Ca^{2+} ATPase), which causes an increase in cytosolic Ca^{2+} as these ions cannot be transported back to the ER (Xuan *et al.* 1992), and represents ER stress which occurs due to disturbed Ca^{2+} homeostasis. These chemicals mimic ER stress induced via different mechanisms and therefore in most experiments both were used, because it was unclear which would be more relevant to vascular calcification. In addition, both calcium and protein folding homeostasis are crucial for bone development, therefore it was important to mimic ER stress that disrupts each of these processes.

ER stress can be inhibited by 4-phenylbutyric acid (PBA), a chemical chaperone (Welch and Brown, 1996). Due to its hydrophobic structure, PBA associates with unfolded proteins and facilitates their folding. Although it cannot completely counter the effects of tunicamycin or thapsigargin, it can attenuate ER stress to an extent.

3.1.3. Potential factors inducing ER stress in vascular calcification

Vascular calcification is a complex, multifactorial process, and therefore it is difficult to single out one inducer that causes it. Nevertheless, there are factors known to contribute to this process. In conditions such as diabetes and CKD, oxidative stress is thought to play a role. Mineral homeostasis dysregulation, high levels of vitamin D and warfarin treatments are also known to contribute to calcification in dialysis patients (Shanahan 2013). Vascular calcification is associated with increased levels of various cytokines, such as BMP-2, TGFβ and TNFα (Kaden *et al.* 2004; Stenvinkel *et al.* 2005; Jian *et al.* 2003). Finally, hydroxyapatite, the result of calcification, has been shown to promote osteogenic differentiation of VSMCs (Sage *et al.* 2011). The effect of these factors on the UPR and whether they can induce ER stress in VSMCs is mostly unknown.

TGFβ1 is a cytokine with an established role in regulating chondrocyte growth by inhibiting hypertrophy and maintaining expression of ECM proteins (Ballock *et al.* 1993). Clasically, TGFβ1 has been associated with maintaining the

contractile phenotype of VSMCs both *in vitro* and *in vivo* (Shah *et al.* 1996; Hirshi *et al.* 1998; Grainger *et al.* 1998). However, at higher concentrations *in vitro* (10ng/ml as opposed to 0.5-2ng/ml) it has been shown to induce VSMC proliferation and activate osteogenic gene expression (Orlandi *et al.* 1994; Simionescu *et al.* 2005). It has also been shown to be present at high levels in calcified human aortic valves (Jian *et al.* 2003). However, another study has shown that VSMCs from SMAD3 knock-out mice (SMAD3 is a mediator of TGFβ1 signalling) calcify more than their wild-type counterparts when exposed to high calcium and phosphate, suggesting that TGFβ signalling suppresses calcification (Shimokado *et al.* 2014). Therefore, the role of TGFβ in regulating VSMC phenotype and calcification in not yet clear. Importantly, TGFβ has been shown to activate the UPR in lung fibroblasts and thus induce ECM protein expression (Baek *et al.* 2011), but its effects on UPR in VSMCs have not been studied.

PDGF is a growth factor crucial for blood vessel formation during embryonic development, where it regulates VSMC and pericyte migration and proliferation (Hellstrom *et al.* 1999). In adult VSMCs PDGF is an important regulator of phenotype, which during injury prompts cells to switch to the synthetic phenotype, lose contractile marker expression, proliferate and synthesise ECM (Wilson *et al.* 1993, Salabei *et al.* 2013). Importantly, PDGF has been shown to promote VSMC calcification *in vitro* (Giachelli *et al.* 2001). ER stress has been shown to protect rat VSMCs from PDGF-induced proliferation and migration. The same study has shown that PDGF did not induce XBP1 splicing or Grp78 and Grp94 expression, but in-depth analysis of UPR activation was not carried out (Yi *et al.* 2012).

BMP-2 is the main osteogenic cytokine and has been widely implicated in vascular calcification, as it is highly expressed in calcified blood vessels (Kaden *et al.* 2004). BMP-2 has been shown to activate ER stress in osteoblasts (Murakami *et al.* 2009). In VSMCs BMP-2 has been shown to activate ER stress via oxidative stress and NADPH oxidases (Liberman *et al.* 2011).

TNFα is a ubiquitous cytokine with many functions, primarily linked to inflammation. It has been associated with vascular calcification, because elevated levels are found in atherosclerotic plaques and in vessels of patients with chronic

kidney disease, a condition which is accompanied by medial calcification and systemic inflammation (Barath *et al.* 1990, Stenvinkel *et al.* 2005). Importantly, TNFα has been shown to activate ER stress in VSMCs, specifically the PERK-ATF4 branch of the UPR in a mouse VSMC line, and thus lead to increased calcification. This pathway was also shown to be activated in aortas, when CKD was induced by 5/6 nephrectomy in mice (Masuda *et al.* 2013). However, activation of other UPR branches by TNFα has not been studied.

Chronic kidney disease results in a range of health complications, all of which impact on VSMC physiology. Mineral dysregulation is thought to be one of the main factors that injure VSMCs in this disease and high levels of calcium and phosphate have been shown to increase calcification of VSMCs *in vitro* (Block *et al.* 1998; Shroff *et al.* 2010; Shanahan *et al.* 2011). Patients with CKD are often administered vitamin D (calcitriol, 1,25-dihydroxyvitamin D3) supplements to counter hypocalcemia and secondary hyperparathyroidism which are the result of disturbed phosphate metabolism. The role of vitamin D in vascular calcification is unclear, as both low and high levels (compared to physiological) have been shown to induce calcification of VSMCs (Jono *et al.* 1998; Wolisi *et al.* 2005; Mizobuchi *et al.* 2009). In addition, vitamin D has been shown to inhibit vascular calcification induced by TNFα (Aoshima *et al.* 2012). In terms of ER stress, vitamin D has been shown to suppress the UPR in macrophages in the context of diabetes (Riek *et al.* 2012). The effect of vitamin D on ER stress pathways in VSMCs has not been studied.

Warfarin is an anticoagulant commonly administered to dialysis patients in order to maintain vascular access. It prevents blood clotting by inhibiting carboxylation of coagulant factors in the liver. Warfarin promotes vascular calcification as one of its side effects is inhibition of MGP carboxylation in the vasculature. MGP is a natural calcification inhibitor, which needs to be carboxylated in order to be effective (Danziger 2008; Willems *et al.* 2014). Warfarin has also been shown to induce calcification of VSMCs *in vitro* (Proudfoot *et al.* 1998; Reynolds *et al.* 2004; Lomashvili *et al.* 2011). The effect of warfarin on ER stress activation has not been previously studied in VSMCs or in fact any other cell type.

Oxidative stress is a well-established inducer of vascular disease, and accompanies atherosclerosis, diabetes and chronic kidney disease (Xue *et al.* 2005; Demer and Tintut, 2014). It has also been implicated in vascular calcification in many studies (Kaneto *et al.* 2005; Byon *et al.* 2008). The link between ER stress and oxidative stress in VSMCs is unclear, as oxidative stress has been shown to induce ER stress (Liberman *et al.* 2011; Chen *et al.* 2014) and some studies make the reverse conclusion that ER stress induces oxidative stress (Nonaka *et al.* 2001; Husa *et al.* 2013).

Calcium and phosphate crystals (hydroxyapatite) form as a result of ongoing vascular calcification. Studies have shown that the crystals themselves can further enhance osteogenic transdifferentiation of VSMCs and increase calcification by inducing apoptosis (Ewence *et al.* 2008; Sage *et al.* 2011, Lei *et al.* 2014). However, whether this occurs via ER stress signalling has not been examined.

3.2. Aims

In this chapter I set out to examine whether ER stress is involved in vascular calcification. Specifically I determined:

1. Expression of ER stress markers and osteogenic genes in healthy, fatty streak and calcified human aortas.
2. Whether factors relevant to vascular calcification promote ER stress in VSMCs.
3. Which branches of the UPR can be activated in human primary VSMCs *in vitro* by tunicamycin and thapsigargin.
4. Whether ER stress was associated with increased calcification and apoptosis of VSMCs.

3.3. Differential expression of ER stress and osteogenic markers between healthy and calcified human aortas

In order to examine whether there are changes in ER stress marker expression in vascular calcification *in vivo*, expression of PERK, ATF6, ATF4 and CHOP was measured in human aortas by quantitative real-time PCR. Ten RNA

samples from healthy, fatty streak and calcified aortas were analysed.

Expression of all four of the examined ER stress markers was lower in fatty streak and calcified vessels compared to healthy. In addition, their expression in calcified vessels was lower than in fatty streak vessels (Figure 3.1.A). For all markers these changes were just trends, but the decrease in PERK expression in calcified aortas was statistically significant. These results suggest that ER stress decreases as vascular disease progresses and leads to calcification.

Next, expression of a number of osteogenic markers was analysed in the same samples in order to examine whether osteogenic differentiation correlated with levels of ER stress markers. Expression of three osteo/chondrogenic transcription factors – Runx2, Osterix and Sox9 and their downstream targets ALP, BSP, OPG and COL1A1 was measured (Figure 3.1.B).

In the fatty streak group expression of all osteogenic markers was decreased compared to healthy samples, which means that their expression followed the same pattern as ER stress markers. However, in the calcified samples levels of expression of Runx2 and Osx were similar to the healthy samples, Sox9, BSP and COL1A1 were slightly increased and only ALP and OPG were decreased. None of these differences were statistically significant. These trends suggest that as vascular disease progresses expression of osteogenic markers at first correlates with ER stress markers, i.e. both are reduced, but later becomes uncoupled and osteogenic gene expression increases independently of ER stress signalling.

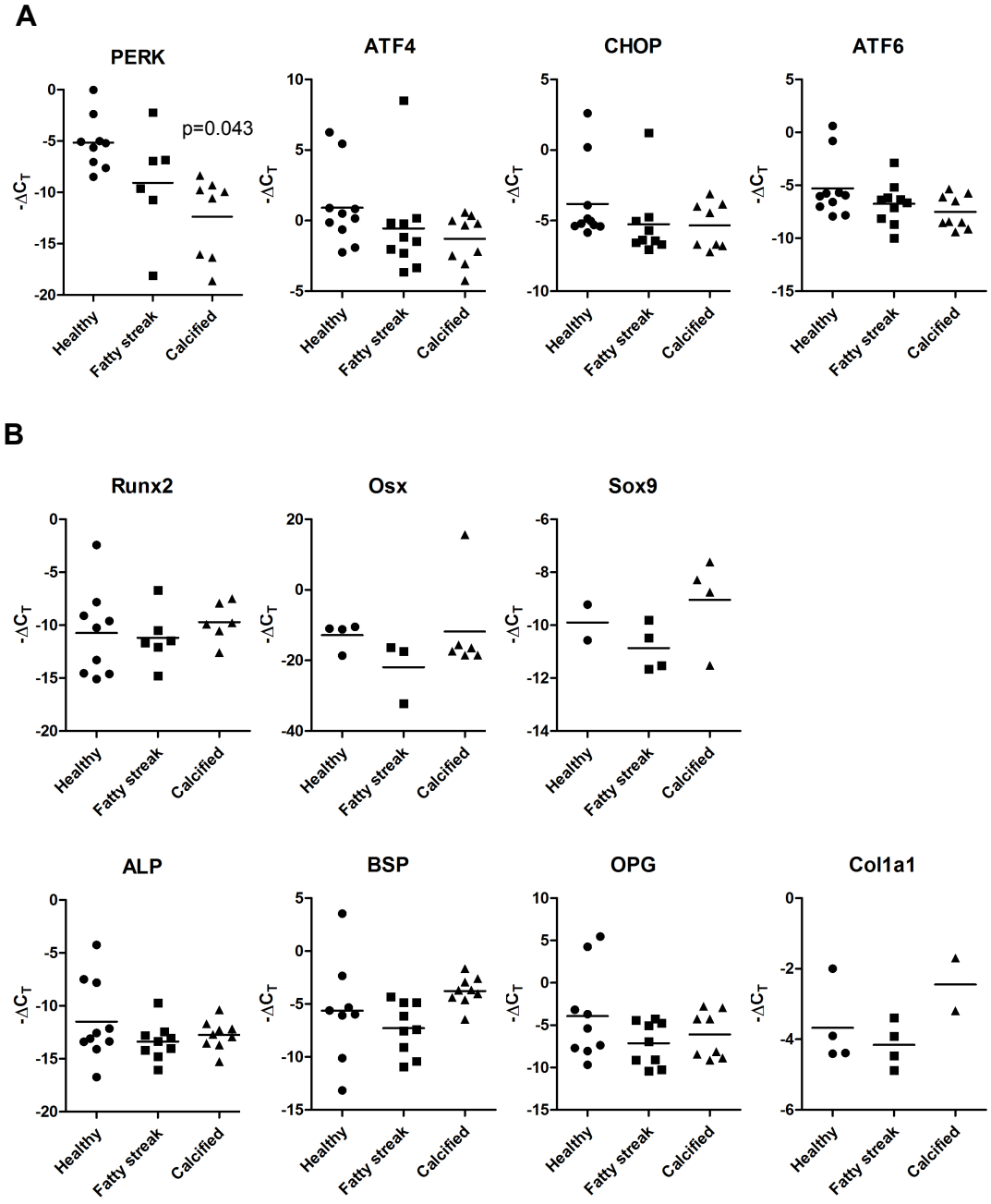

Figure 3.1. Quantitative real-time PCR analysis of **A** ER stress markers and **B** osteo/chondrogenic genes in human aortas. ΔC_T values were calculated relative to GAPDH expression in corresponding samples. Graphs show individual data points and mean, n=2-10, ANOVA with Tukey's *post hoc* tests was performed, p values compared to healthy.

The lack of statistical significance of the observed changes might be partially due to the considerable variability of gene expression within sample groups. This can be explained by the variability in the age, sex and degree of vascular disease in

people, whose aortas were analysed. Table 3.1 shows that patients with calcified aortas were significantly older than people with healthy aortas, which is consistent with the fact that the prevalence of vascular calcification increases with age (Rennenberg *et al.* 2009; Park *et al.* 2012). In addition, for some of the genes the n numbers were low, because samples were excluded from analysis if the real time PCR reactions were not specific (two peaks on the melt curve) or failed completely.

Table 3.1. Demographics of patients, from whom aortic samples were obtained. Differences in mean age were analysed with one-way ANOVA and Tukey's *post hoc* test. ** denotes p between 0.01 and 0.001, in comparison with the healthy group.

Group	Mean Age	Age SD	Females	Males	n
Healthy	38	9	8	2	10
Fatty Streak	43	12	8	2	10
Calcified	51**	7	6	5	11

To further test the relationship between ER stress marker and osteogenic gene expression in the vessel wall, Pearson correlation tests were carried out for expression values of pairs of ER stress versus osteogenic markers for samples from calcified aortas or healthy and fatty streak combined (non-calcified). Figure 3.2.A shows analysis of ATF4 and ALP as an example, the remaining plots are in the Appendix (Figures 7.1 - 7.4). Figure 3.2.B contains a summary of the results and shows that in healthy and fatty streak vessels expression of tested ER stress markers (ATF4, CHOP, ATF6, PERK) in most cases significantly correlated with expression of osteogenic markers Runx2, ALP, BSP and OPG. The exception was PERK, which only correlated with ALP in this data set. SOX9, COL1A1 and OSX were not analysed due to low n numbers. In the dataset consisting of samples from calcified aortas none of the ER stress markers correlated with osteogenic markers, apart form ATF6 and PERK which both correlated with OPG. This is consistent with OPG and ALP being the only two osteogenic genes whose expression was decreased in calcified aortas.

A

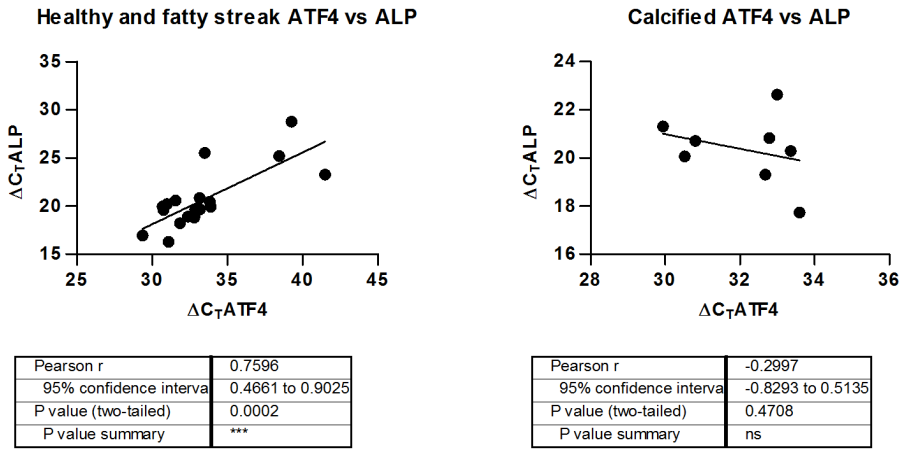

Pearson r	0.7596
95% confidence interva	0.4661 to 0.9025
P value (two-tailed)	0.0002
P value summary	***

Pearson r	-0.2997
95% confidence interva	-0.8293 to 0.5135
P value (two-tailed)	0.4708
P value summary	ns

B

Genes			p value	
			Healthy & Fatty Streak	Calcified
ATF4	vs	Runx2	***	ns
ATF4	vs	ALP	***	ns
ATF4	vs	BSP	**	ns
ATF4	vs	OPG	**	ns
CHOP	vs	Runx2	***	ns
CHOP	vs	ALP	***	ns
CHOP	vs	BSP	**	ns
CHOP	vs	OPG	***	ns
ATF6	vs	Runx2	***	ns
ATF6	vs	ALP	***	ns
ATF6	vs	BSP	**	ns
ATF6	vs	OPG	**	***
PERK	vs	Runx2	ns	ns
PERK	vs	ALP	*	ns
PERK	vs	BSP	ns	ns
PERK	vs	OPG	ns	**

Figure 3.2. Correlation analysis of ER stress versus osteogenic markers. **A.** ΔC_T values of ER stress markers were plotted against ΔC_T values of osteogenic genes. Linear regression was plotted, and a two-tailed Pearson correlation test was carried out. Graphs show individual data points, n=20 for healthy and fatty streak and n=10 for calcified. **B.** Summary of correlation analysis of ER stress versus osteogenic markers; 'ns' denotes p>0.05, * denotes p between 0.05 and 0.01, ** denotes p between 0.01 and 0.001, *** denotes p<0.001.

The results from this section supported the notion that changes in ER stress signalling are associated with vascular disease in human aortas. However, more detailed analysis of ER stress signalling and calcification mechanisms was needed to establish whether ER stress can regulate vascular calcification.

3.4. ER stress is induced by known calcification-promoting factors

Having ascertained that ER stress is involved in vascular calcification, the next important step was to determine what factors that drive calcification are also associated with changes in ER stress. Therefore, expression of ER stress markers was examined after treating cells with some of the well-established inducers of calcification.

3.4.1. Cytokines involved in regulating VSMC phenotype

The first factors tested were TGFβ and PDGF as they have an established role in regulating VSMC phenotype. TGFβ is classically associated with increased contractile differentiation, while PDGF promotes the secretory phenotype of VSMCs as it stimulates ECM secretion and proliferation.

3.4.1.1. TGFβ

VSMCs were treated with 2 ng/ml TGFβ for 5 days, according to a protocol previously established in the laboratory, and expression of ER stress marker mRNA was measured by real-time PCR.

Figure 3.3.A shows that the TGFβ treatment increased the expression of all measured markers: ER stress transducers IRE1 (1.7 ± 0.5 fold increase), ATF6 (1.4 ± 0.5 fold increase) and PERK (1.3 ± 0.17 fold increase), and downstream targets ATF4 (1.6 ± 0.23 fold increase) and CHOP (4.4 ± 2.18 fold increase). The increase in ATF4 expression was statistically significant.

Next, Western blotting for Grp78 and Grp94 was carried out in order to examine whether TGFβ induced changes in ER stress signalling at the protein level. A 1.2-fold increase (±0.45) in expression of Grp78 and 1.2-fold increase of Grp94 (±0.55) was observed consistently in n=3 experiments, however the increases did

not reach statistical significance (Figure 3.3.B and C). Taken together, these results suggest that TGFβ induced ER stress in VSMCs.

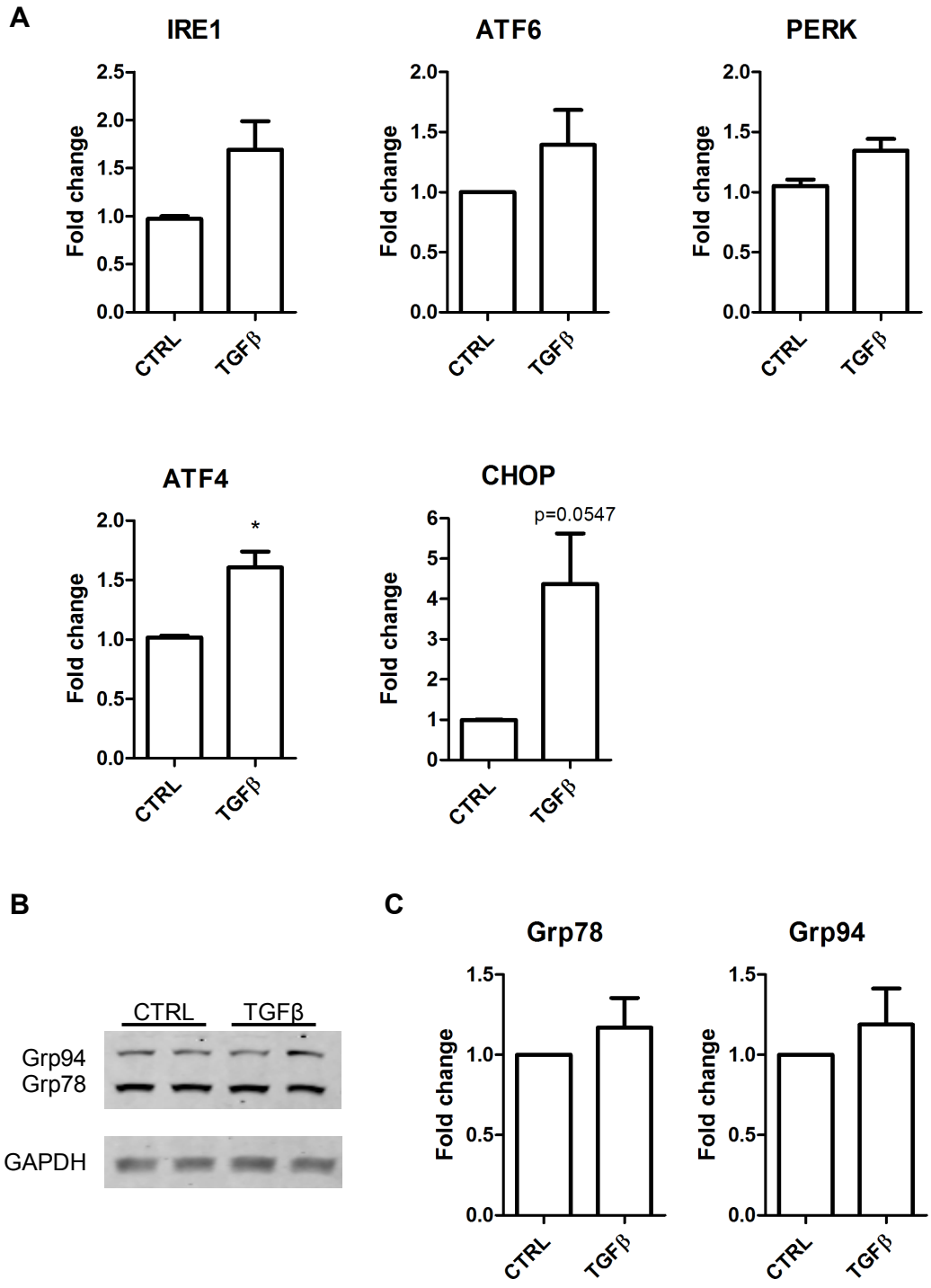

Figure 3.3. ER stress markers in VSMCs treated with TGFβ. Cells were treated with 2ng/ml TGFβ in the presence of 2.5% FBS for 5 days. **A.** ER stress marker expression measured by real-time PCR. **B.** Western blotting for Grp78 and Grp94 and **C.** Quantification of Western blots. All graphs show mean with SEM, n=3, statistical significance of changes was measured using t-tests, * denotes p between 0.05 and 0.01.

3.4.1.2. PDGF

Next, the effect of PDGF treatment on expression of ER stress markers in VSMCs was analysed. Cells were treated with 10ng/ml PDGF for 5 days, according to a protocol previously established in the laboratory.

Expression of ER stress markers measured by real-time PCR did not change after treatment with PDGF (Figure 3.4.A). Grp78 and Grp94 chaperones expression measured by Western blotting was slightly increased (1.4±0.41 fold increase in Grp78, 1.8±1.22 fold increase in Grp94), but the change was not consistent in n=3 experiments. These results suggest that the UPR was not activated in these conditions.

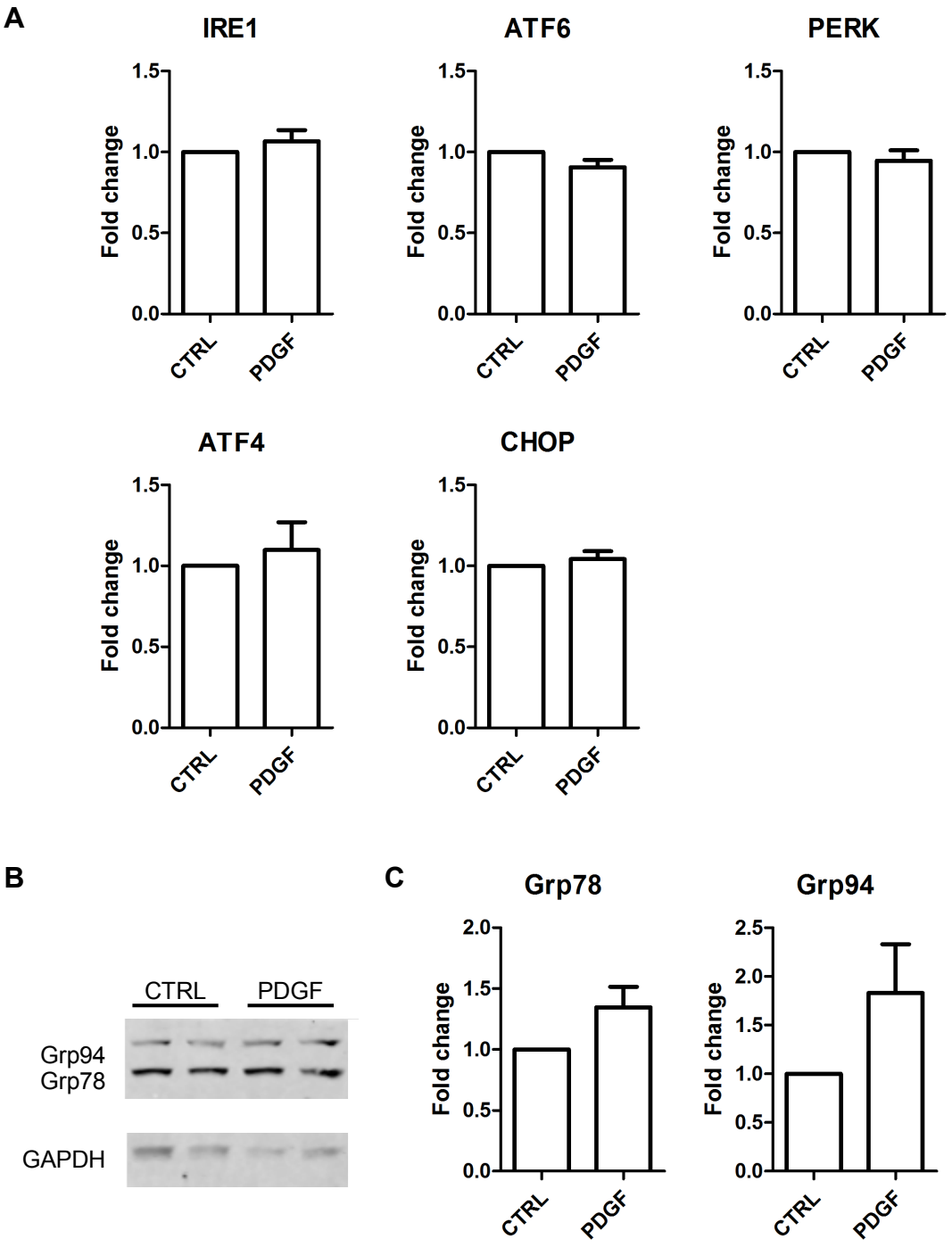

Figure 3.4. ER stress markers in cells treated with PDGF. VSMCs were treated with 10 ng/ml PDGF in the presence of 0.5% FBS for 5 days. A. ER stress marker expression measured by real-time PCR. B. Western blotting for Grp78 and Grp94 and C. Quantification of Western blots. All graphs show mean with SEM, n=3, statistical significance of changes was measured using t-tests.

3.4.2. BMP-2 does not induce ER stress

The next cytokine relevant to calcification, which was hypothesised to promote ER stress in VSMCs was BMP-2. VSMCs were treated with 100ng/ml BMP-2 for 24 hours, in accordance with published literature (Liberman *et al.* 2011). In parallel, cells were also treated with tunicamycin or thapsigargin as a positive control for ER stress. Activation of ER stress markers was measured by real-time PCR and XBP1 splicing assay was carried out.

Figure 3.5.A shows that expression of ATF6, CHOP and ATF4 mRNA measured by real-time PCR did not change after BMP-2 treatment, but increased significantly after thapsigargin treatment. Splicing of XBP1 was not observed in BMP-2 treated VSMCs (Figure 3.5.B).

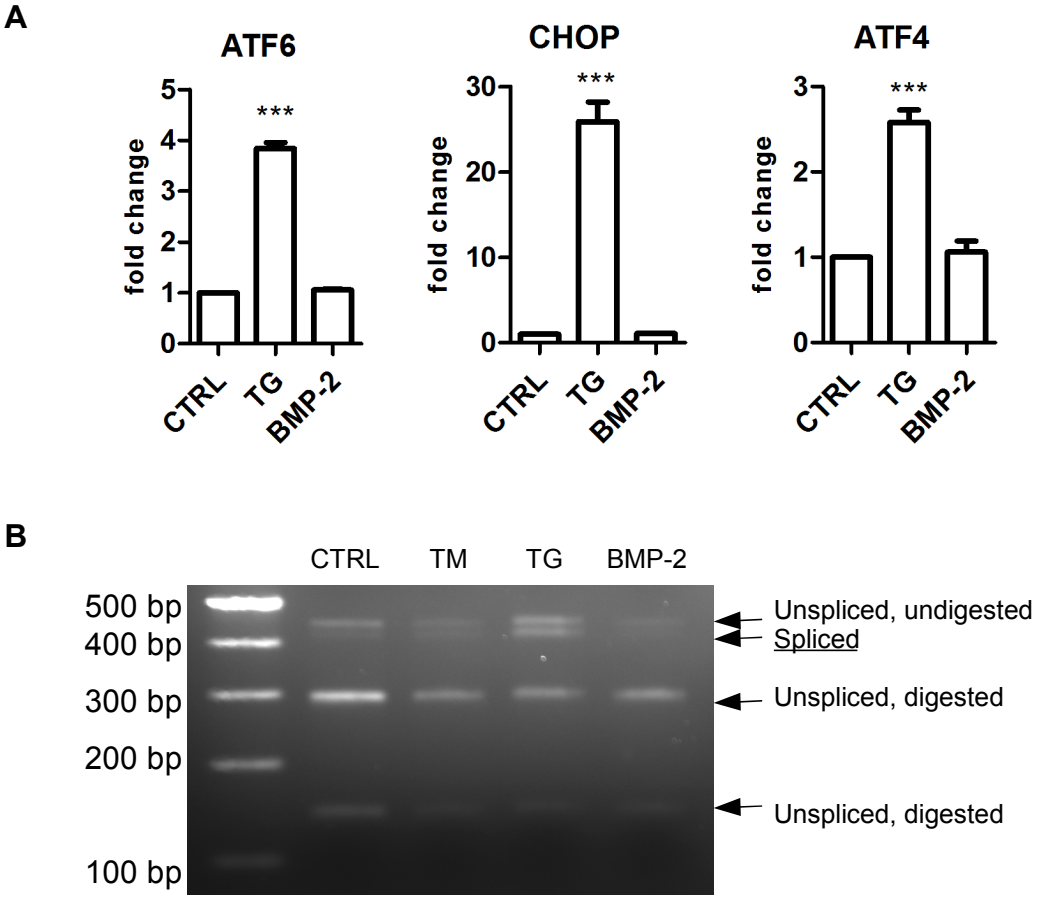

Figure 3.5. ER stress markers in BMP-2-treated VSMCs. Cells were treated with 0.4µg/ml tunicamycin (TM), 0.2µg/ml thapsigargin (TG) or 100ng/ml BMP-2 for 24 hours in medium with 0.5% FBS. **A.** mRNA levels of ATF6, CHOP and ATF4 measured by real-time PCR. Graphs show mean with SEM, n=3, ANOVA and Dunnett's *post hoc* test were carried out. *** denotes $p<0.001$. **B.** XBP1 splicing indicative of UPR activation, n=3, figure shows representative image.

Western blotting for Grp78 and Grp94 chaperones confirmed that ER stress was not activated, as the levels of these proteins did not change with BMP-2 treatment (Figure 3.6.A and quantification B). The results in this section suggest that BMP-2 does not induce ER stress.

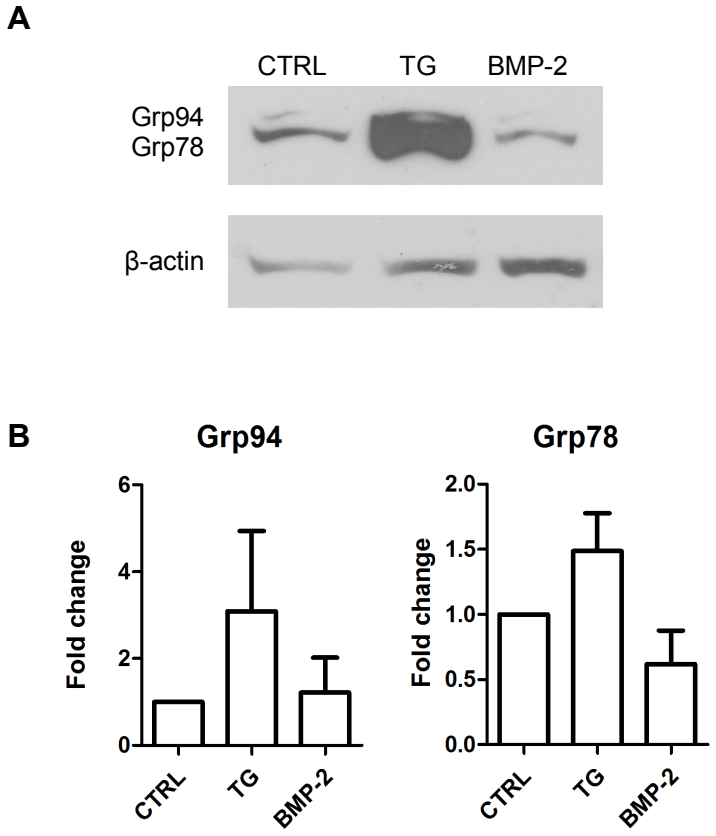

Figure 3.6. BMP-2 does not induce Grp78 and Grp94 expression. Cells were treated with 0.4µg/ml tunicamycin (TM), 0.2µg/ml thapsigargin (TG) or 100ng/ml BMP-2 for 24 hours in medium with 0.5% FBS. **A.** Representative Western blot. **B.** Quantification. Graphs show mean with SEM, n=3, ANOVA and Dunnett's *post hoc* test were carried out.

3.4.3. TNFα increases ER stress in VSMCs

TNFα was previously shown to activate the PERK-ATF4-CHOP branch of the UPR and induce calcification of mouse VSMCs (Masuda *et al.* 2013), but activation of other UPR pathways was not examined in that study. Therefore, expression of all three ER stress transducers and their target genes was examined after TNFα treatment. Cells were treated with 10ng/ml of TNFα for 5 days, according to a

protocol previously established in the laboratory. Expression of ER stress marker mRNA was analysed by real-time PCR and Western blotting.

Surprisingly, TNFα significantly increased expression of IRE1 mRNA (1.7 ± 0.3 fold increase; Figure 3.7.A), and only slightly upregulated expression of PERK (1.2 ± 0.24 fold increase). Levels of ATF6, ATF4 and CHOP remained unchanged. Expression of Grp78 and Grp94 chaperones measured by Western blotting was increased (1.6±0.9 fold increase of Grp78 and 2.2 ± 1.5 of Grp94), and these changes were consistent across n=3 experiments (Figure 3.7.B and C). These results suggest that in human VSMCs TNFα induced the IRE1 rather than PERK branch of the UPR.

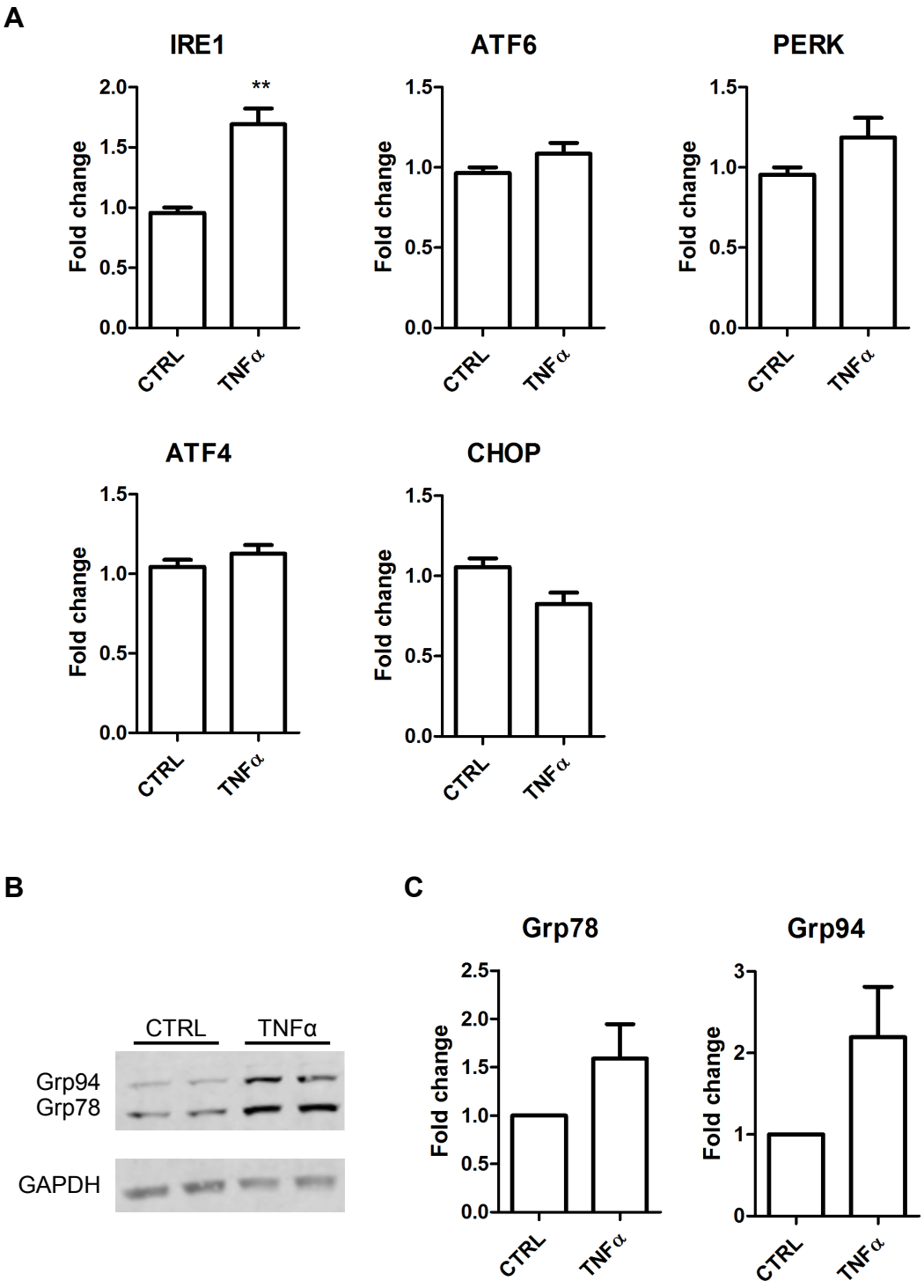

Figure 3.7. ER stress markers in cells treated with TNFα. VSMCs were treated with 10ng/ml TNFα in the presence of 20% FBS for 5 days. **A.** ER stress marker expression measured by real-time PCR. **B.** Western blotting for Grp78 and Grp94 and **C.** Quantification of Western blots. All graphs show mean with SEM, n=3, statistical significance of changes was measured using t-tests, * denotes p between 0.05 and 0.01.

The results in this section show that BMP-2 and PDGF are not involved in activating the UPR in VSMCS, but TGFβ and TNFα possibly are.

3.4.4. Factors involved in CKD

Because chronic kidney disease, and specifically dialysis, is a major risk factor for developing vascular calcification, several factors related to this disease were examined for their ability to induce ER stress in VSMCs.

3.4.4.1. Warfarin induces ER stress in rat aortas

In order to examine whether warfarin induces ER stress in VSMCs, aortic samples from warfarin-fed rats were collected and expression of Grp78 and Grp94 chaperones was examined by Western blotting and compared to that in rats fed a standard diet. Figure 3.8 shows that both chaperones were increased in warfarin fed rats and the change was statistically significant for Grp78 suggesting ER stress was activated in these aortas.

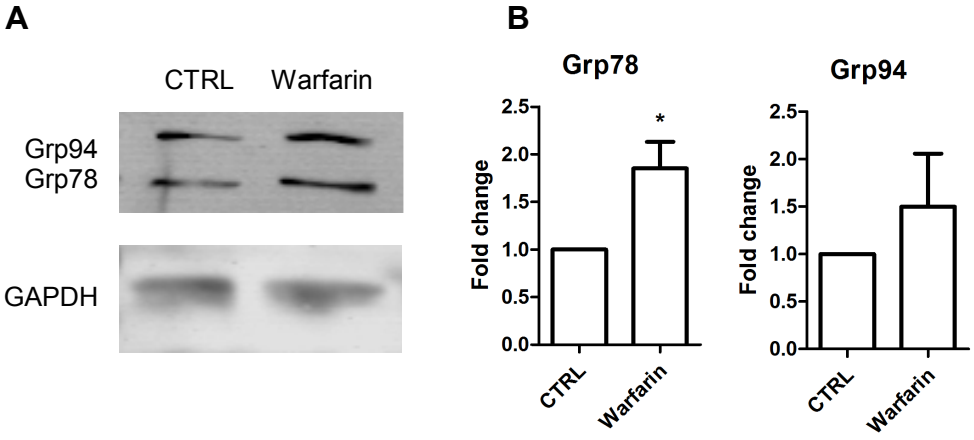

Figure 3.8. Expression of Grp78 and Grp94 chaperones in aortas of warfarin-fed rats. **A.** Western blotting for Grp78 and Grp94 chaperones, figure shows representative image. **B.** Quantification of Western blots. Graphs show mean with SEM, n=3, t-tests have been carried out to examine the statistical significance of observed changes, *denotes p values between 0.05 and 0.01.

Warfarin feeding is an established method of inducing vascular calcification in rats (Price *et al.* 1998; Atkinson *et al.* 2008). Therefore it was interesting to examine whether the increased Grp78 and Grp94 expression localised near calcified

areas of warfarin-fed rat aortas. Immunohistochemistry was carried out for these chaperones, as well as another ER stress marker ATF4 and osteogenic markers ALP and Osterix.

Figure 3.9 shows that expression of Grp78, Grp94 and ATF4 was higher in the warfarin-fed rat aorta compared to control. The expression of these ER stress markers was not limited to the calcified area, as increased staining was observed in the whole width of the vessel wall. In contrast, expression of Osterix and ALP in the vessel wall was similar in both groups of rats, but increased expression was observed around the calcified area.

These results confirm that ER stress chaperone expression was activated in VSMCs in the media of warfarin-fed rat aortas, and that this was accompanied by increased expression of Osterix and ALP in the calcified area, but not the whole of the vessel wall.

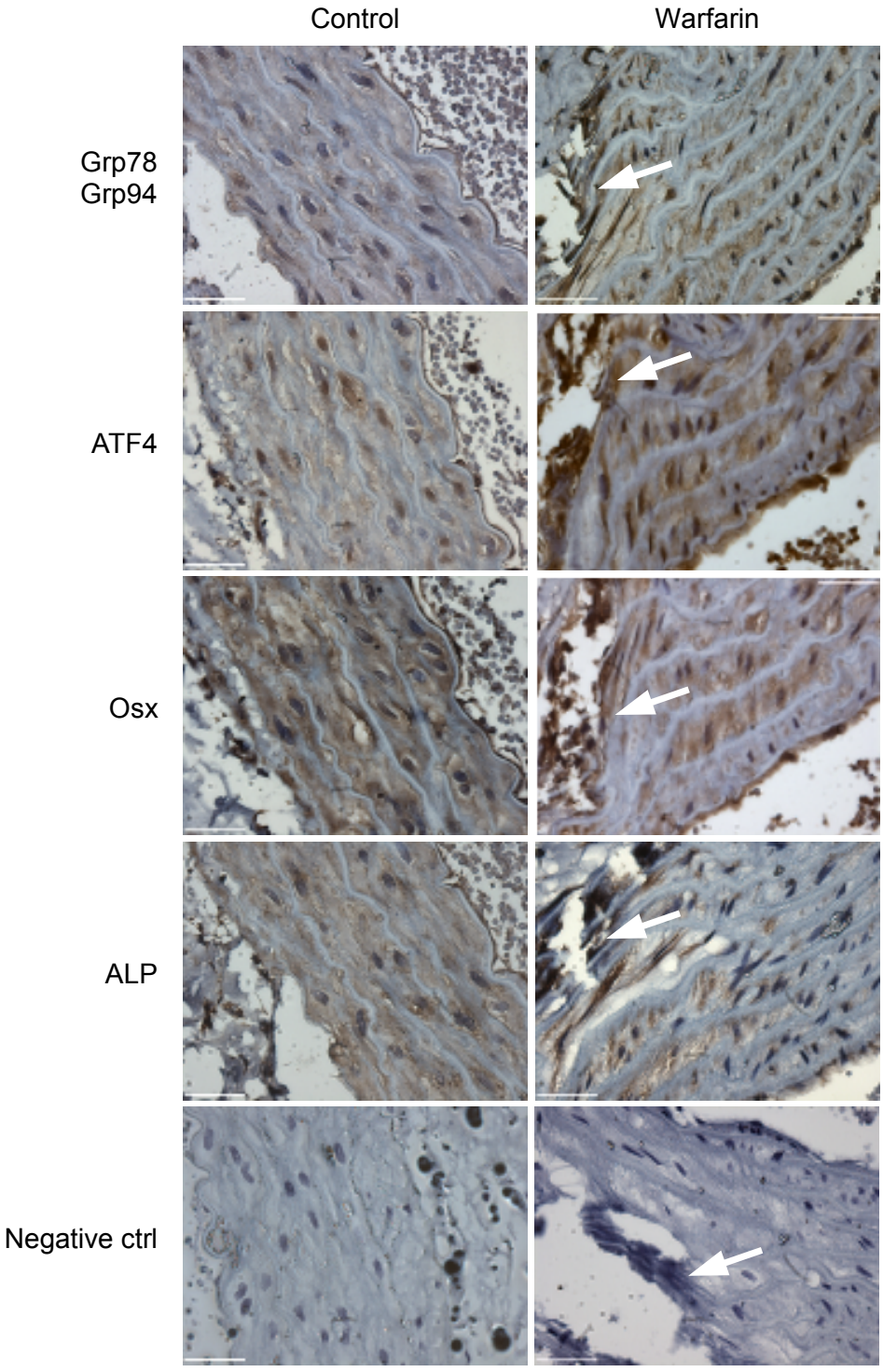

Figure 3.9. Localisation of osteogenic and ER stress markers in aortas of warfarin-fed rats examined by immunohistochemistry. Vessel sections were stained with primary antibodies and HRP-linked secondary antibodies, staining was developed with DAB (brown); the sections were then stained with hematoxylin to visualise nuclei (purple). Arrows point to calcified area in warfarin-fed rat aortas. Negative control – sections stained with secondary antibodies only. N=3, figure shows representative images. Scale bars are 2µm.

The next aim was to examine whether warfarin could also induce ER stress in human primary VSMCs *in vitro.* Cells were treated with a range of concentrations of warfarin, and expression of Grp78 and Grp94 was analysed using Western blotting. Figure 3.10 shows that warfarin increased the expression of both chaperones slightly. Expression of both chaperones was the highest in cells treated with 10µM warfarin (1.7 ± 0.3 fold increase in Grp78, 1.6 ± 0.8 fold increase in Grp94). 10µM is within the upper limit of the therapeutic range of 1.6µM to 9.7µM (Osinbowale *et al.* 2009). Even though the changes were consistent, they were not statistically significant for n=3 experiments.

The results in this subsection suggest that warfarin induces ER stress in rat VSMCs *in vivo* and possibly in human VSMCs *in vitro*.

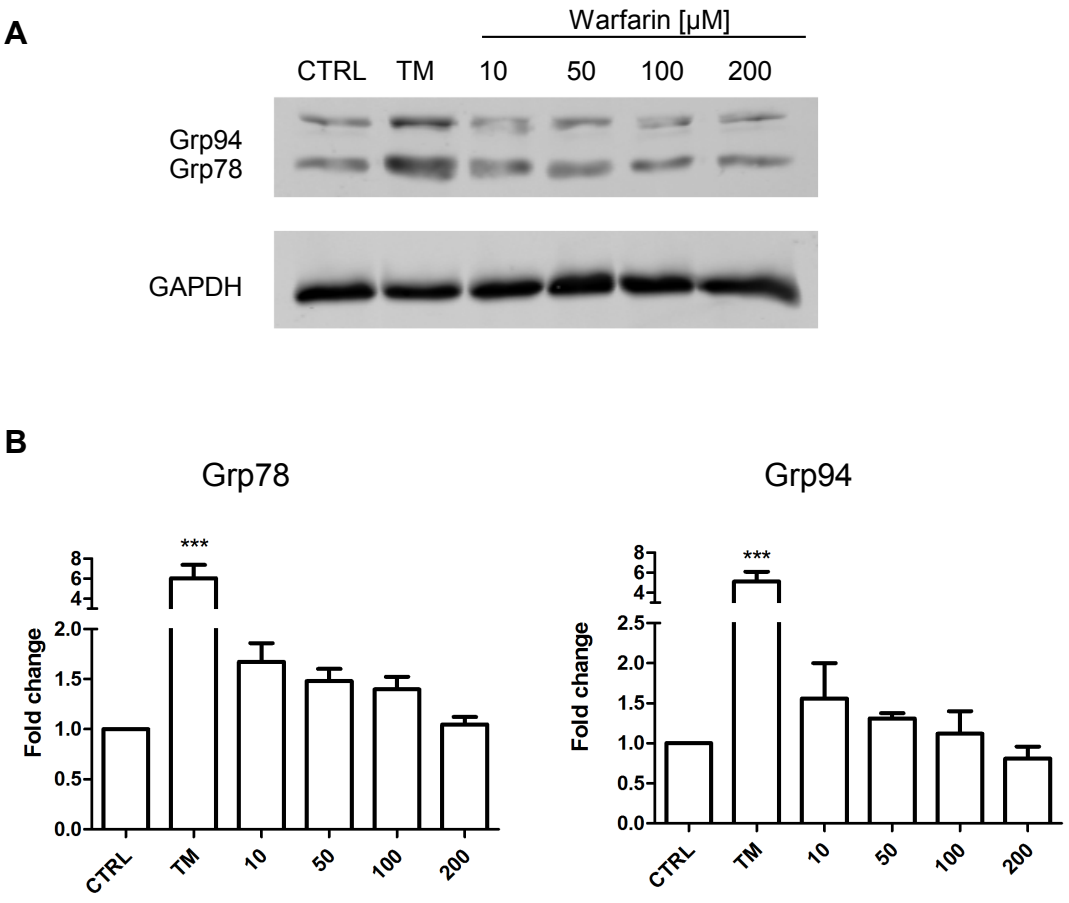

Figure 3.10. Expression of Grp78 and Grp94 chaperones in human primary VSMCs treated with warfarin or 0.2 µg/ml TM for 24 hours. **A.** Western blotting for Grp78 and Grp94 chaperones, figure shows representative image. **B.** Quantification of Western blots. Graphs show mean with SEM, n=3, ANOVA and Dunnett's *post hoc* tests have been carried out to examine the statistical significance of observed changes, ***denotes p<0.001.

3.4.4.2. Oxidative stress is a possible inducer of ER stress

In order to model oxidative stress *in vitro*, VSMCs were treated with hydrogen peroxide (H_2O_2), a source of the highly reactive hydroxyl radical (·OH) (Droge, 2002). Western blotting for Grp78 and Grp94 chaperones was carried out to examine whether oxidative stress can activate the expression of these ER stress markers.

First, a dose response experiment was conducted, with concentrations of H_2O_2 ranging from 2µM to 100µM (considered physiological; Mueller *et al.* 1997). It was observed that 10µM and 20µM H_2O_2 caused an increase in ER stress chaperone expression, and therefore these two concentrations were used for subsequent experiments (Figure 3.11.A). Further analysis revealed that 10µM H_2O_2 induced an average of 1.3±0.6 fold increase of Grp78 expression and a 1.7±0.6 fold increase in Grp94, and 20µM H_2O_2 induced 1.4±0.1 and 1.6±0.6 fold increase in Grp78 and Grp94, respectively (Figure 3.11.B). These results suggest that oxidative stress is a possible inducer of ER stress, but it is unknown why it did not induce Grp78 and Grp94 expression in all experiments.

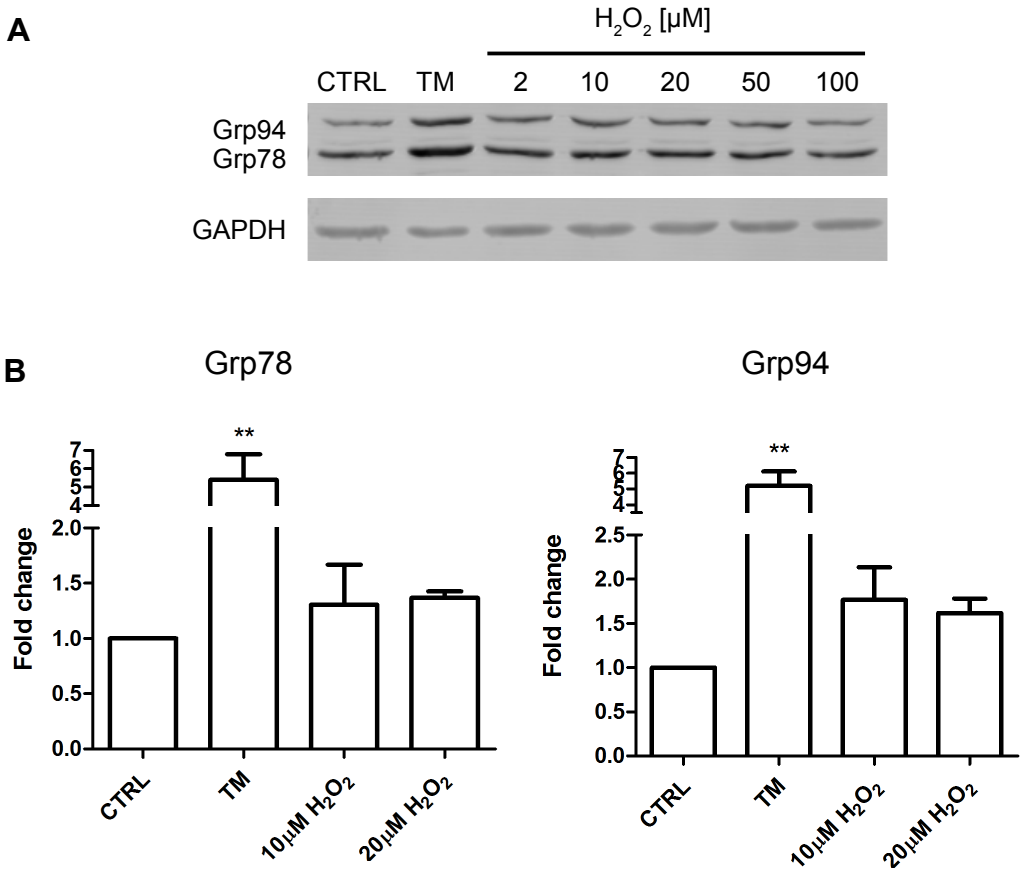

Figure 3.11. ER stress activation in cells treated with hydrogen peroxide (H_2O_2). VSMCs were treated with H_2O_2 or 0.4μg/ml tunicamycin (TM) in the presence of 0.5% FBS for 24h. **A.** Western blotting for Grp78 and Grp94 chaperones - dose response to H_2O_2, n=1. **B.** Quantification of Western blots repeated with just two concentrations of H_2O_2. Graphs show mean with SEM, n=3, statistical significance of changes was measured using ANOVA and Dunnett's *post hoc* test, ** denotes p between 0.01 and 0.001.

3.4.4.3. Hydroxyapatite is possibly an inducer of ER stress in VSMCs

The final potential inducer of ER stress signalling examined were HAp. Cells were treated with 50μg/ml or 150μg/ml HAp for 3 days, the concentration and time-point were used previously in literature to treat VSMCs (Ewence *et al.* 2008).

Western blotting results show that HAp induced an increase in both Grp78 and Grp94 expression at 50μg/ml (3.62±3.07 and 5.3±10.25 fold increases, respectively; Figure 3.12). The results were extremely variable and therefore the changes were not statistically significant. However, there was strong activation in some experiments, hence HAp could be an inducer of ER stress in VSMCs, even though the reasons for such variability are unknown.

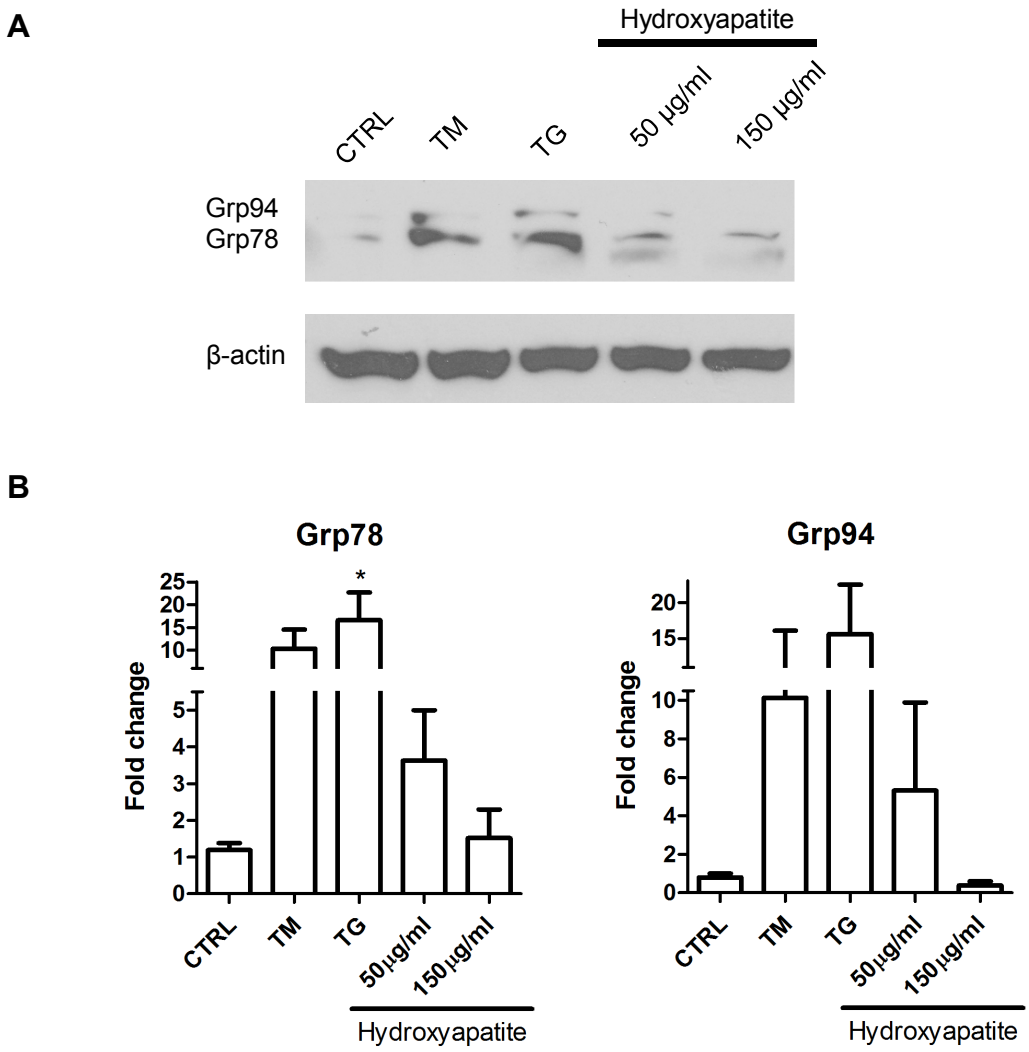

Figure 3.12. ER stress activation in cells treated with hydroxyapatite. VSMCs were treated with hydroxyapatite, 0.02µg/ml tunicamycin (TM) or 0.02µg/ml thapsigargin (TG) in the presence of 5% FBS for 3 days. **A.** Western blotting for Grp78 and Grp94 chaperones, representative image. **B.** Quantification of Western blots. All graphs show mean with SEM, n=3, statistical significance of changes was measured using ANOVA and Dunnett's *post hoc* test, * denotes p between 0.05 and 0.01.

Results presented in this subsection are summarised in Table 3.2. In addition to the mentioned factors, Vitamin D and high levels of calcium and phosphate ions were tested and found not to change the expression of examined ER stress markers markedly. However, it is evident that most of the calcification-related cytokines and CKD-related factors can induce ER stress marker expression in VSMCs. Most of these changes in ER stress marker expression are small but consistent increases.

Table 3.2. Calcification inducers tested for their ability to induce ER stress in VSMCs. Expression of Grp78 and Grp94 was analysed by Western blotting in VSMCs treated with each inducer. For some factors expression of additional ER stress markers (IRE1, PERK, ATF6, CHOP) was examined by real-time PCR. Table shows fold changes, statistically significant changes in expression are indicated with '*'.

Factor		Does it induce Grp78 and Grp94?		Does it induce other markers?
		Grp78	Grp94	
Cytokines	TGFβ	1.25±0.45	1.2±0.55	IRE1: 1.7±0.5 ATF6: 1.4±0.5 PERK: 1.3±0.2 ATF4*: 1.6±0.2 CHOP: 4.4±2.2
	PDGF	1.4±0.41	1.8±1.22	IRE1: 1.1+0.1 ATF6: 0.9±0.1 PERK: 0.9±0.1 ATF4: 1.1±0.3 CHOP: 1.0±0.1
	BMP-2	0.6±0.6	1.2±1.8	ATF6: 1.1±0.0 ATF4: 1.1±0.2 CHOP:1.1±0.0
	TNFα	1.6±0.9	2.2±1.5	IRE1*: 1.7±0.3 ATF6: 1.1±0.1 PERK: 1.2±0.24 ATF4: 1.3±0.1 CHOP: 0.8±0.1
CKD - related	Warfarin	1.7±0.3 – VSMCs 1.9*±0.5 - rat aorta	1.6±0.8 – VSMCs 1.5±1.0 - rat aorta	ATF4↑ (by immunohistochemistry)
	H_2O_2	10μM: 1.3±0.6 20μM: 1.4±0.1	10μM: 1.7±0.6 20μM: 1.6±0.6	Not examined
	HAp	3.6±3.1	5.3±10.3	Not examined
	Vitamin D	0.8±0.4	1.2±0.3	IRE1:1.2±0.2 ATF6: 1.2±0.3 PERK: 0.9±0.2 ATF4:1.6±0.4 CHOP: 1.6±0.4
	Ca+P	1.2±0.2	1.1±0.5	Not examined

3.5. Tunicamycin and thapsigargin increase expression of ER stress markers in VSMCs

Having established that ER stress is potentially associated with vascular calcification and that some calcification-inducing factors can activate ER stress in VSMCs *in vitro* it was important to model ER stress in VSMCs *in vitro* in order to examine its effect on known UPR components, calcification and mechanisms

regulating calcification. First, VSMCs were treated with tunicamycin and thapsigargin for 24 hours and expression of ER stress markers was analysed with quantitative real-time PCR. Results show that expression of all tested ER stress markers (IRE1, ATF6, PERK, together with ATF4 and CHOP, which are downstream targets of PERK) was elevated in VSMCs in response to thapsigargin treatment (Figure 3.13). Tunicamycin upregulated ATF6, ATF4 and CHOP mRNA expression, but did not change IRE1 and PERK expression, suggesting that there are differences in the mechanisms of UPR induction between tunicamycin and thapsigargin.

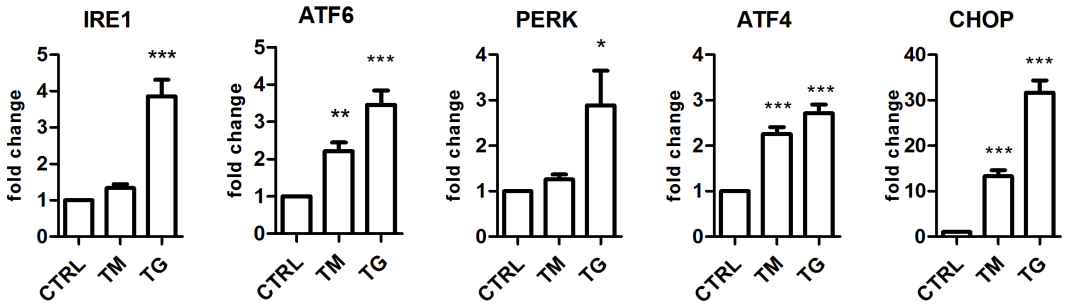

Figure 3.13. Quantitative real-time PCR analysis of ER stress activation in VSMCs. Cells were treated with 0.4µg/ml tunicamycin (TM) or 0.2µg/ml thapsigargin (TG) for 24 hours. N=3, ANOVA with Dunnett's *post hoc* tests were performed. Statistical significance is indicated with asterisks: * denotes p between 0.05 and 0.01, ** denotes p between 0.01 and 0.001, *** denotes p<0.001.

In order to further examine activation of the IRE1-mediated branch of the unfolded protein response, splicing of its downstream target XBP1 was examined. XBP1 splicing is indicative of ER stress and UPR activation. Figure 3.14 shows that XBP1 is spliced even under control conditions, since a faint band corresponding to the spliced PCR product is visible, which reflects the fact that under normal conditions some basal, 'maintenance' levels of ER stress are activated in VSMCs (Wu *et al.* 2006; Tsang *et al.* 2010). However, it is apparent that XBP1 splicing was induced by thapsigargin and to a lesser extent by tunicamycin, as the bands corresponding to spliced XBP1 become more pronounced.

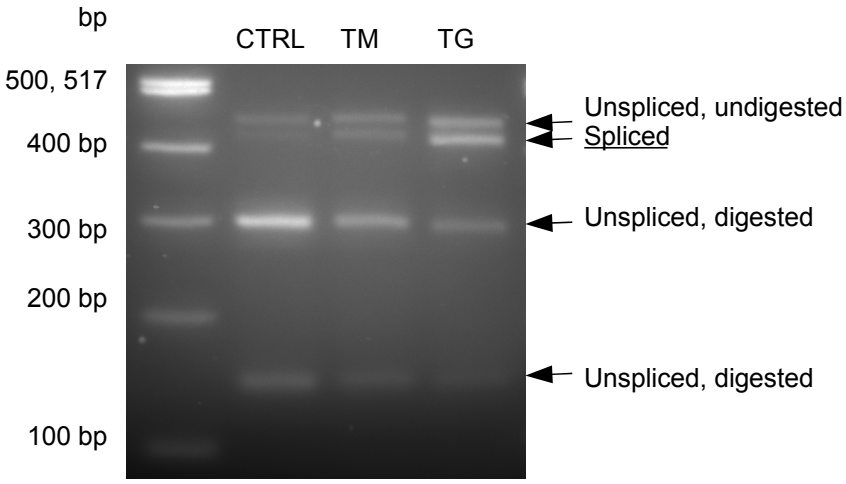

Figure 3.14. Analysis of XBP1 splicing in VSMCs treated with 0.4µg/ml tunicamycin (TM) or 0.2µg/ml thapsigargin (TG) for 24 hours. Tunicamycin and thapsigargin induce XBP1 splicing, a marker of ER stress. N=3, figure shows representative image.

To determine whether mRNA increases corresponded to increased ER stress measured by protein changes, Western blots were performed for the chaperones Grp78 and Grp94, which are downstream targets of all three UPR branches. Figure 3.15 shows that expression of both chaperones was increased by a 24 hour tunicamycin or thapsigargin treatment.

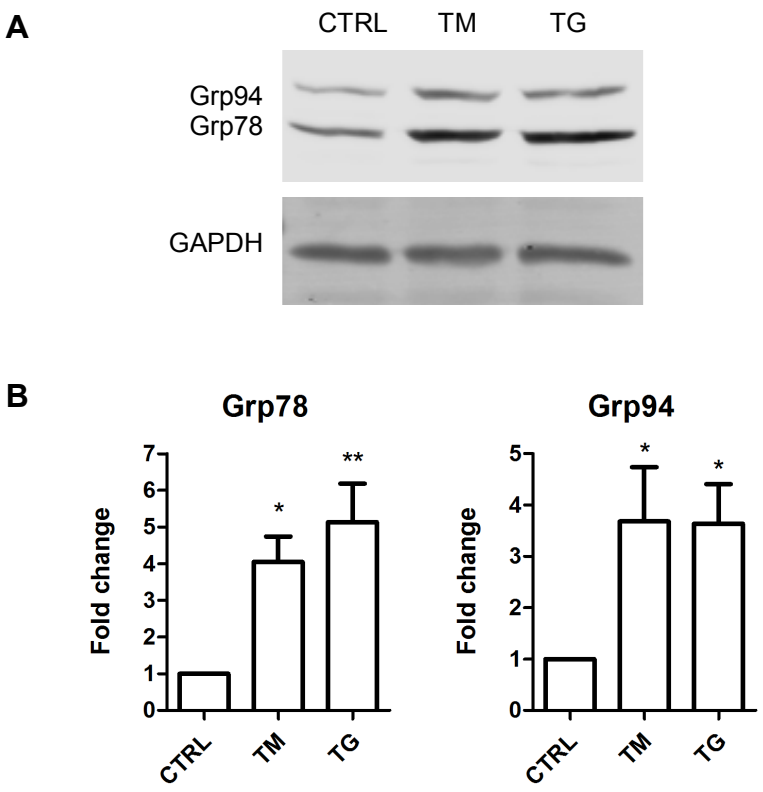

Figure 3.15. Western blotting analysis of Grp78 and Grp94 in response to ER stress in VSMCs treated with 0.4µg/ml tunicamycin (TM) or 0.2µg/ml thapsigargin (TG) for 24 hours**. A.** Representative Western blot showing increased levels of ER stress markers Grp78 and Grp94 as a result of TM and TG treatment. **B.** Quantification of the Western blots. Graph shows mean with SEM, n=8. Statistical significance was tested with ANOVA with Dunnett's *post hoc* tests; * denotes p between 0.05 and 0.01, ** denotes p values between 0.01 and 0.001.

In addition, as shown by immunocytochemistry in Figure 3.16, levels of ER Grp78 and Grp94 chaperones, ER stress transducers IRE1 and phosphorylated PERK (p-PERK) increased as a result of tunicamycin and thapsigargin treatments. Both IRE1 and PERK are localised in the ER membrane. In basal conditions p-PERK localised around the nucleus, and with tunicamycin and thapsigargin the staining was stronger both around the nucleus and in the cytoplasm. IRE1 showed similar nuclear staining at baseline, however upon ER stress treatment the staining became most intensive in a reticular area close to the nucleus, with little staining in the cytoplasm. The staining of both these ER stress transducers is consistent with their ER localisation. The ER is connected with the nuclear membrane and in VSMCs often spreads through the majority of the cell volume, this is illustrated by staining for

Grp78 and Grp94. Western blotting for ATF6, IRE1 and PERK, both total and phosphorylation-specific, was carried out, however it was unsuccessful, most likely due to low abundance of these proteins in VSMCs (data not shown).

Taken together, these changes are indicative of a comprehensive activation of all three unfolded protein response branches and their target genes in VSMCs.

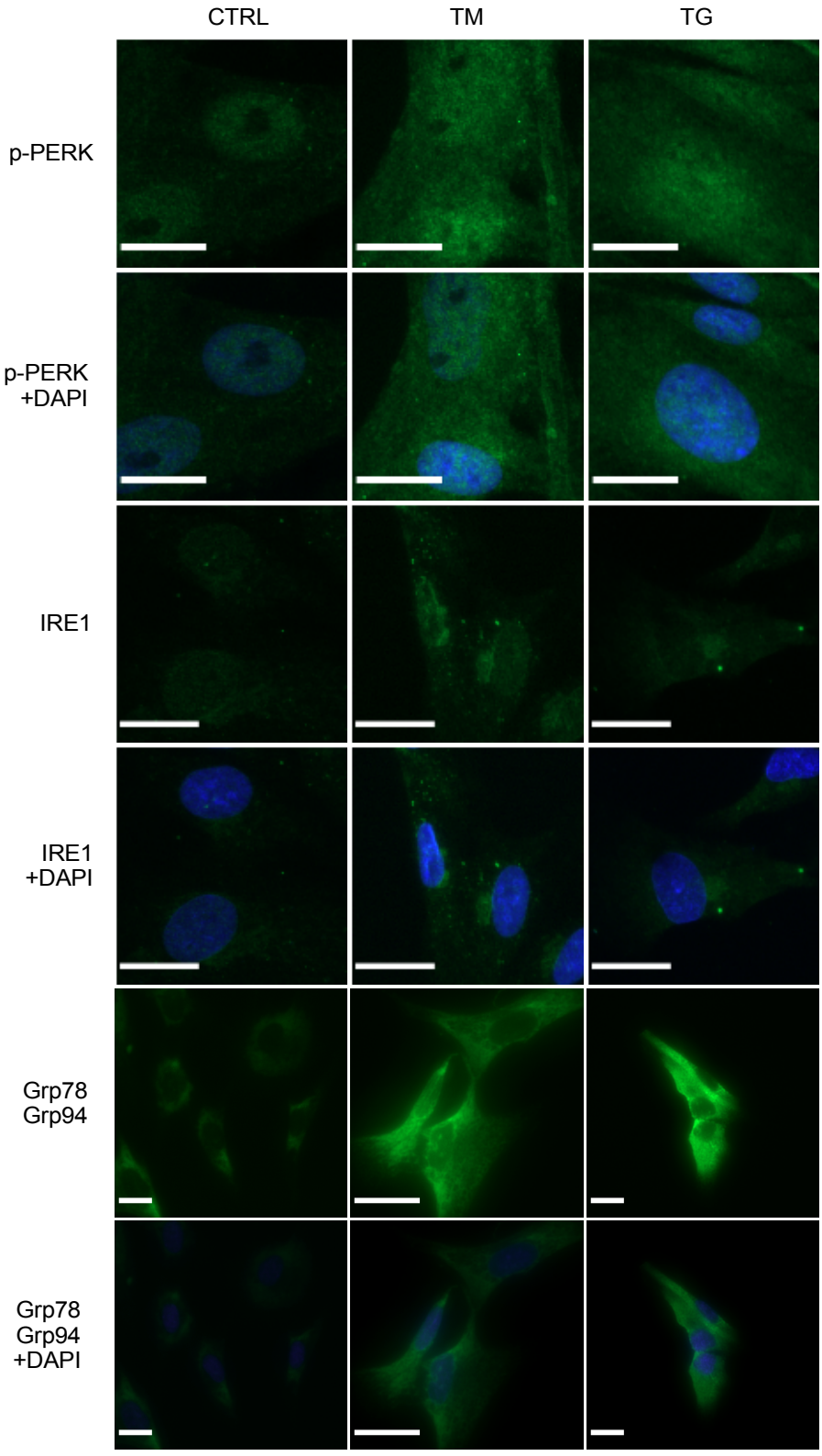

Figure 3.16. Increased levels of phosphorylated PERK (p-PERK), IRE1, Grp78 and Grp94 in response to ER stress treatment visualised by immunocytochemistry. VSMCs were treated with 0.4µg/ml tunicamycin (TM) or 0.2µg/ml thapsigargin (TG) for 24h. N=3, figure shows representative images. Scale bars are 20µm.

Next, I analysed changes in viability, caspase activation and necrosis in VSMCs in response to tunicamycin and thapsigargin treatments. The induction of cell death by the ER stress treatments could interfere with interpretation of subsequent experiments, as it would be impossible to determine whether effects of tunicamycin and thapsigargin are due to UPR signalling or the effect of apoptosis.

Figure 3.17.A shows the results of an MTT assay, where tunicamycin and thapsigargin decreased cell viability in a dose-dependent manner, with the highest concentrations tested (1µg/ml) causing a 60% drop in cell viability compared to untreated cells (for which viability was set as 100%) after a 24 hour incubation. Therefore in subsequent experiments concentrations that did not decrease viability were used - 0.2µg/ml thapsigargin and 0.4µg/ml tunicamycin.

The caspase activation and necrosis assay was performed in order to look at specific cell death pathways (Figure 3.17.B). The 24 hour incubation of VSMCs at baseline condition resulted in approximately 70% of cells being viable (CTRL sample). The addition of 0.2µg/ml thapsigargin and 0.4µg/ml tunicamycin significantly increased the percentage of healthy cells to >80%, via a decrease in apoptosis. The percentage of apoptotic cells was lowered by half. Tunicamycin and thapsigargin did not change the percentage of necrotic cells. Staurosporine (SSP), a known inducer of cell death (Bertrand *et al.* 1994) was used as a positive control and caused a marked increase in both apoptosis and necrosis. These results suggest that tunicamycin and thapsigargin did not induce cell death, but protected cells from apoptosis.

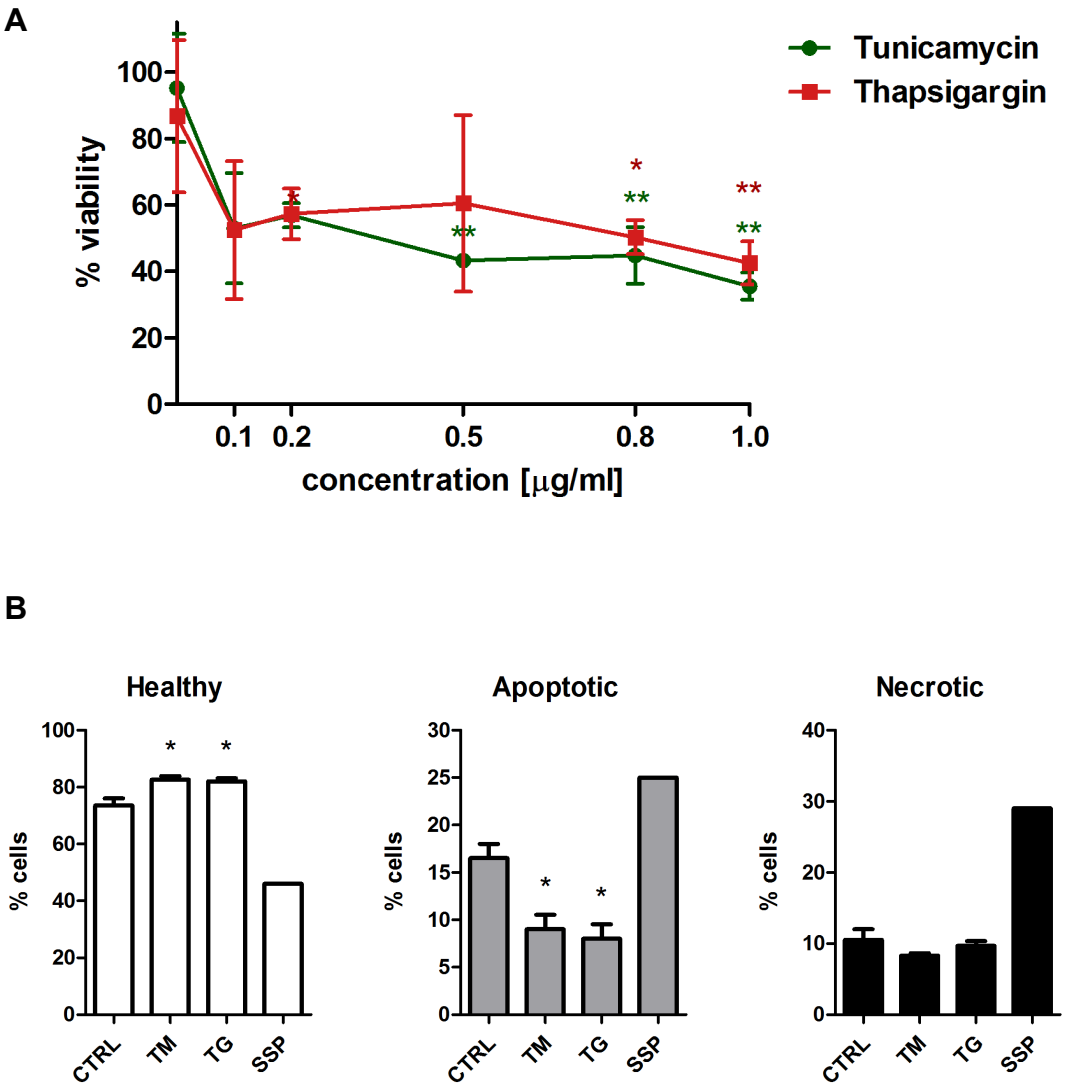

Figure 3.17. VSMC viability in response to ER stress. **A.** Tunicamycin and thapsigargin decrease VSMC viability dose-dependently. Cells were treated with tunicamycin or 0.2μg/ml thapsigargin for 16 hours in M199 with 2% FBS. **B.** TM and TG treatments decrease apoptosis. Cells were treated with 0.4μg/ml tunicamycin (TM) or 0.2μg/ml thapsigargin (TG) for 24 hours in 0.5% FBS with TM and TG for 3h with 0.5μg/ml staurosporine (SSP), caspase activation and necrosis was quantified with the NucleoCounter NC-3000. Graphs show mean with SEM, n=3 (except SSP, where n=1). Statistical significance was tested with ANOVA with Dunnett's *post hoc* tests; * denotes p between 0.05 and 0.01, ** denotes p between 0.01 and 0.001.

3.6. ER stress increases calcification of VSMCs *in vitro*

The next step was to examine whether induction of ER stress influenced calcification of VSMCs *in vitro*. A different treatment protocol was established for this experiment to reflect that vascular calcification is a process that happens over

time. Therefore VSMCs were treated for 8 days and lower concentrations of the ER stress inducers were used. Cells were treated with increased levels of Ca and P (2.7mM Ca^{2+}, 2.5mM PO_4^{3-}) to induce calcification and compared with control cells in medium with physiological Ca and P concentrations (1.8mM and 1mM, respectively) in the presence or absence of low concentrations of the ER stress inducers tunicamycin (0.02µg/ml), thapsigargin (0.01µg/ml) and the ER stress inhibitor PBA.

The optimal concentration of PBA was established based on a dose response experiment (Figure 3.18). Concentrations ranging from 0.05mM to 0.5mM were tested. 0.5mM PBA was chosen for further experiments as it was most effective in decreasing Grp94 expression, Grp78 did not change in this experiment. Higher concentrations were not tested because they were likely to be toxic. There is no literature on the use of PBA in human primary VSMCs, the studies that mention the use of this compound treated rat VSMCs with 5mM PBA, but for a 1 hour treatment (Liu *et al.* 2011b). Therefore for a longer time-point to treat the more sensitive human VSMCs I tested lower concentrations.

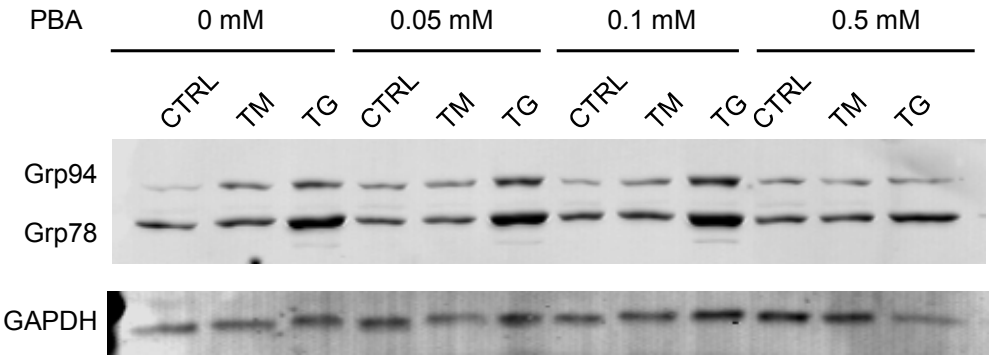

Figure 3.18. Attenuation of ER stress by 4-phenylbutyric acid (PBA). Western blot showing levels of ER stress markers Grp78 and Grp94 in VSMCs treated with 0.02µg/ml tunicamycin (TM) or 0.01µg/ml thapsigargin (TG) and 0-0.5mM PBA in M199 with 5% FBS for 5 days, n=1.

Alizarin Red S staining of cells treated with calcifying conditions (Figure 3.19.A) showed that VSMCs did not calcify when treated with tunicamycin and thapsigargin alone. However in the presence of high Ca and P calcification was increased by the addition of tunicamycin and thapsigargin. This effect was blocked by the ER stress inhibitor PBA.

These results were confirmed by quantification of calcium levels using the o-cresolphthalein assay (Figure 3.19.B). Tunicamycin and thapsigargin alone did not cause a significant increase in calcification. PBA alone and in combination with tunicamycin, thapsigargin and Ca and P did not cause any changes in calcification compared to the control samples (data not shown). Treatment with Ca and P induced calcification (Figure 3.19.B). In the presence of Ca and P tunicamycin induced a 60-fold increase in calcification; this was reduced by PBA by half. In the presence of Ca and P thapsigargin induced a 120-fold increase in calcification. PBA was able to reduce this increase in calcification to approximately 50-fold.

In summary, both tunicamycin and thapsigargin increased calcification of VSMCs in the presence of high Ca and P, and PBA was able to reduce these effects by approximately 50%, suggesting that ER stress can promote calcification in these conditions.

A

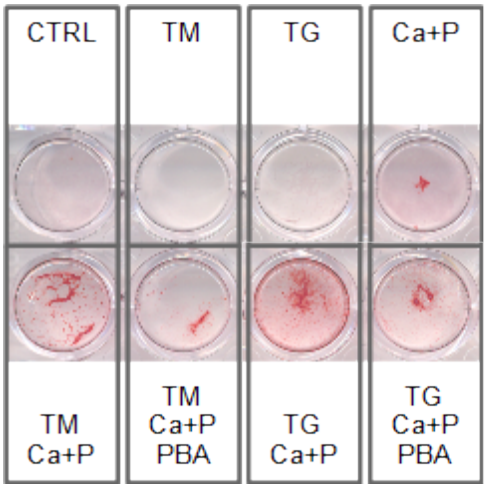

B

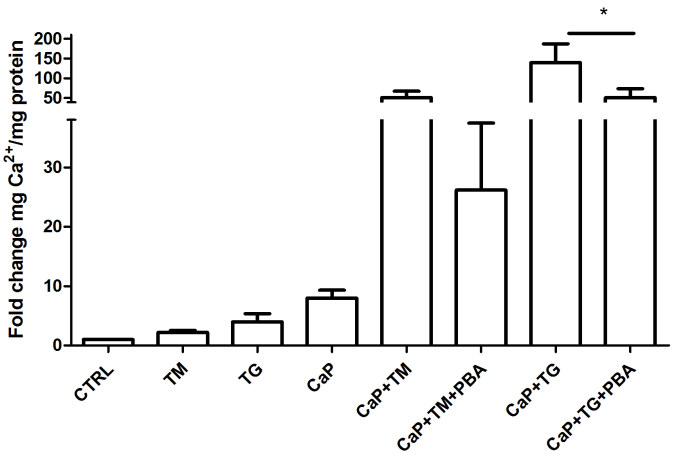

Figure 3.19. ER stress increases calcification of VSMCs. Cells were treated with 2.7mM Ca^{2+}, 2.5mM PO_4^{3-} (CaP), 0.04µg/ml tunicamycin (TM) or 0.01µg/ml thapsigargin (TG), 0.5mM PBA for 8 days in M199 with 5% FBS. **A.** Alizarin Red S staining of VSMCs. **B.** Calcification quantified with the o-cresolphthalein assay. Graph shows mean with SEM, n=5. Statistical significance was tested with ANOVA with Tukey's *post hoc* tests; * denotes p between 0.05 and 0.01. Only relevant comparisons are indicated.

The next step was to examine the effect of the calcification treatments on cell death, since apoptosis is a well-established mechanism contributing to vascular calcification. Figure 3.20 shows that at baseline, after 8 days in treatment conditions cell viability was low, i.e. about 70% of cells had undergone necrosis and apoptosis. This was in stark contrast to the 24 hour time-point, where only around 30% cells were apoptotic or necrotic (Figure 3.17).

Tunicamycin and thapsigargin alone caused only a small and insignificant increase in caspase activation, and did not change the percentage of necrotic cells. High Ca and P treatment did not change the percentage of healthy cells, but changed the ratio of apoptotic and necrotic cells, with a significant increase in necrosis. PBA alone and in combination with tunicamycin, thapsigargin and Ca and P did not cause any changes in cell death rates compared to the control samples (data not shown).

In the presence of Ca and P tunicamycin did not cause a significant change in cell death, and the addition of PBA had no effect on cell viability. However, thapsigargin decreased apoptosis in the presence of Ca and P and increased the percentage of healthy cells. This would suggest that thapsigargin can protect the cells from apoptosis. PBA did not counter this effect.

Importantly, cell death rates were the same in pairs of samples treated with TM versus TM with PBA in the presence of Ca and P, and in corresponding TG treated samples, where differences in calcification levels were observed (Figure 3.19). This means that decreasing ER stress with PBA protected VSMCs from calcification, but not cell death. Therefore the differences in calcification levels between these pairs of samples cannot be attributed to changes in cell death rates. This suggests that cell death is not a mechanism by which ER stress increased calcification.

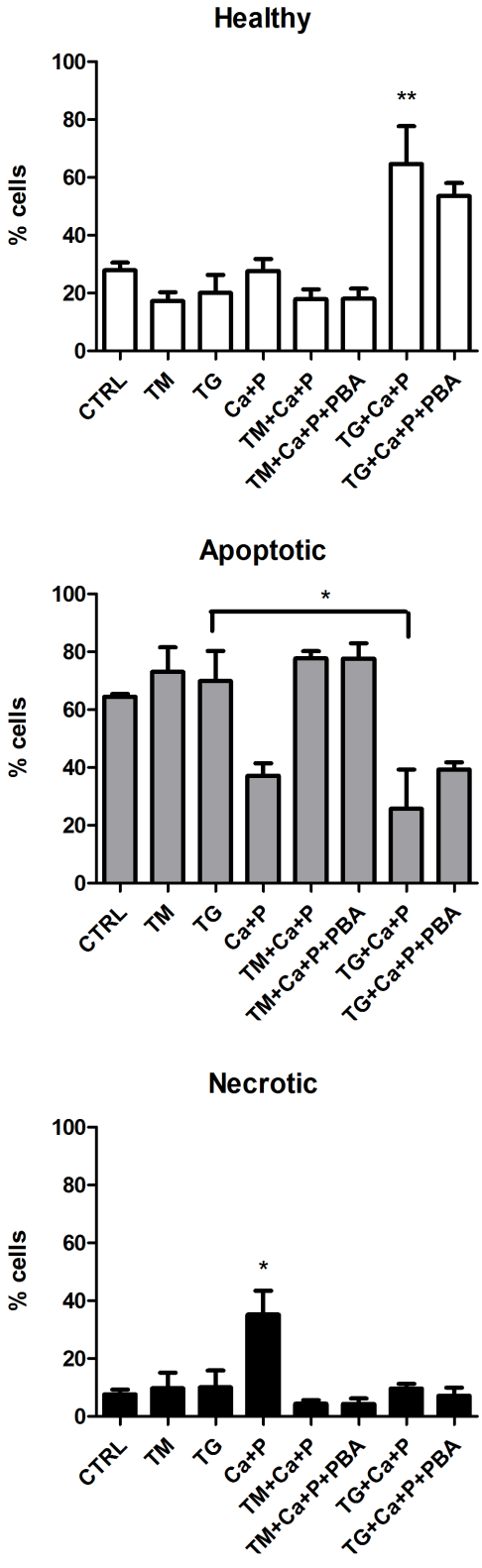

Figure 3.20. The effect of ER stress on caspase activation and necrosis in calcifying VSMCs; measured with the NucleoCounter NC-3000. Cells were treated with 2.7mM Ca^{2+}, 2.5mM PO_4^{3-}, 0.04µg/ml tunicamycin (TM) or 0.01µg/ml thapsigargin (TG), 0.5mM PBA for 8 days in M199 with 5% FBS. Graph shows mean with SEM, n=3. Statistical significance was tested with ANOVA with Tukey's *post hoc* tests; * denotes p between 0.05 and 0.01, ** denotes p between 0.01 and 0.001.

3.7. Discussion

3.7.1. Vascular calcification is associated with changes in ER stress marker expression

In the first part of this chapter I showed that expression of ER stress markers was decreased in fatty streak and calcified human aortic samples compared to healthy. Expression of ER stress markers has never been measured in human aortas before. Studies that examined ER stress activation in the context of VSMC calcification either showed the expression of ER stress markers in cells *in vitro* (Masuda *et al.* 2012, 2013 show increased PERK, ATF4, CHOP expression and XBP1 splicing; Liberman *et al.* 2011 – increased levels of Grp78, p-IRE1 and spliced XBP1) or in rat aortas (Duan *et al.* 2009, 2013 – Grp78, Grp94, PERK, ATF4 and CHOP expression). These studies, contrary to my results, demonstrated that calcification was associated with increased ER stress. However, it is difficult to draw any conclusions from comparing animal studies with my results. In animal models vascular calcification was induced by high dose vitamin D and nicotine. It is impossible to tell how relevant this model is to naturally occurring calcification.

Expression of osteogenic markers in the same human aortic samples was in most cases decreased in fatty streak samples compared to control vessels and increased again to the level of healthy vessels in calcified aortas. The fatty streak represents an earlier stage of atherosclerosis that can progress into calcified lesions (Berliner *et al.* 2005). There is no literature on osteogenic gene expression in fatty streak vessels. Increased expression of osteogenic markers in calcified human aortas is well documented (Shanahan *et al.* 1999a; Tyson *et al.* 2003) and thought to be an indicator of their osteogenic differentiation.

Further analysis of my results showed that expression of osteogenic markers significantly correlated with ER stress markers in healthy and fatty streak but not in calcified aortas, which is a completely novel finding. These results strongly suggests that in the initial stages of vascular disease ER stress regulates osteogenic gene expression in VSMCs. A major limitation of these experiments was the fact that gene expression was analysed only at the mRNA level, and thus might not be

consistent with changes in protein expression. What is more, even though the aortic wall is mainly built of VSMCs, the samples likely have some contributions from endothelial cells and macrophages which might skew the results, as these cell types have been shown to activate ER stress in various circumstances (Sanson *et al.* 2009; Orso *et al.* 2011).

All in all, these results suggest that ER stress regulates expression of osteogenic genes in the initial stages of vascular disease, but that vascular calcification was associated with a decrease in ER stress marker expression in the vessel wall.

3.7.2. Calcification-promoting factors induce ER stress in VSMCs *in vitro*

In order to better understand the relationship between vascular calcification and ER stress it was important to examine whether known calcification-promoting factors can change ER stress marker expression in human primary VSMCs *in vitro*. First, I tested a range of cytokines which are reported to regulate VSMC phenotype or promote vascular calcification in the literature.

I began with TGFβ and PDGF as these two cytokines are known to have opposing effects on the phenotype of VSMCs. TGFβ increased ATF4 and CHOP mRNA expression. In VSMCs *in vitro* the effects of TGFβ are concentration dependent. At low concentrations, consistent with my experiments, it blocks proliferation and promotes the contractile phenotype (Hirschi *et al.* 1998), and unpublished results from our laboratory show that it inhibits calcification of VSMCs. At higher concentrations TGFβ mainly acts by stimulating growth and extracellular matrix production, and has been shown to promote vascular calcification (Orlandi *et al.* 1994; Simionescu *et al.* 2005). As far as ER stress signalling is concerned, in osteoblasts TGFβ has been shown to suppress ATF4 activity by increasing vimentin expression (Lian et al. 2012), but in lung fibroblasts it increased ER stress via ROS production, which in turn stimulated their myofibroblast differentiation (Baek *et al.* 2014). These studies suggest that the effects of TGFβ are context-dependent and the same pathways might have different effects in different cell types. They also suggest that ER stress is activated only in differentiated VSMCs. This is consistent

with my results from human aortas showing that ER stress marker expression decreases as the vessels progress towards calcification and perhaps become dedifferentiated.

Large variation was observed in results from experiments testing different inducers of ER stress. In each repeat of the experiment the inducers caused a change in the same direction, but to a different extent. This suggests that some of the changes did not reach statistical significance because of low n numbers.

PDGF, which induces proliferation and migration of VSMCs, did not induce ER stress in my experiments. This was consistent with the study by Yi and colleagues, who treated cells with PDGF and showed that it did not induce XBP1 splicing or Grp78 and Grp94 chaperones. They also showed that tunicamycin inhibited PDGF signalling in rat primary VSMCs (Yi *et al.* 2012). This suggests that in VSMCs PDGF does not act via the UPR.

Next, I went on to examine whether BMP-2 induced ER stress in VSMCs and I found that it did not. This is in contrast to the findings of Liberman and colleagues, who showed that BMP-2 induced ER stress via oxidative stress, as mentioned above (Liberman *et al.* 2011). In addition, in my experiments BMP-2 was not able to increase the expression of osteogenic genes (data not shown). Research has shown that BMP-2 can increase expression of osteogenic genes, among others Runx2, in VSMCs and thus promote calcification (Chen *et al.* 2006; Li *et al.* 2008). The inconsistency with my results might be explained by the fact that Chen and colleagues used bovine VSMCs and Li *et al.* used twice as much BMP-2 and in both studies VSMCs were treated for longer time-points. A potential issue with my results is that I did not examine a positive control for BMP-2 effects, which would indicate that BMP-2 was active in these treatments. I should have analysed SMAD1 and SMAD5 phosphorylation in order to be sure.

The inflammatory cytokine TNFα significantly upregulated IRE1 mRNA expression. As TNFα promotes calcification, these findings could be a potential mechanism that implicates ER stress in calcification. My results are partially in line with research published by Masuda and colleagues (Masuda *et al.* 2013), who found that TNFα triggered ER stress in mouse VSMCS. However, they report activation of

the PERK, rather than IRE1, branch of the UPR. Again, the difference could be due to the effect of TNFα on ER stress signalling being species-specific. In addition, my experiments were limited to mRNA expression and Western blotting for Grp78 and Grp94 chaperones, which are activated by all three branches, therefore further experiments are needed to explain this difference.

Next, I tested a range of conditions relevant to CKD, as it is one of pathological contexts in which vascular calcification is highly prevalent.

Warfarin, which is administered to dialysis patients, induces expression of ATF4, Grp78 and Grp94 in rat aortas. Experiments with human VSMCs treated with warfarin showed a trend towards an increase of Grp78 and Grp94 expression, indicative of ER stress activation. It seems there would be an obvious link between warfarin treatments and ER stress, as warfarin inhibits carboxylation of proteins, which happens in the ER (Rost *et al.* 2004), and that might be expected to induce ER stress by a mechanism similar to tunicamycin, causing uncarboxylated proteins to accumulate. However, these two processes have not been connected. In addition, it is interesting to note that by immunohistochemistry warfarin increased expression of the ER stress chaperones and ATF4 in the whole vessel wall, but ALP or Osterix only in the calcified area. This is consistent with results from calcified human aortas presented in this chapter because it suggests an uncoupling of ER stress and osteogenic gene expression in calcification in an *in vivo* setting

Hydrogen peroxide treatments did not consistently induce ER stress in VSMCs. Liberman and colleagues (Liberman *et al.* 2011) have found that in human primary coronary artery SMCs oxidative stress induced ER stress, observed as IRE1 phosphorylation, XBP1 splicing and Grp78 expression. However, the authors used BMP-2 to increase ROS production, not hydrogen peroxide and coronary artery VSMCs as opposed to aortic cells in my experiments. Therefore the differences in the results could be due to a different mode of activating oxidative stress and the fact that cells from different vascular bed are known to have different properties (Zhang *et al.* 2014; Leroux-Berger *et al.* 2011). A potential explanation for the variability in my results was the lack of a positive control for oxidative stress, which means I could not confirm whether oxidative stress was indeed activated in each of

the experiments. I carried out Western blotting for hyperoxidised peroxiredoxin, but the antibody did not work (data not shown). Therefore, it is difficult to draw conclusions about oxidative stress and ER stress in VSMCs.

HAp crystals, the endpoint of the process of calcification, were examined for their ability to induce Grp78 and Grp94 expression. I have shown that treatment with synthetic HAp did not consistently increase the expression of these chaperones. The reason why in some experiments an increase was observed, whereas in some they did not change might be due to technical issues, as the crystals are a suspension rather than solution and therefore it is difficult to consistently apply the same amount. In addition, calcium phosphate crystal preparations have been shown to be quite heterogenous with respect to the size of crystals, which might also explain their different effect on cells (Motskin *et al.* 2009). Calcium phosphate particles have been shown to induce osteogenic gene expression and cell death in VSMCs (Ewence *et al.* 2008; Sage *et al.* 2011), but whether they do so via ER stress remains inconclusive. It is also worth noting that the calcium phosphate particles used in the studies mentioned above might have had different properties than the synthetic hydroxyapatite from Sigma, with respect to particle size and calcium to phosphate ratio within the crystals.

Mineral dysregulation, common in dialysis patients with CKD, in my experiments modelled by treating VSMCs with high concentrations of Ca and P, did not induce Grp78 and Grp94 expression. This is in contradiction to the findings of Duan et al. (2013), who have shown that treatment of rat primary VSMCs with similar levels of Ca and β-glycerophosphate as a phosphate donor induced Grp78, Grp94, PERK, ATF4 and CHOP expression. In my experiments I only looked at Grp78 and Grp94 chaperone expression, and not other UPR components. However, these chaperones are activated downstream of all three UPR branches (Wang *et al.* 1998; Wang *et al.* 2000; Luo *et al.* 2003) and therefore serve as a good indicator of ER stress in cells. Based on that I can conclude in human VSMCs high Ca and P treatment does not induce ER stress.

The final CKD-related factor tested was vitamin D. In my experiments I demonstrated that it does not induce Grp78 and Grp94 chaperone expression, or

mRNA of other ER stress markers. In fact there was a trend of vitamin D decreasing ER stress. My results were consistent with the only existing study linking ER stress and vitamin D, which shows that in macrophages similar concentrations of vitamin D attenuate ER stress and thus promote their anti-atherogenic phenotype (Riek *et al.* 2012).

3.7.3. ER stress enhances calcification of VSMCs *in vitro*

To further examine the connection between ER stress and calcification in VSMCs I modelled ER stress *in vitro*. The results show that ER stress can be induced in human primary VSMCs *in vitro* by tunicamycin and thapsigargin and that all three branches of the UPR were activated.

The expression of ER stress markers was activated to a different extent by the two ER stress inducers. Differences in activation of the UPR branches by tunicamycin and thapsigargin have not been studied, but research shows that in VSMCs these two compounds can have different effects on expression of other genes, for example iNOS, and the fact was attributed to the different mechanisms of action of the two inducers (Ohta *et al.* 2011).

In calcification assays the addition of ER stress inducers enhanced VSMC calcification. This is consistent with existing literature showing that increased ER stress leads to calcification (Masuda *et al.* 2012, 2013; Liberman *et al.* 2011; Duan *et al.* 2009, 2013) and suggests that in my experiments ER stress activated mechanisms that lead to calcification. In these experiments tunicamycin and thapsigargin differed in their ability to promote calcification, with thapsigargin increasing calcification more. This suggests that the two inducers might activate different pathways leading to calcification.

One potential mechanism leading to vascular calcification is apoptosis. Duan and colleagues (Duan *et al.* 2013) have shown that calcification of rat VSMCs was associated with ER stress-dependent apoptosis. However, my results show that cell death was not involved in ER stress-enhanced calcification. On the contrary, I demonstrated that thapsigargin decreased the rate of apoptosis. In addition, high levels of Ca and P induced more necrosis alone than in the presence of tunicamycin

and thapsigargin. These results suggest that ER stress protected the cells from cell death. This inconsistency with the study mentioned above might be due to the fact that a different species of cells and a different inducer was used (rat cells and high Ca and P versus human cells and tunicamycin and thapsigargin).

3.7.4. Conclusions

To summarise, in this chapter I showed that vascular calcification is associated with changes in ER stress marker expression. I demonstrated that ER stress can be activated in VSMCs *in vitro* and that it increased calcification in the presence of Ca and P. I also showed this was not associated with increased apoptosis, and that ER stress decreased Ca and P induced cell death. Following from that I examined potential inducers of calcification for their ability to induce ER stress and found that ER stress is activated by factors that both inhibit (TGFβ) or promote (TNFα, warfarin) calcification, suggesting that the connection between ER stress and vascular calcification is complex.

My results also demonstrate that many of the tested ER stress inducers caused a small but consistent increase in ER stress marker expression. This could reflect the fact that a single factor that induces ER stress strongly might not exist, just as no condition in the body is characterised by a change in just one parameter. Vascular calcification is a complex process and is caused by an interplay of a host of factors, each contributing a little. It is therefore likely a host of factors can modulate ER stress, each only to a degree.

In this chapter I explored apoptosis as a mechanism which could mediate ER-stress induced calcification and found that it was not involved. Since expression of osteogenic genes correlated with expression of ER stress markers in human aortas I wanted to explore whether ER stress can influence expression of osteogenic genes in VSMCs *in vitro* and modulate their phenotype.

Chapter 4: ER stress regulates osteo/chondrogenic gene expression in VSMCs

4.1. Introduction

In the previous chapter I established that ER stress increases calcification of VSMCs i*n vitro* in association with a key calcification inducer, such as high Ca and P levels, and that some factors that promote vascular calcification can induce ER stress. This suggests that ER stress might be a component regulating calcification, but is not capable of inducing it alone. I have also shown that changes in calcification in response to ER stress did not involve apoptosis. Expression of osteogenic markers correlated with ER stress markers in healthy and fatty streak vessels but not in calcified aortas. These results suggested that osteo/chondrogenic differentiation of VSMCs could be linked to ER stress signalling and therefore involved in ER stress-regulated VSMC calcification.

4.1.1. Osteo/chondrogenic differentiation of VSMCs

Osteo/chondrogenic differentiation is a result of phenotypic transition of VSMCs. In the vessel wall VSMCs do not differentiate terminally and show phenotypic plasticity. They regulate vascular tone and exist as contractile cells expressing proteins such as SM22α, calponin and myosin, which are proteins associated with the contractile function (Shanahan *et al.* 1993; Shanahan *et al.* 1998). In response to stress and injury VSMCs can proliferate, migrate and secrete ECM proteins, decrease expression of contractility-related genes, and thus they are able to repair the vessel (Shanahan *et al.* 1998; Shanahan *et al.* 1993). In conditions when injury is persistent the phenotypic transition is dysregulated and VSMCs can undergo an unfavourable transdifferentiation into cells with characteristics of osteoblasts or chondrocytes (Iyemere *et al.* 2006). During this process they start expressing osteo/chondrogenic markers (Shanahan *et al.* 1999b; Speer *et al.* 2009). The observation that VSMCs in calcifying blood vessels undergo a phenotypic change to osteoblast/chondrocyte-like cells has led to the idea that vascular

calcification is caused by pathological induction of a process similar to bone formation, which normally only occurs during bone development in the embryo.

4.1.2. ER stress regulates osteo/chondrogenic gene expression in osteoblasts and chondrocytes

Components of all three branches of the UPR (mediated by ER stress transducers IRE1, ATF6 and PERK) have been implicated in transcription of a number of bone specific genes, which have been shown to be involved in vascular calcification.

For example, BMP-2 can activate IRE1 signalling, which results in increased XBP1 expression, and IRE1α and XBP1 are required for maturation of preosteoblasts to osteoblasts. XBP1 also directly activates the promoter of Osterix (Tohmonda *et al.* 2011) and it was shown to be a transcription target of ATF6 in BMP-2 stimulated chondrocytes and to form a complex with Runx2 (Liu *et al.* 2012).

BMP-2 was shown to upregulate CHOP, PERK, ATF4 and ATF6 expression in osteoblasts (Tohmonda *et al.* 2011). A different study, also in osteoblasts, showed that Runx2 activated expression of ATF6, and that ATF6 directly induced transcription of OCN) (Jang *et al.* 2011), suggesting that there is a positive feedback loop between ER stress and osteogenic gene expression.

Knock-outs of PERK and ATF4 in mice cause skeletal dysplasias at birth and postnatal growth retardation (Yang *et al.* 2004b; Saito *et al.* 2011). Furthermore, ATF4 was shown to directly activate transcription of OCN and Ihh (Wang *et al.* 2009).

In addition to the three canonical ER stress transducers (IRE1, ATF6 and PERK) and their signalling pathways, two tissue-specific ER stress transducers OASIS and BBF2H7 have been shown to be involved in osteoblast and chondrocyte maturation, respectively (Murakami *et al.* 2009; Saito *et al.* 2009). Expression of OASIS is induced by BMP-2 signalling in osteoblasts and it activates the transcription of the collagen type 1 gene. Expression of BBF2H7 is induced in chondrocytes by Sox9, the main chondrogenic transcription factor (Hino *et al.* 2014). BBF2H7 activates transcription of Sec23a, a component of the protein coat of secretory

COPII vesicles, which are crucial for secretion of ECM (Saito *et al.* 2009). These two ER stress transducers have not been shown to be expressed in VSMCs.

4.1.3. ER stress in osteogenic differentiation of VSMCs

It is evident that ER stress signalling via the canonical UPR pathways as well as tissue-specific ER stress transducers play a major role in bone formation. Therefore, drawing on the similarities between bone formation and osteo/chondrogenic differentiation of VSMCs, I hypothesized that the UPR is involved in regulating expression of osteo/chondrogenic genes in VSMCs.

Existing studies of ER stress in vascular calcification seem to point to an important role for ATF4 in this process. It has been shown that ATF4 knock-down in mouse VSMCs decreased stearate-induced calcification and expression of OCN, ALP and Pit-1 (Masuda *et al.* 2012). Another study has shown that knock-downs of PERK, ATF4 and CHOP decreased calcification of mouse VSMCs induced by TNFα, and that it was accompanied by a decrease in osteogenic markers Pit-1, OCN, OPG, Osterix, Runx2, and ALP (Masuda *et al.* 2013). In addition, in rat VSMCs, ATF4 knock-down decreased expression of OPN, OCN and Runx2 and ALP activity (Duan *et al.* 2013). Finally, in the only study in human cells, XBP1 was shown to bind and activate the Runx2 promoter in BMP-2-treated coronary artery VSMCs (Liberman *et al.* 2011). However, none of these studies present an in-depth analysis of the UPR component activation or osteogenic gene expression in VSMCs.

In this chapter I set out to characterise the expression of osteo/chondrogenic genes in tunicamycin- and thapsigargin-treated human primary VSMCs *in vitro* and to investigate the effect of specific UPR component knock-downs on the expression of these genes.

4.2. ER stress regulates VSMC phenotype *in vitro*

4.2.1. Regulation of osteogenic gene expression

VSMCs were treated with tunicamycin and thapsigargin for 24 hours and osteogenic gene expression was measured with quantitative real-time PCR. The

analysed osteogenic genes represent three levels of signalling (Figure 4.1), (1) bone formation inducers: BMP-2, (2) transcription factors that act downstream from BMP-2: Runx2, Osterix, Msx2, Dlx5 and Sox9 and (3) ECM proteins and mineralisation regulators whose expression is regulated by the upstream osteo/chondrogenic transcription factors: ALP, BSP, OCN, OPG and COMP. Sox9 and COMP are chondrocyte-specific genes, the rest are characteristic of osteoblasts.

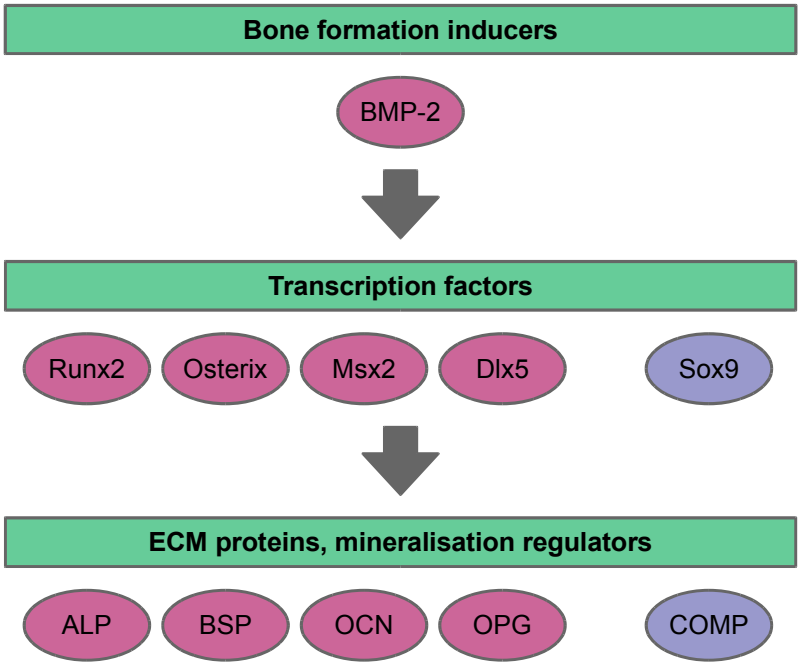

Figure 4.1. Regulation of osteo/chondrogenic gene expression during bone formation. Schematic illustrating components of osteo/chondrogenic pathways, whose expression was examined in subsequent experiments in this chapter.

Expression of BMP-2, the main osteogenic cytokine, decreased in cells treated with both ER stress inducers (Figure 4.2.A).

The expression of chondrogenic transcription factor Sox9 mRNA was decreased by both ER stress inducers, however the expression of its transcriptional target COMP did not change (Figure 4.2.B).

Levels of transcription factors, which are regulated by BMP-2 in osteoblasts, were also changed by ER stress treatments, however they did not follow the same pattern as BMP-2 (Figure 4.2.C). Osterix expression was increased by both inducers. Expression of Runx2 was increased by tunicamycin, but did not change after

thapsigargin treatment. Expression of Msx2 increased after tunicamycin and thapsigargin treatments (1.4 and 1.5-fold increase, respectively) and expression of Dlx5 decreased (0.6 and 0.7-fold change), but these changes were not statistically significant.

A selection of ECM proteins and mineralisation regulators, which are downstream targets of BMP-2 signalling, was examined next (Figure 4.2.D). Expression of BSP, ALP and OPG was significantly increased with at least one of the ER stress inducers. Expression of OCN was not changed by the treatments.

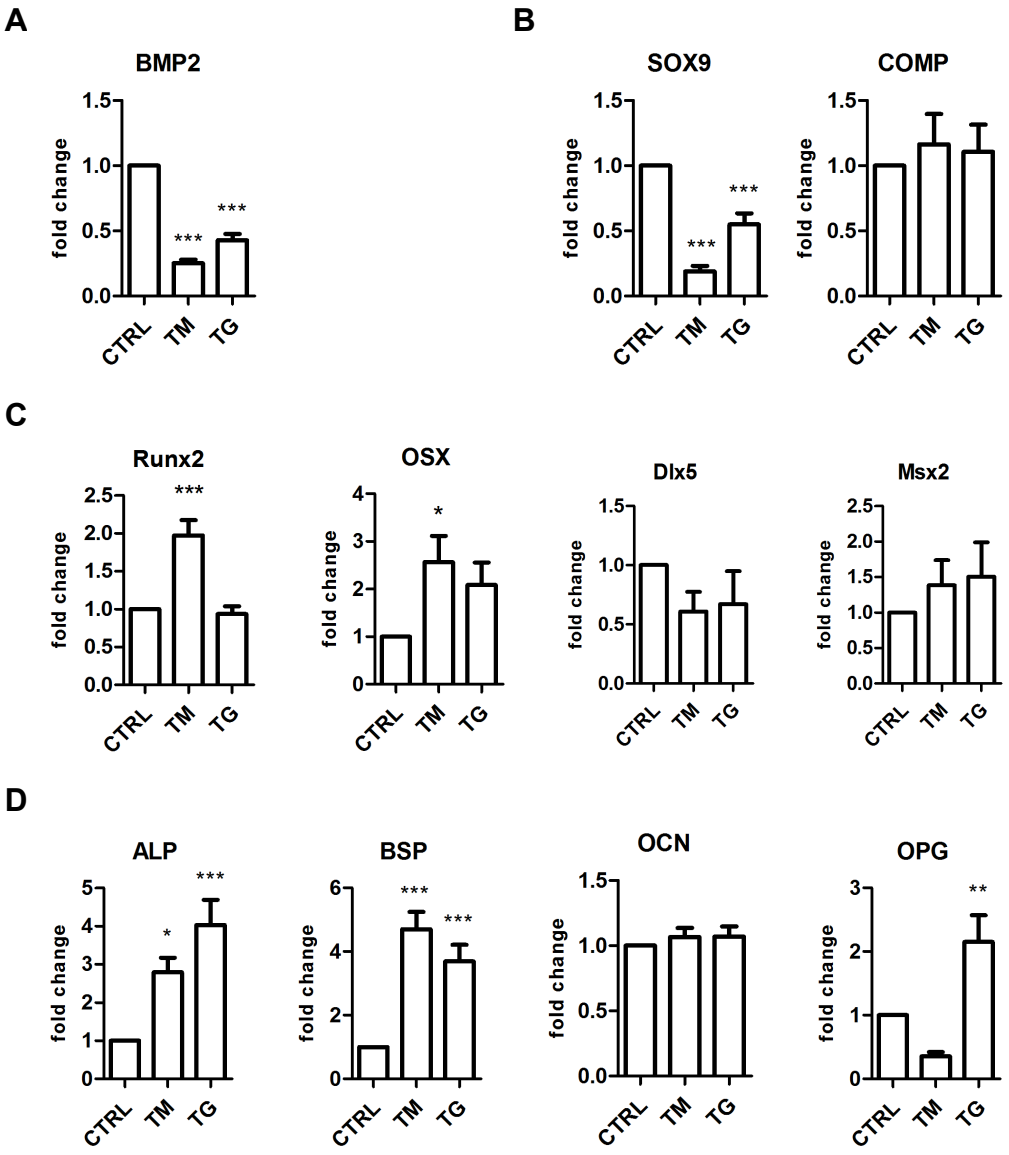

Figure 4.2. Quantitative real-time PCR analysis of osteogenic gene expression in response to ER stress. **A** BMP-2 – inducer of bone formation, **B** chondrogenic genes, **C** osteogenic transcription factors and **D** ECM proteins and mineralisation regulators. VSMCs were treated with 0.4µg/ml tunicamycin (TM) or 0.2µg/ml thapsigargin (TG) for 24 hours. Graphs show n=4-14, mean and SEM, ANOVA with Dunnett's *post hoc* tests was performed. Statistical significance is indicated with asterisks: * denotes p between 0.05 and 0.01, ** denotes p between 0.01 and 0.001, *** denotes p<0.001.

Western blotting analysis was performed in order to examine whether changes in mRNA expression correspond to changes at the protein level.

VSMCs were treated with tunicamycin and thapsigargin in the same

conditions as the real-time PCR experiments, and expression of osteogenic transcription factors was analysed by Western blotting (Figure 4.3.B and C). Runx2 expression did not change in response to ER stress (1.1 fold change with both inducers). Osterix increased 5.8 fold with tunicamycin treatment and decreased 0.3 fold with thapsigargin. Expression levels of Sox9, the main chondrogenic transcription factor, increased by 1.3 fold with tunicamycin, but decreased by 0.8 fold with thapsigargin. None of these changes were statistically significant in n=3 experiments. From the three transcription factors analysed, only in the case of Osterix increased protein levels in tunicamycin-treated cells corresponded with the same trend in mRNA levels measured by real-time PCR.

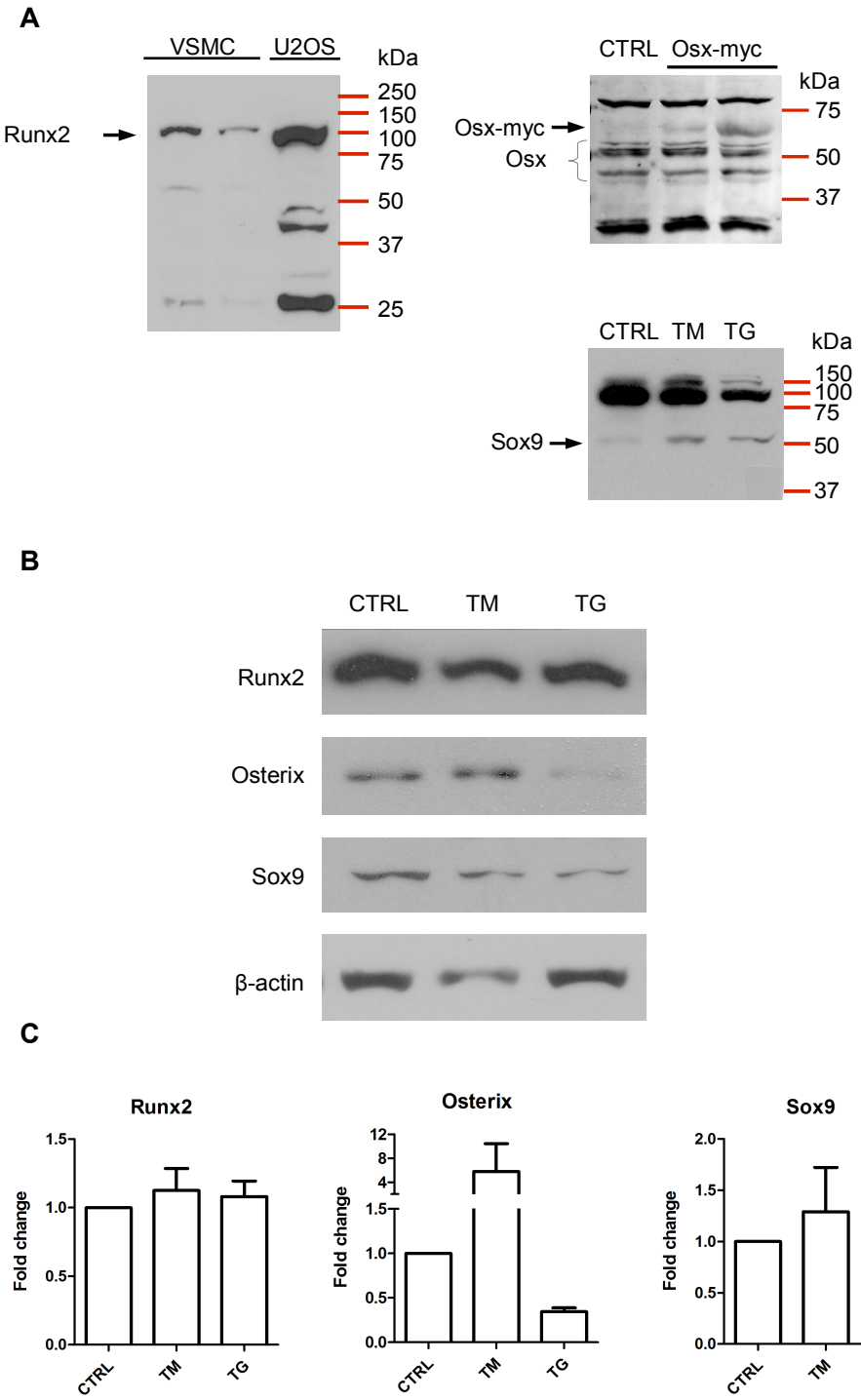

Figure 4.3. Western blotting analysis of osteogenic gene expression in VSMCs. **A.** Validation of antibodies. VSMCs and U2OS cell lysates probed for Runx2 (100kDa specific band, nonspecific 25kDa band). HEK293T cells transfected with an Osterix-myc construct probed for Osterix (bands of 40-50kDa - different states of phosphorylation; 60kDa band - myc-tagged Osterix, nonspecific bands at 25 and 80 kDa). SAOS-2 cell lysates probed for Sox9 (specific 55kDa band, strong nonspecific bands at 100-150kDa). **B.** VSMCs were treated with 0.4µg/ml tunicamycin (TM) or 0.2µg/ml thapsigargin (TG) for 24 hours, representative images. **C.** Quantifications (mean with SEM, n=3, ANOVA with Dunnett's *post hoc* tests was performed).

4.2.2. Osteoblast- and chondrocyte-specific ER stress transducers OASIS and BBF2H7 are expressed in VSMCs

Next, in order to examine whether tissue specific UPR components played a role in osteo/chondrogenic differentiation on VSMCs, expression of ER stress transducers OASIS and BBF2H7 and their target genes was examined. In osteoblasts, OASIS expression is activated by BMP-2, and it leads to increase expression of COL1A1. In chondrocytes, Sox9 activates expression of BBF2H7, which leads to increased expression of Sec23a (Figure 4.4). Expression of both these ER stress transducers has not been shown in VSMCs before.

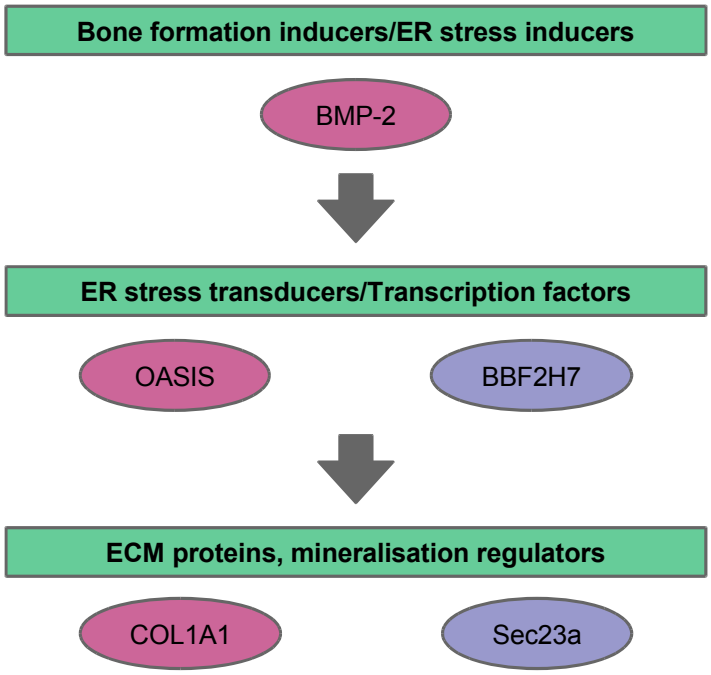

Figure 4.4. Tissue-specific ER stress transducers and regulation of osteo- and chondrogenic signalling pathways.

Real-time PCR analysis showed that expression of OASIS decreased significantly with thapsigargin treatment and did not change with tunicamycin treatment (Figure 4.5.A). Expression of its transcriptional target gene COL1A1 mRNA followed the exact same pattern. Expression of chondrocyte-specific ER stress transducer BBF2H7 mRNA was significantly decreased by tunicamycin and unchanged by thapsigargin treatment. Sec23a, the transcriptional target of BBF2H7 followed the same pattern (Figure 4.5.A).

Expression of OASIS and BBF2H7 was also analysed by Western blotting. Figure 4.5.C and D shows that expression of cleaved OASIS increased 1.6 fold (±0.6) with tunicamycin and did not change with thapsigargin (1.06±0.4 fold change). The levels of full-length BBF2H7 were unchanged by either tunicamycin or thapsigargin (1±0.2 and 1.1±0.2 fold change, respectively).

These results suggest that while ER stress suppressed expression of OASIS and BBF2H7 mRNA, this did not translate into changes at the protein level. COL1A1 and Sec23a mRNA followed the same expression pattern as the transcription factors regulating their expression, they were downregulated by one inducer but not the other. Together this suggests that both these pathways (BMP-2-OASIS-COL1A1 and Sox9-BBF2H7-SEC23A) as a whole were suppressed, each by a different ER stress inducer.

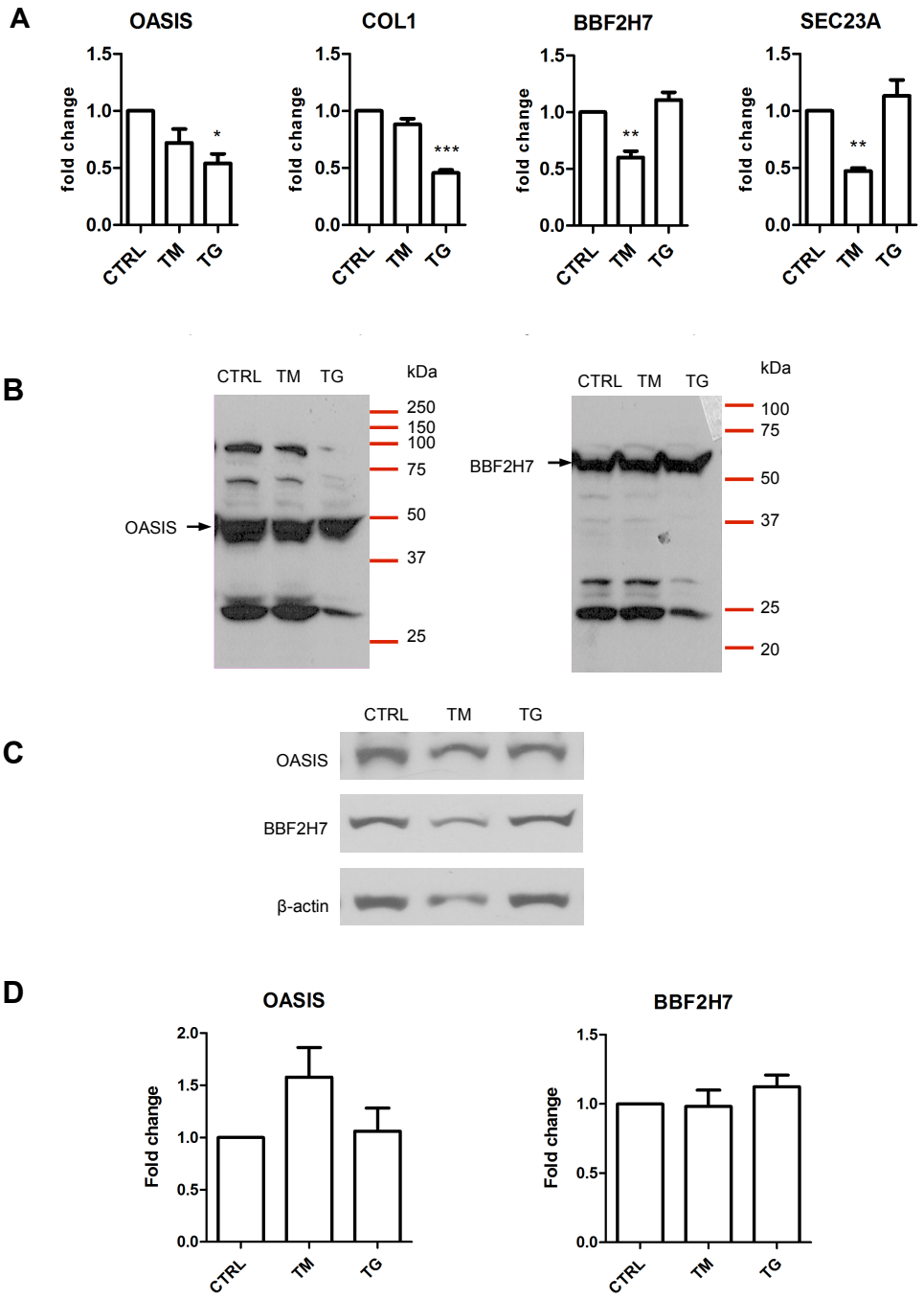

Figure 4.5. Expression of tissue specific ER stress transducers OASIS and BBF2H7 and their target genes in VSMCs. **A.** Real-time PCR analysis. VSMCs were treated with 0.4µg/ml tunicamycin (TM) or 0.2µg/ml thapsigargin (TG) for 24 hours, mean and SEM, n=3, ANOVA with Dunnett's *post hoc* tests was performed, * denotes p between 0.05 and 0.01, ** denotes p between 0.01 and 0.001, *** denotes p<0.001. **B.** Validation of antibodies for Western blotting - U2OS cell lysate probed for OASIS and BBF2H7 (OASIS - a specific 50kDa band corresponding to the cleaved OASIS, several nonspecific 30kDa, 75 kDa and 100kDa bands; BBF2H7 - full-length protein at 80kDa, unspecific bands 25-30kDa). **C.** Western blotting analysis of VSMC lysates probed for OASIS and BBF2H7, representative image. **D.** Quantification of Western blots, n=3, ANOVA with Dunnett's *post hoc* tests was performed.

4.2.3. ER stress downregulates SMC contractile marker expression

Osteogenic differentiation of VSMCs is accompanied by the loss of smooth muscle cell-specific contractile markers (Shanahan *et al.* 1998; Steitz *et al*. 2001; Iyemere *et al.* 2006). Therefore, expression of three components of the smooth muscle cell contractile machinery was examined alongside osteogenic markers, to characterise the effect of ER stress on this aspect of VSMC phenotype.

The mRNA levels of SM22α (TAGLN), a contraction regulating protein, was significantly decreased by both tunicamycin and thapsigargin (0.5±0.2 and 0.6±0.1 fold decrease, respectively; Figure 4.6.A), and this corresponded to a slight decrease in protein expression (0.8±0.1 and 0.9±0.3 fold decrease, respectively; Figure 4.6.B).

Another two markers were only analysed by Western blotting. Protein levels of calponin 1 (CNN1, an actin binding protein) were decreased by 0.9±0.2 and 0.8±0.1 fold by tunicamycin and thapsigargin, respectively (Figure 4.6. B and C). Phosphorylated myosin light chain protein (p-MLC, or MYL2), which is also involved in regulating SMC contraction, was significantly downregulated by both tunicamycin and thapsigargin (0.7±0.1 and 0.5±0.2 fold decrease, respectively; Figure 4.6. B and C). These results suggest that in VSMCs ER stress induces loss of the contractile phenotype.

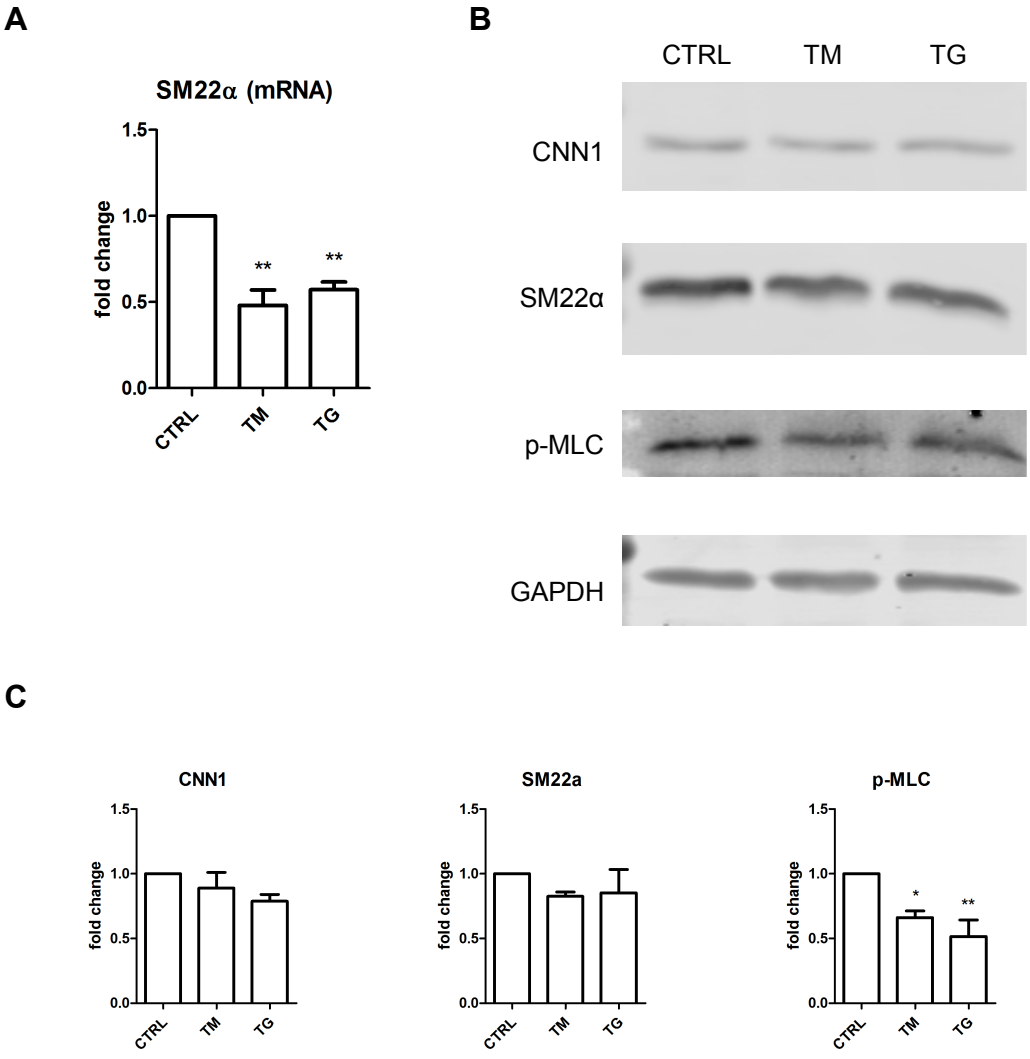

Figure 4.6. Expression of SMC contractile markers in response to ER stress. VSMCs were treated with 0.4μg/ml tunicamycin (TM) or 0.2μg/ml thapsigargin (TG) for 24 hours. **A.** Analysis of SM22α expression by real-time PCR. **B.** Representative Western blots of CNN1, SM22α and p-MLC. **C.** Quantification of western blots. All graphs show n=3, mean with SEM. ANOVA with Dunnett's *post hoc* tests was performed. Statistical significance is indicated with asterisks: * denotes p between 0.05 and 0.01, ** denotes p between 0.01 and 0.001.

The results so far, summarised in Table 4.1, show that tunicamycin- and thapsigargin-induced ER stress has an effect on osteogenic gene and SMC marker expression in VSMCs. From the summary it is apparent that expression of very few of the tested genes did not change with tunicamycin or thapsigargin treatments. Changes in osteogenic and SMC marker expression are consistent with a role of ER stress in VSMC phenotypic modulation.

Looking at real-time PCR results, BMP-2 expression was downregulated, while many of its downstream targets – transcription factors or ECM components were upregulated. This suggests that the expression of the downstream targets is uncoupled from BMP-2 expression in VSMCs in response to ER stress. This is also consistent with results from the previous chapter showing that BMP-2 did not induce ER stress or osteogenic gene expression in VSMCs.

Another observation is that Osterix was the only osteogenic marker which responded to ER stress at the protein level.

Table 4.1. Regulation of osteo/chondrocytic gene and SMC marker expression by ER stress in VSMCs analysed by real-time PCR and Western blotting, fold changes in expression, compared to untreated cells. '*' denote statistically significant changes. Data regarding Dlx5 and Msx2 come from real-time PCR results in the next section of this chapter. †ALP – data in the WB columns are activity levels, experiments shown in the next chapter.

Gene		Description	qPCR		WB	
			TM	TG	TM	TG
1	**BMP-2**	Main bone morphogenetic cytokine.	0.3*	0.4*		
2	**Runx2**	Osteogenic transcription factors downstream of BMP-2, they regulate expression of many extracellular matrix (ECM) components and mineralisation-regulating proteins.	1.9*	0.93	1.1	1.1
3	**Osterix**		2.6*	2.1	5.8	0.3
4	**Dlx5**		0.6	0.7		
5	**Msx2**		1.4	1.5		
6	**BSP**	Bone ECM component, binds hydroxyapatite.	4.7*	3.7*		
7	**ALP†**	Promotes mineralisation by providing phosphate.	2.8*	4*	1.7*	0.8
8	**OPG**	Mineralisation inhibitor.	0.4	2.2*		
9	**OCN**	Late osteoblast marker, regulates mineralisation.	1.1	1.1		
10	**Sox9**	Chondrogenic transcription factor.	0.2*	0.5*	1.3	0.8
11	**COMP**	Cartilage ECM component, target of Sox9.	1.2	1.1		
12	**OASIS**	Osteoblast-specific ER stress transducer.	0.7	0.6*	1.6	1.1
13	**COL1A1**	Bone ECM protein, target of OASIS.	0.9	0.5*		
14	**BBF2H7**	Chondrocyte-specific ER stress transducer.	0.6*	1	1	1.1
15	**SEC23A**	Target of BBF2H7, involved in vesicle transport of ECM proteins.	0.5*	1.1		
16	**SM22α**	VSMC-specific markers, involved in regulating cell contractions.	0.5*	0.6*	0.8	0.9
17	**CNN1**				0.9	0.8
18	**p-MLC**				0.7	0.5*

4.3. Specific UPR pathways regulate osteogenic gene expression in VSMCs

In order to distinguish which ER stress pathways mediate the observed changes in osteo/chondrogenic gene expression, siRNA knock-downs of the canonical ER stress transducers IRE1, PERK, ATF6 as well as ATF4, which is activated downstream of PERK, were carried out. Cells were then treated with tunicamycin and thapsigargin and osteogenic gene expression was measured by real-time PCR. All of the initially tested osteogenic genes were examined (Figure 4.1, Table 4.1). Even though not all changed with ER stress, it was hypothesized that their baseline expression could be controlled by UPR components.

First, expression of all three ER stress transducers (IRE1, ATF6, PERK) and ATF4 was measured to examine whether the siRNA knock-downs were efficient. Figure 4.7 shows that each siRNA smartpool substantially lowered the levels of its target mRNA.

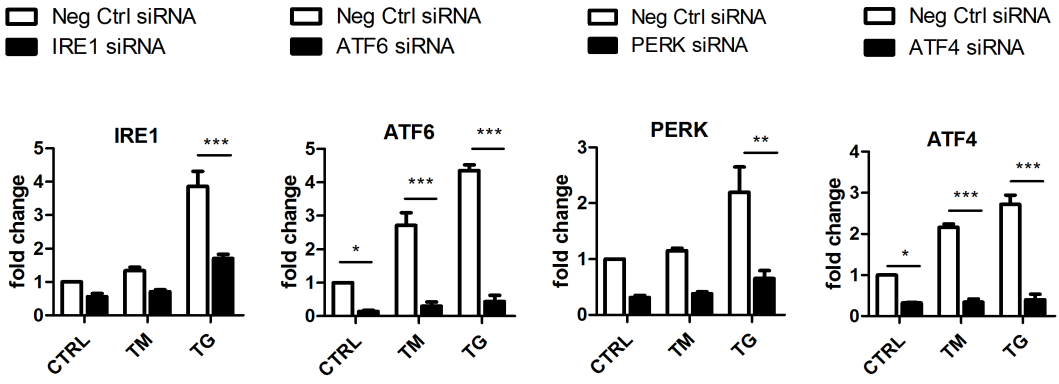

Figure 4.7. Quantitative real-time PCR analysis of ER stress markers in VSMCs treated with with IRE1, ATF6, PERK or ATF4 siRNA or non-targetting siRNA (Neg Ctrl) for 48 hours and then 0.4µg/ml tunicamycin (TM) or 0.2µg/ml thapsigargin (TG) for 24 hours. Graphs show mean and SEM, n=3, ANOVA with Tukey's *post hoc* tests was performed. Statistical significance is indicated with asterisks: * denotes p between 0.05 and 0.01, *** denotes p<0.001.

Next, osteo/chondrogenic gene expression was analysed after knock-down of the UPR components. The first gene analysed was BMP-2, an inducer of bone formation. Knock-downs of ATF6 and ATF4 caused BMP-2 mRNA expression to

increase at baseline, but not in tunicamycin- and thapsigargin-treated cells (Figure 4.8). IRE1 and PERK knock-downs had no effect on BMP-2 expression. These results suggest that in normal conditions ATF4 and ATF6 suppress BMP-2 expression, and that additional factors must exist, apart from the tested UPR components, that regulate BMP-2 expression in ER stress conditions.

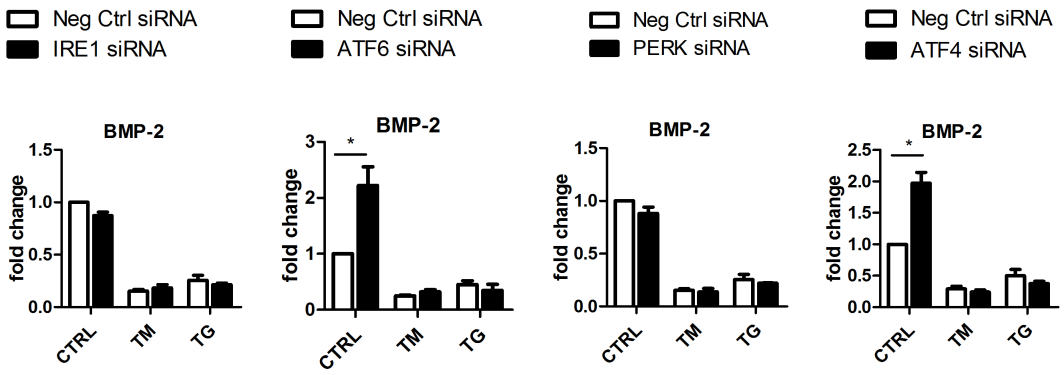

Figure 4.8. Quantitative real-time PCR analysis of BMP-2 expression in VSMCs treated with with IRE1, ATF6, PERK or ATF4 siRNA or non-targetting siRNA (Neg Ctrl) for 48 hours and then 0.4µg/ml tunicamycin (TM) or 0.2µg/ml thapsigargin (TG) for 24 hours. Graphs show n=3, mean with SEM, ANOVA with Tukey's *post hoc* tests was performed. Statistical significance is indicated with asterisks: * denotes p between 0.05 and 0.01.

Next, expression of osteogenic transcription factors, which act downstream of BMP-2, was analysed in the absence of the UPR components (Figure 4.9). Expression of Runx2 mRNA did not change significantly with any of the knock-downs, but increased by approximately 0.5-fold in the absence of ATF4, which suggests that ATF4 could potentially suppress its expression. Expression of Osterix was very variable, therefore only trends were observed – it was decreased by IRE1, PERK and ATF4 knock-downs. Similarly, expression of Msx2 was very variable, but it was decreased approximately 1.5-fold by ATF6 knock-down and increased 2-fold by ATF4 knock-down. Expression of Sox9 was not changed by any of the knock-downs. Dlx5, whose expression was only measured after IRE1 and PERK knock-downs, increased by approximately 0.5-fold after both, but the change was not statistically significant in n=3 experiments.

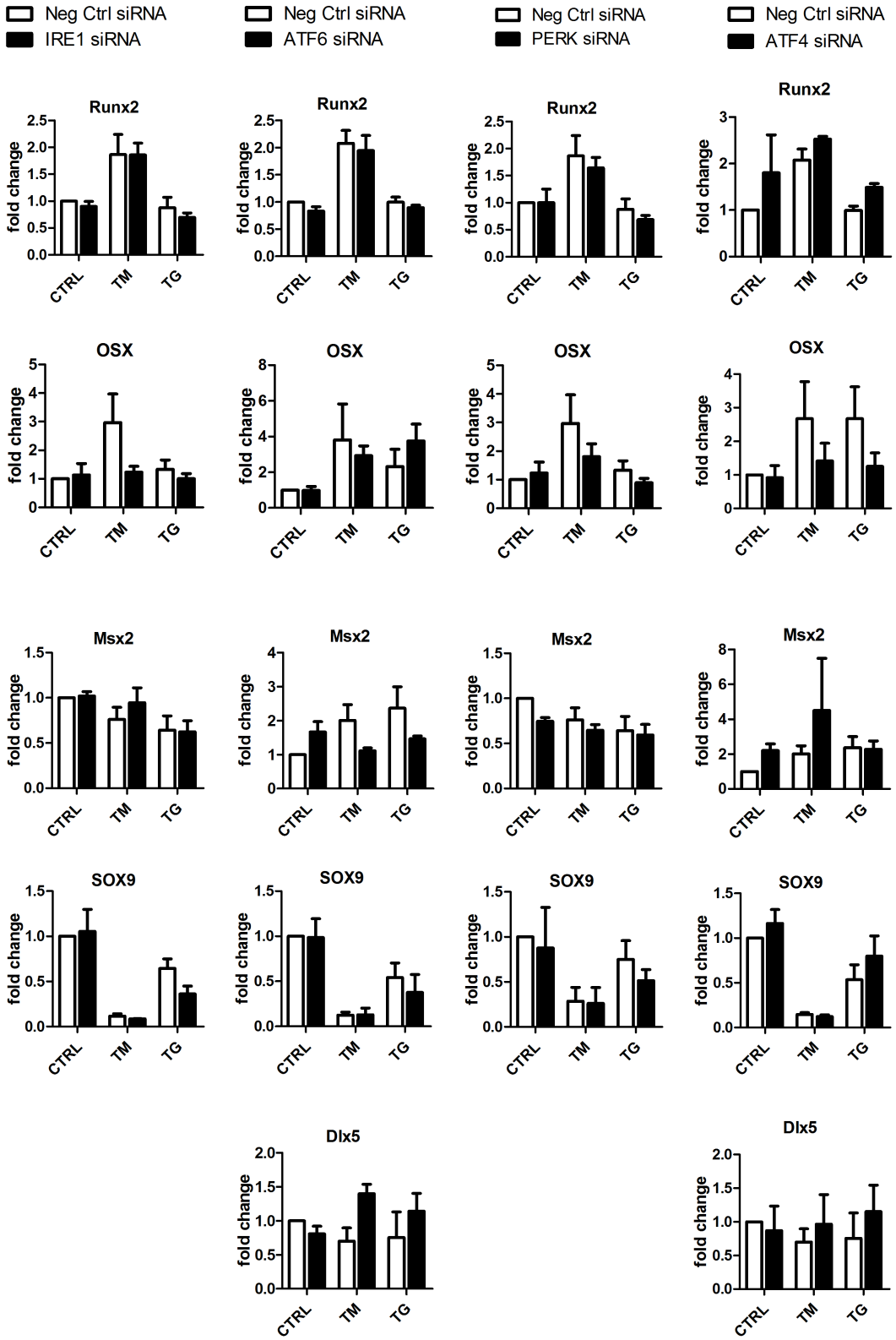

Figure 4.9. Quantitative real-time PCR analysis of osteo/chondrogenic transcription factors in VSMCs treated with with IRE1, ATF6, PERK or ATF4 siRNA or non-targetting siRNA (Neg Ctrl) for 48 hours and then 0.4µg/ml tunicamycin (TM) or 0.2µg/ml thapsigargin (TG) for 24 hours. Graphs show n=3, mean with SEM, ANOVA with Tukey's *post hoc* tests was performed.

Finally, expression of selected ECM and mineralisation-regulating proteins was analysed in the absence of IRE1, ATF6, PERK and ATF4 (Figure 4.10). Results show that ALP expression did not change after IRE1 knock-down, but decreased with ATF6, PERK and ATF4 knock-downs. Only in the absence of ATF4 was the ER-stress induced increase in ALP expression completely attenuated. Expression of BSP increased by approximately 2-fold with IRE1 knock-down, and did not change after knock-downs of the other UPR components. OPG expression was decreased by IRE1 and PERK knock-downs in thapsigargin treated cells. It increased by 0.5-fold with ATF4 knock-down at baseline and in thapsigargin treated cells. None of the changes in OPG expression were statistically significant. OCN expression was analysed only after ATF4 knock-down. Even though OCN expression did not change after tunicamycin and thapsigargin treatments (Figure 4.2), it was increased by the knock-down of ATF4 in all three conditions, and the change was statistically significant in thapsigargin treated cells. This suggests that ATF4 suppressed OCN expression both at baseline and in ER stress conditions.

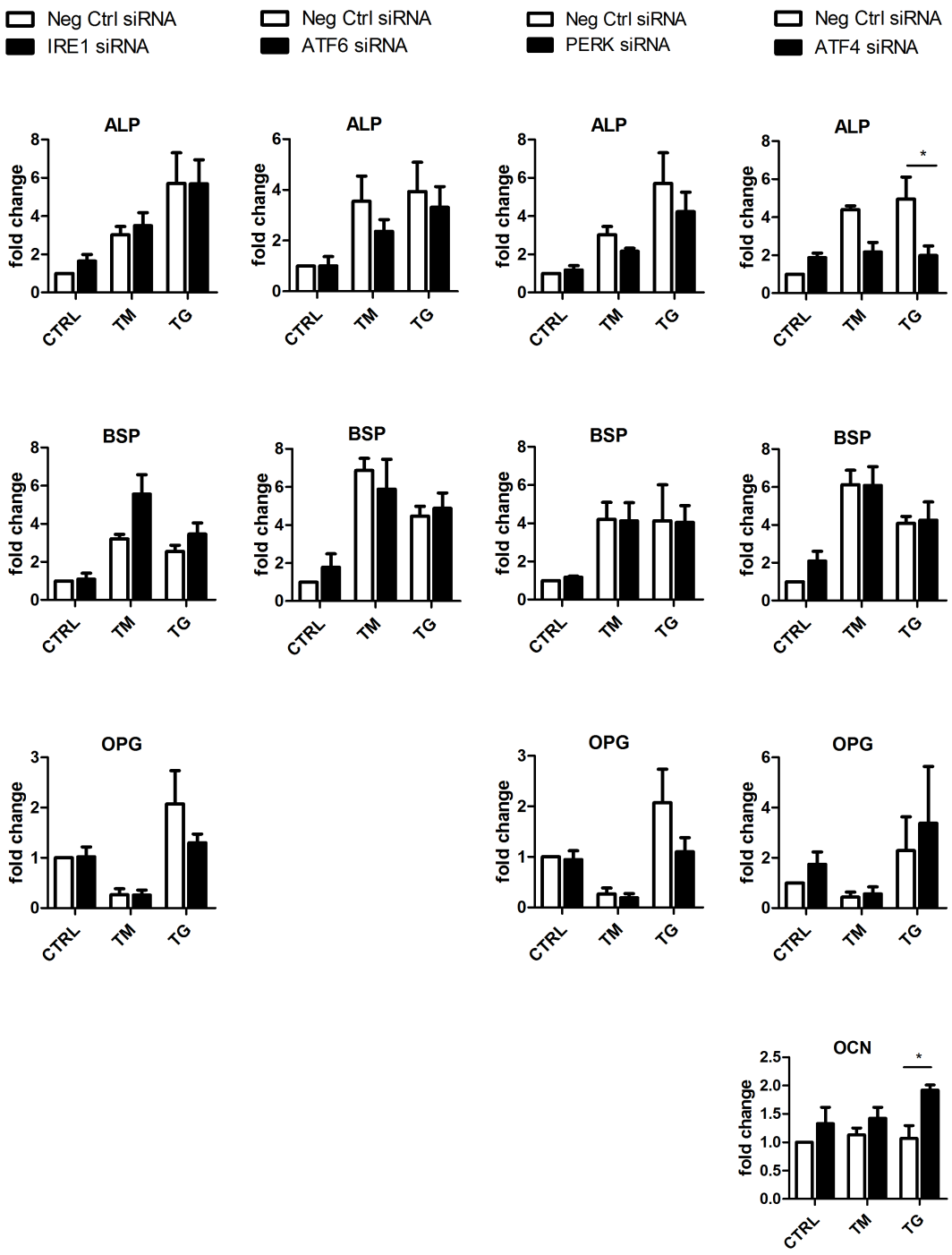

Figure 4.10. Quantitative real time PCR analysis of osteo/chondrogenic genes in VSMCs treated with with IRE1, ATF6, PERK or ATF4 siRNA or non-targetting siRNA (Neg Ctrl) for 48 hours and then 0.4µg/ml tunicamycin (TM) or 0.2µg/ml thapsigargin (TG) for 24 hours. Graphs show n=3, mean with SEM, ANOVA with Tukey's *post hoc* tests was performed. Statistical significance is indicated with asterisks: * denotes p between 0.05 and 0.01.

The knock-down results are summarised in Table 4.2; it is evident that UPR pathways regulate osteogenic gene expression components. The results described in this section are put in the context of UPR signalling in Figure 4.11, which also shows changes that were trends. These results suggest that regulation of osteo/chondrogenic genes by ER stress is very complex, with some genes regulated by more than one branch of the UPR.

Table 4.2. Regulation of osteo/chondrocytic gene and SMC marker expression by UPR components in VSMCs analysed by real-time PCR and Western blotting. Key: '+' denotes increase, '-' decrease and 'o' no change, blank means analysis was not carried out. Statistically significant changes are indicated with '*'. †ALP – data in the WB columns are activity levels, experiments shown in the next chapter.

Gene		Compared to CTRL				Compared to baseline response to ER stress											
		qPCR		WB		IRE1			ATF6			PERK			ATF4		
		TM	TG	TM	TG	CTRL	TM	TG	CTRL	TM	TG	CTRL	TM	TG	CTRL	TM	TG
1	**BMP-2**	-*	-*			o	o	o	+*	o	o	o	o	o	+*	o	o
2	**Runx2**	+	o	o	o	o	o	o	o	o	o	o	o	o	+	+	+
3	**Osterix**	+*	+	+*	-	o	-	o	o	-	o	o	-	o	o	-	-
4	**Dlx5**	o	o						o	+	+				o	+	+
5	**Msx2**	o	o			o	o	o	+	-	-	o	o	o	o	+	o
6	**Sox9**	-*	-*	o	o	o	o	o	o	o	o	o	o	o	o	o	o
7	**BSP**	+*	+*			o	+	o	o	o	o	o	o	o	o	o	o
8	**ALP†**	+*	+*	+*	o	o	o	o	o	-	-	o	-	-	o	-	-*
9	**OPG**	o	+*			o	o	-				o	o	-	o	o	+
10	**OCN**	o	o												+	+	+*

ATF4 knock-down affected expression of the most genes, which is consistent with its well-established roles in bone formation and potentially calcification of VSMCs. However, the knock-down results suggest that ATF4 inhibits expression of OPG, OCN, Msx2, Runx2 and BMP-2, and activates ALP and Osterix (Figure 4.11), which is not consistent with its role as a calcification-promoting transcription factor. In addition, the results show that knock-down of PERK did not cause the same changes in gene expression as knock-down of ATF4, its downstream target, in fact knock-down of PERK did not cause a decrease in ATF4 expression (data not shown). This suggests that in VSMCs ATF4 might also be regulated by other signalling

pathways.

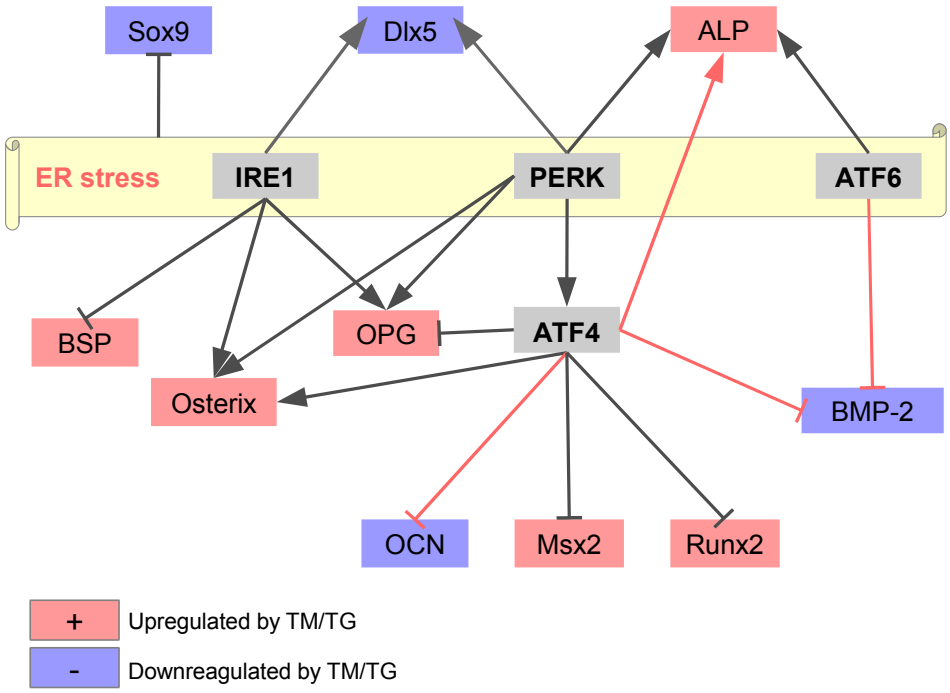

Figure 4.11. Regulation of osteogenic genes by the unfolded protein response transducers IRE1, PERK and ATF6, and PERK downstream target ATF4. Arrows denote activation and blunt ends mean inhibition. Statistically significant changes are marked with red lines. Levels of Sox9 did not change markedly with any of the knock-downs, therefore it was placed outside the UPR signalling pathway.

4.4. Global downregulation of TGFβ signalling in tunicamycin-treated VSMCs

Given the variability in responses shown in the previous experiments, a real-time PCR array was used as a second approach to examine the regulation of osteogenic gene expression in response to ER stress. The expression of a total of 88 genes, including some already examined, was tested by real-time PCR in response to tunicamycin treatment. Tunicamycin was chosen, as in the initial real-time PCR results it changed the expression of more osteogenic genes than thapsigargin.

Figure 4.12 shows that among the genes which could be successfully measured, most decreased in response to ER stress. PHEX and PDGFRB were of special interest, as they were among the few genes whose expression was consistently upregulated.

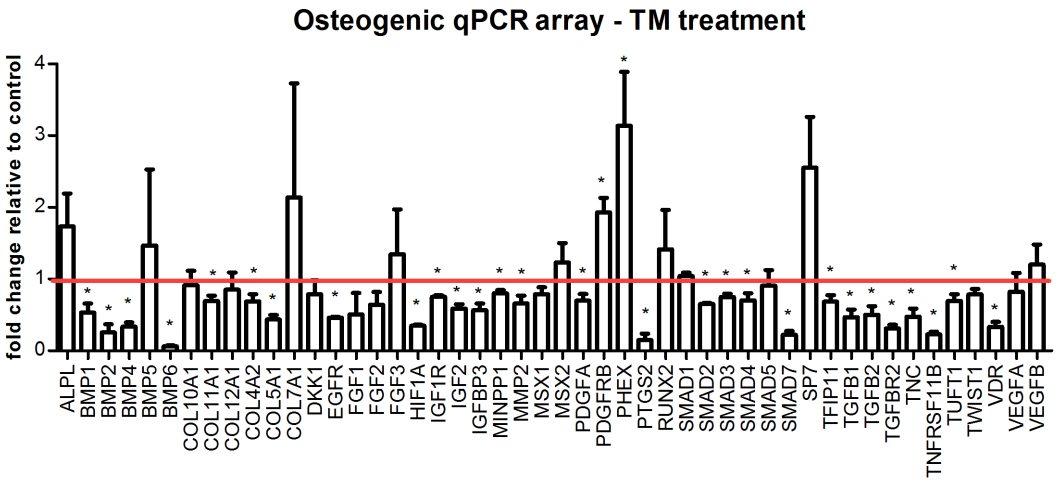

Figure 4.12. Osteogenic real-time PCR array results. VSMCs were treated with 0.4µg/ml tunicamycin for 24 hours. Graph shows mean and SEM, n=3, t-tests were performed for control versus tunicamycin-treated samples for each gene. Statistical significance is indicated with asterisks: * denotes p between 0.05 and 0.01.

To validate some of the differences in gene expression, and to examine whether thapsigargin had the same effect on the genes that showed the biggest changes in the array, conventional real-time PCRs and Western blots were carried out. Figure 4.13.A shows that by real-time PCR BMP-7, COL14A1, PDRGFRB and PHEX were indeed upregulated by tunicamycin, but not thapsigargin. However, MMP8 was upregulated by thapsigargin, not tunicamycin, and MMP9 was downregulated by both treatments. In addition, similar to what was observed in the array, tunicamycin treatment downregulated expression of VDR (both mRNA and protein), but thapsigargin had no effect (Figure 4.13.B). BMP-7, COL14A1, PDRGFRB, PHEX, MMP8 and MMP9 are not known to interact with each other or to be involved in the same signalling pathways.

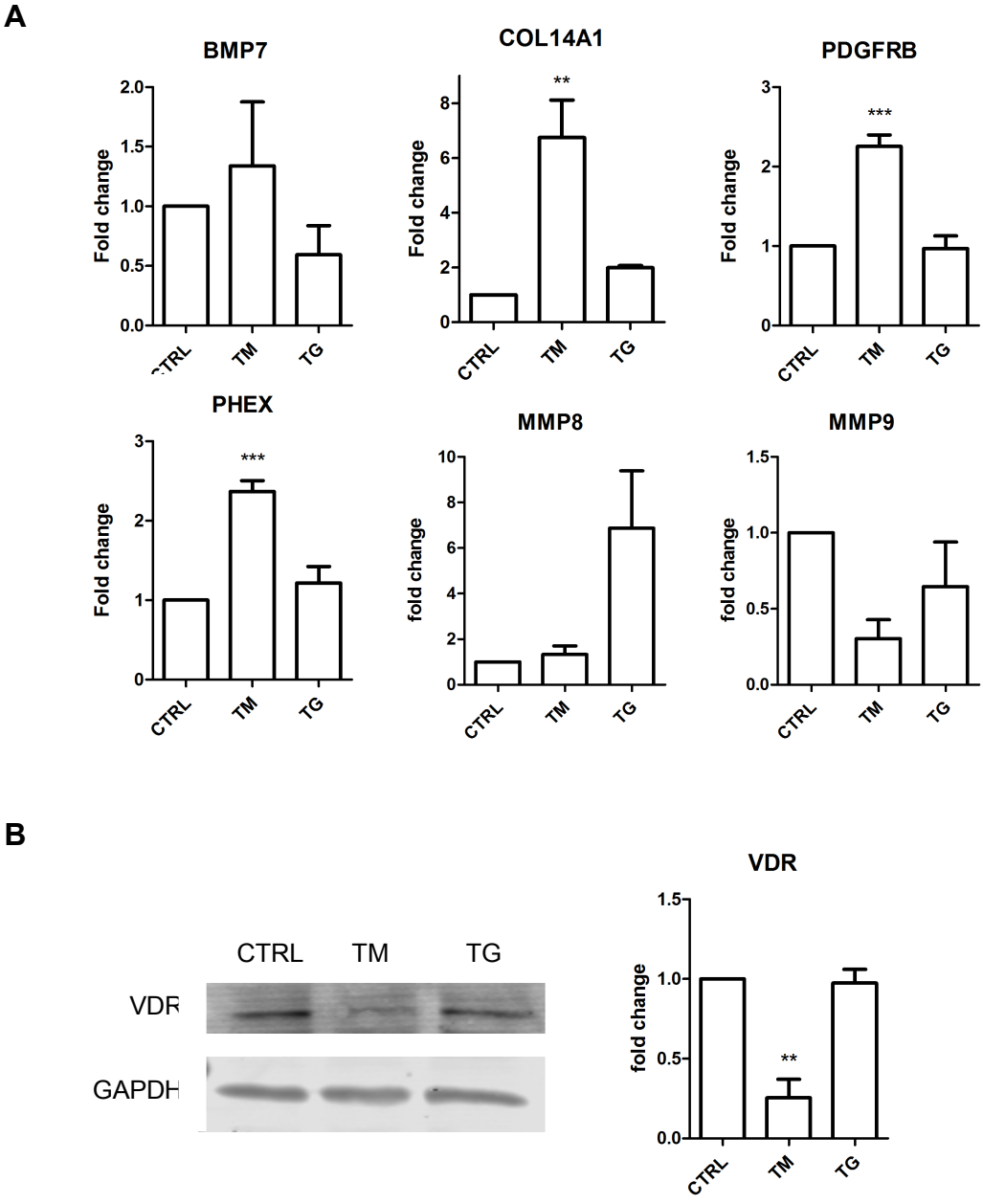

Figure 4.13. Validation of real-time PCR array results **A** by real-time PCR and **B** Western blotting. VSMCs were treated with 0.4µg/ml tunicamycin (TM) or 0.2µg/ml thapsigargin (TG) for 24 hours. Graphs show mean and SEM, n=3, ANOVA with Dunnett's *post hoc* tests was performed. Statistical significance is indicated with asterisks: * denotes p between 0.05 and 0.01, ** denotes p between 0.01 and 0.001, *** denotes p<0.001.

In order to draw conclusions regarding signalling pathways, in which the products of the genes analysed in the array are involved, the array results were combined with a protein-protein interactions network retrieved from online

databases by Cytoscape (Figure 4.14). It became apparent that a large cluster of interacting proteins that were regulated simultaneously belong to the TGFβ family signalling pathways – TGFβs, BMPs and their receptors and SMADs, and that they were downregulated by ER stress.

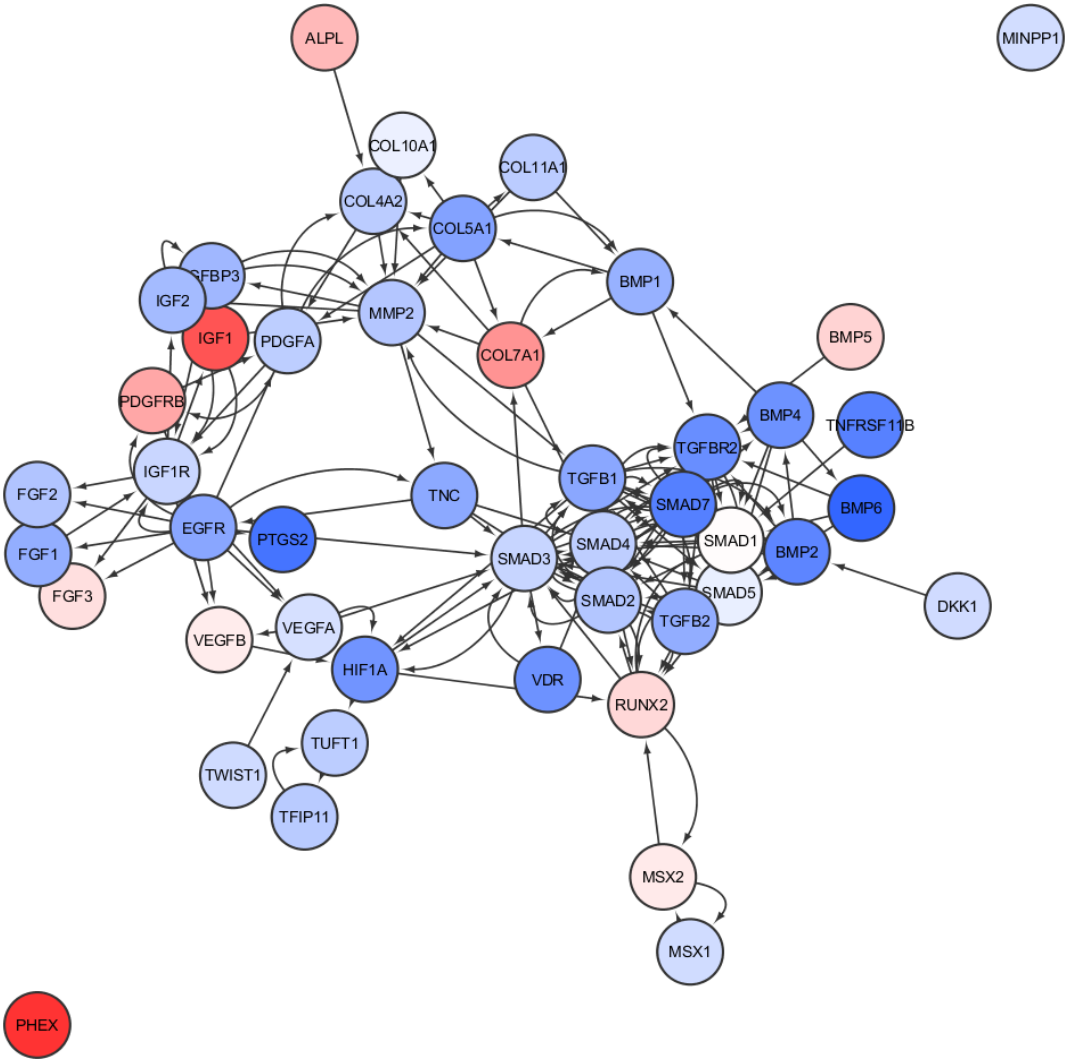

Figure 4.14. Osteogenic array results overlaid over a protein-protein interactions network retrieved by Cytoscape. Expression levels are colour coded – red means upregulation and blue means downregulation, the intensity of the colour reflects the magnitude of the change.

Some of these findings were then validated further by real-time PCR. The results show that tunicamycin treatment decreased TGFBR1 and TGFBR2 mRNA by 0.5-fold, and increased SMAD1, but had no effect on SMAD5 or TGFB2 expression (Figure 4.15). Thapsigargin treatment increased SMAD1 and decreased TGFBR1 mRNA but had no effect on the other tested genes. None of the observed changes

were statistically significant in n=3 experiments (Figure 4.15), which means that the array results were not repeatable and therefore could not be validated.

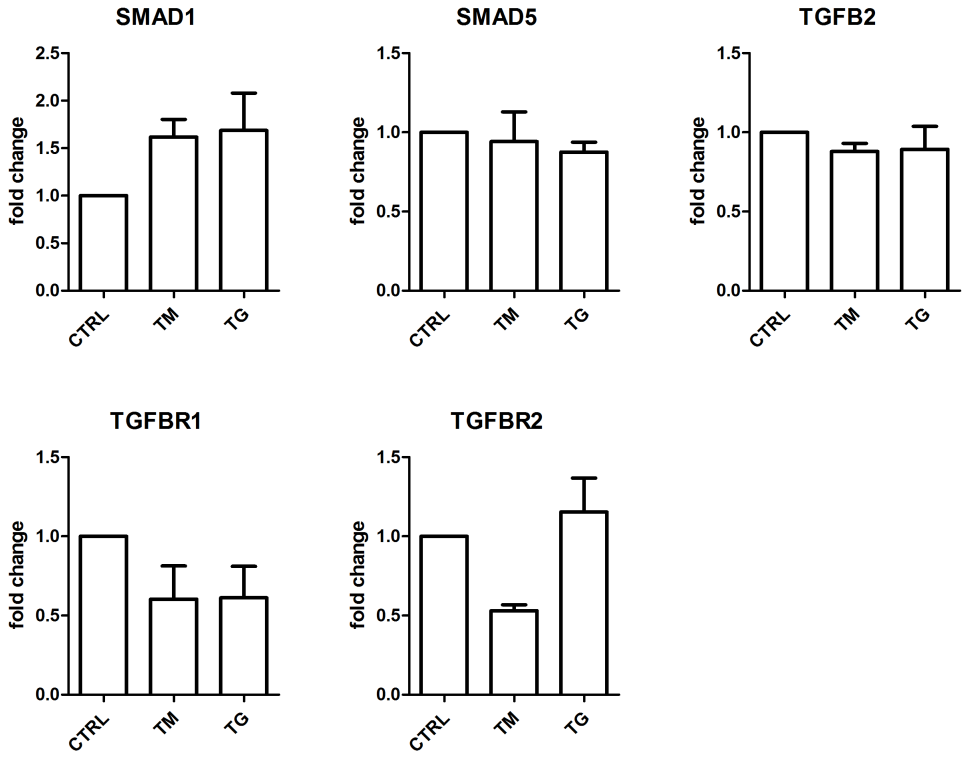

Figure 4.15. Validation of real-time PCR array – TGFβ family signalling. VSMCs were treated with 0.4μg/ml tunicamycin (TM) or 0.2μg/ml thapsigargin (TG) for 24 hours. Graphs show mean and SEM, n=3, ANOVA with Dunnett's *post hoc* tests was performed.

SMAD expression was also analysed by Western blotting. As shown in Figure 4.16, SMAD1 protein expression levels reflect its mRNA, since no change was observed with either of the ER stress treatments. SMAD2 was increased with both ER stress treatments, but the changes were not statistically significant. Thapsigargin (but not tunicamycin) caused a significant decrease in the levels of SMAD3. SMAD4 expression did not change.

In the TGFβ family signalling TGFβ/BMP binding leads to the assembly of a receptor complex in which the type II receptor phosphorylates and activates the type I receptor. Pathway restricted SMADs (SMAD2 and SMAD3 for TGFβ and SMAD1 and SMAD5 for BMPs) are then phosphorylated, which leads to heterodimerization with SMAD4, a common-mediator SMAD. The complex is then translocated to the nucleus, where it binds directly to DNA and affects transcription

of specific genes (Heldin *et al.* 1997). In this light, the fact that SMAD1 expression was increased by tunicamycin and thapsigargin might mean that BMP signalling is increased. Expression of both TGFβ receptors was decreased by ER stress, but SMAD2 and SMAD3 were differentially regulated in these experiments. Therefore it is difficult to draw definite conclusions about this signalling pathway. In addition, because SMADs are activated by phosphorylation, it is important to remember that changes or lack of changes of protein levels might not correspond to actual changes in signalling. These findings were not pursued further as the real-time PCR results were not reproducible and only small changes were observed at the protein level. Therefore it was deemed impractical to test further, phosphorylation-specific antibodies against SMADs.

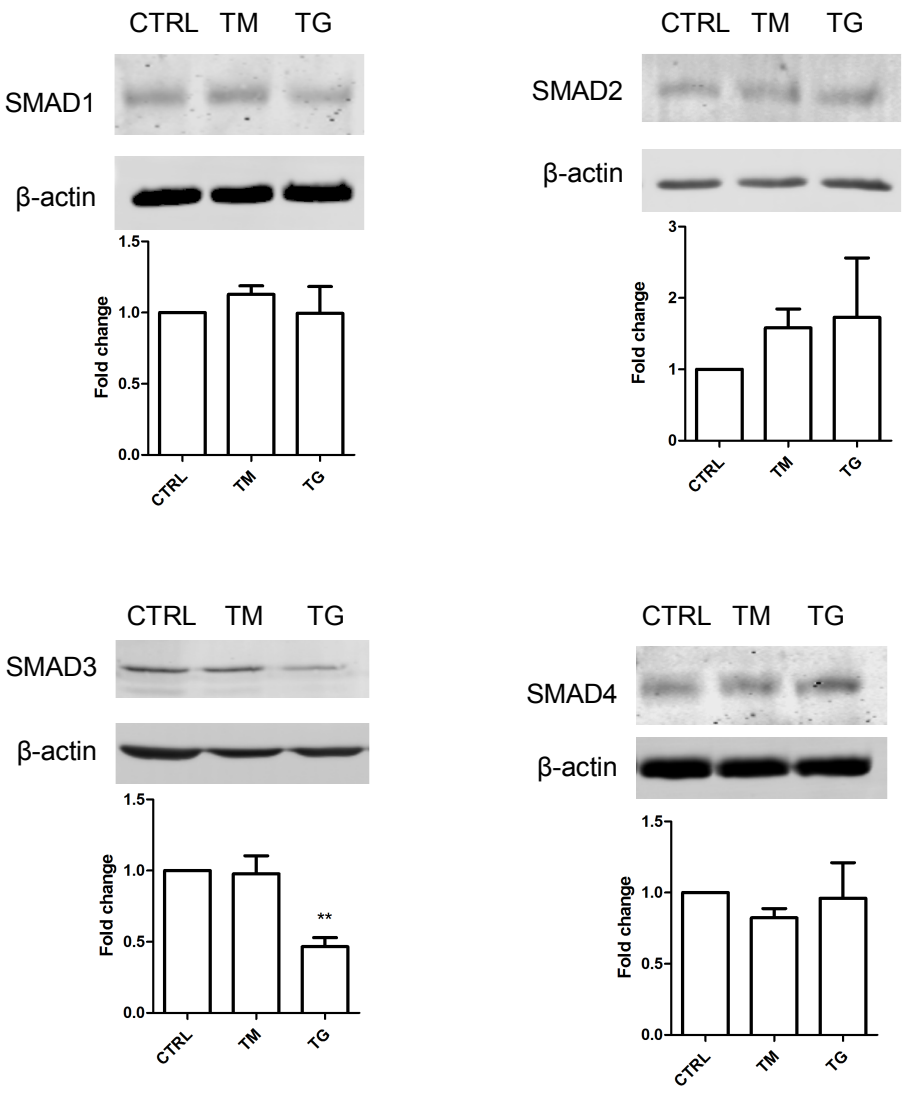

Figure 4.16. Validation of the real-time PCR array – SMAD expression. VSMCs were treated with 0.4µg/ml tunicamycin (TM) or 0.2µg/ml thapsigargin (TG) for 24 hours. Graphs show mean and SEM, n=3, ANOVA with Dunnett's *post hoc* tests was performed. Statistical significance is indicated with asterisks: ** denotes p between 0.01 and 0.001.

4.5. Discussion

In this chapter I have shown that ER stress regulates expression of osteogenic genes in human primary VSMCs via specific unfolded protein response pathways.

4.5.1. ER stress modulates VSMC phenotype

Tunicamycin and thapsigargin treatments changed expression of almost all

examined osteo/chondrogenic genes in VSMCs. Some of the changes were decreases (BMP-2, Sox9 by both inducers, OPG by tunicamycin) and some increases (Runx2 by tunicamycin, Osterix, BSP, OPG by thapsigargin). The fact that all these genes are not regulated in the same direction might reflect the fact that in osteogenic differentiation of VSMCs the expression of these genes has no temporal pattern as it is regulated by aberrant signals, in contrast to osteoblasts where during bone formation these proteins are expressed in a concerted manner, following a strict order. During embryonic development BMP-2 activates Runx2 signalling, Osx, Dlx5 and Msx2 play secondary roles (Nakashima *et al.* 2003, Komori *et al.* 2006, Karsenty *et al.* 2009).

There is a lack of literature on the regulation of osteogenic pathways in VSMCs in the context of vascular calcification, which is surprising because expression of osteogenic genes is widely mentioned as one of the hallmarks of vascular calcification (Shao *et al.* 2006; Speer *et al.* 2009). Osteogenic markers are either reported to be present in calcified arteries or not mentioned at all, which suggests that little thought is given to their regulation and role in VSMCs. My results are therefore the first comprehensive analysis of the effects of ER stress on osteogenic gene expression in VSMCs.

Another important finding is the fact that at the protein level expression of Osterix was upregulated by tunicamycin, but Runx2 was not. Thapsigargin decreased the expression of Osterix at the protein level, but did not change the expression of Runx2. Osterix acts downstream of Runx2 in osteoblasts (Nakashima *et al.* 2002; Matsubara *et al.* 2008), however in VSMCs its regulation by other osteogenic genes is unknown. Runx2 is important for VSMC calcification both *in vivo* and *in vitro*, but mechanisms of its regulation in these cells are unknown (Bostrom *et al.* 2011; Sun *et al.* 2012). My results suggest that in VSMCs an increase in Runx2 expression is not required for an increase in Osterix expression.

I have also included two tissue-specific ER stress transducers OASIS and BBF2H7 in the osteogenic gene analysis and demonstrated that they are expressed in VSMCs, which has not been shown before. I found that their expression was decreased by tunicamycin and thapsigargin. OASIS and BBF2H7 expression was not

examined in subsequent knock-down experiments, because their expression was not induced by ER stress and also because they are ER stress transducers themselves and therefore unlikely to respond to changes in levels of other transducers.

In this chapter I also presented evidence that VSMC contractile marker expression was downregulated by tunicamycin and thapsigargin treatments (SM22α mRNA and p-MLC protein). The expression of these markers in the context of ER stress has not been studied before, therefore these findings are novel. VSMCs have been shown to lose expression of contractile markers when they calcify (Iyemere *et al.* 2006; Speer *et al.* 2009), so these results support the notion that ER stress promotes transdifferentiation to a secretory or osteo/chondrogenic phenotype. Moreover, results from the real-time PCR array show that ER stress increased expression of PDGFRB associated with the synthetic phenotype, and decreased expression of SMAD3 which mediates TGFβ signalling classically associated with contractile differentiation. On the other hand, these results could be interpreted that ER stress induces transition to the synthetic phenotype, which cells assume in response to injury and which provides a way for them to cope with environmental stress. This conclusion is also supported by the fact that ER stress decreased the expression of BMP-2, and that the knock-down of ATF6 and ATF4 increased its expression, which means that although a transition to a secretory phenotype is activated, osteogenic differentiation is not promoted. In addition, in Chapter 3 I showed that pro-contractile TGFβ can induce ER stress. In the light of the current results this is consistent with ER stress protecting from osteogenic phenotype, as a result of TGFβ signalling, and could mean that there is a negative feedback loop of TGFβ activating ER stress and then ER stress inhibiting TGFβ signalling.

4.5.2. Tunicamycin and thapsigargin have different effects on osteogenic gene expression

In the previous chapter I discussed the fact that tunicamycin and thapsigargin enhanced calcification to different extents. This was also reflected in the results presented in this chapter, as tunicamycin and thapsigargin had different

effects on the expression of some osteogenic genes (Runx2, OPG, OASIS, BBF2H7). It is possible that apart from the UPR each inducer activated a separate, ER stress-unrelated signalling pathway, caused for example by secondary effects of the lack of certain glycosylated proteins or excess calcium in the cytoplasm. However, ALP, BMP-2, Osterix and BSP were robustly regulated by both inducers therefore are the most likely associated with ER stress. In addition, in this chapter I showed that osteogenic gene expression is affected by UPR component knock-downs in tunicamycin- and thapsigargin-treated VSMCs, which means that these inducers regulate osteogenic gene expression specifically via ER stress.

4.5.3. ATF4 – a possible inhibitor of VSMC osteogenic differentiation?

An important trend that has emerged from the knock-down experiments is that ATF4 inhibits more osteogenic genes than it activates, as its knock-down more often caused an increase in osteogenic gene expression than a decrease. This is contradictory to studies both in osteoblasts (Yang and Karsenty, 2004a; Saito *et al.* 2011) and in VSMCs (Masuda *et al.* 2012, 2013; Duan *et al.* 2013), where ATF4 has been shown to promote osteogenic gene expression. The idea that ER stress inhibits osteogenic differentiation is not a completely novel notion. It has been shown that tunicamycin inhibited a BMP-2-induced increase in ALP and OCN expression in mouse osteoblasts, however activation of the three canonical UPR branches was not examined in that study (Jang *et al.* 2013). Another study has shown that ATF4 was required for TGFβ-mediated suppression of OCN expression and osteoblast differentiation (Lian *et al.* 2012). The authors of these papers did not comment on the fact, that the majority of evidence suggests the exact opposite role for ER stress and ATF4 in osteoblast differentiation. These studies suggest that even in osteoblasts the role of ER stress signalling is not as clear-cut as suggested in previous reports and might be context dependent. This further supports the notion that ER stress could be a protective mechanism in VSMCs, to provide phenotypic regulation. It should be noted, however, that the experiments described here are short-term treatments with ER stress inducers. In the long-term calcification assays from the previous chapter ER stress enhanced calcification, however, as shown in

the next chapter, this was not accompanied by an increase in ATF4 or ALP expression. That could mean that when ER stress is prolonged it ceases to be protective and promotes calcification.

An alternative explanation for ATF4 inhibiting osteogenic gene expression is that it acts independently of ER stress. In my experiments, the effects of ATF4 knock-down were different from PERK knock-down. In the literature this has not been the case, studies both in osteoblasts and in VSMCs (Saito *et al.* 2011, Masuda *et al.* 2013) show that the effects of these knock-downs are consistent with these two proteins representing the same signalling pathway. However, it is possible that ATF4 is additionally activated by other pathways. It has been shown to be activated by metabolic stress (glucose or amino acid deprivation), hypoxia and oxidative stress as well as ER stress in various tissues (Ameri and Harris, 2008). Low serum conditions used in my experiments could have potentially caused metabolic stress. I have not tested this, but in fibroblasts serum deprivation has been shown to activate ATF4 expression (Dennis *et al.* 2013).

4.5.4. Real-time PCR array provides further evidence for phenotypic regulation of VSMCs by ER stress

I carried out an osteogenic real-time PCR array as a more global approach to identifying the effect of ER stress on osteogenic gene expression. The array results confirmed that activating ER stress with tunicamycin is associated with changes in expression of osteogenic genes in VSMCs. A few were upregulated (BMP-7, PHEX, COL14A1, PDGFRB) but expression of the majority was reduced.

As mentioned previously, the upregulation of PDGFRB, receptor for the cytokine PDGF, could be indicative of cells assuming a secretory, proliferative phenotype (Wilson *et al.* 1993; Salabei *et al.* 2013) in response to ER stress.

BMP-7, a member of the TGFβ family is important for bone formation during embryonic development (Jena *et al.* 1997), but it is also a known inhibitor of vascular calcification (Davies *et al.* 2005). BMP-7 has been shown to play a role in VSMC differentiation and maintaining of their contractile phenotype *in vitro* (Dorai *et al.* 2000). Interestingly, BMP-7 counteracted the action of PDGF and TGFβ1 in an

experiment where both these cytokines were shown to increase cell proliferation (Dorai *et al.* 2001), so its activation by ER stress could be part of a negative feedback loop, where TGFβ activated ER stress but ER stress activated BMP-7, which counteracts pro-secretory aspects of TGFβ signalling.

Another gene found to be upregulated was Collagen 14 α1, whose function is to regulate Collagen type 1 fibril formation (Plenz *et al.* 2003). Interestingly, its expression has been shown to decrease in coronary artery VSMCs after stimulating them with TGFβ1 (Schmidt *et al.* 2006), which is consistent with a contractile phenotype-promoting function of this cytokine. The upregulation of this collagen by tunicamycin in VSMCs supports the notion that a synthetic phenotype is activated by ER stress.

PHEX, another gene found to be increased by tunicamycin in VSMCs, is a zinc metalloendopeptidase, which catalyses cleavage of a group of proteins that regulate mineralisation. Mutations in this gene cause autosomal recessive hypophosphatemic rickets, as PHEX modulates FGF23 expression, which regulates phosphate and vitamin D metabolism (Rowe, 2012). This is the first time it has been shown this gene is expressed in VSMCs, as its role in this cell type is unknown.

Among genes that were found to be downregulated by tunicamycin, of note was a large group of genes related to TGFβ family signalling. I have validated that expression of SMAD3, which carries TGFβ1 signals, is decreased by thapsigargin at the protein level. In the previous chapter I showed that TGFβ1 induces ER stress in VSMCs. Therefore these results suggest that there is a feedback loop of TGFβ1 increasing ER stress and ER stress decreasing TGFβ signalling. This is consistent with studies showing that high levels of TGFβ promote osteogenic differentiation and vascular calcification (Simionescu *et al.* 2005). In light of the previous results from this chapter this suggests that activation of ER stress via TGFβ could be protective, but too much would push the cells towards the osteogenic phenotype, therefore TGFβ must be inhibited by ER stress. In osteoblasts this is in line with results showing that TGFβ suppressed ATF4 activity by increasing vimentin expression, and thus inhibited osteoblast differentiation (Lian *et al.* 2012).

4.5.5. Conclusions

The findings regarding the potential role of ER stress in VSMC phenotype regulation and calcification from these first two chapters are summarised in the schematic in Figure 4.17. In this model ER stress, which can be induced by warfarin or TNFα, upregulates some osteogenic genes via the UPR, which promotes calcification. But at the same time it triggers protective mechanisms, mediated by ATF4, leading to decreased expression of osteogenic genes. TGFβ promotes contractile gene expression, but in certain conditions also the secretory phenotype. Therefore even though TGFβ induces ER stress to activate protective mechanisms, it is also inhibited by ER stress to prevent the maladaptive aspects of TGFβ signalling. The outcome of all these processes might depend on the balance between all the signalling cues, so activating ER stress could both promote calcification and inhibit it, depending on the context.

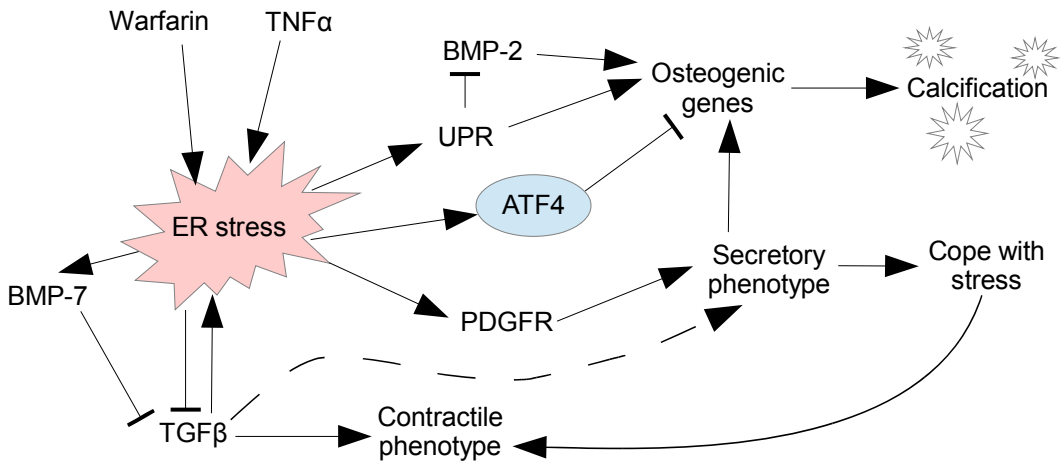

Figure 4.17. Schematic summarising regulation of VSMC phenotype and calcification by ER stress.

In conclusion, the results in this chapter show that regulation of osteogenic genes in VSMCs in response to ER stress is complex and does not recapitulate osteogenic pathways in osteoblasts. Therefore, the next step was to examine the regulation of some of the osteogenic genes in more detail, specifically Osterix and ALP. These two genes were consistently upregulated by both tunicamycin and thapsigargin and little is known about their regulation in VSMCs.

Chapter 5: Investigating regulation of Osterix and alkaline phosphatase expression in response to ER stress in VSMCs

5.1. Introduction

The results in the previous chapter show that Osterix and ALP were consistently upregulated by both tunicamycin and thapsigargin treatments, suggesting that they are likely regulated by ER stress rather than a non-specific effect of the inducers. Both these factors are important for vascular calcification, but little is known about regulation and the roles of these genes in VSMCs.

5.1.1. Osterix

Osterix (OSX, SP7), a zinc-finger transcription factor from the SP1 family, is expressed in MSCs and osteoblasts and is essential for ECM deposition and osteoblast maturation; bone formation does not occur in Osterix knock-out mice (Nakashima *et al.* 2002). Osterix is downstream of BMP-2 signalling, and was shown to act both downstream or independently of Runx2 (Lee *et al.* 2003; Matsubara *et al.* 2008) and downstream of Dlx5 and Msx2 in osteoblasts (Matsubara *et al.* 2008; Ulsamer *et al.* 2008).

Osterix was shown to be expressed in calcified human coronary arteries alongside other bone markers (Alexopoulos *et al.* 2011). It has been demonstrated to be upregulated by Vitamin D, oxidised LDL and hepatocyte growth factor (HGF) in VSMCs *in vitro* (Taylor *et al.* 2011, Zebger-Gong *et al.* 2011, Liu *et al.* 2011a), but there is a poor understanding of what its transcriptional targets and exact functions in those cells are. No transcriptional targets of Osterix have been described in VSMCs and it has not been studied whether its presence is required for calcification. In osteoblasts Osterix was shown to be a transcriptional target of the ER stress transcription factor XBP1 (Tohmonda *et al.* 2011), but otherwise its regulation by ER stress has not been studied.

5.1.2. Alkaline phosphatase

Alkaline phosphatase (ALP, TNAP, ALPL) is an enzyme that catalyses dephosphorylation of PPi, and thus it inactivates this natural calcification inhibitor and provides phosphate ions for HAp crystal formation. Mutations in the ALP gene have been linked to hypophosphatasia, an autosomal recessive disorder, that manifests with decreased bone mineralisation (Henthorn *et al.* 1992). ALP is ubiquitously expressed throughout the body, but increased levels in serum and in the vasculature have been linked to vascular disease and calcification (Kalantar-Zadeh *et al.* 2006, Dreschler *et al.* 2011). Increased expression of ALP accompanies calcification of VSMCs *in vitro* and it is thought to be crucial for this process (Shioi *et al.* 1995, Masuda *et al.* 2013, Duan *et al.* 2013), however not in all studies (Shroff *et al.* 2010). Even though it has a well-established role in vascular calcification, little is known about the regulation of this enzyme in VSMCs or in other tissues. To date only one transcription factor has been shown to regulate ALP expression, PPARγ inhibits its expression in osteoblasts (Lencel *et al.* 2011). No direct links between ALP expression and ER stress have been demonstrated so far.

In this chapter I set out to characterise the cellular localisation of Osterix and the effect of its knock-down on osteogenic differentiation of VSMCs. I also wanted to investigate whether ALP expression is directly regulated by ER stress-related transcription factors in VSMCs and if ALP activity changes in ER stress-induced calcification.

5.2. The function of Osterix in VSMCs

In the initial experiments in Chapter 4 I showed that Osterix mRNA expression was upregulated both by tunicamycin and thapsigargin treatments (Figure 4.2). However, Osterix protein levels were upregulated by tunicamycin and downregulated by thapsigargin (Figure 5.1 and 4.3). Expression of Osterix was not consistently affected by the knock-down of any ER stress transducer, but the knock-down of IRE1 and ATF4 caused an approximately 50% decrease in Osterix expression (Figure 4.9). All these results suggested that Osterix is regulated by the UPR.

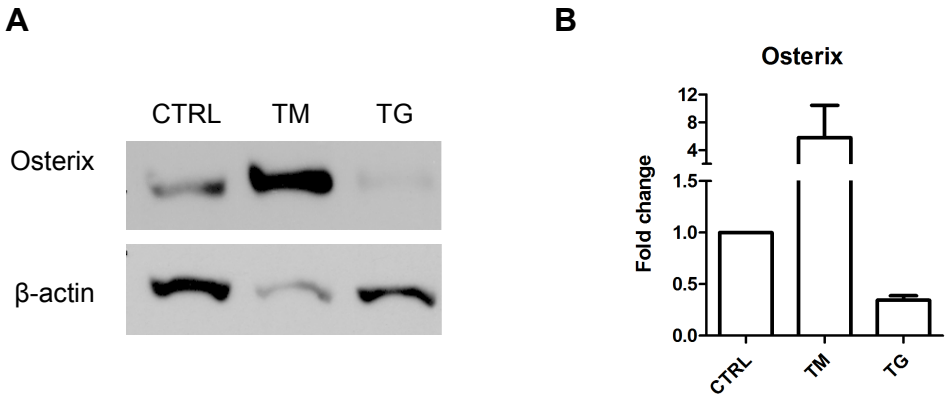

Figure 5.1. Osterix expression in response to ER stress. VSMCs were treated with 0.4μg/ml tunicamycin (TM) or 0.2μg/ml thapsigargin (TG) for 24 hours. **A.** Representative blot and **B.** quantification. Graph shows mean and SEM, n=3, ANOVA with Dunnett's *post hoc* tests was performed.

In parallel experiments I set out to characterise the function of Osterix in VSMCs. First, immunocytochemical analysis was performed to examine the subcellular localisation of Osterix. The results show that in VSMCs Osterix was localised in the nucleus and in the cytoplasm in foci (Figure 5.2.A). To test antibody specificity SAOS-2 osteosarcoma cells were stained for Osterix alongside VSMCs. In SAOS-2, Osterix was present mostly in the nuclei, but only some cells expressed it at high levels. Cytoplasmic foci were not observed, but weak grainy staining was present in the cytoplasm.

To further confirm the cytoplasmic localisation of Osterix in VSMCs, nuclear fractionation was carried out, followed by Western blotting, both for VSMCs and SAOS-2 cells (Figure 5.2.B). In both cell types Osterix was detected in both fractions, however higher amounts were present in the cytoplasmic fractions. That suggests that the cytoplasmic foci in VSMCs represent specific Osterix staining. Lower amounts of Osterix in the nuclei of SAOS-2 cells are consistent with the fact that high levels of nuclear Osterix were only observed in only a small number of these cells.

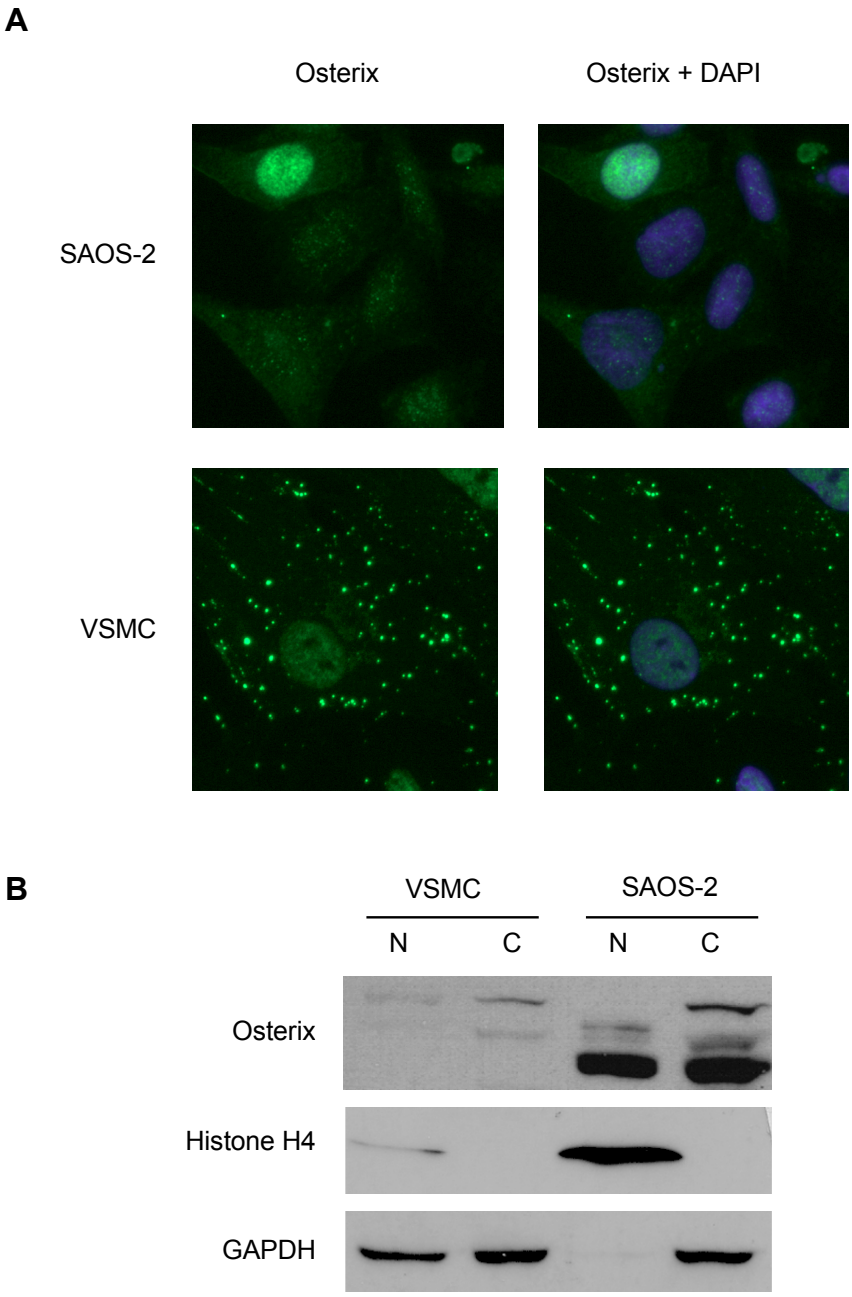

Figure 5.2. Subcellular localisation of Osterix in VSMCs and SAOS-2 cells. **A**. Immunoctyochemistry shows that in VSMCs Osterix localises to cytoplasmic foci **B.** Nuclear fractionation and Western blotting analysis confirmed that Osterix was localised in the cytoplasm. 'C' – cytoplasmic fraction, 'N' – nuclear fraction. N=3 for both experiments, representative images are shown.

In order to identify which cellular organelles these cytoplasmic Osterix foci associated with, immunocytochemical co-stainings with various vesicular organelle markers were carried out. Among the proteins examined were lysosome and late endosome marker LAMP-1 (Rohrer *et al.* 1996), early endosome marker EEA1 (Mu

et al. 1995) or multivesicular body marker CD63 (Kobayashi *et al.* 2000) (Figure 5.3). Osterix did not co-localise with any of these markers, which suggests that it is not localised in any of these organelles in VSMCs.

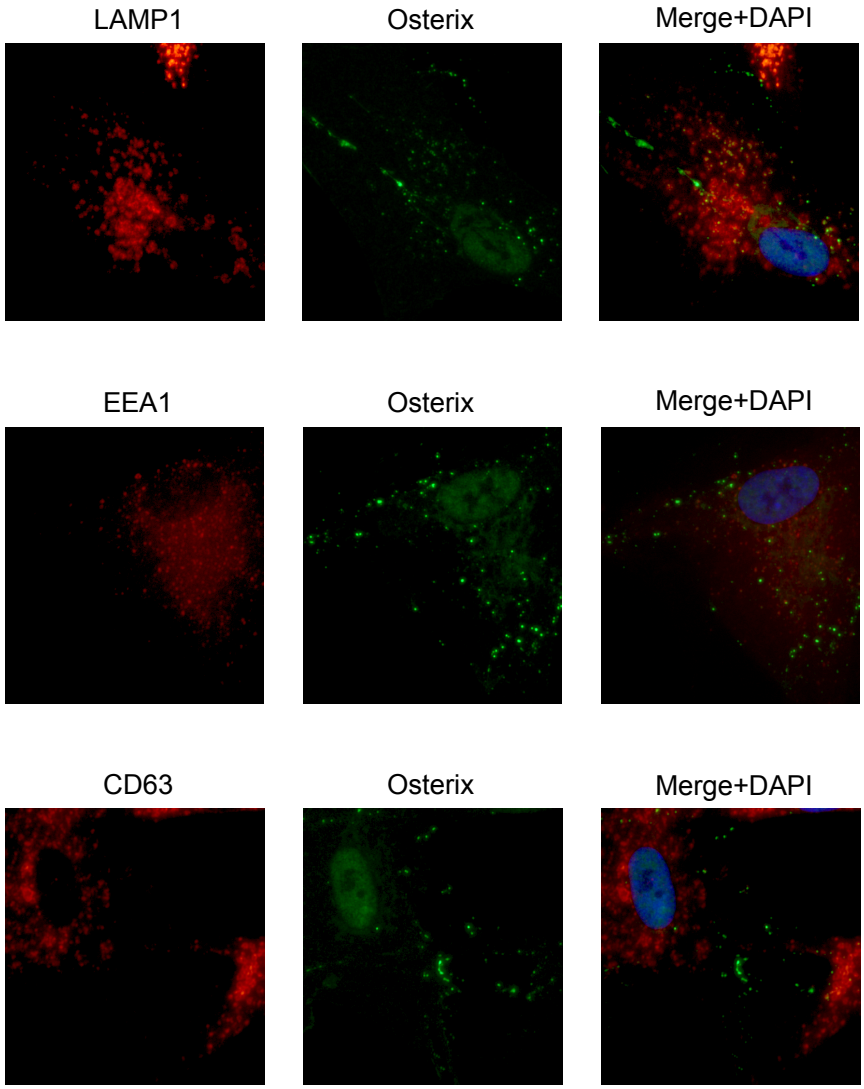

Figure 5.3. Analysis of Osterix foci in VSMCs by immunocytochemistry. VSMCs were co-stained with for Osterix (green) and lysosome and late endosome marker LAMP-1, early endosome marker EEA1 and multivesicular body marker CD63 (red). None of these markers co-localised with Osterix. N=3, figure shows representative images.

At the same time, siRNA knock-downs of Osterix were carried out as a different approach to elucidating its function in VSMCs. The ultimate goal was to examine whether expression of osteogenic genes in response to ER stress is affected by the absence of Osterix.

A protocol previously optimised for siRNA knock-downs of UPR components was used and then VSMCs were treated with tunicamycin and thapsigargin for 24 hours. Figure 5.4.A shows that this method resulted in only a very small decrease in Osterix mRNA, measured by real-time PCR. Figure 5.4.B and C show that at the same time-point levels of Osterix protein did not change at all. Therefore, a different protocol was used with a 7 day incubation of cells with the siRNA oligonucleotides. The results show that using this protocol Osterix protein expression was decreased by approximately 50% (Figure 5.4.B and C). The effectiveness of the siRNA oligonucleotides was tested in SAOS-2 cells, and they were effective in knocking down Osterix in this cell line (Figure 5.4.A, B and C). Interestingly however, Western blotting analysis of Osterix in SAOS-2 cells showed that the siRNA was more effective in knocking down some phosphorylation forms of Osterix better than others. It has been shown previously that Osterix can exhibit different phosphorylation forms, which are visualised as separate bands on a Western blot (Ortuno *et al.* 2010). SAOS-2 and VSMCs differ in the proportions in which these are present (Figure 5.2 and Figure 5.4). Perhaps Osterix was difficult to knock-down in VSMCs because some phosphorylation forms are sequestered in the cytoplasmic foci and therefore are more stable. In addition, alternative splice variants have been described for Osterix (Milona *et al.* 2003), that are possibly not targeted by the siRNA used.

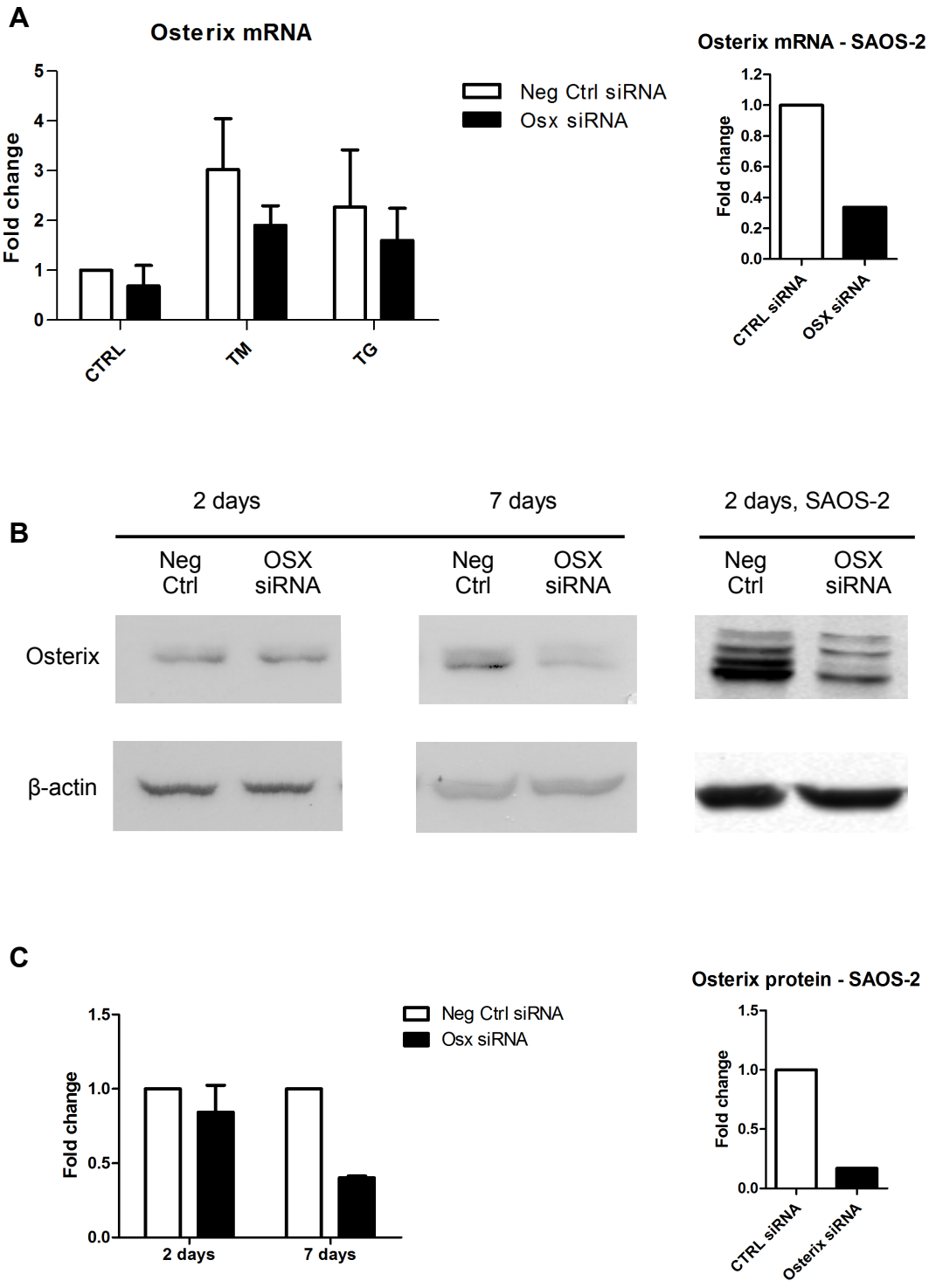

Figure 5.4. SiRNA knock-down of Osterix. VSMCs and SAOS-2 cells were incubated with siRNA against Osterix for 2 or 7 days and then treated with 0.4µg/ml tunicamycin (TM) or 0.2µg/ml thapsigargin (TG) for 24 hours. **A.** Levels of Osterix mRNA measured by real-time PCR after 2 days of siRNA treatment, n=3. **B.** Western blotting for Osterix, after 2 or 7 days incubation with siRNA. **C.** Quantification of Western blots, n=3 for 2 days, n=2 for 7 days, n=1 for SAOS-2 cells.

Several other approaches including retroviral and lentiviral vectors carrying shRNA targeting Osterix, and an Osterix-targetting microRNA were used in order to achieve a more robust knock-down in VSMCs. These were also tested in SAOS-2 cells, as they endogenously express high levels of Osterix.

MiR125b, an Osterix-targeting miRNA (Goettsch *et al.* 2011), was applied to VSMCs and SAOS-2 cells, according to a protocol similar to siRNA transfections. Osterix expression was measured at the mRNA and protein levels (Figure 5.5). The miRNA was not effective in knocking down Osterix in either cell type. Additional experiments were carried out in order to optimise the amount of the transfection reagent and the miRNA applied to cells but with no success (data not shown).

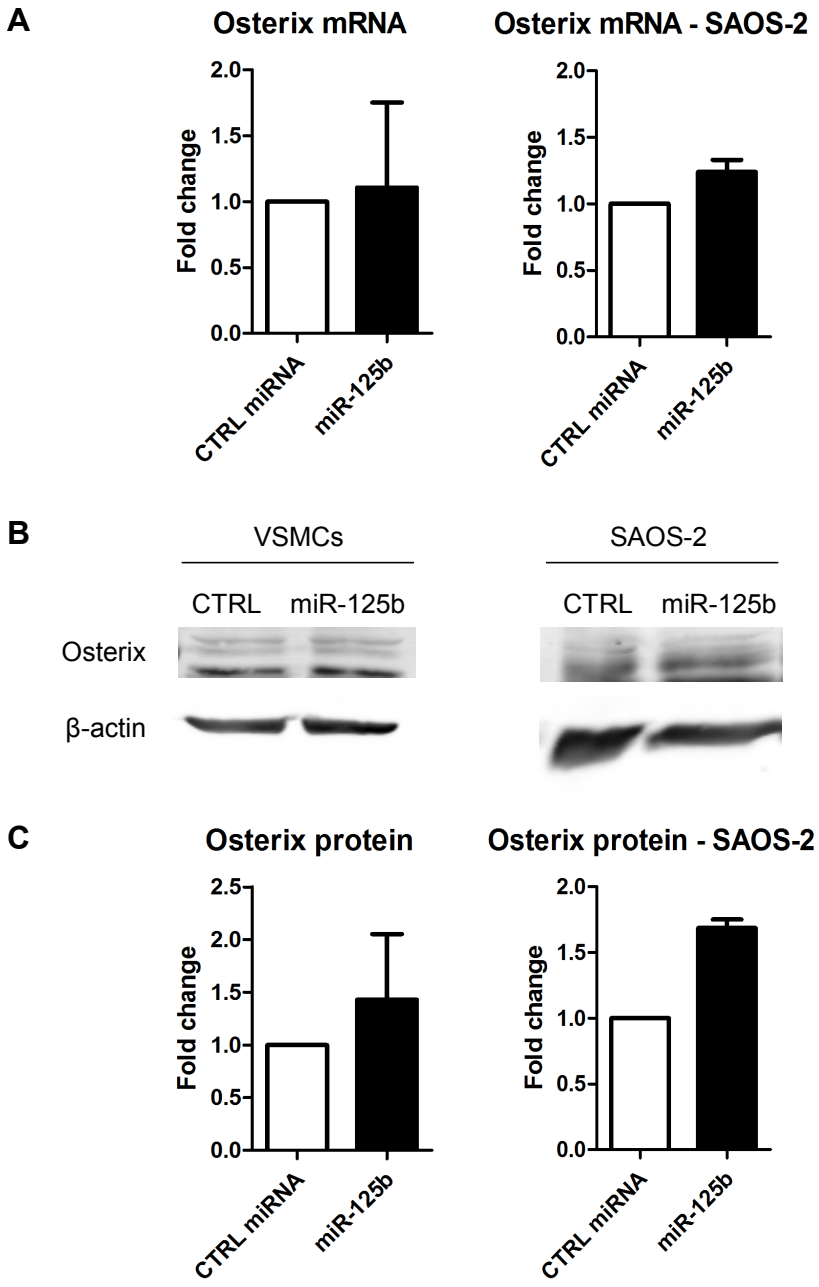

Figure 5.5. MiRNA knock-down of Osterix. VSMCs and SAOS-2 cells were incubated with miR-125b for 2 days **A.** Levels of Osterix mRNA measured by real-time PCR, n=2. **B.** Western blotting for Osterix, representative images. **C.** Quantification of Western blots, n=3 for VSMCs, n=2 for SAOS-2 cells.

Next, PG13 cells constitutively producing retroviruses carrying human Osterix cDNA, a Osterix shRNA knock-down cassette or empty retroviruses were obtained (Zhu *et al.* 2012). Media from these cells (containing retroviruses) were applied to SAOS-2 cells and levels of Osterix were analysed by Western blotting. The

results show that neither the overexpression or knock-down of Osterix worked (Figure 5.6). Several transduction protocols were also tested, including different incubation times, centrifuging cells in culture plates with the viral supernatants, different concentrations of the viral media and transducing also VSMCs, NIH 3T3 and C2C12 cells, but none proved effective (data not shown).

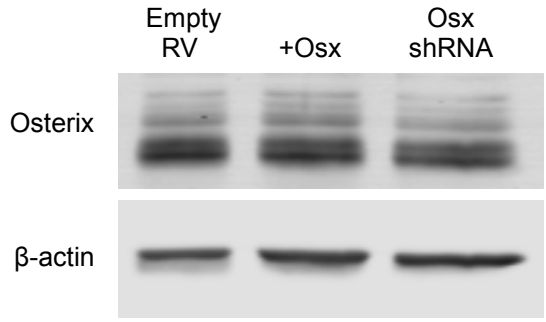

Figure 5.6. Retroviral overexpression and knock-down of Osterix in SAOS-2 cells. SAOS-2 cells were incubated with viral supernatants 2 days. Western blotting for Osterix, n=1.

Finally, commercially available lentiviral particles carrying shRNA Osterix knock-down cassettes were purchased. They were applied to VSMCs and SAOS-2 cells at different multiplicity of infections (MOI), according to the manufacturer's protocol. Four different viral clones in total were tested, each expressing a different Osterix-targeting shRNA, and an empty vector was used as a control. Figure 5.7 shows results for one clone as an example. Osterix levels were analysed using Western blotting and the lentiviruses were found to be ineffective in both VSMCs and SAOS-2 cells.

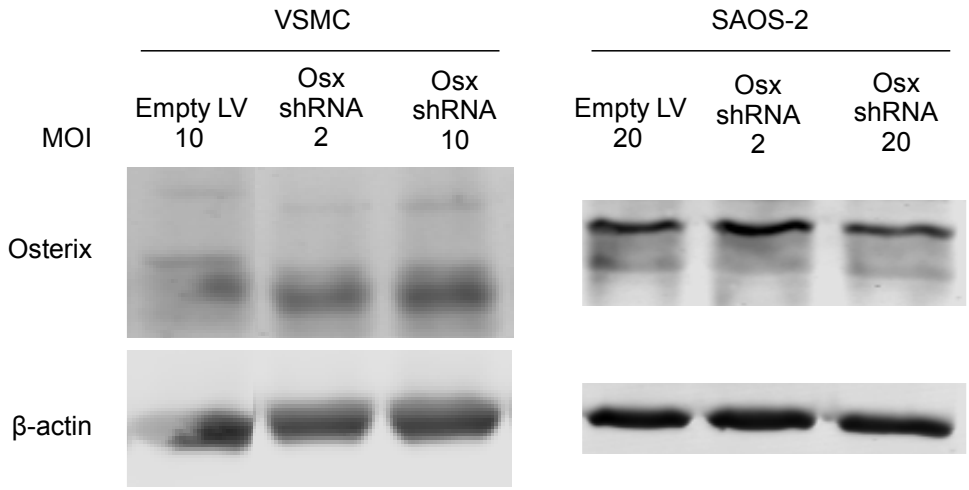

Figure 5.7. Lentiviral knock-down of Osterix. VSMCs and SAOS-2 cells were incubated with lentiviruses expressing shRNA against Osterix for 2 days according to the manufacturer's protocol. Western blotting for Osterix, n=1.

In order to test lentiviral transduction efficiencies, the same vector expressing GFP was purchased and tested in SAOS-2 cells. GFP expression levels were observed with a fluorescent microscope. At MOI of 20 the transduction efficiency was extremely low, explaining why the lentiviral vectors did not work (Figure 5.8) and showing that the commercially available lentiviruses were of poor quality.

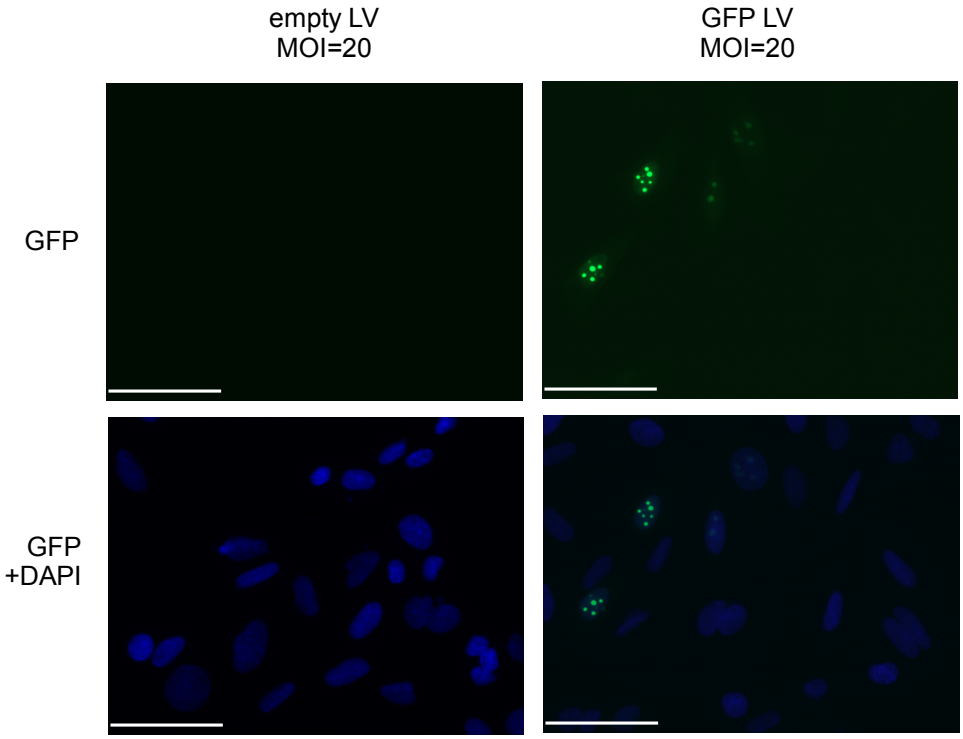

Figure 5.8. Test of lentiviral vector transduction efficiency. SAOS-2 cells were incubated with lentiviruses expressing GFP for 2 days according to the manufacturer's protocol, stained with nuclear dye DAPI, fixed with PFA, mounted in Mowiol mounting media and visualised in a fluorescent microscope. Scale bars are 60 μm.

To summarise, it has proven difficult to knock-down Osterix in VSMCs using siRNA or miRNA approaches. Knock-down using viral vectors was not successful due to technical difficulties. Therefore no further experiments on Osterix were carried out.

5.3. Regulation of ALP expression and activity by ER stress in VSMCs *in vitro*

5.3.1. ALP expression and activity are ATF4-dependent

The analysis of osteogenic gene expression presented in Chapter 2 shows that ALP mRNA levels measured by real-time PCR were consistently upregulated in VSMCs treated with tunicamycin and thapsigargin (Figure 5.9.A). Therefore, ALP activity was measured in order to examine whether changes in mRNA levels corresponded to differences in activity of this enzyme. ALP activity was significantly

increased (two-fold change) by tunicamycin treatment, but it did not change with thapsigargin treatment (Figure 5.9.B). This suggests ALP expression was upregulated by ER stress, but only tunicamycin triggered signalling events that lead to the activation of this enzyme.

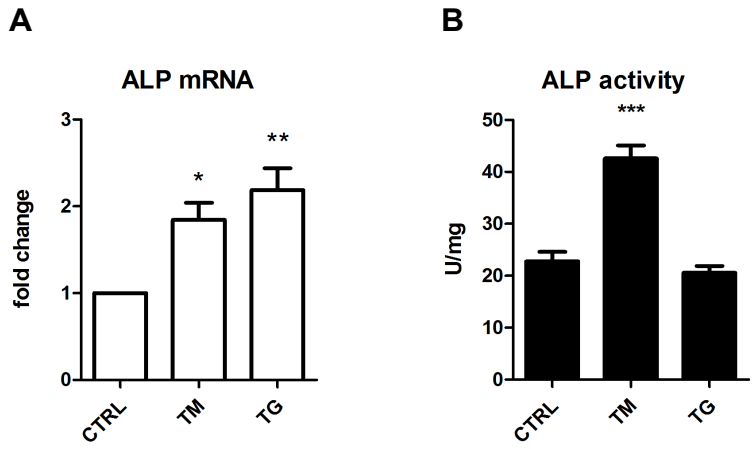

Figure 5.9. Alkaline phosphatase **A.** mRNA levels and **B.** activity are upregulated by ER stress. VSMCs were treated with 0.4µg/ml tunicamycin (TM) or 0.2µg/ml thapsigargin (TG) for 24 hours. Graphs show mean and SEM, n=3, ANOVA with Dunnett's *post hoc* tests was performed. Statistical significance is indicated with asterisks: * denotes p between 0.05 and 0.01, ** denotes p between 0.01 and 0.001, *** denotes p<0.001.

I next set out to determine whether ALP expression and activity can be directly regulated by UPR signalling in this context. ALP expression and activity levels have been shown to be ATF4-dependent in calcifying rat and mouse VSMCs *in vitro* (Masuda *et al.* 2013; Duan *et al.* 2013). In addition, in my experiments siRNA knock-down of ATF4 caused the largest decrease in ALP mRNA expression of all the UPR component knock-downs (Figure 4.10 and 5.10.A), therefore I measured ALP activity after ATF4 knock-down to check if the decrease in mRNA observed earlier corresponded to a decrease in ALP activity. The results in Figure 5.10.B show that ALP activity was increased by tunicamycin, and this increase was blocked by ATF4 knock-down. Activity at baseline and in thapsigargin-treated cells was not affected by ATF4 knock-down. This confirmed that ALP activity levels are ATF4-dependent in tunicamycin-treated cells.

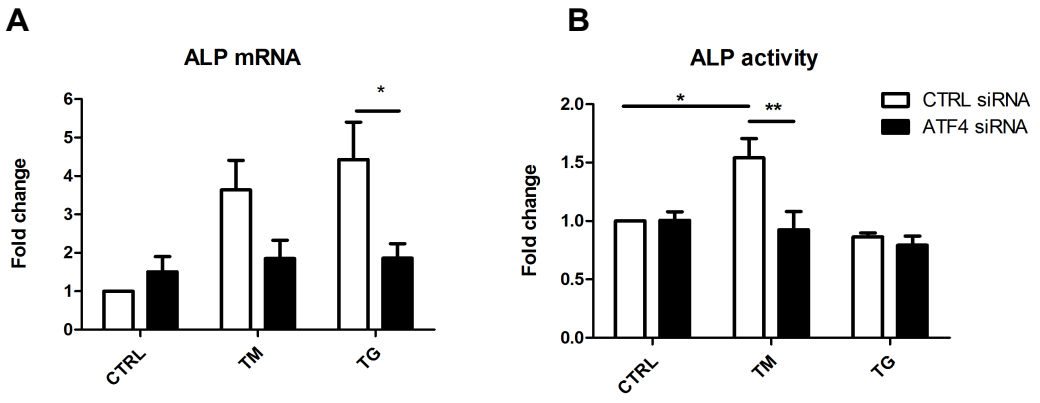

Figure 5.10. ATF4 knock-down causes a decrease in ALP **A.** mRNA expression and **B.** activity. VSMCs were treated with ATF4 siRNA for 48 hours and then 0.4μg/ml tunicamycin (TM) or 0.2μg/ml thapsigargin (TG) for 24 hours. Graphs show mean and SEM, n=3, ANOVA with Tukey's *post hoc* tests was performed. Statistical significance is indicated with asterisks: * denotes p between 0.05 and 0.01, ** denotes p between 0.01 and 0.001.

5.3.2. Identification of ALP transcription regulators

The next set of experiments aimed at establishing whether the increase in ALP mRNA expression in tunicamycin- and thapsigargin-treated VSMCs was due to increased transcription. The first step was to examine whether ALP promoter activity is regulated by ER stress. Ten constructs containing fragments of the 5'-upstream region of the human ALP gene spanning from -122 to -4556 (counting from the first nucleotide of the initiation codon) cloned in front of a firefly luciferase gene were obtained (Figure 5.11). Construct 1 contained the full length sequence of the examined promoter fragment and constructs 2-10 were deletion constructs derived from construct 1, which means each consecutive fragment was shorter than the one before. VSMCs were transfected with each of the 10 constructs, treated with tunicamycin and thapsigargin for 24 hours and luciferase promoter assays were carried out.

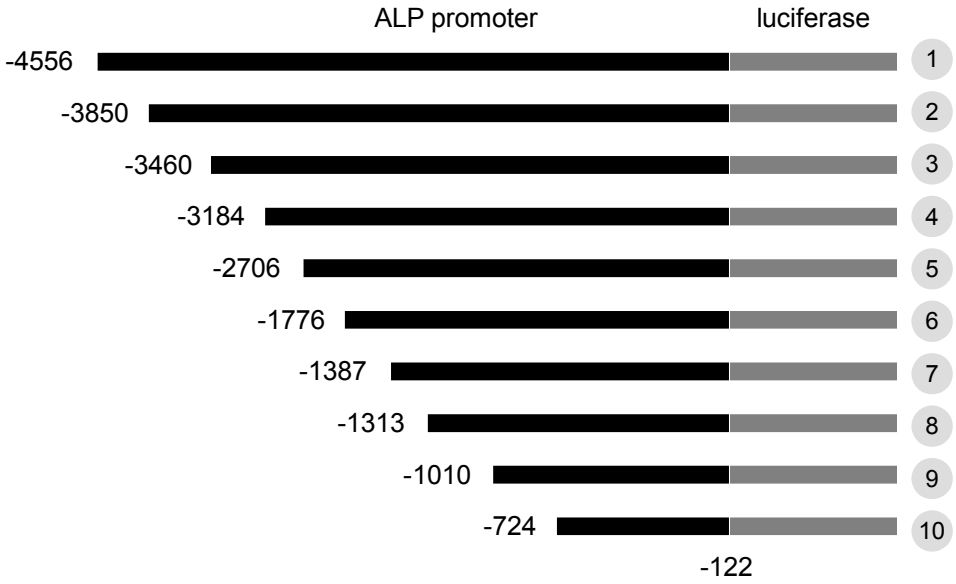

Figure 5.11. Schematic showing ALP promoter constructs for luciferase assay. Construct 1 represents the full length fragment and constructs 2-10 are shorter fragments derived by deleting increasing portions of the full length. Based of figure from Orimo *et al.* 2005.

Preliminary luciferase assay results (n=1) show that constructs 1, 3, 5, 6, 7, 9 and 10 contained fragments of the ALP promoter that were transcriptionally active in VSMCs. Furthermore, expression of luciferase was activated further in constructs 3, 5, 6 and 7 by thapsigargin treatment, and construct 6 and 7 also by tunicamycin (Figure 5.12.A).

Further assays were carried out to validate results for constructs from which expression was regulated by ER stress. The results confirmed that thapsigargin induced activity of promoter fragments 3, 5, 6 and 7. However, in this set of experiments, tunicamycin did not have an effect on ALP promoter activity (Figure 5.12.B). These results further support the notion that tunicamycin and thapsigargin regulate ALP via different pathways. They also suggest that tunicamycin-responsive elements of the promoter might not have been encompassed by the constructs used, that could explain why ALP promoter activity was not increased by tunicamycin and enzyme activity and mRNA expression was.

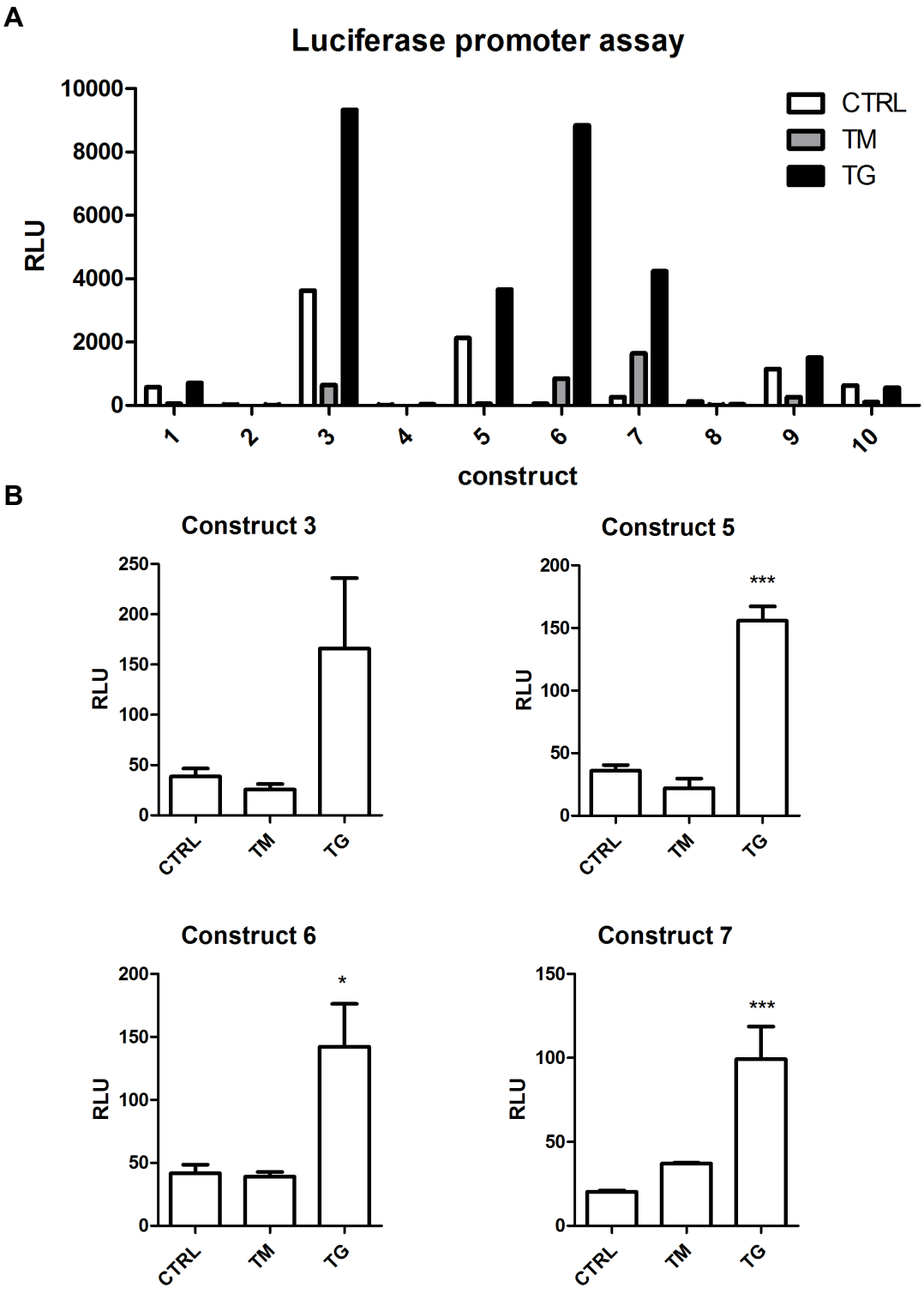

Figure 5.12. ALP promoter activity in response to ER stress - luciferase reporter assays. VSMCs were transfected with luciferase constructs for 24 hours and then treated with 0.4µg/ml tunicamycin (TM) or 0.2µg/ml thapsigargin (TG) for 24 hours. **A.** Overview of all promoter activity in all 10 constructs, n=1. **B.** Validation of luciferase activity for constructs 3, 5, 6 and 7. Graphs show mean and SEM, n=3, ANOVA with Dunnett's *post hoc* tests was performed. Statistical significance is indicated with asterisks: * denotes p between 0.05 and 0.01, *** denotes p<0.001.

Based on the luciferase assay results with the deletion constructs it was possible to infer which sequences activate and which suppress transcription from the examined fragment of the ALP promoter, as the level of reporter gene expression is the outcome of influences of both types of sequences. It was concluded that the examined fragment of the promoter region likely contains three silencing sequences, surrounded by sequences that activate transcription. Figure 5.13.A shows a schematic representation of the proposed silencers and enhancers in each of the luciferase constructs. Constructs 2, 4 and 8 showed no luciferase activity, and therefore likely contain silencing sequences, which when not surrounded by activators inhibit transcription. It is also apparent that the promoter fragment shared by constructs 3 to 7 contains a sequence that is highly active in VSMCs and inducible by ER stress and therefore of interest.

A

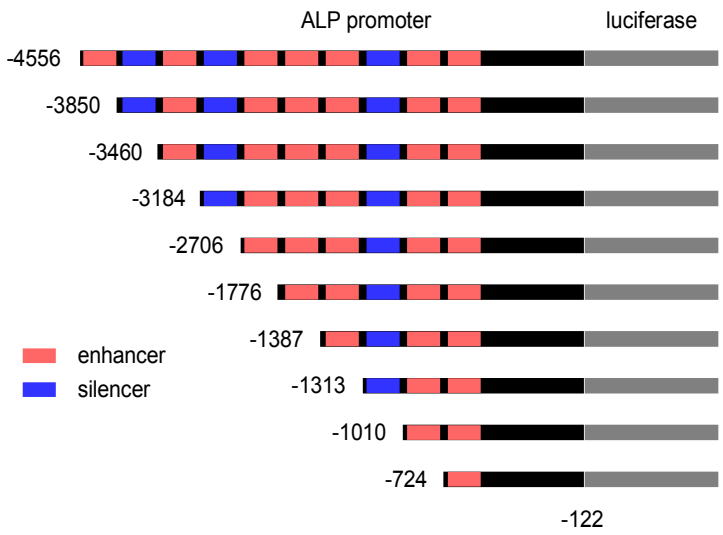

B

Construct	Luciferase activity		
	Baseline	**TM**	**TG**
1	+	-	+
2	-	-	-
3	++	+	+++
4	-	-	-
5	++	-	++
6	-	+	+++
7	+	++	+++
8	-	-	-
9	+	-	+
10	+	-	+

Figure 5.13. Enhancers and silencers within the ALP promoter. **A.** Schematic of ALP promoter constructs with potential regions activating (red) and inhibiting (blue) transcription in VSCMs based on **B.** luciferase assay results. '+' denotes degrees of activation, '-' denotes lack of promoter activity.

The next step was to investigate whether there are any ER stress-related transcription factor binding sites within the sequence encompassed by the promoter constructs, whether ATF4 is one of them, and whether they are located in the discovered enhancer sequences. Therefore, the promoter sequence was

subjected to bioinformatics analysis with Genomatix Matinspector, which contains a database of known transcription factor consensus binding sequences.

Figure 5.14.A shows a schematic representation of the whole examined promoter fragment; several binding sites for ATF6, ATF4, CHOP and XBP1 were predicted in this sequence (the full annotated sequence can be found in the Appendix, Figure 7.5). Figure 5.14.B shows where each of these predicted binding sites is located in each luciferase construct.

Two ATF6 binding sequences were identified, both in activator regions present in constructs 1-5. Two XBP1 binding sequences were shown to be present in an activator region present in all constructs. A CREB/ATF binding sequence was found in an activator only present in construct 1. There were two ATF4 binding sites predicted, one localised in a silencer sequence and one in an enhancer, located in a region of the promoter encompassed by constructs 1 to 5. This fact further supported the notion that ATF4 could be a direct regulator of ALP expression.

It is also interesting that CHOP and ATF4 binding sites were found in a silencer fragment that did not induce any luciferase expression (constructs 1 and 2, Figure 5.14.B), suggesting that these transcription factors might be involved in inhibiting rather than promoting ALP expression in response to ER stress.

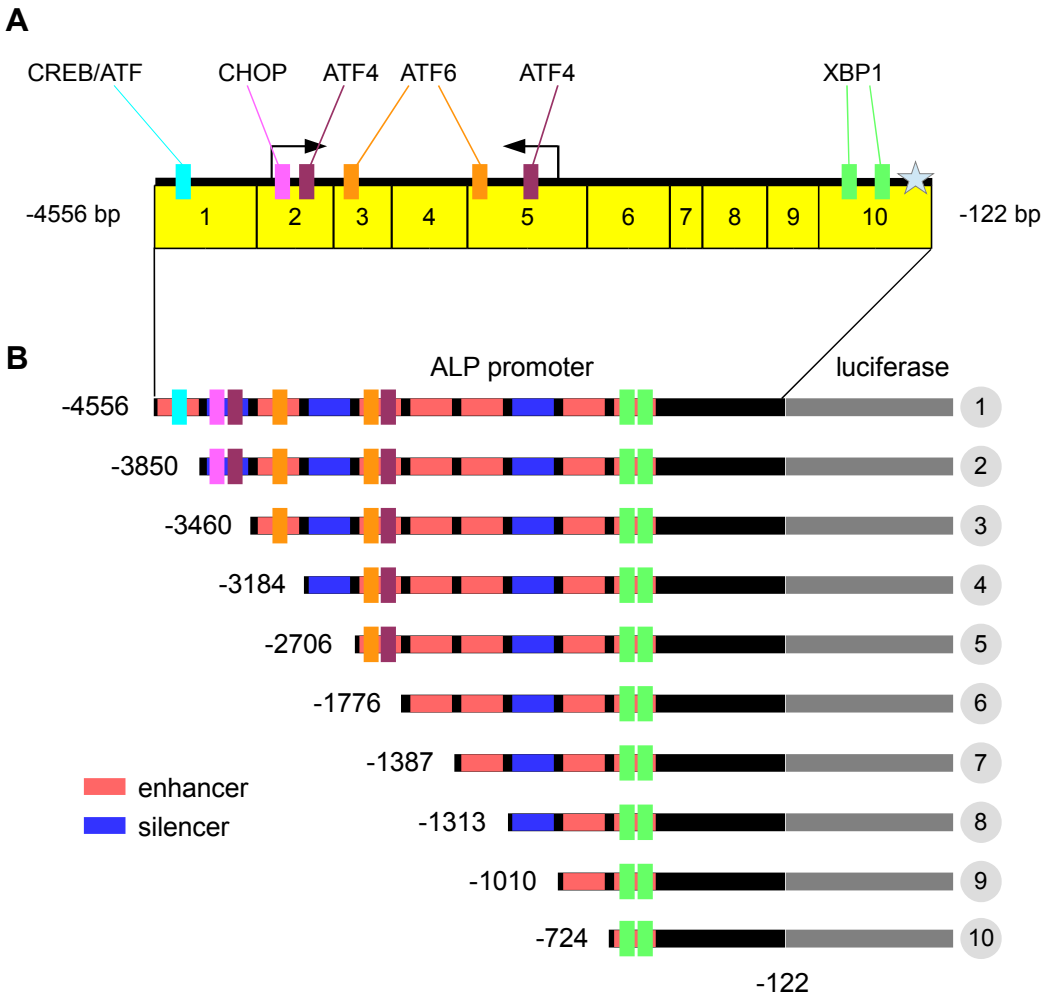

Figure 5.14. ER stress-related transcription factor binding sites mapped to the ALP promoter. **A.** Schematic of the full length of the examined promoter fragment, numbers 1-10 refer to luciferase constructs, in which a given fragment is at the end. Blue star marks the transcription start site. Arrows indicate the fragment used for DNA binding assays in later experiments. **B.** Localisation of transcription factor binding sites in enhancer and silencer fragments of the ALP promoter constructs. Potential regions activating transcription (enhancers) are marked red and regions inhibiting ALP transcription (silencers) in VSCMs are marked blue.

To examine whether ATF4 indeed plays a direct role in activation of the examined fragment of the ALP promoter, luciferase assays were performed with simultaneous ATF4 siRNA knock-down. VSMCs were transfected with luciferase vectors for 24 hours, then incubated with siRNA for 24 hours and finally treated with tunicamycin and thapsigargin for 24 hours. Constructs which showed high promoter activity in response to tunicamycin or thapsigargin were used in these experiments. Constructs 3 and 5 were chosen, as they had an ATF4 binding site

predicted. Constructs 6 and 7 were also used, even though no ATF4 binding sites were predicted for these fragments of the promoter. The rationale behind these choices was that if ATF4 activated expression from the ALP promoter fragments in construct 3 and 5, siRNA knock-down of ATF4 would decrease luciferase expression from these two constructs, but not from constructs 6 and 7, which did not contain the ATF4 binding sites. Construct 1 and 2 were not used, even though they contained another ATF4 binding site, because they showed very low promoter activity in the initial experiments.

The results of the luciferase assays were inconclusive as the readings were very variable, with no statistically significant differences (Figure 5.15). There was a trend that ATF4 knock-down decreased the activity of promoter fragments 3, 5 and 6 at baseline. It also decreased activity of cells transfected with construct 5 and treated with thapsigargin and construct 7 with tunicamycin. However, ATF4 knock-down increased activity of construct 3 in tunicamycin-treated cells. Therefore, there was no ground to confirm or exclude ATF4 as a regulator of ALP activity.

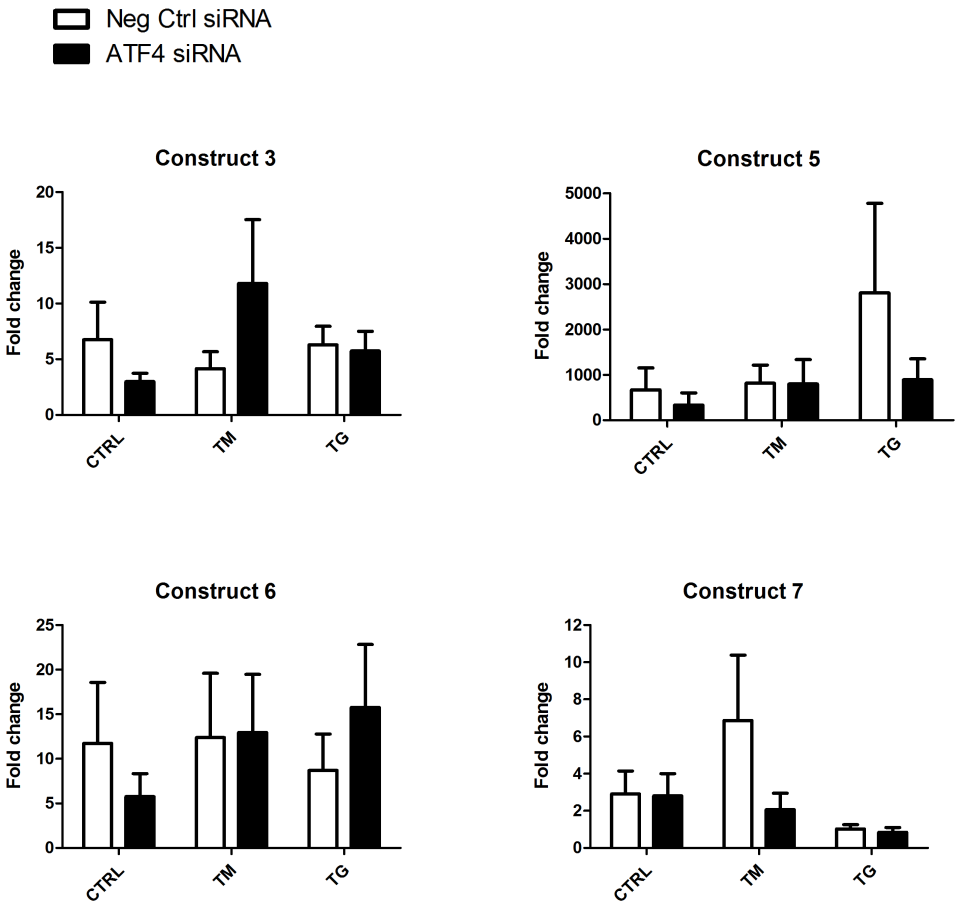

Figure 5.15. ALP promoter activity after ATF4 siRNA knockdown. VSMCs were transfected with luciferase vectors for 24 hours, then incubated with siRNA for 24 hours and treated with 0.4µg/ml tunicamycin (TM) or 0.2µg/ml thapsigargin (TG) for 24 hours. Graphs show mean and SEM, n=3, ANOVA with Tukey's *post hoc* tests was performed.

Since the results of luciferase assays were inconclusive, a different approach was used to examine whether ATF4 directly regulates ALP promoter activity. The fragment of the promoter containing both potential ATF4 binding sites (-3631 to -2048bp from the first intron, encompassed by constructs 2 to 5, marked with two arrows in Figure 5.14.A) was amplified using biotinylated primers. The product was conjugated onto magnetic streptavidin beads. The beads were then incubated with VSMC nuclear extracts, washed and proteins eluted off the DNA were analysed by Western blotting to detect ATF4.

Figure 5.16 shows that ATF4 was not detected in the eluted extracts. The presence of a band corresponding to ATF4 in the lane with an unprocessed nuclear

extract suggested that either ATF4 did not bind to the tested promoter fragment, or that it was present in amounts too small to be detected by Western blotting.

The gels used for ATF4 Western blots were stained with Coomassie Brilliant Blue, to visualise all proteins present on both samples. Figure 5.16 shows that proteins were detected in the pulldown sample. This suggested that there might be other proteins than ATF4, binding the examined fragment of the ALP promoter.

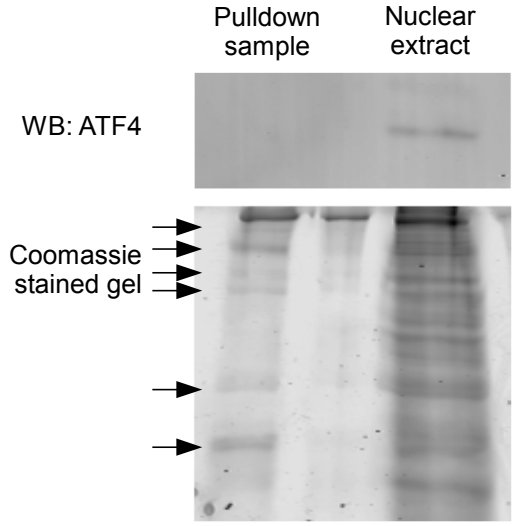

Figure 5.16. DNA binding assay to identify proteins bound to the ALP promoter and Western blotting for ATF4 (WB). The fragment of the ALP promoter containing potential ATF4 binding sites was amplified using biotinylated primers and conjugated onto magnetic streptavidin beads. The beads were then incubated with VSMC nuclear extracts, washed and proteins were eluted off the DNA and analysed by Western blotting. Coomassie gel demonstrates that even though ATF4 was not detected in the pulldown sample, other proteins were present (arrows). N=3, figure shows representative images.

Therefore, the DNA binding experiment was repeated and proteins bound to the examined fragment of ALP promoter were analysed using a proteomics mass spectrometry approach to identify additional factors that might regulate its activity.

A thapsigargin-treated nuclear extract was used for the proteomic experiment to increase the chances of finding protein-ALP promoter interactions relevant to ER stress. Thapsigargin was chosen for this experiment, as it was associated with more consistently increased promoter activity in the luciferase assays. The nuclear extract was bound and eluted from the biotinylated DNA on beads (pulldown sample) and compared to an aliquot of the same extract incubated

with beads without DNA (negative CTRL) to control for nonspecific binding to the beads (Figure 5.17). Both samples were resolved on an acrylamide gel which was stained with Coomassie. Even though there were many bands in the lane with the negative control, there were a few that were present only in the pulldown sample (indicated with arrows in Figure 5.17). Corresponding fragments of both lanes (marked with red boxes in Figure 5.17) were excised from the gel and subjected to liquid chromatography-mass spectrometry (LC-MS/MS).

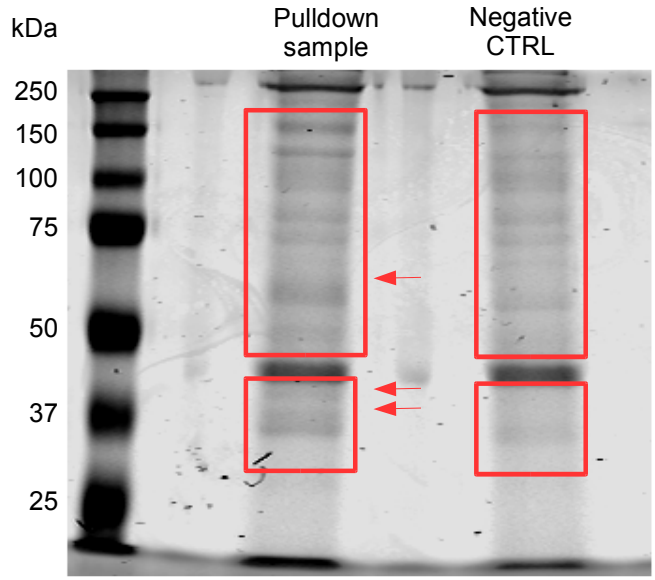

Figure 5.17. Coomassie-stained acrylamide gel used for proteomics analysis of proteins bound to the ALP promoter. Nuclear extracts were bound and eluted off the biotinylated DNA on beads and analysed by SDS-PAGE. Arrows indicate bands unique for the pulldown sample. Red boxes indicate fragments of gel that were excised and analysed by LC-MS/MS.

The mass spectrometry analysis identified 447 different proteins with 95% or more probability, for which more that 1 peptide was present, in both lanes. ATF4 was not among them. 166 of these proteins were present only in the pulldown sample and not in the negative control. 17 of these have transcription regulating activity. Table 5.1 contains a summary of information about these proteins.

None of the 17 identified proteins are known to be regulated by ER stress or associated with the ALP promoter, however three have bone-related functions. DDX5 has been shown to act as a co-activator for Runx2 and to regulate osteoblast

differentiation (Jensen *et al.* 2008). Another protein identified in the analysis was β-catenin, which belongs to the Wnt signalling pathway and is crucial for bone formation and has been implicated in vascular calcification (Shao *et al.* 2005). Finally, THRAP3 interacts with PPARγ, which has been shown to suppress ALP promoter activity in osteoblasts (Katano *et al.* 2013, Lencel *et al.* 2011, Woldt *et al.* 2005).

Table 5.1. Transcription-regulating proteins that bind to the ALP promoter, identified by LC-MS/MS. Information was retrieved from Genecards (http://www.genecards.org/).

Protein	Gene	Accession number	No peptides	Information	Activator (+) Repressor (-)
Staphylococcal nuclease domain-containing protein 1	SND1	SND1_HUMAN	18	Functions as a bridging factor between STAT6 and the basal transcription factor. Plays a role in PIM1 regulation of MYB activity. Functions as a transcriptional coactivator for the Epstein-Barr virus nuclear antigen 2 (EBNA2).	+
Far upstream element-binding protein 1	FUBP1	FUBP1_HUMAN	19	This gene encodes a ssDNA binding protein that activates the far upstream element (FUSE) of c-myc and stimulates expression of c-myc in undifferentiated cells. This protein has been shown to function as an ATP-dependent DNA helicase. May act both as activator and repressor of transcription.	+/-
Probable ATP-dependent RNA helicase DDX5	DDX5	DDX5_HUMAN	11	Involved in the alternative regulation of pre-mRNA splicing. Involved in transcriptional regulation; the function is independent of the RNA helicase activity. Transcriptional coactivator for estrogen receptor ESR1, androgen receptor AR and p53/TP53. Synergizes with DDX17 and SRA1 RNA to activate MYOD1 transcriptional activity and involved in skeletal muscle differentiation. Transcriptional coactivator for RUNX2 and involved in regulation of osteoblast differentiation. Acts as transcriptional repressor in a promoter-specific manner; the function probably involves association with histone deacetylases, such as HDAC1.	+/-
Transcription intermediary factor 1-beta	TRIM28	TIF1B_HUMAN	8	Nuclear corepressor for KRAB domain-containing zinc finger proteins (KRAB-ZFPs). Mediates gene silencing by recruiting. Enhances transcriptional repression by coordinating the methylation and acetylation of histones. May play a role as a coactivator for CEBPB and NR3C1 in the transcriptional activation of ORM1. Also corepressor for ERBB4. Inhibits E2F1 activity. Important regulator of CDKN1A/p21(CIP1). Mediates the nuclear localization of KOX1, ZNF268 and ZNF300 transcription factors.	+/-
Nuclear receptor subfamily 1 group I member 2	NR1I2	NR1I2_HUMAN	5	Nuclear receptor that binds and is activated by variety of endogenous and xenobiotic compounds. Transcription factor that activates the transcription of multiple genes involved in the metabolism and secretion of potentially harmful xenobiotics, drugs and endogenous compounds. Binds to a response element in the promoters of the CYP3A4 and ABCB1/MDR1 genes.	+

Protein	Gene	Accession number	No peptides	Information	Activator (+) Repressor (-)
Probable ATP-dependent RNA helicase DDX17	DDX17	DDX17_HUMAN	9	RNA-dependent ATPase. Involved in transcriptional regulation. Transcriptional coactivator for estrogen receptor ESR1. Synergizes with DDX5 and SRA1 RNA to activate MYOD1 transcriptional activity and probably involved in skeletal muscle differentiation.	+
ATP-dependent RNA helicase DDX1	DDX1	DDX1_HUMAN	6	ATP-dependent RNA helicase, able to unwind both RNA-RNA and RNA-DNA duplexes. May play a role in RNA clearance at DNA double-strand breaks . Together with RELA, acts as a coactivator to enhance NFκB-mediated transcriptional activation. Acts as a positive transcriptional regulator of cyclin CCND2 expression. Binds to the cyclin CCND2 promoter region.	+
Pre-mRNA-processing factor 6	PRPF6	PRP6_HUMAN	6	Involved in pre-mRNA splicing as component of the U4/U6-U5 tri-snRNP complex, one of the building blocks of the spliceosome. Enhances transactivation activity of AR, as well as transactivation activity of NR3C1, but does not affect estrogen-induced transactivation.	+
RNA-binding protein 14	RBM14	RBM14_HUMAN	5	This gene encodes a ribonucleoprotein that functions as a general nuclear coactivator, and an RNA splicing modulator. Interacts with thyroid hormone receptor-binding protein (TRBP), and is required for transcription activation.	+
Splicing factor 1	SF1	SF01_HUMAN	4	Necessary for the ATP-dependent first step of spliceosome assembly. Binds to the intron branch point sequence (BPS) 5'-UACUAAC-3' of the pre-mRNA. May act as transcription repressor.	+/-
Thyroid hormone receptor-associated protein 3	THRAP3	TR150_HUMAN	3	Involved in pre-mRNA splicing. Involved in response to DNA damage. Cooperatively with HELZ2, enhances the transcriptional activation mediated by PPARG, maybe through the stabilization of the PPARG binding to DNA in presence of ligand. May play a role in the terminal stage of adipocyte differentiation.	+
Proliferation-associated protein 2G4	PA2G4	PA2G4_HUMAN	3	Acts a co-repressor of the androgen receptor (AR) and is regulated by the ERBB3 ligand neuregulin-1/heregulin (HRG). Inhibits transcription of some E2F1-regulated promoters, probably by recruiting histone acetylase (HAT) activity. Mediates cap-independent translation of specific viral IRESs (internal ribosomal entry site).	-
Zinc finger protein 207	ZNF207	ZN207_HUMAN	3	GO annotations related to this gene include heparin binding and sequence-specific DNA binding transcription factor activity. Expressed in human VSMCs. Has something to do with kinetochore and mitotic spindle.	?
Catenin beta-1	CTNNB1	CTNB1_HUMAN	3	Key downstream component of the canonical Wnt signalling pathway. In the presence of Wnt ligand, CTNNB1 is not ubiquitinated and accumulates in the nucleus, where it acts as a coactivator for transcription factors of the TCF/LEF family, leading to activate Wnt responsive genes. Involved in the regulation of cell adhesion. Acts as a negative regulator of centrosome cohesion.	+

Protein	Gene	Accession number	No peptides	Information	Activator (+) Repressor (-)
26S protease regulatory subunit 6A	PSMC3	PRS6A_HUMAN	2	This gene encodes one of the ATPase subunits of the 26S proteasome, a member of the triple-A family of ATPases that have chaperone-like activity.	?
Protein AATF	AATF	AATF_HUMAN	2	May function as a general inhibitor of the histone deacetylase HDAC1. Binding to the pocket region of RB1 may displace HDAC1 from RB1/E2F complexes, leading to activation of E2F target genes and cell cycle progression. Conversely, displacement of HDAC1 from SP1 bound to the CDKN1A promoter leads to increased expression of this CDK inhibitor and blocks cell cycle progression.	+

Further bioinformatics analysis did not predict binding sites for any of these proteins in the examined ALP promoter fragment. However, some of them might not have known consensus sequences or not have DNA-binding domains and therefore interact with the promoter indirectly. This appeared to be true for β-catenin, which activates transcription of its targets by forming a complex with TCF and LEF (Novak *et al.* 1999; Westendorf *et al.* 2004). The bioinformatics analysis has revealed that a TCF/LEF binding site is present in the analysed fragment of the ALP promoter (Figure 5.18; full annotated sequence is in the Appendix, Figure 7.5). The binding site is localised in a silencer region present in constructs 1-4, which was responsible for the lack of promoter activity of construct 4 (Figure 5.12 and 5.13). This suggests that β-catenin could be involved in repressing transcription of ALP.

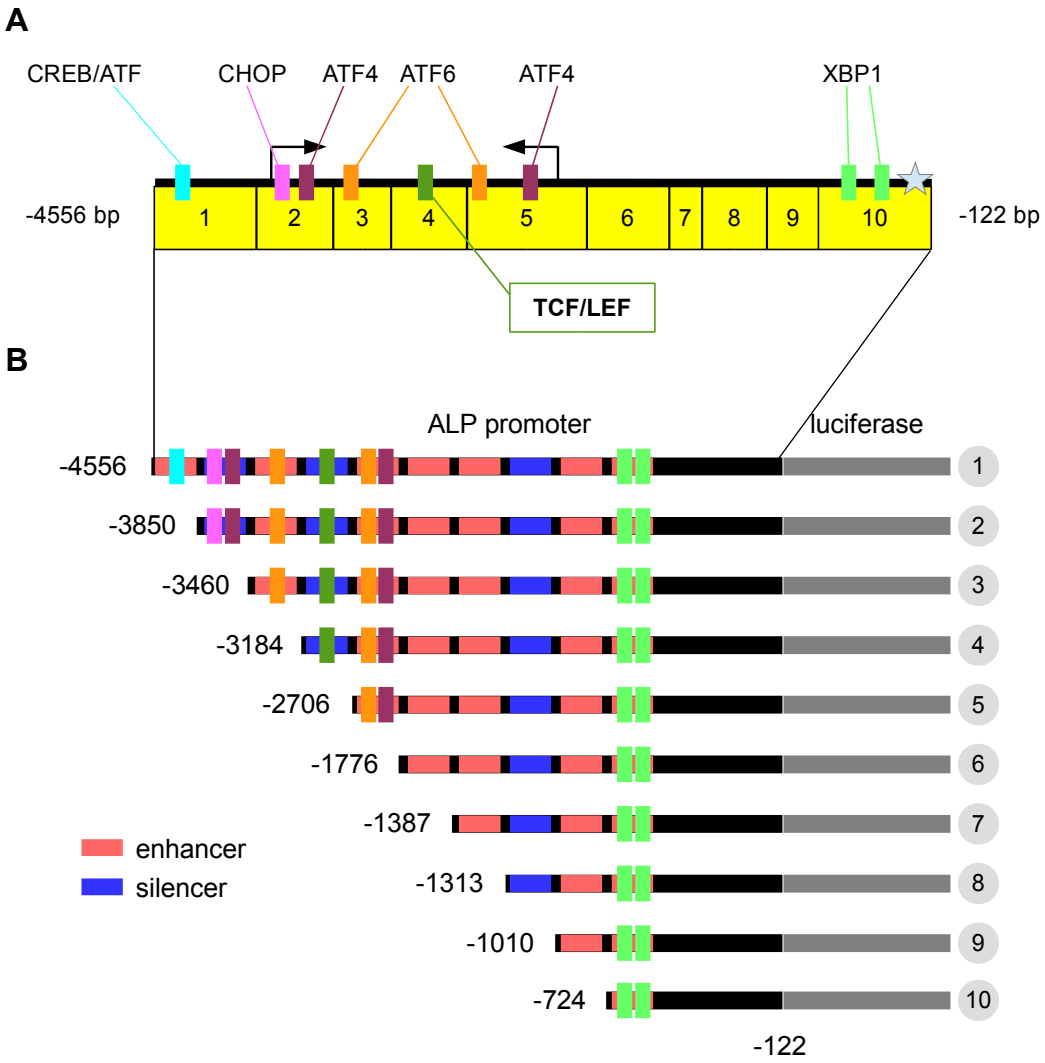

Figure 5.18. Analysed ALP promoter region with TCF/LEF binding site mapped. **A.** Schematic of the examined promoter fragment, numbers 1-10 refer to constructs. Blue star marks the transcription start site. Arrows indicate the fragment used for DNA binding assays. **B.** Localisation of transcription factor binding sites in enhancer and silencer fragments of the ALP promoter constructs. Potential regions activating transcription (enhancers) are marked red and regions inhibiting ALP transcription (silencers) in VSCMs are marked blue.

Taken together these results strongly suggest that ATF4 does not bind the tested fragment of ALP promoter. However, other proteins potentially involved in regulating ALP expression in VSMCs have been identified.

5.4. Alkaline phosphatase activity in mouse aortic rings

Even though ATF4 was not shown to be a direct regulator of ALP it was still important to investigate the role of ALP in ER-stress enhanced calcification. The first step was to examine whether ER stress inducers have the same effect on ALP activity in an *ex vivo* setting of mouse aortic rings. Aortas were harvested from wild type mice, cut into rings, treated with tunicamycin and thapsigargin for 24 hours and then ALP activity was measured. Corresponding samples were collected for Western blotting analysis.

Western blotting for Grp78 and Grp94 confirmed that ER stress was induced in these conditions (Figure 5.19.B and C). Results of activity assays showed that there was a lot of variability in baseline ALP activity in the aortic rings. After tunicamycin treatment ALP activity was slightly decreased, but the change was not statistically significant. Thapsigargin did not induce an overall change in ALP activity levels (Figure 5.19.A). These results suggest that in mouse VSMCs in a vessel wall ER stress did not induce ALP activity in the tested conditions.

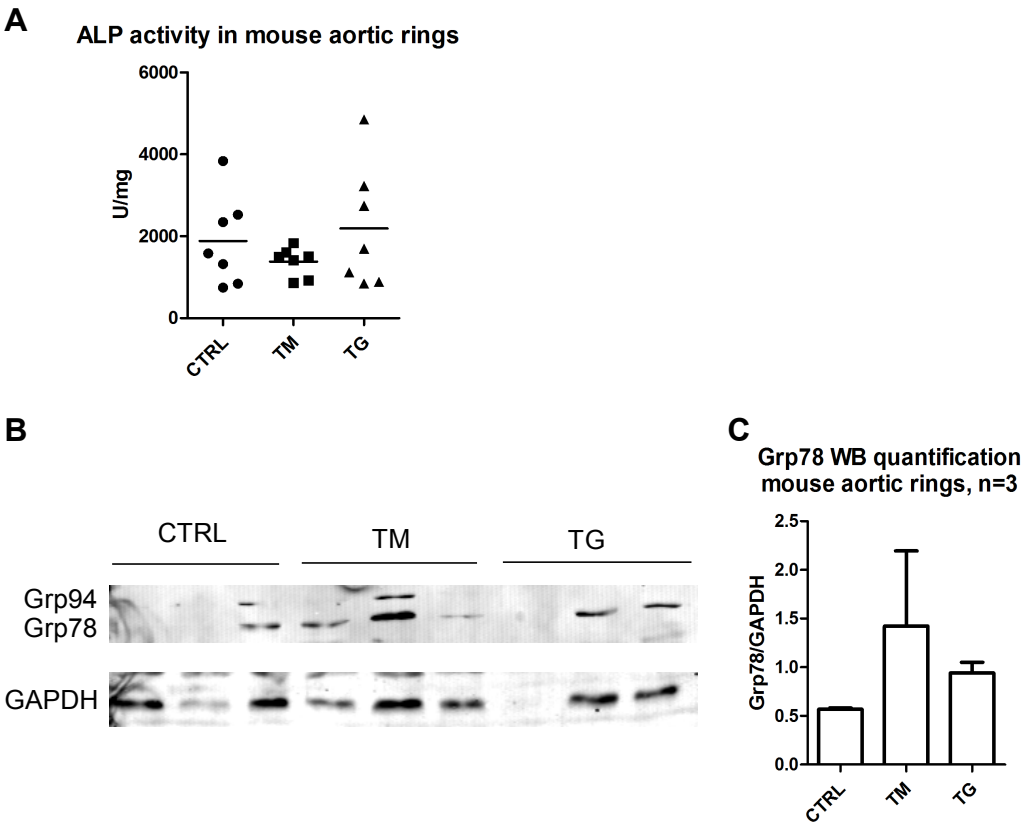

Figure 5.19. Alkaline phosphatase activity **i**n mouse aortic rings. **A.** Activity measured after a 24 hour treatment with 0.4µg/ml tunicamycin (TM) or 0.2µg/ml thapsigargin (TG) and normalised to the weight of each aortic ring. Graph shows data points and mean, n=7, ANOVA with Dunnett's *post hoc* tests was performed. **B.** Western blotting for ER stress markers Grp78 and Grp94 confirms that ER stress was induced in these conditions. **C.** Quantification of Grp78 western blot. Graph shows mean and SEM, n=3, ANOVA with Dunnett's *post hoc* tests was performed.

To investigate the possibility that a longer time-point might be required to elicit a more consistent response to ER stress in terms of ALP activity in mouse aortic rings, a long-term experiment was carried out. In this experiment aortic rings were incubated with tunicamycin or thapsigargin for 36 hours, 7 days and 14 days. At each time-point the vessels were collected for ALP activity measurement and Western blotting and at 14 days they were also collected for histological analysis.

Results show that at all three time-points both tunicamycin and thapsigargin caused a decrease in alkaline phosphatase activity (Figure 5.20.A) and that at 14 days this change was statistically significant. Figure 5.20.B shows a comparison of ALP activity levels at baseline (CTRLs) at the three different time-points and

highlights the fact that at baseline ALP activity increased after 7 days and then dropped significantly after 14 days.

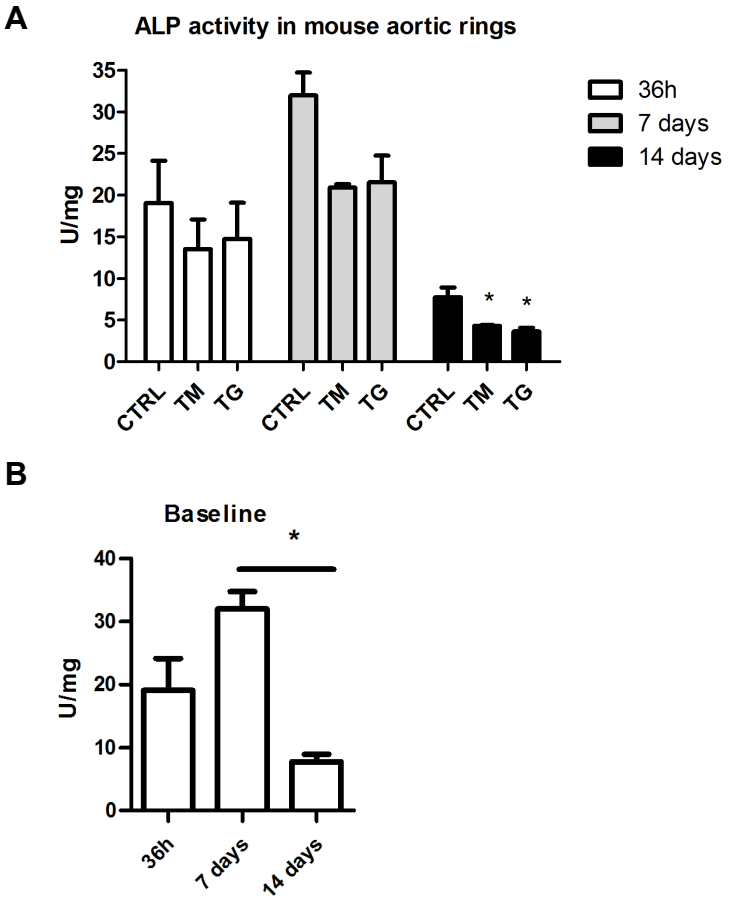

Figure 5.20. Alkaline phosphatase activity in mouse aortic rings – long term experiment. **A.** Comparison of ALP activity measured after treatment with 0.4µg/ml tunicamycin (TM) or 0.2µg/ml thapsigargin (TG) at different time-points and normalised to the weight of each aortic fragment. **B.** Comparison of baseline ALP activity (CTRL samples) across the three time-points. All graphs show mean and SEM, n=3, ANOVA with Dunnett's *post hoc* tests was performed * denotes p between 0.05 and 0.01.

Western blots for Grp78 and Grp94 were carried out to examine whether ER stress was activated in VSMCs by incubating vessels in tunicamycin and thapsigargin at these time-points. The results show that both at 36 hours and 7 days the expression of these chaperones was increased compared to control, although at 7 days it was the case in only one sample out of three (Figure 5.21A and B). At the 14 day time-point hardly any protein was detectable making it difficult to reach any

conclusions.

Histological analysis of aortic rings treated for 14 days revealed that in tunicamycin- and thapsigargin-treated rings there were very few nuclei in the vessel wall, compared with the CTRL sample (Figure 5.21.C). This suggests that the ER stress treatments induced cell death at this time-point. This could explain why ALP activity decreased at this time-point, as only viable cells are able to sustain the synthesis of this enzyme. However, it does not explain why baseline ALP activity dropped after 14 days (Figure 5.20.B), as cells in the CTRL vessel were still alive.

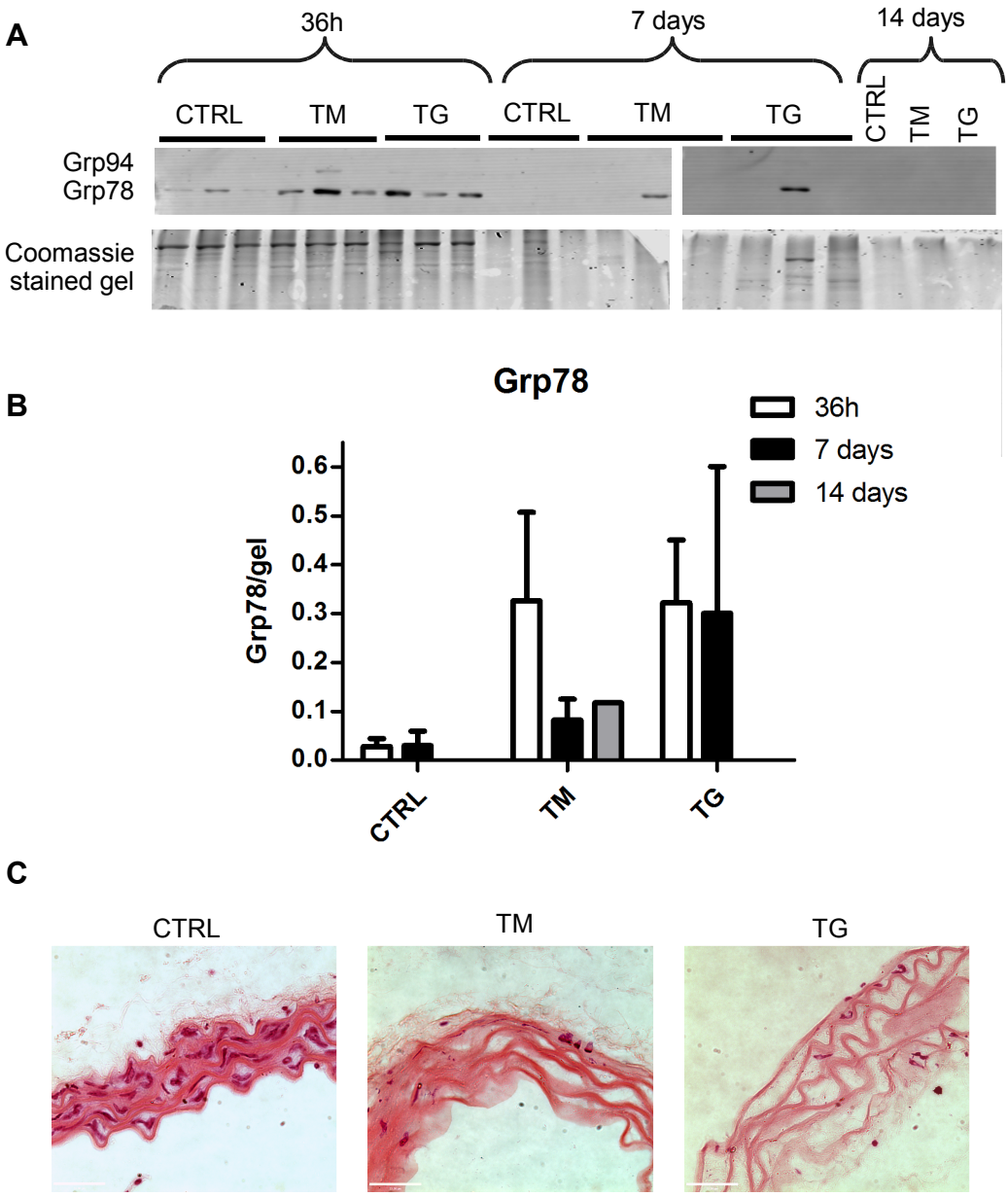

Figure 5.21. ER stress activation in mouse aortic rings. **A.** Western blot showing expression of ER stress markers Grp78 and Grp94 after treatment with 0.4µg/ml tunicamycin (TM) or 0.2µg/ml thapsigargin (TG) at different time-points. **B.** Quantification of the Western blot, normalised to the Coomassie stained gel. Graph shows mean and SEM, n=3, except at 14 days, where n=1, ANOVA with Tukey's *post hoc* tests was performed. **C.** Hematoxylin and eosin staining of mouse aortas treated with TM and TG for 14 days, scale bars are 33 µm.

The results so far show that tunicamycin, but not thapsigargin, increased ALP activity in human VSMCs *in vitro*, and that both inducers caused a decrease in ALP activity in mouse aortic rings. Therefore, it can be concluded that ER stress regulates ALP activity in VSMCs, however in a blood vessel wall the activity of this

enzyme is likely affected by other factors. Next, ALP expression and activity were examined in the context of ER stress-enhanced calcification of VSMCs *in vitro* in order to establish the importance of this enzyme for this process.

5.5. Alkaline phosphatase activity is not required for ER stress-enhanced calcification of VSMCs *in vitro*

In Chapter 3 I showed that tunicamycin and thapsigargin enhanced VSMC calcification *in vitro*, and that could be inhibited by PBA (Figure 3.19). Similar, in the experiments shown here cells were treated with tunicamycin and thapsigargin in the presence of high levels of Ca and P and ER stress inhibitor PBA, ALP expression was measured with real-time PCR and Western blotting and ALP activity assays were carried out.

Figure 5.22 shows a comparison of mRNA, protein and activity levels. Tunicamycin and thapsigargin alone did not change ALP mRNA levels in the calcification assay conditions. This is in contrast to results shown earlier in this chapter in short-term experiments. The difference between these two experiments is that here, for the purpose of calcification assays, approximately 10 times lower concentrations of tunicamycin and thapsigargin were used, and for 8 days instead of 24 hours. However, in the long-term calcification assay conditions tunicamycin and thapsigargin increased ALP protein expression. This did not, however, translate into higher activity levels, as ALP activity was slightly decreased by both ER stress inducers. This suggests that in these conditions ER stress does not induce ALP activity and also that ALP is synthesized inactive and needs an activation step for the protein levels to correspond to activity.

Surprisingly, Ca and P alone, i.e. the baseline calcifying condition, did not induce ALP mRNA, protein or activity levels suggesting that ALP is not required for cells to calcify.

In the presence of high Ca and P levels tunicamycin and thapsigargin did not change ALP mRNA expression, but increased protein expression compared to baseline and to Ca and P alone. Again, this did not translate into higher activity levels. This suggests that an increase in ALP activity is not required for ER stress-

enhanced calcification.

The addition of PBA to VSMCs treated with thapsigargin in the presence of high Ca and P increased ALP mRNA levels by approximately 50%, but did not change protein or activity levels. Addition of PBA did not change ALP mRNA, protein or activity levels in tunicamycin treated cells, both in the presence or absence of high Ca and P. This further confirms that ER stress does not play a role in regulating ALP in calcifying conditions.

In summary, calcifying conditions and ER stress caused an increase in protein but not mRNA levels of ALP, and did not induce any significant changes in ALP activity, suggesting ALP is not a major factor driving ER stress-induced VSMC calcification.

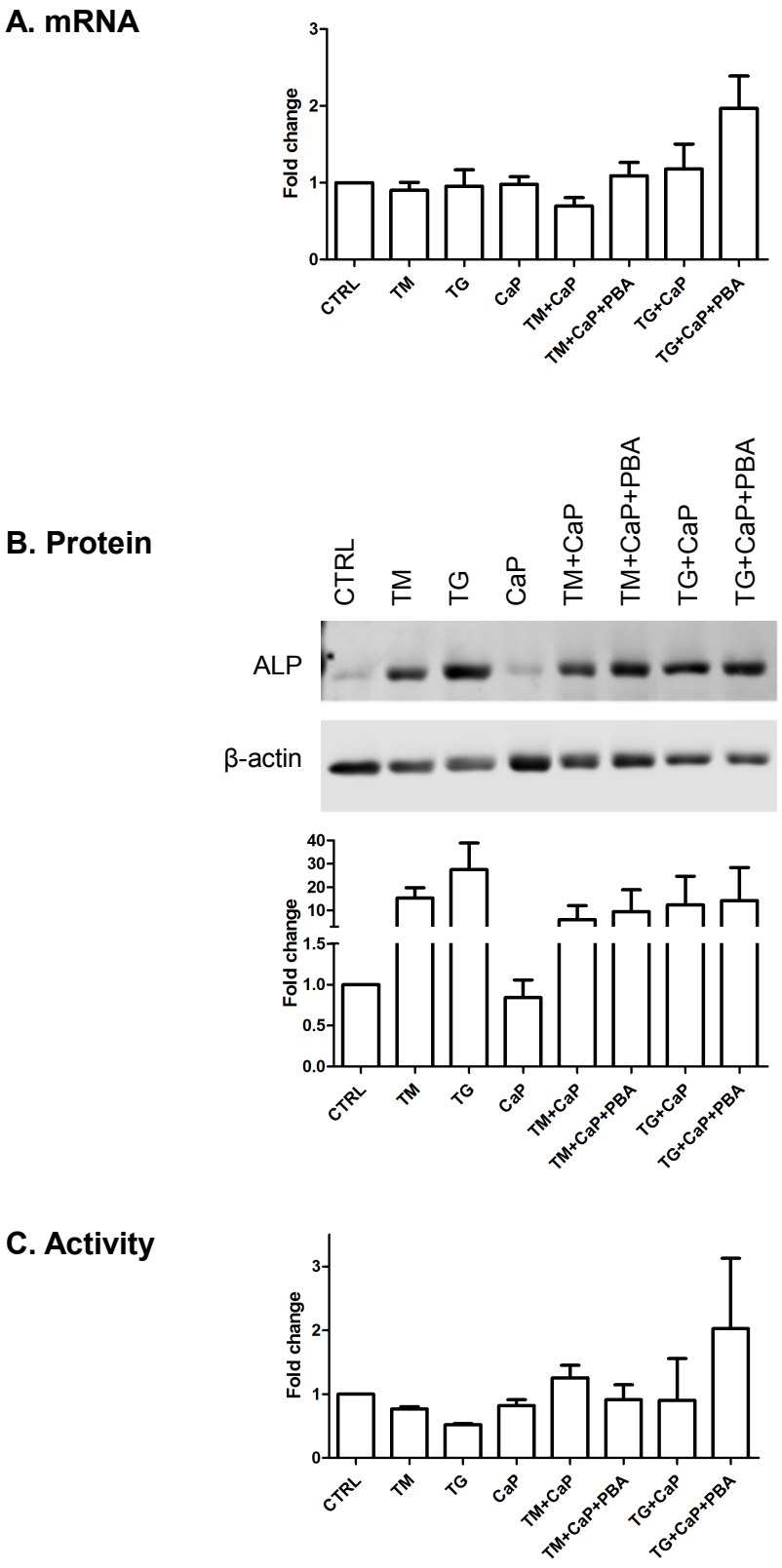

Figure 5.22. ALP in a calcifying VSMCs. Cells were treated with 2.7mM Ca^{2+}, 2.5mM PO_4^{3-}, 0.04µg/ml tunicamycin (TM) or 0.01µg/ml thapsigargin (TG), 0.5mM PBA for 8 days. **A.** Real-time PCR analysis of mRNA levels. **B.** Western blotting and quantification of protein levels **C.** ALP activity. Graphs show mean and SEM, n=3, ANOVA with Tukey's *post hoc* tests was performed.

Western blotting for Grp78 and Grp94 was carried out at the same conditions to examine whether ER stress was activated in these experiments. Figure 5.23 shows that tunicamycin and thapsigargin alone increased the expression of these two chaperones approximately 10 and 25-fold. High Ca and P treatment alone did not change the expression of these ER stress markers. Grp78 and Grp94 expression was increased by Ca and P in combination with tunicamycin and thapsigargin, when compared to tunicamycin and thapsigargin or Ca and P alone. PBA did not change the levels of these chaperones. None of these changes were statistically significant, due to high variability in the levels of induction on thee chaperones by ER stress. Nevertheless, tunicamycin and thapsigargin increased their expression in each of the three experiments carried out, and increases in Grp78 and Grp94 always coincided with an increase in ALP protein expression.

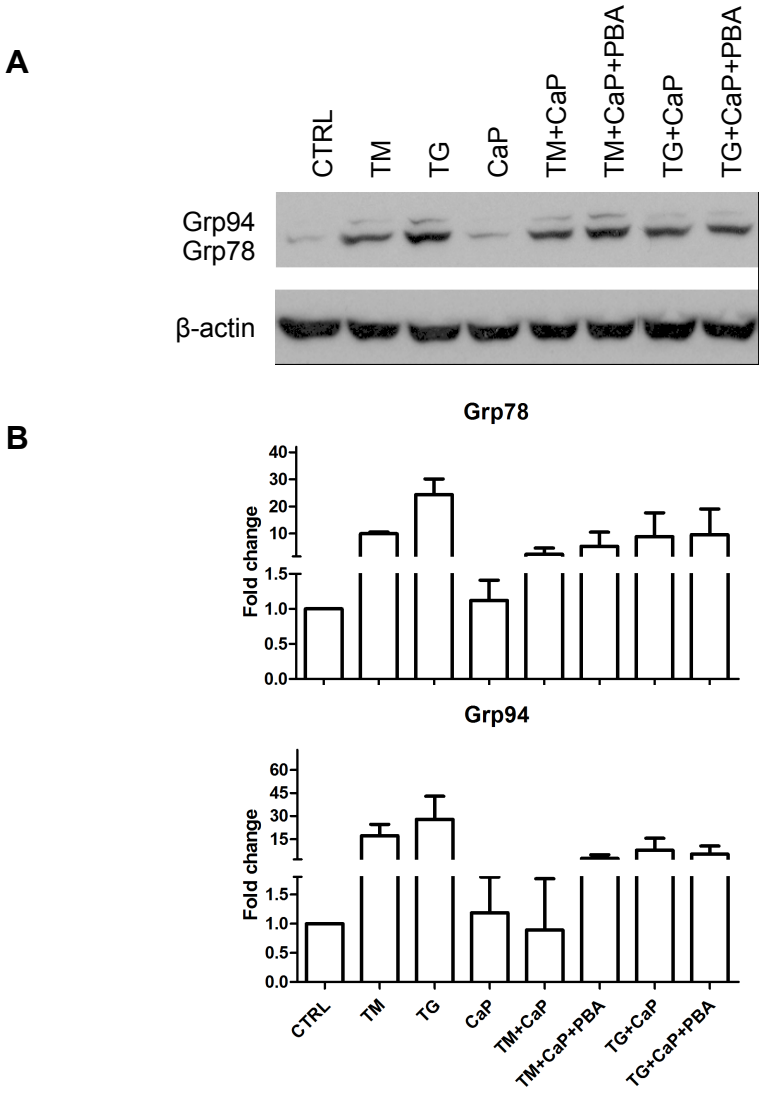

Figure 5.23. Levels of ER stress markers Grp78 and Grp94 in calcifying VSMCs. Cells were treated with 2.7mM Ca^{2+}, 2.5mM PO_4^{3-}, 0.04µg/ml tunicamycin (TM) or 0.01µg/ml thapsigargin (TG), 0.5mM PBA for 8 days. **A.** Representative Western blot. **B.** Quantifications. Graphs show mean and SEM, n=3, ANOVA with Tukey's *post hoc* tests was performed.

Expression of ATF4 mRNA was measured in the same calcifying conditions (Figure 5.24) in order to examine whether it followed the same expression pattern as ALP. This was thought likely since ATF4 knock-down decreased ALP expression. ATF4 mRNA expression was slightly increased with tunicamycin and thapsigargin alone, and in combination with Ca and P. PBA did not have an effect on ATF4 mRNA expression in these conditions. These results show that increased expression of ATF4 is not required for VSMCs to calcify and that it did not follow the same

expression pattern as ALP.

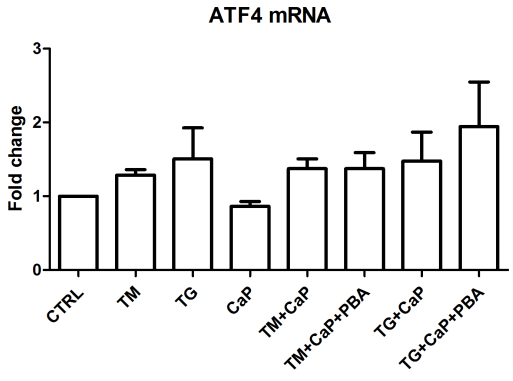

Figure 5.24. ATF4 expression in calcifying VSMCs. Cells were treated with 2.7mM Ca^{2+}, 2.5mM PO_4^{3-}, 0.04µg/ml tunicamycin (TM) or 0.01µg/ml thapsigargin (TG), 0.5mM PBA for 8 day, after that real-time PCR was carried out. Graph shows mean and SEM, n=3, ANOVA with Tukey's *post hoc* tests was performed.

The results in this section show that in calcifying VSMCs, both in the presence and absence of ER stress, ALP expression or activity did not change. In addition, ATF4 expression did not change significantly either.

5.6. Discussion

In this chapter I have explored regulation of Osterix and ALP expression in response to ER stress in VSMCs.

5.6.1. Osterix expression is regulated by ER stress

I have shown that expression of Osterix is regulated by ER stress in VSMCs. This has not been previously studied in VSMCs, but is consistent with studies in mouse osteoblasts, where Osterix expression was induced by thapsigargin (Tohmonda *et al.* 2011). In VSMCs Osterix localised to cytoplasmic foci of unknown function. Literature on the function of Osterix in VSMCs is very limited and does not offer explanations as to the subcellular localisation of this transcription factor, its location in the cytoplasm has not been previously described.

Osterix was mentioned as a marker of osteogenic differentiation in studies

of the effects of Vitamin D, oxidised LDL and hepatocyte growth factor (HGF) in VSMCs *in vitro* (Taylor *et al.* 2011; Zebger-Gong *et al.* 2011; Liu *et al.* 2011a), but signalling downstream of Osterix has not been looked at. Numerous studies in osteoblasts and mesenchymal stem cells have shed light onto its functions in bone development and highlight its importance in osteoblast differentiation (Zhang *et al.* 2010b). In-depth investigation of the role of Osterix was not performed, as it was not possible to achieve an efficient knock-down of this protein in human primary VSMCs.

In a study in SAOS-2 cells (Peng *et al.* 2013) the half-life of Osterix protein was estimated to be 12 hours, with a 36 hour cycloheximide treatment decreasing its levels below levels detectable by Western blotting. This suggests that the 48 hour siRNA treatment protocol used in my experiments should have been effective, and a 7 day treatment should have resulted in completely abolishing the protein, but this was not the case. However, literature reports of siRNA knock-down of Osterix, do not show complete knock-down at the protein level (Fan *et al.* 2007; Park and Kim 2013) suggesting that an approximately 50% knock-down that I have achieved could be sufficient to observe the effects of Osterix knock-down.

Goettsch *et al.* describe a miRNA targetting Osterix, miR-125b, which is expressed in VSMCs. But rather than showing that it decreases Osterix expression when applied to cells, they show that blocking miR-125b increases Osterix expression and VSMC calcification (Goettsch *et al.* 2011). In the light of these findings my results suggest that Osterix is not a direct target of miR-125b.

5.6.2. ALP activity is regulated by ER stress in VSMCs *in vitro*

In the second part of this chapter I have shown that ALP mRNA and activity were significantly increased by a short term, acute ER stress treatment of human primary VSMCs *in vitro.* Interestingly, activity was only upregulated by tunicamycin and not thapsigargin. This further adds to the evidence that tunicamycin and thapsigargin have different effects on osteogenic gene expression in VSMCs.

In this chapter I show strong evidence supporting the conclusion that ATF4 does not bind the examined fragment of the ALP promoter region (-3631 to

-2048bp from the first intron), despite the fact that siRNA knock-down experiments showed that the presence of ATF4 is required for ER stress-induced ALP expression and bioinformatics analysis predicted two ATF4 binding sites in this fragment of the ALP promoter. There are several possible explanations for this. Firstly, bioinformatics predictions are not always accurate. Another reason could be that ATF4 might not be a direct regulator of ALP expression, it could act via other, unknown downstream factors whose expression would be downregulated after ATF4 knock-down. Moreover, the ATF4-responsive element could be located further upstream or downstream of the examined promoter fragment as some regulatory elements are known to be located very far from the genes they regulate (Kleinjan and van Heyningen, 2005). This is supported by the fact that tunicamycin caused an increase in ALP mRNA expression and enzyme activity levels, but not promoter activity. That suggests that the examined fragment of the ALP promoter did not contain elements responsive to tunicamycin activation. This in turn means that ATF4 could still be an activator of the ALP promoter, but the analysis did not encompass the right region of the promoter.

Instead of confirming that ATF4 binds to the ALP promoter region I identified 3 other proteins that could potentially perform this function - DDX5, β-catenin and THRAP3. All 3 are known to be involved in osteoblast differentiation, but were not previously implicated in regulating ALP expression in VSMCs. β-catenin is of special interest, as binding sites for its well known interacting partners TCF/LEF (Novak *et al.* 1999) were found in the examined fragment of the ALP promoter. Further experiments are needed to validate the interactions of these factors with the ALP promoter and to explore whether they can be induced by ER stress and how.

5.6.3. ER stress does not induce ALP activity in mouse aortic rings

In mouse aortic rings (an *ex vivo* model) ALP activity did not change significantly regardless of ER stress inducer used. The inconsistency of results between experiments in human VSMCs and mouse aortic rings could be explained by species differences. There have been studies showing differences in VSMCs from different species (Bonin and Damon, 1994). Another reason why VSMCs and mouse

rings might have responded differently could be that cells in culture and the vessel wall differ in their phenotype/ differentiation status and therefore have different abilities to respond to ER stress treatments (Shanahan and Weissberg, 1998; Shroff *et al.* 2010). Because of that it is difficult to conclude what these results could mean in terms of ER stress regulation of VSMC phenotype.

5.6.4. The role of ALP activity in ER stress-enhanced calcification is unclear

I demonstrated that calcification of VSMCs enhanced by ER stress was not accompanied by significant changes in ALP expression or activity in human VSMCs. Many studies consider an increase in ALP activity as an early marker of osteogenic transdifferentiation of VSMCs (Shanahan *et al.* 1999a; Lomashvili *et al.* 2008; Schoppet and Shanahan, 2008). It has also been shown to be activated during ER-stress mediated calcification in rat and mouse VSMCs (Masuda *et al.* 2013; Duan *et al.* 2013). On the other hand, there have been studies showing that its activity levels can be uncoupled from expression of other osteogenic markers such as Runx2 and not increase after high Ca and P treatment (Shroff *et al.* 2010) or in fact that calcification of VSMCs can occur without osteogenic differentiation altogether (O'Neill and Adams, 2014). This might be the case in my model of calcification *in vitro*, as in experiments in Chapter 3 VSMCs calcified more in the presence of ER stress transducers, but here I have shown that this was not accompanied by an increase in ALP activity or ATF4 expression. To have a complete picture of what is happening in this model of calcification, expression of more osteogenic genes would have to be examined. Another explanation for the lack on an increase in ALP activity could be a wrong time-point. My calcification experiments took 8 days and ALP activity and expression was measured on the last day. It is possible that increased ALP is required in initial stages of calcification and decreased by the time the measurements were carried out.

In the calcification experiments ALP activity levels did not correspond to protein expression patterns, suggesting the enzyme is expressed but not active. In addition to that, it has been observed that thapsigargin increased ALP promoter activity and mRNA expression, but not enzyme activity, at the 24 hour time-point. It

has been shown before that ALP needs to be activated in order to form a functional enzyme. This requires a two-step mechanism via protein stabilization followed by enzyme conversion with zinc loaded by zinc transporter complexes (Fukunaka *et al.* 2011). Interestingly, it has been shown that ablation of zinc transporter proteins ZnT5 and Znt7, which are involved in ALP activation and provide other proteins folded in the ER with zinc ions needed for their activation can induce ER stress and activate the unfolded protein response (Ishihara *et al.* 2006). This highlights the importance of zinc homeostasis for ER function and suggests that UPR signalling can increase the expression of ALP in VSMCs, but ER stress might inhibit formation of a functional enzyme by disrupting zinc homeostasis. However, it has not been tested whether ER stress disrupts zinc homeostasis.

5.6.5. Conclusions

In conclusion, it has emerged that regulation of both Osterix and ALP expression in response to ER stress in human primary VSMCs is complex and different from that in mouse and rat cells. In addition, the results in this chapter support the notion that increased ALP activity is not required for ER-stress-enhanced calcification. Analysis of additional osteogenic genes is required before conclusions about the regulation of osteogenic differentiation by ER stress and its contribution to VSMC calcification can be made.

Chapter 6: Conclusions and future work

6.1. ER stress promotes calcification

In the course of this thesis I presented evidence that ER stress promotes vascular calcification. I demonstrated that pro-calcific factors including warfarin and TNFα as well as TGFβ can induce ER stress in VSMCs, showing that factors relevant to calcification *in vivo* can induce this stress response. I also examined potential mechanisms via which ER stress could increase VSMC calcification *in vitro*. Apoptosis was ruled out, as it was found that ER stress actually protected cells from death, contrary to published literature (Duan *et al.* 2013).

Osteogenic differentiation was concluded to be a possible mechanism, as expression of osteogenic markers correlated with ER stress markers in healthy and fatty streak human aortas, suggesting that ER stress regulates expression of osteogenic genes in the initial stages of vascular disease. In addition, in rat aortas warfarin induced ER stress and expression of Osterix and ALP in calcified areas. Finally, ER stress upregulated expression of some osteogenic genes (Osterix, ALP, BSP, OPG) in VSMCs *in vitro* after short term treatments. I demonstrated that these changes in gene expression were mediated by specific UPR pathways. In the same conditions VSMC contractile markers SM22α and p-MLC were decreased, which was consistent with decreased expression of some components of the TGFβ signalling pathway which promotes differentiation (Shah *et al.* 1996; Hirschi *et al.* 1998). A decrease in contractile gene expression is one of the hallmarks of osteogenic conversion of VSMCs (Iyemere *et al.* 2006). My results are also consistent with literature showing that ER stress is associated with increased osteogenic gene expression in VSMCs (Liberman *et al.* 2011; Masuda *et al.* 2012, 2013; Duan *et al.* 2013).

There are other mechanisms via which ER stress could enhance calcification, one of them is an increase in Grp78 chaperone expression. Grp78 has been shown to be expressed on the cell surface (Zhang *et al.* 2010), to bind to type 1 collagen and to facilitate ECM mineralisation by nucleating calcium phosphate crystal formation (Ravindran *et al.* 2011). I have shown that in VSMCs Grp78 expression

was increased by tunicamycin and thapsigargin treatments in long-term calcification assays in the presence of Ca and P, so it is possible that Grp78 was responsible for the ER stress-enhanced increase of calcification of VSMCs *in vitro* in response to ER stress. My immunocytochemistry experiments show that both in untreated cells and when ER stress was induced, Grp78 was only localised in the ER and cytoplasm, and therefore not exposed to the ECM. However, it is possible that the chaperone was loaded into matrix vesicles (MVs) that are known to nucleate matrix mineralisation. MV release is a well established mechanism that mediates calcification (Kapustin *et al.* 2011, Kapustin and Shanahan, 2012) and previous studies in our laboratory have shown that MVs from calcifying VSMCs contain ER components and Grp78 among them (data not shown), suggesting that ER stress might play a role in vesicle-mediated calcification. Therefore, in further experiments calcification assays should be carried out in the absence of Grp78 to investigate whether it is required for VSMC calcification. It would also be interesting to examine whether ER stress can influence the number and calcification-inducing properties of MVs released by VSMCs.

Another mechanism that could potentially link ER stress and vascular calcification is autophagy. There is abundant evidence that ER stress can lead to activation of autophagy (Ogata *et al.* 2006, Hoyer-Hansen and Jaattela 2007). In addition, ATF4 has been shown to regulate autophagy in the context of hypoxia in cancer cells (Rzymski *et al.* 2009). Autophagy has been demonstrated to protect VSMCs from calcification induced by high levels of phosphate ions or TGFβ (Dai *et al.* 2013, Liu *et al.* 2014). However, the link between ER stress and autophagy in vascular calcification has not been studied. My preliminary experiments showed that very high concentrations of tunicamycin and thapsigargin (1μg/ml for 24h, which is 5 times higher that what I used in experiments) can induce expression of LC3-II, a marker of autophagy (data not shown), however I have not studied activation of autophagy in calcification assays.

An important limitation of my experiments is the fact that most experiments were carried out as replicates from one biological sample (VSMCs from one donor). Therefore, future experiments should include validating the results in other VSMC

isolates. Nevertheless, my results provide the first insight into the effects of ER stress on human aortic VSMCs calcification and phenotype, as these cells were not studied in research described in existing literature on ER stress in vascular calcification. Liberman *et al.* (2011) used coronary artery cells and did not mention how many donors the cells were from; Masuda *et al.* (2012, 2013) carried out all their experiments on a mouse cell line (MOVAS-1) and Duan *et al.* (2013) used rat VSMCs, which are genetically homogeneous.

6.2. Could ER stress be a protective mechanism?

Even though the majority of my findings suggest that ER stress promotes vascular calcification, there is some data that do not support this conclusion.

Firstly, in calcified human aortas expression of ER stress markers is decreased and expression of osteogenic genes increased, suggesting that these two processes are uncoupled in the late stages of vascular disease. In addition, in calcified rat aortas expression of osteogenic genes did not follow the same pattern as ER stress markers, seeing that ER stress markers were increased in the whole vessel wall and osteogenic markers only in the calcified area, further suggesting that ER stress does not drive expression of these genes during calcification.

As mentioned above I found that ER stress modelled in VSMCs *in vitro* increased the expression of some osteogenic genes in short term treatments. However, in long term calcification assays, ALP activity and ATF4 expression were not increased by ER stress both in the presence and absence of calcification media. This is contrary to what has been shown in studies by Masuda *et al.* and Duan *et al.*, which found that ATF4 is a key mediator of the changes in osteogenic gene expression and that an increase in ALP activity accompanies ER stress-mediated VSMC calcification (Masuda *et al.* 2012, 2013; Duan *et al.* 2013). I have not investigated the expression of other genes in long term calcification assays, but analysis of some key osteogenic markers in the context of calcification assays is necessary to ascertain whether ER stress can induce osteogenic differentiation in the long term. Further to this, I have shown evidence that ER stress suppressed expression of pro-osteogenic BMP-2, increased expression of calcification inhibitor

BMP-7 and that ATF4 inhibits expression of a number of osteogenic genes in VSMCs.

Even though the majority of the literature points to ER stress having a pro-osteogenic effect on both osteoblasts (Tohmonda *et al.* 2011; Jang *et al.* 2011; Saito *et al.* 2011) and VSMCs (Liberman *et al.* 2011; Masuda *et al.* 2012, 2013; Duan *et al.* 2013), the idea that ER stress inhibits osteogenic differentiation is not a completely novel notion. It has been shown that ATF4 was required for TGFβ-mediated suppression of OCN expression and osteoblast differentiation (Lian *et al.* 2012). This is important, as I have shown that in VSMCs TGFβ activated ATF4 expression. It has also been demonstrated that tunicamycin inhibited a BMP-2-induced increase in ALP and OCN expression in mouse osteoblasts (Jang *et al.* 2013), which is consistent with my results showing that ER stress decreased expression of BMP-2. Another recent study has shown that low levels of ER stress induce osteoblastic differentiation of bone marrow stromal cells, but high levels had an inhibitory effect (Nakamura *et al.* 2013).

In addition, *in vitro*, ER stress protected VSMCs from apoptosis, an important mechanism which promotes calcification. Interestingly, a study in mouse VSMCs lacking the ENPP1 enzyme (which synthesizes the natural mineralisation inhibitor PPi) showed that the absence of CHOP (which mediates ER stress-induced apoptosis) in these conditions increased calcification (Serrano *et al.* 2014). This suggests that in the absence of PPi CHOP protected cells from calcification.

I have shown that TGFβ, which promotes contractile differentiation, can induce ER stress in VSMCs. Together with results showing that also pro-calcific warfarin and TNFα can induce ER stress this suggests that ER stress is activated when cells undergo phenotypic changes, regardless of what induces them and regardless of whether the cells are becoming more contractile or more synthetic. This fact further supports the notion that ER stress is a physiological, adaptive mechanism (Wu *et al.* 2006; Moore and Hollien, 2012). However, I also demonstrated that ER stress modelled by tunicamycin and thapsigargin induces features of a secretory phenotype in VSMCs, such as decrease of contractile markers, suggesting that ER stress does not mediate a pro-contractile expression programme. My findings could therefore mean that the pro-contractile features of

TGFβ signalling are perhaps not mediated by ER stress, but the pro-calcific are (as shown by Simionescu *et al.* 2005 and Liu *et al.* 2014). It is unclear why TGFβ has a dual effect on VSMC phenotype and it is likely context-dependent.

It would be interesting to further analyse what phenotypic changes TNFα and warfarin induce and whether they are mediated by ER stress by using ER stress inhibitors. Apart from PBA used in experiments here, specific inhibitors of IRE1 and PERK have recently been described and could be used for these experiments to determine which UPR pathways are involved in phenotypic regulation of VSMCs (Cross *et al.* 2012; Axten *et al.* 2012). In addition, in order to examine if ER stress is involved in physiological phenotypic regulation, or whether it is a mechanism only activated in response to pathological conditions, it would be also interesting to examine the levels of ER stress marker expression in VSMCs from different phases of vascular development, representing different stages of VSMC differentiation (Majesky, 2007).

6.3. Regulation of osteogenic genes by ER stress

6.3.1. The function of Osterix in VSMCs remains unknown

I demonstrated that expression of Osterix is increased in VSMCs by tunicamycin, suggesting that it could play a role in ER stress-regulated osteogenic differentiation. Expression of this osteogenic transcription factor was not analysed in published studies of ER stress in VSMCs to date, therefore my findings with regards to Osterix are novel. An important next step would be to examine Osterix expression in VSMCs calcifying in the presence of ER stress inducers, in order to investigate whether it plays a role in ER stress-enhanced calcification of VSMCs *in vitro*.

In depth studies of the function and target genes of Osterix in VSMCs were prevented by the inability to knock it down efficiently in these cells. Obtaining VSMC-specific Osx knock-out mice would be a way to overcome this problem. Mice with floxed Osterix have been described before (Nishimura *et al.* 2012). They were used to create a cartilage-specific Osterix knock-out, as they were crossed with mice

expressing Cre from the type 2 collagen promoter. Contrary to global Osterix knock-out mice, in which bone formation did not occur at all, in mice with chondrocyte-specific Osterix knock-out endochondral bone formation was arrested at the hypertrophic chondrocyte stage (Nishimura *et al.* 2012). In order to achieve a VSMC-specific Osterix knock-out, the Osterix-floxed mice could be crossed with mice expressing Cre under the SM22α promoter. SM22α-Cre mice have been used previously to knock out Runx2 in VSMCs (Sun *et al.* 2012). Osteogenic gene expression in response to ER stress could be examined in cells from VSMC-specific Osterix knock-out mice. The mice could be fed a calcification inducing diet (Atkinson *et al.* 2008) or treated with tunicamycin (Liang *et al.* 2013), and osteogenic gene expression could be examined in their aortas, which would elucidate the function of Osterix in VSMC calcification.

In addition, since it is unknown what regulates Osterix expression in VSMCs, it is necessary to analyse the Osterix promoter in order to explain the mechanisms by which its expression is upregulated by ER stress. An XBP1 binding site has already been identified in the Osterix promoter region and XBP1 has been shown to bind this promoter in mouse embryonic fibroblasts (Tohmonda *et al.* 2011). Therefore, it would be interesting to examine whether XBP1 binds the Osterix promoter in human primary VSMCs, or perhaps if ATF4 is involved, since its knock-down caused a small decrease in Osterix expression.

6.3.2. The role of ALP in VSMC calcification is unclear

I showed that ALP expression and activity are increased by ER stress in VSMCs, but not in the context of calcification. Its levels did not change in cells calcifying *in vitro* in the absence of ER stress inducers. ALP expression was not different in calcified human aortas compared to healthy. These results suggest that an increase in ALP activity is not required in all instances of calcification, both in the context of ER stress and not. There have been studies showing that calcification can occur without an increase in ALP activity (Shroff *et al.* 2010), even though the majority of published research shows that ALP activity is increased in VSMCs calcifying in the presence of ER stress (Masuda *et al.* 2012, 2013; Duan *et al.* 2013)

or in calcification induced by other factors (Shioi *et al.* 1995). This fact has several possible explanations. It could mean that in some conditions VSMCs are already expressing enough ALP in order to hydrolyse PPi and mineralise. It could also mean that upregulation of ALP is one of many redundant mechanisms contributing to calcification and therefore calcification can occur without it if other mechanisms are activated. Another alternative is that increased ALP activity is only required in initial stages of mineralisation and that I measured it at too late a time-point. Therefore, in order to better understand the function of ALP in VSMCs calcification, a time-course experiment measuring ALP activity at several stages of VSMC calcification is necessary.

I also attempted to examine whether ATF4 is a direct regulator of the ALP promoter and cannot conclude that it is, even though I have demonstrated that ALP activity is ATF4-dependent in VSMCs, consistent with published literature (Duan *et al.* 2013). However, since ALP is often reported to be increased in the context of calcification and it was increased by ER stress treatments it is important to find out more about its regulation. To date only one direct regulator of ALP expression has been described, PPARγ (Lencel *et al.* 2011). Interestingly, in DNA binding assays combined with proteomics analysis I found that THRAP3, which is known to form complexes with PPARγ, to bind the ALP promoter, strongly suggesting that it might be a novel regulator of ALP expression. In addition, DDX5, which forms complexes with Runx2 (Jensen *et al.* 2008) and β-catenin, which forms complexes with TCF/LEF (Novak *et al*. 1999), for which I found a binding site in the ALP promoter, could also be potential regulators of ALP expression. Additional DNA binding assays should be carried out to validate binding of these factors and also in order to examine whether the binding sites for XBP1, ATF6 and CHOP predicted in the ALP promoter are real.

6.4. Conclusion

To summarise, I presented evidence supporting the notion that the role of ER stress in VSMC calcification is not as unequivocally calcification-promoting as the literature to date has suggested, as it also promotes protective changes in the VSMC

phenotype. My findings contribute to the existing understanding of molecular mechanisms of vascular calcification. However, more studies are needed to fully understand the role of ER stress in regulating VSMC phenotype and calcification.

Chapter 7: Appendix

7.1. Osteogenic gene and ER stress marker expression in human aortas – correlation tests

Pearson correlation tests were carried out for expression values of pairs of ER stress versus osteogenic markers for samples from calcified aortas (n=10) or healthy and fatty streak combined (non-calcified, n=20). Figure 7.1 shows analysis of osteogenic markers vs ATF4, Figure 7.2 shows the analysis for ATF6, Figure 7.3 shows CHOP and Figure 7.4 PERK.

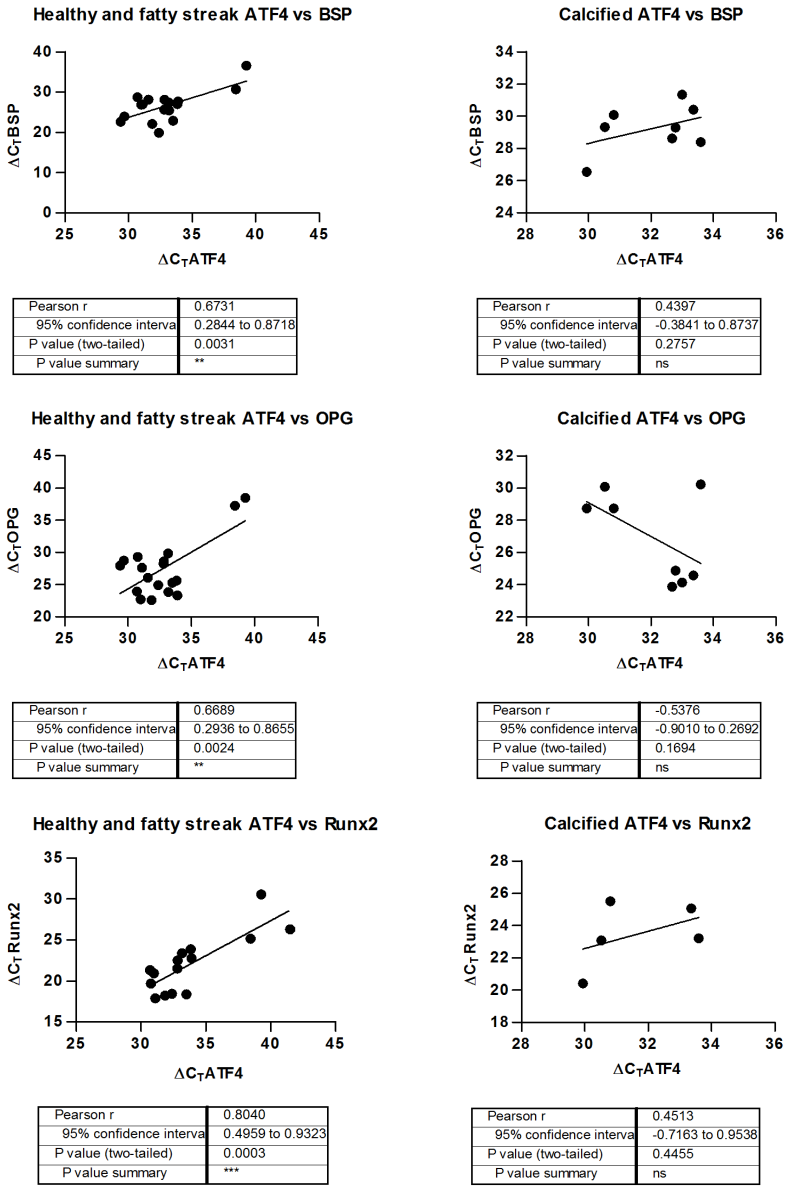

Figure 7.1. Correlation analysis of **ATF4** versus osteogenic markers expression in human aortas. ΔC_T values of ER stress markers were plotted against ΔC_T values of osteogenic genes. Linear regression was plotted, and a two-tailed Pearson correlation test was carried out. Graphs show individual data points.

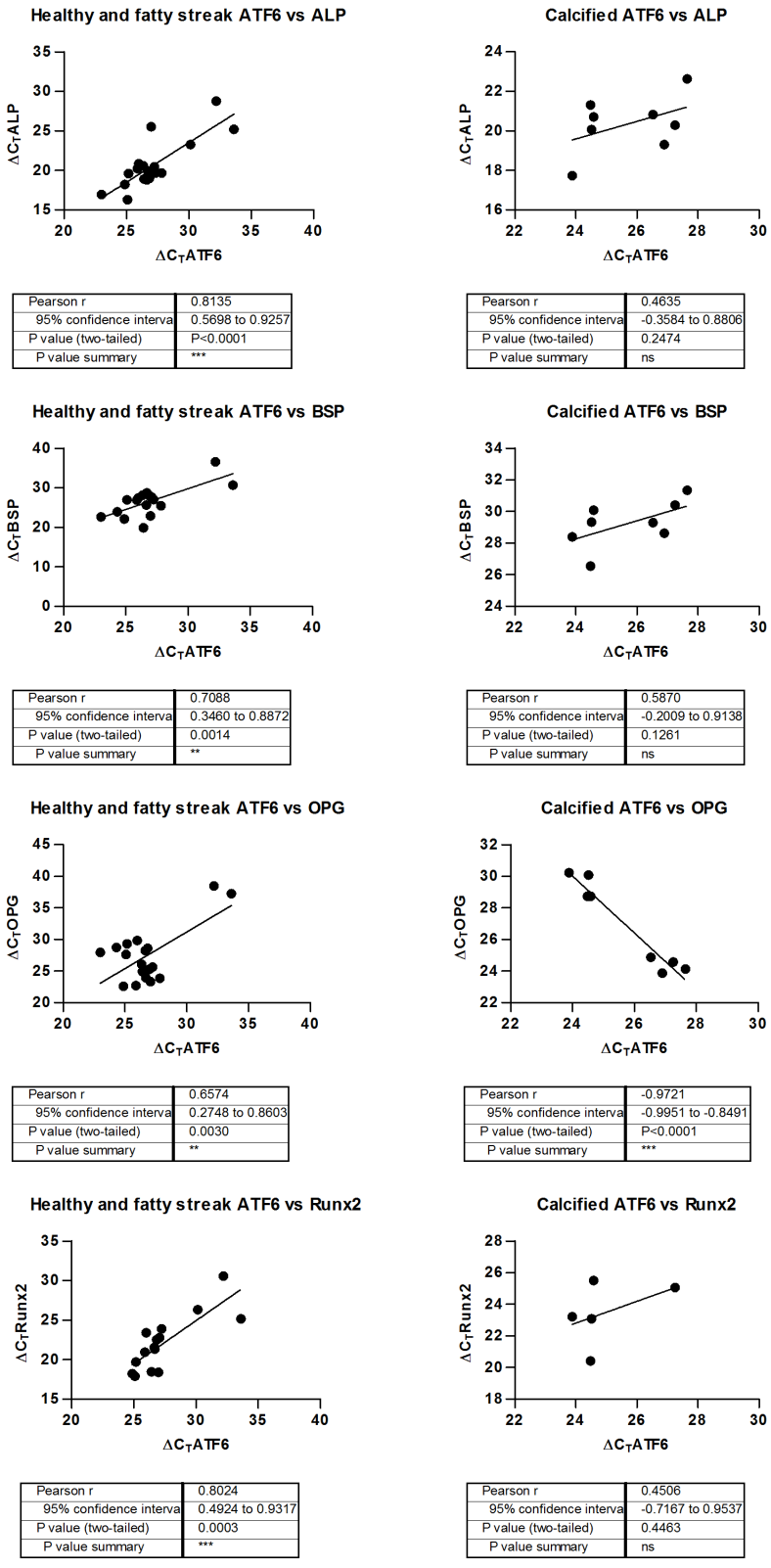

Figure 7.2. Correlation analysis of **ATF6** versus osteogenic markers expression in human aortas. ΔC_T values of ER stress markers were plotted against ΔC_T values of osteogenic genes. Linear regression was plotted, and a two-tailed Pearson correlation test was carried out. Graphs show individual data points.

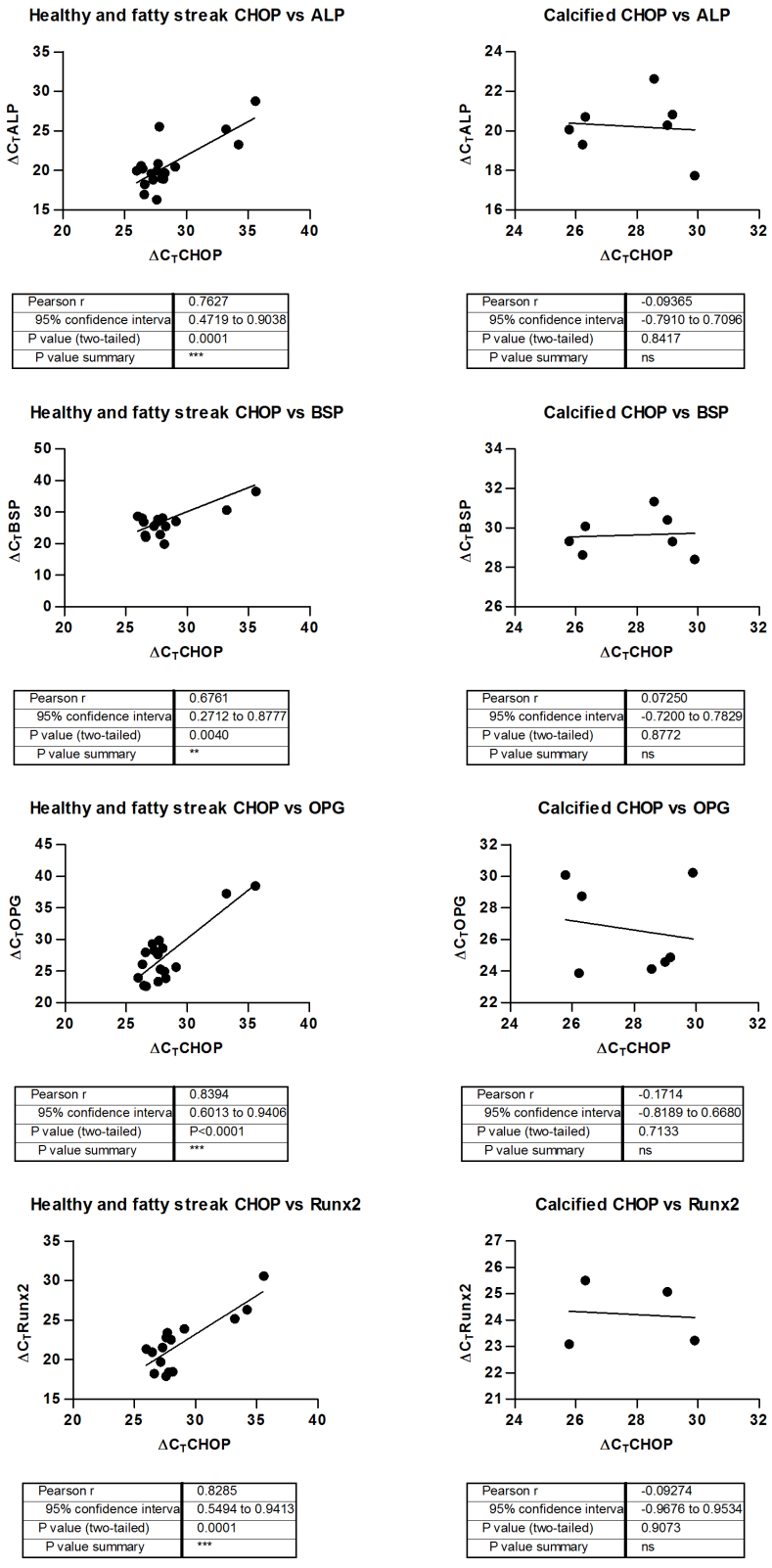

Figure 7.3. Correlation analysis of **CHOP** versus osteogenic markers expression in human aortas. ΔC_T values of ER stress markers were plotted against ΔC_T values of osteogenic genes. Linear regression was plotted, and a two-tailed Pearson correlation test was carried out. Graphs show individual data points.

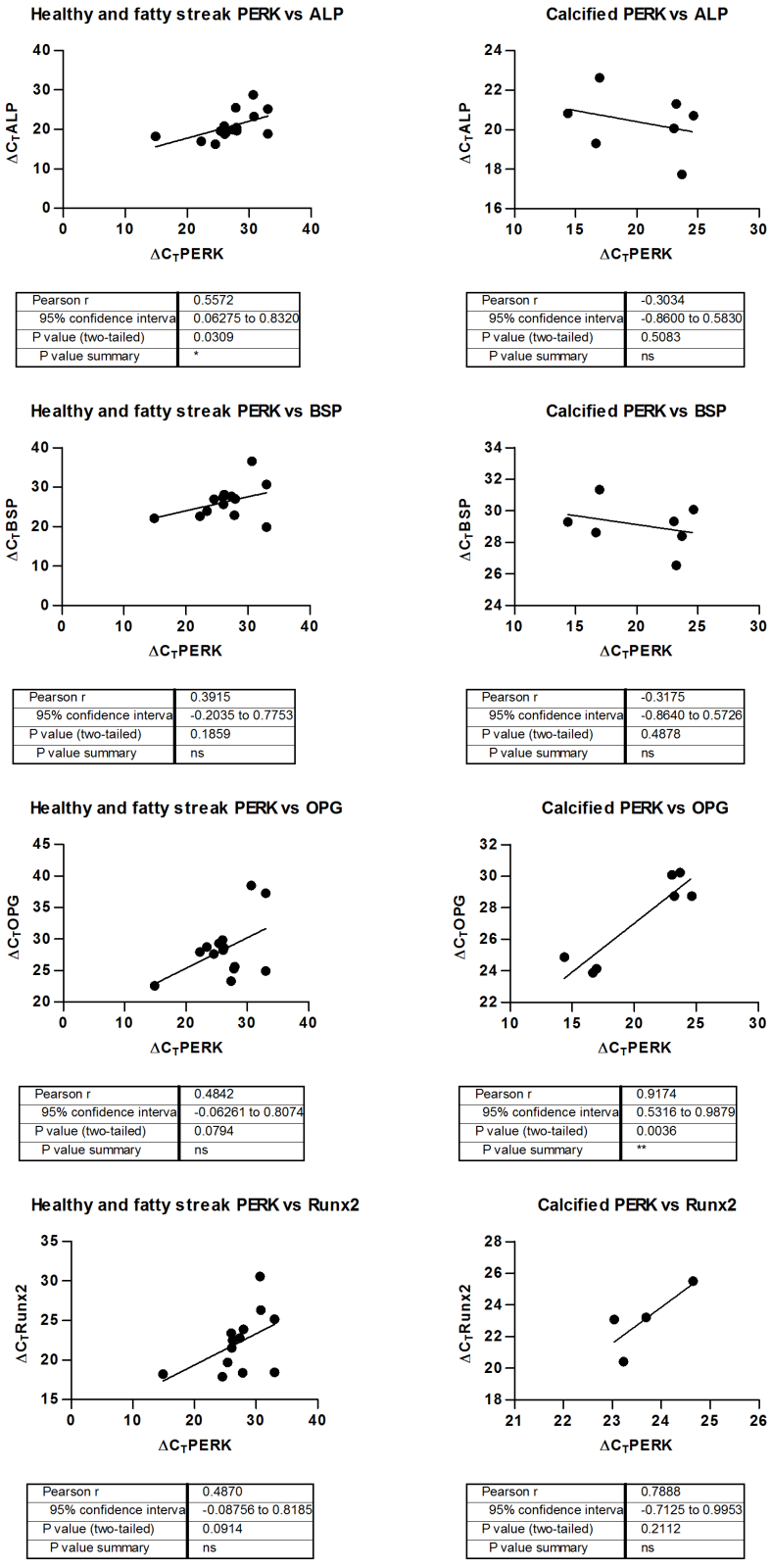

Figure 7.4. Correlation analysis of **PERK** versus osteogenic marker expression in human aortas. ΔC_T values of ER stress markers were plotted against ΔC_T values of osteogenic genes. Linear regression was plotted, and a two-tailed Pearson correlation test was carried out. Graphs show individual data points.

7.2. ALP promoter sequence

The ALP promoter region sequence (-122 to -4556 from the start of the first intron, Orimo *et al.* 2005) was subjected to bioinformatics analysis with Genomatix Matinspector, which contains a database of transcription factor consensus binding sequences. Figure 7.5. shows the full sequence with binding sites for ATF6, ATF4, CHOP, XBP1 and TCF/LEF annotated.

```
   1  ACTGGGATTA CAGGCGTGTG CCACTGTGCC CGGCCCCTGT TATCTTACTA ACTTACTTAT
  61  TAATGTTTGT TGTTTATTAT CTACCTTCCC AACTAAAGTG TCAGTTCCGT GAGGATAAAC
 121  ATTCTGTTTT GTTCACTGGT ATGTCCAGTT CCTAGAAGGG TGCCTGCTGC AGAGCAGGCA
 181  TCCAATAAAC ATTTGTTGAA TGAATAAGGT TGCCAAGTCT GCCTGGGATA ACAGCCTGCT
 241  CACTGGAAAG GTGACGATGA CAACAGTGAT GGTGCTTTGG TGTTGCAGGG AGGAGCAAGT
                  CREB/ATF

 301  TAAATCTCAC CTATAAAGAT CTTTCCATCA GGCTGCAGAC ACAGAGGGAG TCCCCAGCAA
 361  CAATAGCTCA TATATGCTTC AGTTTCCTCA TCCGTGAAGA GAGAATAAAA GTCCCTACTT
 421  TTATTAGCGT CCAATTGCCC TGGCCACGGC AGCATTGTCG GTTTAATGAT GCTGCTTCGG
 481  CTGTCGTAGT CTCTTCCACC TCATGCCTTT TGGTTCATTT TTTAACTGAG TTAAAGGTGG
 541  GGCTGTAGGT GGCACTGGGA ATCAAATGGC TGAACTTGTG CTCAGGCCTG GGCTTGAGAT
 601  AAAATGACCC CTTTAGTCCA AGCATCAAAA CAGACCAAGG TTTCAGGCCC CCTTGCCTTT
 661  AAATAGATTT CAGGGATTAT TTTCTCCAGC CCTAGACCAC AGCTGACTCC TCACCGCCTC
 721  TCCACGAACA GACCTCAGAG TTTTGTTTTC TCTGTCTCTC TCCTTTCTTT CTCCTTTATC
 781  TCTGTCTACT GAGGTCCTGG CTGTCCCCCT GCCCCACCCT ACCCTATGCT CTTGGGCTTC
 841  TGGCCTCATC TCTAACTTAG CTTCTAATTT TTTCTCTTCT TTTCCTTTCT TTTTTTGAAA
 901  CAGAGTCTCA CTCTGTCACC CAGGCTGGAG TGTAGTGGCG TGATCTCAGC TCACTGCAAC
                                                              CHOP

 961  CTCTGCCTCC AGGGTTCAAG CGTTTCTCGT GCCTCAGCCT CCCAAGTAGC TGGGACTACA
1021  GGTGTGCGTC ACCTTGCTCG GCTAATTTTT ATGTTTTCAG TAGAGACGGG GTTTCACCGT
        ATF4

1081  GTTGGCCAGG CTGGTCTCAA ACTCCGGACC TCAGGTGATC CACCTGCCTA GCCTCCCAAA
1141  GTGCTGGGAT TACAGGCATG AGCCACCACG CCCGGCCTAA CTTAGCTTCT AATTCTAATG
                                  ATF6

1201  CCTGGTGAAC CTCTTAAATT TTTTTTTCCC AAGACAAAGT CTCACTCTGT TGGCCAGGCT
1261  GGAGTGCAGG GGTGTGATCA TAGCTCACTG CAGACTCTAA CTCCTGGACA CAAGAGACCC
1321  TCCCATCTTG GCCTCCCAAA GTGCTGGGAT TACAGGCGTG AGCCACCATG CCTGGCCTGC
1381  CTAGTGAACT TGAAGGTCTA GCTTGCGGCA CAGGCTCATG GCATGCACTT AACAGATACG
1441  GAATAAATGG ATGAATGGAA AAAGCCCTGG ACTGGGAATA GTAAACCTGG TAACCAAACC
1501  CAGCTCTGAC CCTGACCTGT AAGTAACTAC TATCTCTGGC CTTGGTGTAC CCCATGTATA
1561  GTGGGGATTG TAAACACCTG CCCTGCCCAC CTTATGATAC TGCTGTGAGA CTCAAAAGAC
1621  ATCATTAGCT CTTAGGCACA GGGAGCTTGG AGGTTAAATC CAATTTGTTT AGTTTTCAAC
1681  AAGGAAGTGG TGCCCCAGGG ACAATGATGG AGAGAAATCG AATGTAATGA GCTGTTGCCA
1741  CCAGCTGAGT GGTCCTGAAA TCATGGCATC TGGGTTGCAC TTAGAGATTG TCCAGTTCAA
                                                          TCF/LEF

1801  AAGGCCAGAA GGAATCTGAA CCTCGATGGG AAAAGTGACT TGCTCAGCTC CCCAGCAAGC
1861  CAGGGCAGAG CTGGAGGATG GACTGGAGTC TCCTGGTTCC AGGTCCAGGA CTTCTTTCCG
1921  CTGTGTTGAC AGAGCCAGGA GGAGGGGCAC CCGGGGAGCA GGGGAGGCAA GGGCTGCTGG
1981  ATGCCCCATC TCAGTTGAAT TCTCCTTGAG GGACCCAGCC CAGGAGCAGA GTAAGAGGGT
2041  TTGAGGGTGG AAGGTGGCAG GGCTGGCCAA GCAGTATAGT CCCTGCTGCT GATAACCAAT
2101  CCCTGAAATC CCGAGGTGGA GGGACTTGAG GGCAAATCAC AGACATGGGG GACCTAATGC
2161  TGGCCATGTG GCTCAACCAG AAGTGCCCGT CCCTCATAGC TTTGGGGAGA TCAGAAGTCA
2221  GGGATAGGGT CGGGTGTGGT GGCTCATGCC TGTAATCCCA TCACTTTGGG ATAAGGAGGC
2281  AGGGGGATCA CTTGAGCTTA GGAGTTCGAG ACCAGCCTGA GCAACATAGC AAAACCCTGT
2341  TCTTTACAAA AAAATACAAA AATTAGCCGG GCGTGGTGGT GCACACCTGT AGTCCTGGCT
                                  ATF6
```

```
2401  GCTGGGGAGG CTGAGGTGGG AAGATCACTT GAGCCCGGGA GGTCGAGGCT GCAGTGAGCT
2461  GACATCATGC TACTGCATTC CAGCCTAGGC AATAGAGTGG GACCCTGTCT CAAAAAAAAA
           ATF4

2521  AAAAAAAAAA AGTCAGGGGT GCTGGCCCCA TGATAGGTGC AATGGGTGCC TCCAATTCCC
2581  TCTGGCTCTG CCTCCCAGCC TCTGTCCAAG CAACAGGCAG ATTTTCCATG CCTGGGGACT
2641  TGCCCCTGGC TCACTGATGA TGATACCATC TTAAGTCTCC TGGAATCCTT AAACCCTTCC
2701  TTGGCATTTG TGAGCAAGTA TTGAGCCCCT CCCATGTTTT AGGCCCAGTG CTGGGTGCTT
2761  TCACCTGCAA TTTCTTACAG AGGATGGTAT TTCCTAAACT CCATTCATTT GCTACCTCCA
2821  TGATTTTTGC CATATCACCC AACCCATGAA ATACATAAAT AAATAGTATT TACTCAATAT
2881  TTTGACTCAC TTTTAAAAAA CATAAACTTA TCTGAAAAGG GAACCTATGT CACGCCTCTA
2941  AATAAACAGT ATCAACCAAA AATACAAAAG AAACAAAAAT AAATACAAAG ACATTCTTGG
3001  TTTCTGGCAC CAGGCCCCAG TTCTGGCTCC AACCTTACTG AGAAGTCACA TGATCTCTCT
3061  GGGCCTCAGT TTTCTCCTCT GGAAAATGGA GCTTTTGGAA GTTAATGCAT GCACAGTGCC
3121  TGGCCCTGAG ACTGGCATGG AGTGAGTGGA AGAGAGGTTG CCTGACCTGG CTAAAATTGG
3181  TTCTCTGGGC AGACATTTTC CCAAGGGCCA CTGAGAAGAC CCTCCTGTTA GGAGTCAGTG
3241  AGCTCTGTCG CTGGAGGCAT TCAAACAGAG CCTGCGGACT TCTCACTGCG AAGTTGCCCA
3301  GAGAATTCAG TGCTCAGAGG AAAGGGAGTG GTTATTCCAT CAGAGCTGGT TCCCCAGGAG
3361  CGGGAGCAGG GCCTGTAGCA CCCAGCCTCT GTCCCTGGCT CCCGTCTATC CGGGATTTTA
3421  GCGTTTCCTC TGTAGTTTTC AAGCACTGTC TCATATGACT CTCGCACCAG CGAGAGGCCA
3481  GGGGAGATGG TGTCTGCCTG TTAAAGAGGG GCAGGCTGGT CCACATAGGT CAAGTGACTT
3541  GGCCAAGGTC ACCAGAGCAG AGTTTTGAAC TTGAGCTGTC TGACTCAACT GCCTGGGAAG
3601  TGCCTGCCCC TCCTCTGGCA TCCAGGGAGC ATGTCCTGGG GCTCTGGCTG GGACATAGCC
3661  GGACACCTGC GGGCCCTTTA CGTCTCTAAA GAGAGAAAGA GGGAAGGGCC CCTGTCTAGG
3721  GGGTGGTTTC CCTCCAGATG CCACCCCTCC GAGGTCCCCT TCTGCTTCTT CTTGCGGTAG
3781  CCAGGGAGGC AGCCCACGGG CAGGGAAGCG GGGGTGGGGG TGCAGAGTCA GAGGTGCACG
                                                          XBP1

3841  TGGACAGAGA CAGAGAGACA GGGACACGTG GGCAGAGACG GATAAAGACA GAGACCCAGA
                              XBP1

3901  GAAAGCCAGA TATGTTGACA GACACAGAGA CAGACGCCAG AGAGGAAGGC AGACAAAGAG
3961  ACGGGTGGAG ACAAAGACTC CCACCAAGAG ACGCAGAAGG AAGATGCCGA CGGTAAAGAC
4021  AAAACAGGAG ACGCGCGCAA GGAGCAGGTC AGAGCCCAGG CTCGCTGAGA GAGGAAGGGC
4081  TGGGCTGGGG CAGCCCGGAG GCAGAGAGAC CGAGAGTGCG GGGCGGGCGA GGGACGCCAG
4141  GGCCGCGTCA CCCCAGCCCG TTCCTAGCTC CGCTCCCGGC AGGGGGCGCC CTGGCCTCGT
4201  GGCACGACCG GCCCGCGGGG CGCGGGGCTC GGGCCGGGGG CGGGGCCGGG GCCGGGCTGG
4261  GGAGGGGTTG GGGCCGGGGG CGGGGGAGGG GGCGGGCTGC CCGGGCCTCA CTCGGGCCCC
4321  GCGGCCGCCT TTATAAGGCG GCGGGGGTGG TGGCCCGGGC CGCGTTGCGC TCCCGCCACT
                                                    TSS

4381  CCGCGCCCGC TATCCTGGCT CCGTGCTCCC ACGCGCTTGT GCCTGGACGG ACCC
```

Figure 7.5. ER stress-related transcription factor binding sites mapped to ALP promoter region (-122 to -4556 from the start of the first intron). TSS - transcription start site. Underline – fragment used for DNA binding assays and proteomic analysis.

References

Acampora, D., Merlo, G.R.*, et al.* (1999). "Craniofacial, vestibular and bone defects in mice lacking the Distal-less-related gene Dlx5." Development **126**(17): 3795-3809.

Akiyama, H. (2008). "Control of chondrogenesis by the transcription factor Sox9." Modern Rheumatology **18**(3): 213-219.Alexopoulos, A., Peroukides, S.*, et al.* (2011). "Implication of bone regulatory factors in human coronary artery calcification." Artery Research **5**(3): 101-108.

Alexopoulos, A., Peroukides, S.*, et al.* (2011). "Implication of bone regulatory factors in human coronary artery calcification." Artery Research **5**(3): 101-108.

Ameri, K. and Harris, A. (2008). "Molecules in focus: Activation transcription factor 4" The International Journal of Biochemistry & Cell Biology **40**: 14–21

Anderson, H.C. (2003). "Matrix vesicles and calcification." Current Rheumatology Reports **5**(3): 222-226.

Aoshima, Y., Mizobuchi, M., *et al.* (2012). "Vitamin D receptor activators inhibit vascular smooth muscle cell mineralization induced by phosphate and TNF-α." Nephrology Dialysis Transplantation **27**: 1800–1806.

Atkinson, J. (2008). "Age-related medial elastocalcinosis in arteries: mechanisms, animal models, and physiological consequences." The Journal of Applied Physiology **105**:1643-1651.

Axten, J.M., Medina, J.R., *et al.* (2012). "Discovery of 7-Methyl-5-(1-{[3-(trifluoromethyl)phenyl]acetyl}-2,3-dihydro-1H-indol-5-yl)-7H-pyrrolo[2,3d] pyrimidin-4-amine (GSK2606414), a Potent and Selective First-in-Class Inhibitor of Protein Kinase R (PKR)-like Endoplasmic Reticulum Kinase (PERK)." Journal of Medicinal Chemistry **55**: 7193−7207.

Baek, H.A., Kim, D.S., *et al.* (2011). "Involvement of Endoplasmic Reticulum Stress in Myofibroblastic Differentiation of Lung Fibroblasts." Americam Journal of Respiratory Cell and Molecular Biology **46**: 731–739.

Baek, W.Y., Kim, Y.J., *et al.* (2013). "Osterix is required for cranial neural crest-derived craniofacial bone formation." Biochemical and Biophysical Research Communications **432**(1): 188-192.

Baek, J.E., Choi, J.Y., *et al.* (2014). "Skeletal analysis and differential gene expression in Runx2/Osterix double heterozygous embryos." *Biochemical and Biophysical Research Communications* **451:** 442–448.

Balica, M., Boström, K.*, et al.* (1997). "Calcifying Subpopulation of Bovine Aortic Smooth Muscle Cells Is Responsive to 17β-Estradiol." Circulation **95**(7): 1954-1960.

Ballock, R.T., Heydemann, A.*, et al.* (1993). "TGF-β1 prevents hypertrophy of epiphyseal chondrocytes: Regulation of gene expression for cartilage matrix proteins and metalloproteases." Developmental Biology **158**(2): 414-429.

Barath, P., Fishbein, M.C.*, et al.* (1990). "Detection and localization of tumor necrosis factor in human atheroma." The American Journal of Cardiology **65**(5): 297-302.

Berliner, J.A., Navab, M., *et al.* (2005). ”Atherosclerosis: Basic Mechanisms” Circulation **91**:2488-2496.

Bertrand, R., Solary, E., *et al.* (1994). “Induction of a Common Pathway of Apoptosis by Staurosporine” Experimental Cell Research **211**: 314-321.

Bi, W., Deng, J.M.*, et al.* (1999). "Sox9 is required for cartilage formation." Nat Genet **22**(1): 85-89.

Bialek, P., Kern, B., *et al.* (2004). “A Twist Code Determines the Onset of Osteoblast Differentiation” Developmental Cell **6**: 423–435.

Block, G.A., Hulbert-Shearon, T.E.*, et al.* (1998). "Association of Serum Phosphorus and Calcium x Phosphate Product With Mortality Risk in Chronic Hemodialysis Patients: A National Study." American Journal of Kidney Diseases **31**(4): 607-617.

Bonin, L.R. and Damon, D.H. (1994). Vascular cell interactions modulate the expression of endothelin-1 and platelet-derived growth factor BB.” American Journal of Physiology **267** (Heart Circulation Physiololgy 36): H1698-H1706.

Bostrom, K., Watson, K.E.*, et al.* (1993). "Bone morphogenetic protein expression in human atherosclerotic lesions." Journal of Clinical Investigation **91**(4): 1800-1809.

Bostrom, K., Rajamannan N.M., *et al. (*2011). “The Regulation of Valvular and Vascular Sclerosis by Osteogenic Morphogens” Circulation Research **109**: 564-577.

Brändström, H., Gerdhem, P.*, et al.* (2004). "Single Nucleotide Polymorphisms in the Human Gene for Osteoprotegerin are Not Related to Bone Mineral Density or Fracture in Elderly Women." Calcified Tissue International **74**(1): 18-24.

Bucay, N., Sarosi, I.*, et al.* (1998). "osteoprotegerin-deficient mice develop early onset osteoporosis and arterial calcification." Genes & Development **12**(9): 1260-1268.

Byon, C.H., Javed, A.*, et al.* (2008). "Oxidative Stress Induces Vascular Calcification through Modulation of the Osteogenic Transcription Factor Runx2 by AKT Signaling." The Journal of Biological Chemistry **283**(22): 15319-15327.

Cai, Z., Li, F., *et al.* (2013). "Endoplasmic Reticulum Stress participates in Aortic Valve Calcification in Hypercholesterolemic Animals" Arteriosclerosis, Thrombosis, and Vascular Biology **33**: 2345-3254.

Calfon, M., Zeng, H.*, et al.* (2002). "IRE1 couples endoplasmic reticulum load to secretory capacity by processing the XBP-1 mRNA." Nature **415**(6867): 92-96.

Cao, S.S. And Kaufman R.J. (2014). "Endoplasmic Reticulum Stress and Oxidative Stress in Cell Fate Decision and Human Disease." Antioxidants and Redox Signaling **21**(3): 396-413.

Carthew, R.W. and Sontheimer, E.J. (2009). "Origins and Mechanisms of miRNAs and siRNA." Cell **136**: 642–655.

Chen, N.X., O'Neill, K.D., *et al.* (2006). "The mechanisms of uremic serum-induced expression of bone matrix proteins in bovine vascular smooth muscle cells." Kidney International **70**: 1046–1053.

Chen, G., Deng, C., *et al.* (2012). "TGF-β and BMP Signaling in Osteoblast Differentiation and Bone Formation." International Journal of Biological Sciences **8**(2): 272-288.

Chen, Y., Wang, X., *et al.* (2014). "Upregulated expression of PERK in spinal ligament fibroblasts from the patients with ossification of the posterior longitudinal ligament." European Spine Journal **23**: 447–454

Cheng, W.P., Hung, H.F., *et al.* (2008). "The molecular regulation of GADD153 in apoptosis of cultured vascular smooth muscle cells by cyclic mechanical stretch." Cardiovascular Research **77**: 551-559.

Clarke, M.C.H., Littlewood, T.D.*, et al.* (2008). "Chronic Apoptosis of Vascular Smooth Muscle Cells Accelerates Atherosclerosis and Promotes Calcification and Medial Degeneration." Circulation Research **102**: 1529-1538.

Clauss, I.M., Gravallese, E.M.*, et al.* (1993). "In Situ Hybridization Studies Suggest a Role for the Basic Region-Leucine Zipper Protein hXBP-1 in Exocrine Gland and Skeletal Development During Mouse Embryogenesis " Developmental Dynamics **197**: 146-156.

Collin-Osdoby, P. (2004). "Regulation of Vascular Calcification by Osteoclast Regulatory Factors RANKL and Osteoprotegerin." Circulation Research **95**(11): 1046-1057.

Cross, B.C.S., Bond, P.J., *et al.* (2012). “The molecular basis for selective inhibition of unconventional mRNA splicing by an IRE1-binding small molecule.” Proceedings of the National Academy of Sciences **109**(15): E869-78.

Dai, X.Y., Zhao, M.M., *et al.* (2013). “Phosphate-induced autophagy counteracts vascular calcification by reducing matrix vesicle release.” Kidney International **83**: 1042-1051.

Danciu, T.E., Li, Y., *et al.* (2102). “The Basic Helix Loop Helix Transcription Factor Twist1 is a Novel Regulator of ATF4 in Osteoblasts.” Journal of Cellular Biochemistry **113**: 70-79.

Danziger, J. (2008). "Vitamin K-dependent Proteins, Warfarin, and Vascular Calcification." Clinical Journal of the American Society of Nephrology **3**: 1504-1510.

Das, I., Png, C.W., *et al.* (2013). “Glucocorticoids alleviate intestinal ER stress by enhancing protein folding and degradation of misfolded proteins.” Journal of Experimental Medicine **210**(6): 1201-1216.

Davies, M.R., Lund, R.J., *et al.* (2005). "Low Turnover Osteodystrophy and Vascular Calcification Are Amenable to Skeletal Anabolism in an Animal Model of Chronic Kidney Disease and the Metabolic Syndrome." Journal of the American Society of Nephrology **16**(4): 917-928.

Deegan, S., Saveljeva, S., *et al.* (2013). “Stress-induced self-cannibalism: on the regulation of autophagy by endoplasmic reticulum stress.” Cellular and Molecular Life Sciences **70**: 2425-2441.

Demer, L.L. and Tintut, Y. (2014). “Inflammatory, Metabolic, and Genetic Mechanisms of Vascular Calcification.” Arteriosclerosis, Thrombosis, and Vascular Biology **34**:715-723.

Dennis, M.D., McGhee, N.K., *et al.* (2013). “Regulated in DNA damage and development 1 (REDD1) promotes cell survival during serum deprivation by sustaining repression of signaling through the mechanistic target of rapamycin in complex 1 (mTORC1).” Cellular Signalling **25**: 2709-2716.

DeVries-Seimon, T., Li, Y., *et al.* (2005). "Cholesterol-induced macrophage apoptosis requires ER stress pathways and engagement of the type A scavenger receptor." Journal of Cell Biology **171**(1): 61-73.

Dimcheff, D.E., Askovic, S., *et al.* (2003). "Endoplasmic Reticulum Stress Is a Determinant of Retrovirus-Induced Spongiform Neurodegeneration." Journal of Virology **77**(23): 12617-12629.

Dorai, H., Vukicevic, S., *et al.* (2000). "Bone morphogenetic protein-7 (osteogenic protein-1) inhibits smooth muscle cell proliferation and stimulates the expression of markers that are characteristic of SMC phenotype in vitro." Journal of Cellular Physiology **184**(1): 37-45.

Dorai, H. and Sampath T.K. (2001). “Bone Morphogenetic Protein-7 Modulates Genes that Maintain the Vascular Smooth Muscle Cell Phenotype in Culture.” The Journal of Bone and Joint Surgery **83A**(S1): 70-78.

Dreschler, C., Verdujin, M., *et al.* (2011). “Bone Alkaline Phosphatase and Mortality in Dialysis Patients.” Clinical Journal of the American Society of Nephrology **6**: 1752-1759.

Droge, W. (2002). “Free Radicals in the Physiological Control of Cell Function” Physiological Reviews **82**: 46-95.

Duan, X., Zhou, Y*., et al.* (2009). "Endoplasmic reticulum stress-mediated apoptosis is activated in vascular calcification." Biochemical and Biophysical Research Communications **387**: 694–699.

Duan, X.H., Chang, J.R., *et al.* (2013). “Activating transcription factor 4 is involved in endoplasmicvreticulum stress-mediated apoptosis contributing to vascular calcification.” Apoptosis **18**(9): 1132-1144.

Dzau, V.J., Braun-Dullaeus, R.C., *et al.* (2002). “Vascular proliferation and atherosclerosis: New perspectives and therapeutic strategies.” Nature Medicine **8**(11): 1249-1256.

Ewence, A.E., Bootman, M*., et al.* (2008). "Calcium Phosphate Crystals Induce Cell Death in Human Vascular Smooth Muscle Cells: A Potential Mechanism in Atherosclerotic Plaque Destabilization." Circulation Research **103**: e28-e34.

Fan, D., Chen, Z., *et al.* (2007). “Osterix Is a Key Target for Mechanical Signals in Human Thoracic Ligament Flavum Cells.” Journal of Cellular Physiology **211**: 577-584.

Feil, S., Hofmann, F., *et al.* (2004). “SM22α Modulates Vascular Smooth Muscle Cell Phenotype During Atherogenesis.” Circulation Research **94**: 863-865.

Fietta, P. and Manganelli, P. (2002). “Is fibrillin-1 the link between ankylosing spondylitis and Marfan's syndrome?.” The Journal of Rheumatology **29**(8): 1800-1808.

Freedman, B.I., Bowden, D.W*., et al.* (2009). "Bone morphogenetic protein 7 (BMP7) gene polymorphisms are associated with inverse relationships between vascular calcification and BMD: The diabetes heart study." Journal of Bone and Mineral Research **24**(10): 1719-1727.

Frid, M.G., Shekhonin, B.V., *et al.* (1992). “Phenotypic Changes of Human Smooth Muscle Cells during Development: Late Expression of Heavy Caldesmon and Calponin.” Developmental Biology **153**: 185-193.

Fujii, Y., Khoshnoodi, J*., et al.* (2006). "The effect of dexamethasone on defective nephrin transport caused by ER stress: A potential mechanism for the therapeutic action of glucocorticoids in the acquired glomerular diseases." Kidney International **69**(8): 1350-1359.

Fukui, M., Senmaru, T*., et al.* (2011). "17β-Estradiol attenuates saturated fatty acid diet-induced liver injury in ovariectomized mice by up-regulating hepatic senescence marker protein-30." Biochemical and Biophysical Research Communications **415**(2): 252-257.

Fukunaka, A., Kurokawa, Y., *et al.* (2011). "Tissue Nonspecific Alkaline Phosphatase Is Activated via a Two-step Mechanism by Zinc Transport Complexes in the Early Secretory Pathway." The Journal of Biological Chemistry **286**: 16363-16373.

Galvin, K.M., Donovan, M.J*., et al.* (2000). "A role for Smad6 in development and homeostasis of the cardiovascular system." Nat Genet **24**(2): 171-174.

Garg, A.D., Kaczmarek, A*., et al.* (2012). "ER stress-induced inflammation: does it aid or impede disease progression?" Trends in Molecular Medicine **18**(10): 589-598.

Giachelli, C.M., Jono, S., *et al.* (2001). "Vascular Calcification and Inorganic Phosphate." American Journal of Kidney Diseases **38**(4): S34-S37.

Goettsch, C., Rauner, M*., et al.* (2011). "miR-125b Regulates Calcification of Vascular Smooth Muscle Cells." The American Journal of Pathology **179**(4): 1594–1600.

Gorlach, A., Klappa, P., *et al.* (2006). "The Endoplasmic Reticulum: Folding, Calcium Homeostasis, Signaling, and Redox Control." Antioxidants and Redox Signaling **8**(9): 1391-1418.

Grainger, D.J., Metcalfe, J.C., *et al.* (1998). "Transforming growth factor-β dynamically regulates vascular smooth muscle differentiation in vivo." Journal of Cell Science **111**: 2977-2988

Guo, F.J., Xiong, Z., *et al.* (2013). "ATF6 upregulates XBP1S and inhibits ER stress-mediated apoptosis in osteoarthritis cartilage." Cellular Signalling **26**: 332-342

Guo, F.J., Jiang, R., *et al.* (2014). "IRE1a constitutes a negative feedback loop with BMP2 and acts as a novel mediator in modulating osteogenic differentiation." Cell Death and Disease **5**: e1239.

Guo, F.J., Jiang, R., et al. (2014b). "Regulation of chondrocyte differentiation by IRE1α depends on its enzymatic activity." Cellular Signalling **26**: 1998–2007.

Guo, Y.S., Sun, Z., *et al.* (2014c). "17β-Estradiol inhibits ER stress-induced apoptosis through promotion of TFII-I-dependent Grp78 induction in osteoblasts." Laboratory Investigation **94**: 906-916.

Haas, M.J., Raheja, P*., et al.* (2012). "Estrogen-dependent inhibition of dextrose-induced endoplasmic reticulum stress and superoxide generation in endothelial cells." Free Radical Biology and Medicine **52**(11-12): 2161-2167.

Han, X., Zhou, J., et al. (2013). “IRE1αdissociates with BiP and inhibits ER stress-mediated apoptosis in cartilage development.” Cellular Signalling **25**: 2136–2146.

Harding, H.P., Zhang, Y*., et al.* (1999). "Protein translation and folding are coupled by an endoplasmic-reticulum-resident kinase." Nature **397**(6716): 271-274.

Harding, H.P., Zhang, Y*., et al.* (2000). "Perk Is Essential for Translational Regulation and Cell Survival during the Unfolded Protein Response." Molecular Cell **5**: 897–904.

Harding, H.P., Zeng, H*., et al.* (2001). "Diabetes Mellitus and Exocrine Pancreatic Dysfunction in Perk -/- Mice Reveals a Role for Translational Control in Secretory Cell Survival." Molecular Cell **7**: 1153–1163.

Hashimoto, S., Ochs, R.L*., et al.* (1998). "Chondrocyte-derived apoptotic bodies and calcification of articular cartilage." Proceedings of the National Academy of Sciences **95**(6): 3094-3099.

Haze, K., Yoshida, H*., et al.* (1999). "Mammalian Transcription Factor ATF6 Is Synthesized as a Transmembrane Protein and Activated by Proteolysis in Response to Endoplasmic Reticulum Stress." Molecular Biology of the Cell **10**: 3787–3799.

Heldin, C.H., Miyazono, K., *et al.* (1997). “TGF-bsignalling from cell membrane to nucleus through SMAD proteins.” Nature **390**: 465-471.

Hellstrom, M., Kalen, M., et al. (1999). “Role of PDGF-B and PDGFR-β in recruitment of vascular smooth muscle cells and pericytes during embryonic blood vessel formation in the mouse.” Development **126**: 3047-3055.

Henthorn, P.S., Raducha, M., *et al.* (1992). “Different missense mutations at the tissue-nonspecific alkaline phosphatase gene locus in autosomal recessively inherited forms of mild and severe hypophosphatasia.” Proceedings of the National Academy of Sciences **89**: 9924-9928.

Herrmann, S.M., Whatling, C*., et al.* (2000). "Polymorphisms of the Human Matrix Gla Protein (MGP) Gene, Vascular Calcification, and Myocardial Infarction." Arteriosclerosis, Thrombosis, and Vascular Biology **20**: 2386-2393.

Hino, K., Saito, A., *et al.* (2014). “Master Regulator for Chondrogenesis, Sox9, Regulates Transcriptional Activation of the Endoplasmic Reticulum Stress Transducer BBF2H7/CREB3L2 in Chondrocytes.” The Journal of Biological Chemistry **289**(20): 13810–13820.

Hirschi, K.K., Rohovsky, S.A., *et al.* (1998). “PDGF, TGF-b, and Heterotypic Cell–Cell Interactions Mediate Endothelial Cell–induced Recruitment of 10T1/2 Cells and Their Differentiation to a Smooth Muscle Fate.” The Journal of Cell Biology **141**(3): 805–814.

Hitomi, J., Katayama, T., *et al.* (2004). “Involvement of caspase-4 in endoplasmic reticulum stress-induced apoptosis and Aβ-induced cell death.” The Journal of Cell Biology **165**(3): 347–356.

Hollien, J. and Weissman, J.S. (2006). “Decay of Endoplasmic Reticulum-Localized mRNAs During the Unfolded Protein Response.” Science **312**(104): 104-107.

Hoshino, T., Chow, L., *et al.* (2009). “Mechanical Stress Analysis of a Rigidn Inclusion in Distensible Material: a Model of Atherosclerotic Calcification and Plaque Vulnerability.” American Journal of Physiology – Heart and Circulatory Physiology **297**(2): H802-H810.

Hosoi, T., Sasaki, M.*, et al.* (2008). "Endoplasmic reticulum stress induces leptin resistance." Molecular Pharmacology **74**(6): 1610-1619.

Howard, T.D., Paznekas, W.A., *et al.* (1997). “Mutations in TWIST, a Basci Helix-Loop-Helix Transcription factor, in Saethre-Chotzen syndrome.” Nature Genetics **15**: 36-41.

Hoyer-Hansen, M. and Jaattela, M. (2007). “Connecting endoplasmic reticulum stress to autophagy by unfolded protein response and calcium.” Cell Death and Differentiation **14**: 1576–1582.

Huang, Q.Q., Fisher, S.A., *et al.* (1999). “Forced Expression of Essential Myosin Light Chain Isoforms Demonstrates Their Role in Smooth Muscle Force Production.” The Journal of Biological Chemistry **274** (49): 35095–35098.

Husa, M., Petursson, F., *et al.* (2013). “C/EBP homologous protein drives pro-catabolic responses in chondrocytes.” Arthritis Research & Therapy **15**: R218.

Ichida, F., Nishimura, R.*, et al.* (2004). "Reciprocal Roles of Msx2 in Regulation of Osteoblast and Adipocyte Differentiation." Journal of Biological Chemistry **279**(32): 34015-34022.

Ichikawa, S., Imel, E.A.*, et al.* (2007). "A homozygous missense mutation in human KLOTHO causes severe tumoral calcinosis." Journal of Clinical Investigation **117**(9): 2684-2691.

Iribarren, C., Husson, G.*, et al.* (2007). "Plasma Leptin Levels and Coronary Artery Calcification in Older Adults." Journal of Clinical Endocrinology & Metabolism **92**(2): 729-732.

Ishihara, K, Yamazaki, T., et al. (2006). “Zinc Transport Complexes Contribute to the Homeostatic Maintenance of Secretory Pathway Function in Vertebrate Cells.” Journal of Biological Chemistry **281**(26): 17743-17750.

Iyemere, V.P., Proudfoot, D.*, et al.* (2006). "Vascular smooth muscle cell phenotypic plasticity and the regulation of vascular calcification." Journal of Internal Medicine **260**(3): 192-210.

Izumi, S., Saito, A., *et al.* (2012). “The Endoplasmic Reticulum Stress Transducer BBF2H7 Suppresses Apoptosis by Activating the ATF5-MCL1 Pathway in Growth Plate Cartilage.” The Journal of Biological Chemistry **287**(43): 36190–36200.

Jahnen-Dechent, W., Schinke, T*., et al.* (1997). "Cloning and Targeted Deletion of the Mouse Fetuin Gene." The Journal of Biological Chemistry **272**(50): 31496-31503.

Jang, W.G., Kim, E.J*., et al.* (2011). "BMP2 Protein Regulates Osteocalcin Expression via Runx2-mediated Atf6 Gene Transcription." The Journal of Biological Chemistry **287**(2): 905-915.

Jang, W.G., Kim, E.J., *et al.* (2013). “Tunicamycin negatively regulates BMP2-induced osteoblast differentiation through CREBH expression in MC3T3E1 cells.” BMB Reports **44**(11): 735-740.

Jena, N., Martín-Seisdedos, C*., et al.* (1997). "BMP7 null mutation in mice: Developmental defects in skeleton, kidney, and eye." Experimental Cell Research **230**(1): 28-37.

Jensen, E.D., Niu, L., *et al.* (2008). “p68 (Ddx5) Interacts With Runx2 and Regulates Osteoblast Differentiation.” Journal of Cellular Biochemistry **103**: 1438–1451.

Jian, B., Narula, N*., et al.* (2003). "Progression of aortic valve stenosis: TGF-{beta}1 is present in calcified aortic valve cusps and promotes aortic valve interstitial cell calcification via apoptosis." The Annals of Thoracic Surgery **75**(2): 457-465.

Jono, S., Nishizawa, Y., et al. (1998) “Parathyroid Hormone–Related Peptide as a Local Regulator of Vascular Calcification Its Inhibitory Action on In Vitro Calcification by Bovine Vascular Smooth Muscle Cells.” Arteriosclerosis, Thrombosis, and Vascular Biology **17**:1135-1142

Kaden, J.J., Bickelhaupt, S*., et al.* (2004). "Expression of bone sialoprotein and bone morphogenetic protein-2 in calcific aortic stenosis." The Journal of heart valve disease **13**(4): 560-566.

Kalantar-Zadeh, K., Kuwae, N., et al. (2006). “Survival predictability of time-varying indicators of bone disease in maintenance hemodialysis patients.” Kidney International **70**: 771–780.

Kalra, S.S. and Shanahan, C.M. (2012). "Vascular calcification and hypertension: Cause and effect." Annals of Medicine **44**(SUPPL. 1): S85-S92.

Kaneto, H., Matsuoka, T*., et al.* (2005). "Oxidative stress, ER stress, and the JNK pathway in type 2 diabetes." The Journal of Molecular MEdicine **83**: 429-439.

Kapustin, A.N., Davies, J.D.*, et al.* (2011). "Calcium regulates key components of vascular smooth muscle cell-derived matrix vesicles to enhance mineralization." Circulation Research **109**(1): e1-e12.

Kapustin, A.N. and Shanahan, C.M. (2012). "Calcium Regulation of Vascular Smooth Muscle Cell–Derived Matrix Vesicles." Trends in Cardiovascular Medicine **22**(5): 133-137.

Karsenty, G., Kronenberg, H.M.*, et al.* (2009). "Genetic Control of Bone Formation." Annual Review of Cell and Developmental Biology **25**: 629-648.

Karwowski, W., Naumnik, B.*, et al.* (2012). "The mechanism of vascular calcification - a systematic review." Medical Science Monitor **18**(1): RA1-11.

Kassan, M., Galán, M.*, et al.* (2012). "Endoplasmic reticulum stress is involved in cardiac damage and vascular endothelial dysfunction in hypertensive mice." Arteriosclerosis, Thrombosis, and Vascular Biology **32**(7): 1652-1661.

Katagiri, T. and Takahashi, N. (2002). "Regulatory mechanisms of osteoblast and osteoclast differentiation." Oral Diseases **8**(3): 147-159.

Katano, A., Satoh, T., *et al.* (2013). "THRAP3 Interacts with HELZ2 and Plays a Novel Role in Adipocyte Differentiation." Molecular Endocrinology **27**(5): 769 –780.

Kedi, X., Ming, Y.*, et al.* (2009). "Free cholesterol overloading induced smooth muscle cells death and activated both ER- and mitochondrial-dependent death pathway." Atherosclerosis **207**(1): 123-130.

Ketteler, M., Bongartz, P.*, et al.* (2003). "Association of low fetuin-A (AHSG) concentrations in serum with cardiovascular mortality in patients on dialysis: a cross-sectional study." The Lancet **361**(9360): 827-833.

Ketteler, M., Vermeer, C.*, et al.* (2002). "Novel Insights into Uremic Vascular Calcification: Role of Matrix Gla Protein and Alpha-2-Heremans Schmid Glycoprotein/Fetuin." Blood Purification **20**: 473-476.

Kim, J.W., Choi, H., *et al.* (2014). "transcriptional Factor AtF6 is Involved in Odontoblastic Differentiation." Journal of Dental Research **93**(5): 483-48.

Kleinjan, .A., and van Heyningen, V., (2005). "Long-Range Control of Gene Expression: Emerging Mechanisms and Disruption in Disease." American Journal of Human Genetics **76**: 8–32.

Kobayashi, T., Vischer, U.M.*, et al.* (2000). "The Tetraspanin CD63/lamp3 Cycles between Endocytic and Secretory Compartments in Human Endothelial Cells." Molecular Biology of the Cell **11**(5): 1829-1843.

Komori, T. (2006). "Regulation of Osteoblast Differentiation by Transcription Factors." Journal of Cellular Biochemistry **99**: 1233–1239.

Ketteler, M., Vermeer, C*., et al.* (2002). "Novel Insights into Uremic Vascular Calcification: Role of Matrix Gla Protein and Alpha-2-Heremans Schmid Glycoprotein/Fetuin." Blood Purification **20**: 473-476.

Kondo, S., Saito, A*., et al.* (2007). "BBF2H7, a Novel Transmembrane bZIP Transcription Factor, Is a New Type of Endoplasmic Reticulum Stress Transducer."

Kooptiwut, S., Mahawong, P., *et al.* (2014). "Estrogen reduces endoplasmic reticulum stress to protect against glucotoxicity induced-pancreatic β-cell death." Journal of Steroid Biochemistry and Molecular Biology **139**: 25-32.

Kozutsumi, Y., Segal, M., *et al.* (1988). "The presence of malfolded proteins in the endoplasmic reticulum signals the induction of glucose-regulated proteins." Nature **332**: 462-464.

Kuro-o, M., Matsumura, Y*., et al.* (1997). "Mutation of the mouse klotho gene leads to a syndrome resembling ageing." Nature **390**(6655): 45-51.

Lee, M.-H., Kwon, T.-G*., et al.* (2003). "BMP-2-induced Osterix expression is mediated by Dlx5 but is independent of Runx2." Biochemical and Biophysical Research Communications **309**: 689-694.

Lee, H.L., Woo, K.M., *et al.* (2010). "Tumor necrosis factor-aincreases alkaline phosphatase expression in vascular smooth muscle cells via MSX2 induction." Biochemical and Biophysical Research Communications **391**: 1087-1092.

Lehtinen, A.B., Burdon, K.P*., et al.* (2007). "Association of α2-Heremans-Schmid Glycoprotein Polymorphisms with Subclinical Atherosclerosis." Journal of Clinical Endocrinology & Metabolism **92**(1): 345-352.

Lei, Y., Sinha, A., *et al.* (2014). "Hydroxyapatite and calcified elastin induce osteoblast-like differentiation in rat aortic smooth muscle cells." Experimental Cell Research 323(1): 198-208.

Lencel, P., Delplace, S., *et al.* (2011). "TNF-α stimulates alkaline phosphatase and mineralization through PPARγ inhibition in human osteoblasts." Bone **48**: 242-249.

Leroux-Berger, M., Queguiner, I., *et al.* (2011). "Pathologic Calcification of Adult Vascular Smooth Muscle Cells Differs on Their Crest or Mesodermal Embryonic Origin." Journal of Bone and Mineral Research **26**(7): 1543-1553.

Li, X., Yang, H.Y*., et al.* (2008). "BMP-2 promotes phosphate uptake, phenotypic modulation, and calcification of human vascular smooth muscle cells." Atherosclerosis **199**(2): 271-277.

Lian, N., Lin, T., *et al.* (2012). “Transforming Growth Factor#Suppresses Osteoblast Differentiation via the Vimentin Activating Transcription Factor 4 (ATF4) Axis.” The Journal of Biological Chemistry **287**(43): 35975-35984.

Liang, B., Wang, S., *et al.* (2013). “Aberrant Endoplasmic Reticulum Stress in Vascular Smooth Muscle Increases Vascular Contractility and Blood Pressure in Mice Deficient of AMP-Activated Protein Kinase-α2 In Vivo.” Arteriosclerosis, Thrombosis, and Vascular Biology **33**: 595-604.

Liberman, M., Johnson, R.C*., et al.* (2011). "Bone morphogenetic protein-2 activates NADPH oxidase to increase endoplasmic reticulum stress and human coronary artery smooth muscle cell calcification." Biochemical and Biophosical Research Communications **413**: 436-441.

Lim, K., Lu, T.S*., et al.* (2012). "Vascular Klotho Deficiency Potentiates the Development of Human Artery Calcification and Mediates Resistance to Fibroblast Growth Factor 23." Circulation **125**(18): 2243-2255.

Liu, F., Hata, A*., et al.* (1996). "A human Mad protein acting as a BMP-regulated transcriptional activator." Nature **381**(6583): 620-623.

Liu, C., Zhang, Y., *et al.* (2007). “Transcriptional activation of cartilage oligomeric matrix protein by Sox9, Sox5, and Sox6 transcription factors and CBP/p300 coactivators.” Frontiers in Bioscience **12**: 3899-3910.

Liu, Y., Wang, T., *et al.* (2011a). “HGF/c-Met signalling promotes Notch3 activation and human vascular smooth muscle cell osteogenic differentiation in vitro.” Atherosclerosis **219**: 440-447.

Liu, Y., Wang, X., *et al.* (2011b). “Wogonin ameliorates lipotoxicity-induced apoptosis of cultured vascular smooth muscle cells via interfering with DAG-PKC pathway.” Acta Pharmacologica Sinica **32**: 1475-1482.

Liu, Y., Zhou, J*., et al.* (2012). "XBP1S Associates with RUNX2 and Regulates Chondrocyte Hypertrophy." Journal of Biological Chemistry.

Liu, D., Cui, W., *et al.* (2014). “Atorvastatin Protects Vascular Smooth Muscle Cells From TGF-β1-Stimulated Calcification by Inducing Autophagy via Suppression of the β-Catenin Pathway.” Cellular Physiology and Biochemistry **33**: 129-141.

Livak, K.J. and Schmittgen, T.D. (2001). “Analysis of Relative Gene Expression Data Using Real-Time Quantitative PCR and the $2^{-\Delta\Delta CT}$ Method.” Methods **25**: 402-408.

Lomashvili, K.A., Garg, P*., et al.* (2008). "Upregulation of alkaline phosphatase and pyrophosphate hydrolysis: Potential mechanism for uremic vascular calcification." Kidney International **73**(9): 1024-1030.

Lomashvili, K.A., Wang, X*., et al.* (2011). "Matrix gla protein metabolism in vascular smooth muscle and role in uremic vascular calcification." Journal of Biological Chemistry **286**(33): 28715-28722.

London, G.M. (2011). "Arterial calcification: cardiovascular function and clinical outcome." Nefrologia **31**(6): 644-647.

Luo, G., Ducy, P*., et al.* (1997). "Spontaneous calcification of arteries and cartilage in mice lacking matrix GLA protein." Nature **386**(6620): 78-81.

Luo, S., Baumeister, P*., et al.* (2003). "Induction of Grp78/BiP by Translational Block." The Journal Of Biological Chemistry **278**(39): 37375–37385.

Mackie, E.J., Ahmed, Y.A., *et al.* (2008). "Endochondral ossification: How cartilage is converted into bone in the developing skeleton." The International Journal of Biochemistry and Cell Biology **40**: 46–62.

Maiuri, M.C., Zalckvar, E*., et al.* (2007). "Self-eating and self-killing: Crosstalk between autophagy and apoptosis." Nature Reviews Molecular Cell Biology **8**(9): 741-752.

Makowski, A.J., Uppuganti, S., *et al.* (2014). "The loss of activating transcription factor 4 (ATF4) reduces bone toughness and fracture toughness." Bone **62**: 1–9.

Masuda, M., Ting, T.C*., et al.* (2012). "Activating transcription factor 4 regulates stearate-induced vascular calcification." Journal of Lipid Research **53**(8): 1543-1552.

Masuda, M., Miyazaki-Anzai, S., *et al.* (2013). "PERK-eIF2a-ATF4-CHOP Signaling Contributes to TNFa-Induced Vascular Calcification." The Journal of the American Heart Association **2**(5): e000238.

Matsubara, T., Kida, K*., et al.* (2008). "BMP2 Regulates Osterix through Msx2 and Runx2 during Osteoblast Differentiation." The Journal of Biological Chemistry **283**(43): 29119-29125.

Michigami, T. (2013). "Regulatory mechanisms for the development of growth plate cartilage." Cellular and Molecular Life Sciences **70**: 4213-4221.

Miller, J.D., Chu, Y*., et al.* (2008). "Dysregulation of Antioxidant Mechanisms Contributes to Increased Oxidative Stress in Calcific Aortic Valvular Stenosis in Humans." Journal of the American College of Cardiology **52**(10): 843-850.

Milona, M., Gough, J.E., *et al.* (2003). "Expression of alternatively spliced isoforms of human Sp7 in osteoblast-like cells." BMC Genomics **4**(43).

Minamino, T. and Kitakaze, M. (2012). "ER stress in cardiovascular disease." Journal of Molecular and Cellular Cardiology **48**: 1105–1110.

Mizobuchi, M., Ogata, H., et al. (2009). "Vitamin D and vascular calcification in chronic kidney disease." Bone **45**: S26-S29.

Moe, S.M. and Chen, N.X. (2005). "Inflammation and vascular calcification." Blood Purification **23**(1): 64-71.

Moore, K. and Hollien, J. (2012). “The Unfolded Protein Response in Secretory Cell Function.” The Annual Review of Genetics **46**: 165-183.

Mori, K., Shioi, A.*, et al.* (1999). "Dexamethasone enhances in vitro vascular calcification by promoting osteoblastic differentiation of vascular smooth muscle cells." Arteriosclerosis, Thrombosis, and Vascular Biology **19**(9): 2112-2118.

Motskin, M., Wrights, D.M., *et al.* (2009). “Hydroxyapatite nano and microparticles: Correlation of particle properties with cytotoxicity and biostability.” Biomaterials **30**: 3307–3317

Mu, F.-T., Callaghan, J.M.*, et al.* (1995). "EEA1, an Early Endosome-Associated Protein." Journal of Biological Chemistry **270**(22): 13503-13511.

Mueller, S., Riedel, H.D., *et al.* (1997). “Determination of Catalase Activity at Physiological Hydrogen Peroxide Concentrations.” Analytical Biochemistry **245**: 55-60.

Munroe, P.B., Olgunturk, R.O.*, et al.* (1999). "Mutations in the gene encoding the human matrix Gla protein cause Keutel syndrome." Nat Genet **21**(1): 142-144.

Murakami, T., Saito, A.*, et al.* (2009). "Signalling mediated by the endoplasmic reticulum stress transducer OASIS is involved in bone formation." Nature Cell Biology **11**(10): 1205-1211.

Murakami, T., Hino, S., et al. (2010). “Distinct mechanisms are responsible for osteopenia and growth retardation in OASIS-deficient mice.” Bone **48**(3): 514-523.

Musunuru, K., Nasir, K.*, et al.* (2008). "A synergistic relationship of elevated low-density lipoprotein cholesterol levels and systolic blood pressure with coronary artery calcification." Atherosclerosis **200**(2): 368-373.

Nakagawa, T., Zhu, H., *et al.* (2000). “Caspase-12 mediates endoplasmic reticulum-specific apoptosis and cytotoxicity by amyloid-β.” Nature **403**: 98-103.

Nakagawa, Y., Ikeda, K.*, et al.* (2010). "Paracrine osteogenic signals via bone morphogenetic protein-2 accelerate the atherosclerotic intimal calcification in vivo." Arteriosclerosis, Thrombosis, and Vascular Biology **30**(10): 1908-1915.

Nakamura, S., Miki, H., *et al.* (2013). “Activating transcription factor 4, an ER stress mediator, is required for, but excessive ER stress suppresses osteoblastogenesis by bortezomib.” International Journal of Hematology **98**: 66–73.

Nakashima, K. and de Crombrugghe, B. (2003). "Transcriptional mechanisms in osteoblast differentiation and bone formation." Trends in Genetics **19**(8): 458-466.

Nakashima, K., Zhou, X*., et al.* (2002). "The Novel Zinc Finger-Containing Transcription Factor Osterix Is Required for Osteoblast Differentiation and Bone Formation." Cell **108**: 17-29.

Neven, E., Dauwe, S*., et al.* (2007). "Endochondral bone formation is involved in media calcification in rats and in men." Kidney Int **72**(5): 574-581.

Neven, E., Persy, V., *et al.* (2010). "Chondrocyte Rather Than Osteoblast Conversion of Vascular Cells Underlies Medial Calcification in Uremic Rats." Arteriosclerosis, Thrombosis, and Vascular Biology **30**: 1741-1750.

New, S.E., Goettsch, C., *et al.* (2013). "Macrophage-Derived Matrix Vesicles: An Alternative Novel Mechanism for Microcalcification in Atherosclerotic Plaques." Circulation Research **113**: 72-77.

Niederhoffer, N., Bobryshev, Y.V., *et al.* (1997). "Aortic Calcification Produces by Vitamin D3 plus Nicotine." Journal of Vascular Rsearch **34**: 386-398.

Nikaido, T., Yokoya, S*., et al.* (2001). "Expression of the novel transcription factor OASIS, which belongs to the CREB/ATF family, in mouse embryo with special reference to bone development." **116**: 141–148.

Nishimura, R., Kato, Y*., et al.* (1998). "Smad5 and DPC4 Are Key Molecules in Mediating BMP-2-induced Osteoblastic Differentiation of the Pluripotent Mesenchymal Precursor Cell Line C2C12." The Journal of Biological Chemistry **4**: 1872-1879.

Nishimura, R., Wakabayashi, M., *et al.* (2012). "Osterix Regulates Calcification and Degradation of Chondrogenic Matrices through Matrix Metalloproteinase 13 (MMP13) Expression in Association with Transcription Factor Runx2 during Endochondral Ossification." The Journal of Biological Chemistry **287**(40): 33179-33190.

Nonaka, H., Tsujino, T., *et al.* (2001). "Taurine Prevents the Decrease in Expression and Secretion of Extracellular Superoxide Dismutase Induced by Homocysteine." Circulation **104**: 1165-1170.

Novak, A. and Dedhar, S. (1999). "Signaling through#-catenin and Lef/Tcf." Cellular and Molecular Life Sciences **56**: 523-537.

O'Neill, W.C. and Adams, A.L. (2014). "Breast arterial calcification in chronic kidney disease: absence of smooth muscle apoptosis and osteogenic transdifferentiation." Kidney International **85**: 668-676.

Obeng, E.A. and Boise, L.H. (2005). "Caspase-12 and Caspase-4 Are Not Required for Caspase-dependent Endoplasmic Reticulum Stress-induced Apoptosis." The Journal of Biological Chemistry **280**(33): 29578-29587.

Ogata, M., Hino, S., *et al.* (2006). “Autophagy Is Activated for Cell Survival after Endoplasmic Reticulum Stress.” Molecular And Cellularbiology **26**(24): 9220–9231

Ohta, S., Hattori, Y., *et al.* (2011). “Differential Modulation of Immunostimulant-Triggered NO Production by Endoplasmic Reticulum Stress Inducers in Vascular Smooth Muscle Cells.” Journal of Cardiovascular Pharmacology **57**(4): 434-438.

Okawa, A., Nakamura, I*., et al.* (1998). "Mutation in Npps in a mouse model of ossification of the posterior longitudinal ligament of the spine." Nature Genetics **19**(3): 271-273.

Olden, K., Pratt, R.M*., et al.* (1979). "Evidence for role of glycoprotein carbohydrates in membrane transport: Specific inhibition by tunicamycin." Proceedings of the National Academy of Science **76**(2): 791-795.

O'Neill, W.C. And Adams, A.L. (2014). “Breast arterial calcification in chronic kidney disease: absence of smooth muscle apoptosis and osteogenic transdifferentiation.” Kidney International **85**(3): 668-676.

Orimo, H. and Shimada, T. (2005). “Regulation of the human tissue-nonspecific alkaline phosphatase gene expression by all-trans-retinoic acid in SaOS-2 osteosarcoma cell line.” Bone **36:** 866 – 876.

Orlandi, A., Ropraz, P., *et al.* (1994). “Proliferative Activity and α-Smooth Muscle Actin Expression in Cultures Rat Aortic Smooth Muscle Cells Are Differently Mudulated by Transforming Growth Factor-β1 and Heparin.” Experimental Cell Research **214**: 528-536.

Orsó, E., Grandl, M*., et al.* (2011). "Oxidized LDL-induced endolysosomal phospholipidosis and enzymatically modified LDL-induced foam cell formation determine specific lipid species modulation in human macrophages." Chemistry and Physics of Lipids **164**(6): 479-487.

Osako, M.K., Nakagami, H*., et al.* (2010). "Estrogen inhibits vascular calcification via vascular RANKL system: Common mechanism of osteoporosis and vascular calcification." Circulation Research **107**(4): 466-475.

Osawa, M., Tian, W*., et al.* (2005). "Association of α2-HS glycoprotein (AHSG, fetuin-A) polymorphism with AHSG and phosphate serum levels." Human Genetics **116**(3): 146-151.

Osinbowale, O., Malki, M., *et al.* (2009). “An algorithm for managing warfarin resistance.” Cleveland Clinic Journal of Medicine **76**(12): 724-730.

Parhami, F., Tintut, Y*., et al.* (2001). "Leptin Enhances the Calcification of Vascular Cells." Circulation Research **88**(9): 954-960.

Parhami, F., Basseri, B*., et al.* (2002). "High-Density Lipoprotein Regulates Calcification of Vascular Cells." Circulation Research **91**(7): 570-576.

Park, J., Jang, H., *et al.* (2012). “ER stress-inducible ATF3 suppresses BMP2-induced ALP expression and activation in MC3T3-E1 cell.” Biochemical and Biophysical Research Communications **443**: 333–338.

Park, S.Y. and Kim, J.E. (2013). “Differential gene expression by Osterix knockdown in mouse chondrogenic ATDC5 cells.” Gene 518: 368–375.

Peng, Y., Shi, K., *et al.* (2013). “Characterization of Osterix Protein Stability and Physiological Role in Osteoblast Differentiation.” PloS ONE 8(2): e56451.

Pereira, L., Andrikopoulos, K*., et al.* (1997). "Targetting of the gene encoding fibrillin-1 recapitulates the vascular aspect of Marfan syndrome." Nat Genet **17**(2): 218-222.

Plenz, G.A.M., Deng, M.C., *et al.* (2003). “Vascular collagens: spotlight on the role of type VIII collagen in atherogenesis.” Atherosclerosis **166**: 1-11.

Price, P.A., Faus, S.A., *et al.* (1998). “Warfarin Causes Rapid Calcification of the Elastic Lamellae in Rat Arteries and Heart Valves.” Arteriosclerosis, Thrombosis, and Vascular Biology **18**: 1400-1407.

Proudfoot, D., Skepper, J.N*., et al.* (1998). "Calcification of Human Vascular Cells In Vitro Is Correlated With High Levels of Matrix Gla Protein and Low Levels of Osteopontin Expression." Arteriosclerosis, Thrombosis, and Vascular Biology **18**: 379-388.

Proudfoot, D., Skepper, J.N*., et al.* (2000). "Apoptosis Regulates Human Vascular Calcification In Vitro: Evidence for Initiation of Vascular Calcification by Apoptotic Bodies." Circulation Research **87**: 1055-1062.

Proudfoot, D. and Shanahan, C.M. (2001). "Biology of Calcification in Vascular Cells: Intima versus Media." Herz **26**(4): 245-251.

Proudfoot, D., Davies, J.D*., et al.* (2002). "Acetylated Low-Density Lipoprotein Stimulates Human Vascular Smooth Muscle Cell Calcification by Promoting Osteoblastic Differentiation and Inhibiting Phagocytosis." Circulation **106**(24): 3044-3050.

Qiao, J.H., Mertens, R.B., *et al.* (2003). “Cartilaginous Metaplasia in Calcified Diabetic Peripheral Vascular Disease: Morphologic Evidence of Enchondral Ossification.” Human Pathology **34**(4): 402–407.

Ramirez, F., Gayraud, B*., et al.* (1999a). "Marfan syndrome: New clues to genotype-phenotype correlations." Annals of Medicine **31**(3): 202-207.

Ramirez, F. and Pereira, L. (1999b). "Mutations of extracellular matrix components in vascular disease." The Annals of Thoracic Surgery **67**(6): 1857-1858.

Rao, R.V., Ellerby, H.M., *et al.* (2004). “Coupling endoplasmic reticulum stress to the cell death program.” Cell Death and Differentiation **11**: 372–380.

Rasheed, Z. and Haqqi, T.M. (2012). “Endoplasmic reticulum stress induces the expression of COX-2 through activation of eIF2α, p38-MAPK and NF-κB in advanced glycation end products stimulated human chondrocytes.” Biochimica et Biophysica Acta **1823**: 2179–2189.

Ravindran, S., Gao, Q*., et al.* (2011). "Stress Chaperone GRP-78 Functions in Mineralized Matrix Formation." The Journal Of Biological Chemistry **286**(11): 8729–8739.

Ravindran, S., Gao, Q., *et al.* (2012). “Expression and distribution of grp-78/bip in mineralizing tissues and mesenchymal cells.” Histochemistry abd Cell Biology **138**: 113–125.

Reimold, A.M., Iwakoshi, N.N*., et al.* (2001). "Plasma cell differentiation requires the transcription factor XBP-1." Nature **412**(6844): 300-307.

Ren, X., Shao, H., *et al.* (2009). “Advanced Glycation End-products Enhance Calcification in Vascular Smooth Muscle Cells.” The Journal of International Medical Research **37**: 847-854.

Rennenberg, R.J.M., Kessels, A.G.H., *et al.* (2009). “Vascular calcifications as a marker of increased cardiovascular risk: A meta-analysis.” Vascular Health and Risk Management **5**: 185–197.

Reynolds, J.L., Joannides, A.J*., et al.* (2004). "Human Vascular Smooth Muscle Cells Undergo Vesicle-Mediated Calcification in Response to Changes in Extracellular Calcium and Phosphate Concentrations: A Potential Mechanism for Accelerated Vascular Calcification in ESRD." Journal of the American Society of Nephrology **15**: 2857–2867.

Reynolds, J.L., Skepper, J.N*., et al.* (2005). "Multifunctional Roles for Serum Protein Fetuin-A in Inhibition of Human Vascular Smooth Muscle Cell Calcification." Journal of the American Society of Nephrology **16**: 2920-2930.

Riek, A.E., Oh, J., *et al*. (2012). “Vitamin D Suppression of Endoplasmic Reticulum Stress Promotes an Antiatherogenic Monocyte/Macrophage Phenotype in Type 2 Diabetic Patients.” The Journal of Biological Chemistry **287**(46): 38482-38494.

Rohrer, J., Schweizer, A*., et al.* (1996). "The targeting of Lamp1 to lysosomes is dependent on the spacing of its cytoplasmic tail tyrosine sorting motif relative to the membrane." The Journal of Cell Biology **132**(4): 565-576.

Ron, D. and Walter, P. (2007). "Signal integration in the endoplasmic reticulum unfolded protein response." Nature Reviews Molecular Cell Biology **8**: 519-530.

Rost, S., Fregin, A., *et al.* (2004), “Mutations in VKORC1 cause warfarin resistance and multiple coagulation factor deficiency type 2.” Nature **427**: 537-541.

Rowe, P.S.N. (2012). “Regulation of Bone–Renal Mineral and Energy Metabolism: The PHEX, FGF23, DMP1, MEPE ASARM Pathway.” Critical Reviews in Eukaryotic Gene Expression **22**(1): 61–86.

Rutsch, F., Ruf, N.*, et al.* (2003). "Mutations in ENPP1 are associated with 'idiopathic' infantile arterial calcification." Nature Genetics **34**(4): 379-381.

Rzymski, T., Milani, M., *et al.* (2009). “Role of ATF4 in regulation of autophagy and resistance to drugs and hypoxia.” Cell Cycle **8**(23): 3838-3847.

Sage, A.P., Tintut, Y., *et al.* (2010). “Regulatory mechanisms in vascular calcification.”Nature Reviews Cardiology **7**: 528–536.

Sage, A.P., Lu, X., *et al*. (2011). “Hyperphosphatemia-induced nanocrystal upregulate the expression of bone morphogenetic protein-2 and osteopontin genes in mouse smooth muscle cells in vitro.” Kidney International **79**(4): 414-22.

Saito, A., Hino, S.I.*, et al.* (2009). "Regulation of endoplasmic reticulum stress response by a BBF2H7-mediated Sec23a pathway is essential for chondrogenesis." Nature Cell Biology **11**(10): 1197-1204.

Saito, A., Ochiai, K.*, et al.* (2011). "Endoplasmic ReticulumStress Response Mediated by the PERK-eIF2a-ATF4 Pathway Is Involved in Osteoblast Differentiation Induced by BMP2." The Journal of Biological Chemistry **286**(6): 4809-4818.

Salabei, J.K., Cummins, T.D., et al. (2013). “PDGF-mediated autophagy regulates vascular smooth muscle cell phenotype and resistance to oxidative stress.” Biochemical Journal **451**: 375–388.

Sano, R. and Reed, J.C. (2013). “ER stress-induced cell death mechanisms.” Biochimica et Biophysica Acta **1833**:3460–3470.

Sanson, M., Augé, N.*, et al.* (2009). "Oxidized low-density lipoproteins trigger endoplasmic reticulum stress in vascular cells: Prevention by oxygen-regulated protein 150 expression." Circulation Research **104**(3): 328-336.

Schafer, C., Heiss, A.*, et al.* (2003). "The serum protein α2–Heremans-Schmid glycoprotein/fetuin-A is a systemically acting inhibitor of ectopic calcification." The Journal of Clinical Investigation **112**(3): 357-366.

Schmidt, A., Lorkowski, S., *et al.* (2006). “TGF-β1 generates a specific multicomponent extracellular matrix in human coronary SMC.” European Journal of Clinical Investigation **36**: 473-482.

Schoppet, M. and Shanahan, C.M. (2008). “Role for alkaline phosphatase as an inducer of vascular calcification in renal failure?” Kidney International **73**: 989-991.

Scorrano, L., Oakes, S.A., *et al.* (2013). “BAX and BAK Regulation of Endoplasmic Reticulum Ca2+: A Control Point for Apoptosis.” Science **300**(135): 135-139.

Serrano, R.L., Yu, W., *et al.* (2014). “Mono-allelic and bi-allelic ENPP1 deficiency promote post-injury neointimal hyperplasia associated with increased C/EBP homologous protein expression.” Atherosclerosis **233**: 493-502.

Shah, N.M., Groves, A.K., *et al.* (1996). “Alternative Neural Crest Cell Fates Are Instructively Promoted by TGFβ Superfamily Members.” Cell **85**: 331-343.

Shah, G.N., Bonapace, G., *et al.* (2004). "Carbonic anhydrase II deficiency syndrome (osteopetrosis with renal tubular acidosis and brain calcification): Novel mutations in CA2 identified by direct sequencing expand the opportunity for genotype-phenotype correlation." Human Mutation **24**(3): 272-272.

Shamu, C.E. and Walter, P. (1996). "Oligomerization and phosphorylation of the Irelp kinase during intracellular signaling from the endoplasmic reticulum to the nucleus." The EMBO Journal **15**(12): 3028-3039.

Shanahan, C.M., Weissberg, P.L., *et al.* (1993). "Isolation of gene markers of differentiated and proliferating vascular smooth muscle cells." Circulation Research **73**(1): 193-204.

Shanahan, C.M., Cary, N.R.B., *et al.* (1994). "High expression of genes for calcification-regulating proteins in human atherosclerotic plaques." Journal of Clinical Investigation **93**(6): 2393-2402.

Shanahan, C.M. and Weissberg, P.L. (1998). "Smooth muscle cell heterogeneity: Patterns of gene expression in vascular smooth muscle cells in vitro and in vivo." Arteriosclerosis, Thrombosis, and Vascular Biology **18**(3): 333-338.

Shanahan, C.M., Cary, N.R.B., *et al.* (1999a). “Medial Localization of Mineralization-Regulating Proteins in Association With Monckeberg’s Sclerosis: Evidence for Smooth Muscle Cell–Mediated Vascular Calcification.” Circulation **100**: 2168-2176.

Shanahan, C.M. and Weissberg, P.L. (1999b). “Smooth Muscle Cell Phenotypes in Atherosclerotic Lesions.” Current Opinion in Lipidology **10**: 507-513.

Shanahan, C.M. (2005). "Vascular Calcification." Current Opinion in Nephrology and Hypertension **14**: 361-367.

Shanahan, C.M., Crouthamel, M.H., *et al.* (2011). "Arterial Calcification in Chronic Kidney Disease: Key Roles for Calcium and Phosphate." Circulation Research **109**(6): 697-711.

Shanahan, C.M. (2013) “Mechanisms of vascular calcification in CKD - evidence for premature ageing?” Nature Reviews Nephrology **9**: 661-670.

Shao, J.S., Cheng, S.L.*, et al.* (2005). "Msx2 promotes cardiovascular calcification by activating paracrine Wnt signals." Journal of Clinical Investigation **115**(5): 1210-1220.

Shao, J.S., Cai, J., *et al.* (2006). "Molecular Mechanisms of Vascular Calcification: Lessons Learned From The Aorta." Arteriosclerosis, Thrombosis, and Vascular Biology **26**: 1423-1430.

Shimokado, A., Sun, Y., et al. (2014). "Smad3 plays an inhibitory role in phosphate-induced vascular smooth muscle cell calcification." Experimental and Molecular Pathology **97**: 458–464.

Shioi, A., Nishizawa, Y.*, et al.* (1995). "β-Glycerophosphate accelerates calcification in cultured bovine vascular smooth muscle cells." Arteriosclerosis, Thrombosis, and Vascular Biology **15**(11): 2003-2009.

Shroff, R.C. and Shanahan, C.M. (2007). "The Vascular Biology of Calcification." Seminars in Dialysis **20**(2): 103-109.

Shroff, R.C., McNair, R.*, et al.* (2008). "Muscle Cell Apoptosis Dialysis Accelerates Medial Vascular Calcification in Part by Triggering Smooth Muscle Cell Apoptosis." Circulation **118:** 1748-1757.

Shroff, R.C., McNair, R., *et al.* (2010). "Chronic Mineral Dysregulation Promotes Vascular Smooth Muscle Cell Adaptation and Extracellular Matrix Calcification." Journal of the American Society of Nephrology **21**: 103–112.

Simionescu, A., Philips, K.*, et al.* (2005). "Elastin-derived peptides and TGF-β1 induce osteogenic responses in smooth muscle cells." Biochemical and Biophysical Research Communications **334**(2): 524-532.

Speer, M.Y. and Giachelli, C.M. (2004). "Regulation of cardiovascular calcification." Cardiovascular Pathology **13**: 63-70.

Speer, M.Y., Yang, H.-Y.*, et al.* (2009). "Smooth Muscle Cells Give Rise to Osteochondrogenic Precursors and Chondrocytes in Calcifying Arteries." Circulation Research **104**(6): 733-741.

Spicer, S.S., Lewis, S.E.*, et al.* (1989). "Mice carrying a CAR-2 null allele lack carbonic anhydrase II immunohistochemically and show vascular calcification." The American Journal of Pathology **134**(4): 947-954.

Sriburi, R., Jackowski, S.*, et al.* (2004). "XBP1: a link between the unfolded protein response, lipid biosynthesis, and biogenesis of the endoplasmic reticulum." The Journal of Cell Biology **167**(1): 35-41.

Steitz, S.A., Speer, M.Y., *et al.* (2001), "Smooth Muscle Cell Phenotypic Transition Associated With Calcification: Upregulation of Cbfa1 and Downregulation of Smooth Muscle Lineage Markers." Circulation Research **89**: 1147-1154.

Stenvinkel, P., Wang, K. et al. (2005). “Low fetuin-A levels are accociated with cardiovascular death: Impact of variations in the gene encoding fetuin.” Kidney International **76**: 2383-2392.

Sun, Y., Byon, C.H., *et al.* (2012). “Smooth Muscle Cell–Specific Runx2 Deficiency Inhibits Vascular Calcification.” Circulation Research **111**: 543-552.

Symoens, S., Malfait, F., *et al.* (2013). “Deficiency for the ER-stress transducer OASIS causes severe recessive osteogenesis imperfecta in humans.” Orphanet Journal of Rare Diseases **8**:154.

Szegezdi, E., Logue, S.E., *et al.* (2006). "Mediators of endoplasmic reticulum stress-induced apoptosis." EMBO reports **7**(9): 880-885.

Tanaka, K., Yamaguchi, T., *et al.* (2013). “Advanced glycation end products suppress osteoblastic differentiation of stromal cells by activating endoplasmic reticulum stress.” Biochemical and Biophysical Research Communications **438**: 463-467.

Tanaka, K., Kaji, H., *et al.* (2014). “Involvement of the Osteoinductive Factors, Tmem119 and BMP-2, and the ER Stress Response PERK–eIF2a–ATF4 Pathway in the Commitment of Myoblastic into Osteoblastic Cells.” Calcified Tissue International **94**: 454–464.

Tang, A., Wang, A., *et al.* (2012). “Differentiation of multipotent vascular stem cells contributes to vascular diseases.” Nature Communications **3**: 875.

Taylor, J., Butcher, M., *et al.* (2011). "Oxidized Low-Density Lipoprotein Promotes Osteoblast Differentiation in Primary Cultures of Vascular Smooth Muscle Cells by Up-regulating Osterix Expression in an Msx2-Dependent Manner." Journal of Cellular Biochemistry **112**: 581-588.

Ting, T.C., Miyazaki-Anzai, S., *et al.* (2011). “Increased Lipogenesis and Stearate Accelerate Vascular Calcification in Calcifying Vascular Cell.” The Journal of Biological Chemistry 286 (27): 23938-23949.

Tintut, Y., Patel, J., *et al.* (2000). "Tumor Necrosis Factor-α Promotes In Vitro Calcification of Vascular Cells via the cAMP Pathway." Circulation **102**(21): 2636-2642.

Tohmonda, T., Miyauchi, Y., *et al.* (2011). "The IRE1a–XBP1 pathway is essential for osteoblast differentiation through promoting transcription of Osterix." EMBO reports **12**: 451-457.

Tohmonda, T., Yoda, M., et al. (2013). “The IRE1α-XBP1 Pathway Positively Regulates Parathyroid Hormone (PTH)/PTH-related Peptide Receptor Expression and Is Involved in PTH-induced Osteoclastogenesis.” The Journal of Biological Chemistry **288**(3): 1691-1695.

Travers, K.J., Patil, C.K., *et al.* (2000). "Functional and genomic analyses reveal an essential coordination between the unfolded protein response and ER-associated degradation." Cell **101**(3): 249-258.

Tsang, K.Y., Chan, D., *et al.* (2010). "In vivo cellular adaptation to ER stress: survival strategies with double-edged consequences." Journal of Cell Science **123**: 2145-2154.

Tyson, K.L., Reynolds, J.L., *et al.* (2003). "Arteriosclerosis, Thrombosis, and Vascular Biology." **23**: 489-494.

Ulsamer, A., Ortuno, M.J., *et al.* (2008). "BMP-2 Induces Osterix Expression through Up-regulation of Dlx5 and Its Phosphorylation by p38." The Journal of Biological Chemistry **283**(7): 3816-3826.

Urano, F., Wang, X.Z., *et al.* (2000). "Coupling of Stress in the ER to Activation of JNK Protein Kinases by Transmembrane Protein Kinase IRE1." Science **287**: 664-666.

Vattem, K.M. and Wek, R.C. (2004). "Reinitiation involving upstream ORFs regulates ATF4 mRNA translation in mammalian cells." Proceedings of the National Academy of Sciences of the United States of America **101**(31): 11269-11274.

Walter, P. and Ron, D. (2011). "The Unfolded Protein Response: From Stress Pathway to Homeostatic Regulation." Science **334**: 1081-1086.

Wang, X.Z., Harding, H.P., *et al.* (1998). "Cloning of mammalian Ire1 reveals diversity in the ER stress responses." The EMBO Journal **17**(19): 5708-5717.

Wang, Y., Shen, J., *et al*. (2000). "Activation of ATF6 and an ATF6 DNA binding site by the ER stress response." The Journal of Biological Chemistry **275**(35): 27013-27020.

Wang, W., Lian, N., *et al.* (2009). "Atf4 regulates chondrocyte proliferation and differentiation during endochondral ossification by activating Ihh transcription." Development **136**: 4143-4153.

Wang, Z., Jiang., Y., *et al.* (2012a)."Advanced glycation end-product Nε-carboxymethyl-Lysine accelerates progression of atherosclerotic calcification in diabetes." Atherosclerosis **221**: 387- 396.

Wang, W., Lian, N., *et al.* (2012b). "Chondrocytic Atf4 regulates osteoblast differentiation and function via Ihh." Development **139**: 601-611.

Wang, X., Guo, B., *et al.* (2013). "miR-214 targets ATF4 to inhibit bone formation." Nature Medicine **19**(1): 93-100.

Watson, K.E., Boström, K., *et al.* (1994). "TGF-beta 1 and 25-hydroxycholesterol stimulate osteoblast-like vascular cells to calcify." The Journal of Clinical Investigation **93**(5): 2106-2113.

Weber, C. and Noels, H. (2011). “Atherosclerosis: current pathogenesis and therapeutic options.” Nature Medicine **17**(11): 1410-1422.

Wei, J., Sheng, X.*, et al.* (2008). "PERK Is Essential for Neonatal Skeletal Development to Regulate Osteoblast Proliferation and Differentiation." Journal of Cellular Physiology **217**: 693-707.

Welch, W. and Brown, C.R. (1996). “Influence of Molecular and Chemical Chaperones on Protein Folding.” Cell Stress and Chaperones **1**(2): 109-115.

Westendorf, J.J., Kahler, R.A., *et al.* (2004). “Wnt signaling in osteoblasts and bone diseases.” Gene **341**: 19 – 39.

Willems, B.A., Vermeer, C., *et al.* (2014). “The realm of vitamin K dependent proteins: Shifting from coagulation toward calcification.” Molecular Nutrition and Food Research **58**: 1620-1635.

Wilson, E., Mai, Q., *et al.* (1993). “Mechanical Strain Induces Growth of Vascular Smooth Muscle Cells via Autocrine Action of PDGF.” The Journal of Cell Biology **123**(3): 741-747.

Woldt, E., Terrand, J., *et al.* (2005). “The nuclear hormone receptor PPARγ counteracts vascular calcification by inhibiting Wnt5a signalling in vascular smooth muscle cells.” Nature Communications **3**:1077.

Wolisi, G.O. and Moe, S.M. (2005). "The Role of Vitamin D in Vascular Calcification in Chronic Kidney Disease." Seminars in Dialysis **18**(4): 307-314.

Wu, J. and Kaufman, R.J. (2006). “From acute ER stress to physiological roles of the Unfolded Protein Response.” Cell Death and Differentiation **13**: 374-384.

Wu, L., Wang, D., *et al.* (2014). “Endoplasmic reticulum stress plays a role in the advanced glycation end product-induced inflammatory response in endothelial cells.” Life Sciences **110**: 44-51.

Xiong, Y., Zhang, J., et al. (2014) “Human leptin protein activates the growth of HepG2 cells by inhibiting PERK-mediated ER stress and apoptosis.” Molecular Medicine Reports **10**(3): 1649-1655

Xu, Z., Ji, G.*, et al.* (2012). "SOX9 and myocardin counteract each other in regulating vascular smooth muscle cell differentiation." Biochemical and Biophysical Research Communications **422**(2): 285-290.

Xuan, Y.T., Wang, O.L.*, et al.* (1992). "Thapsigargin stimulates Ca2+ entry in vascular smooth muscle cells: nicardipine-sensitive and -insensitive pathways " American Journal of Physiology **262**(Cell Physiol. 31): C1258-C1265.

Xue, X., Piao, J.-H.*, et al.* (2005). "Tumor Necrosis Factor α (TNFα) Induces the Unfolded Protein Response (UPR) in a Reactive Oxygen Species (ROS)-dependent Fashion, and the UPR Counteracts ROS Accumulation by TNFα." Journal of Biological Chemistry **280**(40): 33917-33925.

Yamabe, S., Hirose, J., *et al.* (2013). "Intracellular accumulation of advanced glycation end products induces apoptosis via endoplasmic reticulum stress in chondrocytes." The FEBS Journal **280**: 1617-1629.

Yamaguchi, H. and Wang, H.G. (2004). "CHOP Is Involved in Endoplasmic Reticulum Stress-induced Apoptosis by Enhancing DR5 Expression in Human Carcinoma Cells." The Journal of Biological Chemistry **279**(44): 45495-45502.

Yang, X. and Karsenty, G. (2004a). "ATF4, the Osteoblast Accumulation of Which Is Determined Post-translationally, Can Induce Osteoblast-specific Gene Expression in Non-osteoblastic Cells." The Journal of Biological Chemistry **279**(45): 47109–47114.

Yang, X., Matsuda, K.*, et al.* (2004b). "ATF4 Is a Substrate of RSK2 and an Essential Regulator of Osteoblast Biology: Implication for Coffin-Lowry Syndrome." Cell **117**: 387–398.

Yao, Y., Jumabay, M., *et al.* (2013). "A Role for the Endothelium in Vascular Calcification"Circulation Research **113**: 495-504.

Yi, N., Chen, S.Y., *et al.* (2012). "Tunicamycin Inhibits PDGF-BB-Induced Proliferation and Migration of Vascular Smooth Muscle Cells Through Induction of HO-1." The Anatomical Record **295**: 1462-1472.

Yin, Q.Q., Dong, C.F., *et al.* (2012). "AGEs Induce Cell Death via Oxidative and Endoplasmic Reticulum Stresses in Both Human SH-SY5Y Neuroblastoma Cells and Rat Cortical Neurons." Cell Mol Neurobiol (2012) 32:1299–1309

Yoshida, H., Matsui, T.*, et al.* (2001). "XBP1 mRNA Is Induced by ATF6 and Spliced by IRE1 in Response to ER Stress to Produce a Highly Active Transcription Factor." Cell **107**: 881-891.

Yousfi, M., Lasmoles, F., *et al.* (2002). "TWIST inactivation reduces CBFA1/RUNX2 expression and DNA bindingto the osteocalcin promoter in osteoblasts." Biochemical and Biophysical Research Communications **297**: 641-644.

Yu, S., Zhu, K., et al. (2013). "ATF4 Promotes β-Catenin Expression and Osteoblastic Differentiation of Bone Marrow Mesenchymal Stem Cells." Interntional Journal of Biological Sciences **9**(3): 256-266.

Zebboudj, A.F., Imura, M.*, et al.* (2002). "Matrix GLA Protein, a Regulatory Protein for Bone Morphogenetic Protein-2." Journal of Biological Chemistry **277**(6): 4388-4394.

Zebger-Gong, H., Muller, D*., et al.* (2011). "1,25-Dihydroxyvitamin D3-induced aortic calcifications in experimental uremia: up-regulation of osteoblast markers, calcium-transporting proteins and osterix." Journal of Hypertension **29**: 339-348.

Zhang, H. and Bradley, B. (1996). “Mice deficient for BMP2 are nonviable and have defects in amnion/chorion and cardiac development.” Development **122**: 2977-2986.

Zhang, P., McGrath, B*., et al.* (2002). "The PERK Eukaryotic Initiation Factor 2a Kinase Is Required for the Development of the Skeletal System, Postnatal Growth, and the Function and Viability of the Pancreas." Molecular and Cellular Biology **22**(11): 3864-3874.

Zhang, K. and Kaufman, R.J. (2008). “From endoplasmic-reticulum stress to the inflammatory response.” Nature **45**: 455-462.

Zhang, Y., Liu, R., *et al.* (2010a). “Cell Surface Relocalization of the Endoplasmic Reticulum Chaperone and Unfolded Protein Response Regulator GRP78/BiP.” The Journal of Biological Chemistry **285**(20): 15065–15075.

Zhang, C. (2010b). ”Transcriptional regulation of bone formation by the osteoblast-specific transcription factor Osx.” Journal of Orthopaedic Surgery and Research **5**(37).

Zhang, X.W., Zhang, B.Y., *et al.* (2014). “Twist-related protein 1 negatively regulated osteoblastic transdifferentiation of human aortic valve interstitial cells by directly inhibiting runt-related transcription factor 2.” The Journal of Thoracic and Cardiovascular Surgery **148**(4): 1700-1708.

Zhu, F., Friedman, M.S., *et al.* (2012). “The Transcription Factor Osterix (SP7) Regulates BMP6-Induced Human Osteoblast Differentiation.” Journal of Cellular Physiology **227**: 2677-2685.

Zinszner, H., Kuroda, M., *et al.* (1998). “CHOP is implicated in programmed cell death in response to impaired function of the endoplasmic reticulum.“ Genes and Development **12**: 982-995.